

Biochemical differences in the modes of synaptic vesicle release between control and streptozotocin-induced diabetic rats and possible relationship to changes in behaviour

by

Mansi Harish Patel

A thesis submitted in partial fulfilment for the requirements of the degree of MSc (by Research) at the University of Central Lancashire, Preston, UK.

Date of Submission: June 2011

Student Declaration

I declare that while registered as a candidate for the research degree, I have not been a registered candidate or enrolled student for another award of the University or other academic or professional institution. No material contained in the thesis has been used in any other submission for an academic award and is solely my own work.

Signature _____

Mansi. Harish. Patel

Type of Award: MSc (by Research)

School : School of Pharmacy and Biomedical Sciences

Abstract

In order to understand the huge complexity of brain function, and to determine the mechanisms underlying various psychiatric (e.g. schizophrenia) and neuronal disorders (Alzheimer's disease), it is imperative that the basic machinery involved in neuronal transmission is fully elucidated. This involves exocytosis of synaptic vesicles (SVs) and subsequent release of neurotransmitter. SVs can exocytose by two different modes: full fusion (FF) and kiss-and-run (K&R). There is much debate as to whether SV fusion in the nerve terminal can occur via K&R mode of exocytosis and this has been studied herein, using cerebrocortical synaptosomes from adult rats. Switching between the two modes depends upon the secondary messenger calcium and protein phosphorylation reactions. Dr. Ashton has previously demonstrated that an increase in intracellular calcium levels regulates the switch between these modes of exocytosis, and thus the role of voltage-gated calcium channels (VGCCs) was studied. Blockade of L-type (but not N- and P-type) VGCCs switch K&R exocytosis to FF mode in control terminals, indicating that such channels contribute to the calcium increase that induces K&R mode. These results (for the first time) demonstrate that distinct VGCC subtypes contribute to the specific mode of exocytosis. Very surprisingly, it has been discovered that in diabetic terminals (prepared from streptozotocin treated rats: a model for type 1 diabetes), higher amount of K&R exocytosis occurs relative to non-diabetic terminals due to a higher stimulus evoked change in intracellular calcium. Whether this was due to an over-activation of certain VGCCs was studied. Fascinatingly, L-type channels did not regulate the mode of exocytosis but diabetic terminals displayed a higher dependence on N-type channels. Blockade of calcium/calmodulin dependent kinase II (CaMKII) was found to inhibit completely the release of reserve pool (RP) of vesicles, with no effect on readily releasable pool (RRP) of vesicles in control terminals. However, by studying the release of just the RRP of SV it was discovered that, inhibition of CaMKII leads to a switch from K&R to FF, suggesting this enzyme when activated can phosphorylate substrate proteins that induces K&R mode of exocytosis. Inhibition of myosin II induces a switch from K&R to FF in both control and diabetic terminals; although results suggest that myosin II may only regulate the fusion mode of the RRP. In control terminals, blockade of calcineurin

induces more K&R. By blocking both myosin II and calcineurin in control synaptosomes, more K&R was apparent. This indicates that RP of vesicles switch to K&R mode of exocytosis independently of the role of myosin II, and that calcineurin exclusively works on RP of vesicles. The inhibition of dynamins switched the mode of exocytosis of the RP of SVs from K&R to FF in diabetic terminals, whilst failing to regulate the mode of exocytosis of the RRP for both control and diabetic terminals when a strong stimulus was applied. It has been established that inhibition of protein phosphatase 2A and activation of protein kinase C induces RRP that undergo K&R in control terminals to FF mode of exocytosis. Similar experiments were performed on diabetic terminals. Each drug treatment alone switched the RRP vesicles in diabetic terminals to undergo FF, but the dual treatment switched all vesicles that previously underwent K&R (i.e. the RRP and some RPs) to a FF mode of exocytosis. The results obtained should help future research to understand precisely the molecular mechanisms that occur in the switching of the mode of different pools of SVs.

The diabetic terminals respond differently to various drugs that perturb protein phosphorylation, $[Ca^{2+}]_i$ and specific phospho-proteins. We hypothesised that these characterized biochemical changes may affect synaptic plasticity and could result in some behavioural changes. With the long-term goal of establishing a link between the biochemical and behavioural findings, which may represent subtle changes in synaptic plasticity, difference in the behaviours of STZ-induced diabetic rats in comparison to the age-matched control rats were measured. A newly developed behaviour registration system, Laboratory Animal Behaviour Observation, Registration and Analysis System (LABORAS) was utilized. The diabetic animals showed significantly decreased locomotive and rearing behaviour whilst the grooming, drinking and eating behaviour was substantially increased over this period. Intriguingly, whilst the incidence of locomotive behaviour was decreased in diabetic animals, the average speed and distance covered over a period of 24hrs was significantly more in such rats than the control rats. These initial observations established behavioural differences that could be related to the biochemical changes seen, and future experiments will attempt to find a correlation between these.

Table of Contents

Abstract.....	iii
Acknowledgements.....	xix
Abbreviations.....	xxi
CHAPTER I. INTRODUCTION.....	1
I.1 Brain Cells/ Neurons.....	1
I.2 Synapses and the process of exocytosis.....	2
I.2.1 Initiation and Propagation of Action Potential.....	6
I.3 Role of Calcium ions in the process of exocytosis.....	7
I.3.1 T-type calcium channels.....	10
I.3.2 L-Type (long lasting) Calcium channels.....	11
I.3.3 N-Type (for Non-L and Neuronal) channels.....	12
I.3.4 P/Q-type Calcium channels.....	13
I.4 Synaptic vesicles and their various pools.....	16
I.4.1 Synaptic Vesicle cycle.....	18
I.5 Modes of Exocytosis.....	20
I.5.1 Full Fusion.....	20
I.5.2 Kiss-and-run.....	22
I.6 Process of Endocytosis.....	24
I.7 Proteins that participate in the process of exocytosis and endocytosis.....	26
I.7.1 Synapsin.....	26
I.7.2 Clathrin.....	29
I.7.3 Dynamin.....	32

I.8 Soluble N-Ethyl-maleimide-sensitive factor (NSF) attachment protein receptors (SNAREs).....	34
I.8.1 Role of SNAREs and SNAPs.....	37
I.9 Secondary messengers.....	40
I.9.1 Calcium/calmodulin dependent kinase.....	40
I.9.2 Protein Kinase C.....	43
I.9.3 Protein Phosphatases.....	45
I.9.3.1 PP2A.....	45
I.9.3.2 PP2B/Calcineurin.....	45
I.9.4 Myosin Family.....	46
I.9.4.1 Myosin-II.....	47
I.10 Synaptic plasticity.....	42
I.10.1 Post-Translational Modification of Endocytotic Proteins.....	48
I.10.2 NT Receptors/trafficking system.....	49
I.10.3 Neurotoxicity.....	50
I.11 Background Results.....	53
I.12 Diabetes Mellitus.....	55
I.13 Symptoms.....	50
I.14 Cognitive Dysfunction.....	57
I.14.1 Hypoglycaemia and brain.....	60
I.14.2 Hyperglycaemia and neuronal deficient.....	61
I.14.3 Hyperglycaemia and neuronal regeneration.....	64
I.15 Behavioural Studies.....	66

I.16 Rationale Behind the methods used.....	67
I.16.1 Synaptosomes.....	67
I.16.2 Glutamatergic synaptic transmission.....	68
I.16.3 FM2-10 dye assay to study the mode of exocytosis.....	71
I.16.4 Fura-2AM experiments.....	72
I.16.5 Three stimuli employed in this study.....	72
I.16.6 STZ as a model.....	73
I.17 Aims and Hypothesis of the Research.....	75
CHAPTER II. REGULATION OF THE MODE OF EXOCYTOSIS IN CONTROL AND DIABETIC TERMINALS.....	77
II.1 MATERIALS AND METHODS.....	77
II.1.1 Animal house.....	77
II.1.2 Biochemical Assays.....	78
II.1.3 Preparation of Synaptosomes.....	79
II.1.4 Glutamate Assay.....	81
II.1.5 FM2-10 Dye Assay.....	82
II.1.6 Fura-2-acetoxymethyl ester Assay.....	84
II.1.7 Statistical Analysis.....	86
II. 2 RESULTS.....	87
II.2.1 Role of P-type VGCCs.....	87
II.2.2 Role of L-type channel.....	93
II.2.3 Role of N-type VGCCs.....	98

II.2.4 Role of P-, Q- and N-type VGCCs.....	108
II.2.5 CaMKII define mode of exocytosis for RRP.....	110
II.2.6 Myosin II is unaltered in diabetic synaptosomes.....	117
II.2.7 Inhibition of Protein Phosphatase 2B/Calcineurin increases the kiss-and-run mode of exocytosis in control synaptosomes.....	119
II.2.8 Dual effect of Myosin II and PP2B inhibitor.....	121
II.2.9 Effect of the inhibition of dynamin on Control Terminals.....	122
II.2.10 Dual effect of Dynamin and Myosin II inhibitor.....	124
II.2.11 Dynamin inhibition switches the RPs to full fusion in Diabetic terminals.....	125
II.2.12 Role of Protein Phosphatase 2A.....	130
II.2.13 Protein Kinase C switches some SVs to full fusion mode of exocytosis in diabetic terminals.....	133
II.2.14 Dual treatment by inhibiting PP2A and activating PKC switches all the pool of SVs to full fusion in diabetic terminals.....	136
II.3 DISCUSSIONS.....	141
II.3.1 Role of VGCCs.....	141
II.3.2 Role of Calcium/Calmodulin dependent Kinase II.....	144
II.3.3 Role of Myosin II.....	145
II.3.4 Role of Calcineurin.....	146
II.3.5 Role of Dynamins.....	148
II.3.6 Dual effect of Dynamin and Myosin II inhibitor.....	150
II.3.7 Role of Protein Phosphatase 2A and Protein Kinase C.....	150
II.3.8 Summary of Results obtained.....	150

II.4 CONCLUSIONS AND FUTURE STUDIES.....	156
CHAPTER III. MONITORING BEHAVIOURAL CHANGES IN DIABETIC RATS USING LABORAS.....	157
III.1.1 Laboratory Animal Behaviour Observation, Registration and Analysis System.....	157
III.2.1 Materials and Methods.....	162
III.2.2 Statistical Analysis.....	163
III.3 RESULTS.....	164
III.3.1 Comparison of weights.....	164
III.3.2 Locomotor activity.....	167
III.3.3 Immobility.....	174
III.3.4 Rearing.....	177
III.3.5 Grooming.....	180
III.3.6 Drinking.....	183
III.3.7 Eating.....	185
III.3.8 Undefined.....	189
III.4 DISCUSSION.....	192
III.5 CONCLUSIONS AND FUTURE STUDIES.....	197
CHAPTER IV. GENERAL CONCLUSIONS.....	198
CHAPTER V. REFERENCES.....	200
CHAPTER VI. APPENDICES.....	228

List of Figures and Tables

Chapter I: Introduction

<u>Figure A.</u> Schematic View of an Excitatory Synapse Formed by an Axonal Varicosity onto a Dendritic Spine	4
<u>Figure B.</u> Synaptic Transmission	5
<u>Figure C.</u> Pedigree segregating the A454T mutation and protein location of the amino acid change.....	16
<u>Figure D.</u> The classic three-pool model of synaptic vesicle.....	18
<u>Figure E.</u> The classical synaptic vesicle cycle	19
<u>Figure F.</u> Neurotransmitter Release at Active Zones under Low- and High-Stimulation Frequencies	21
<u>Figure G.</u> Part of the ‘Vesicle Cycle’ of Exo and Endocytosis	23
<u>Figure H.</u> Multiple synaptic vesicle retrieval pathways in central nerve terminals.....	26
<u>Figure I.</u> Presynaptic terminal depicting the main stages of the synaptic vesicle cycle, characterized by complete fusion and clathrin-mediated endocytosis:	27
<u>Figure J.</u> Synapsins located near the reserve pools at the ultrastructural level i.e near the vicinity of the AZ	28
<u>Figure K.</u> Model for the formation of a clathrin-coated pit and the selective incorporation of integral membrane proteins into clathrin-coated vesicles	31
<u>Figure L.</u> Dyansore-reversible inhibitor of dynamin	34
<u>Figure M.</u> Diagram summarizing the main features of the model of how synaptotagmins and SNAREs cooperate in Ca ²⁺ -dependent membrane fusion ...	35
<u>Figure N.</u> Synaptic vesicle and plasma membrane proteins important for vesicle docking and fusion	37

<u>Figure O.</u> Schematic model depicting the organization of the non-releasable and releasable vesicles vis-à-vis the voltage-gated calcium channel, syntaxin 1A, SNAP-25, and synaptotagmin.....	39
<u>Figure P.</u> Schematic Representation of Activation and Role of CaM Kinase II in Neuronal Cells:	42
<u>Figure Q.</u> Memory consolidation needs PTMs and protein synthesis	49
<u>Figure i.</u> Background Results	54
<u>Figure R.</u> Physiological fates due to the increased glucose level	63
<u>Figure S.</u> Dynamics of FM-dye terminal staining in the two models of neurotransmitter release	70
<u>Figure T.</u> Schematic representation of the toxic effects of the glucose streptozotocin in β -cells, which produce chemical diabetes	71
<u>Figure U.</u> The Tecan GENios Pro	79
 <u>Chapter II: Regulation of the Mode of Exocytosis in Control and Diabetic Terminals</u>	
<u>Table II.A:</u> Wavelengths used for experimental study	86
<u>Figure 1:</u> No effect of HK5C evoked Glu release \pm 50nM Aga TK on (A) Control synaptosomes and (B) Diabetic synaptosomes	88
<u>Figure 2:</u> 50 nM Aga TK significantly perturbs HK5C evoked $[Ca^{2+}]_i$ release using Fura-2AM on (A) Control synaptosomes and (B) Diabetic synaptosomes...89	89
<u>Figure 3:</u> 50 nM Aga TK action on HK1.25C evoked Glu release is significant in(A) control synaptosomes , but has no effect in (B) Diabetic synaptosomes.....91	91
<u>Figure 4:</u> No change in HK5C evoked FM2-10 dye release incontrol synaptosomes treated with 50 nM Aga TK.....	92
<u>Figure 5:</u> 1 μ M Nif fails to perturb the Glu release evoked by HK5C in (A) Control synaptosomes and (B) Diabetic synaptosomes (Barba, 2010).....	93

<u>Figure 6:</u> 1µM Nif perturbs HK1.25C evoked Glu release in (A) control synaptosomes but has not effect in (B) diabetic synaptosomes	95
<u>Figure 7:</u> HK5C evoked FM2-10 release is increased in the presence of 1µM Nif in (A) Control terminals but is not changed in (B) Diabetic terminals.....	96
<u>Figure 8:</u> Similar amount of FM2-10 dye release observed in Control terminals evoked with HK5C and treated with 0.8µM OA or 1µM Nif.....	97
<u>Figure 9:</u> Application of 1µM Nif significantly decreases HK5C evoked $[Ca^{2+}]_i$ in control terminals	98
<u>Figure 10:</u> 1µM GVIA has no effect on HK5C evoked Glu release 1µM GVIA in (A) Control synaptosomes but has an effect in (B) Diabetic synaptosomes.....	99
<u>Figure 11:</u> There is a significant decrease in HK5C evoked change in $[Ca^{2+}]_i$ upon addition of 1µM GVIA in (A) Control synaptosomes and in (B) Diabetic synaptosomes	100
<u>Figure 12:</u> 1µM GVIA perturbs HK1.25C evoked Glu release in control synaptosomes	101
<u>Figure 13:</u> No change in the FM2-10 dye release in control terminals evoked with HK5C following treatment with 1µM GVIA.....	102
<u>Figure 14:</u> 100 nM GVIA has no effect on HK5C evoked (A) Glu release or (B) FM2-10 dye release on diabetic nerve terminals	103
<u>Figure 15:</u> 150 nM GVIA has no effect on (A) HK5C evoked Glu release but has a small but non-significant effect on (B) HK5C evoked FM2-10 dye release in diabetic nerve terminals	104
<u>Figure 16:</u> 200 nM GVIA has no effect on (A) HK5C evoked Glu release but has a small but non-significant effect on (B) HK5C evoked FM2-10 dye release in diabetic nerve terminals	105
<u>Figure 17:</u> 300 nM GVIA has no effect on (A) HK5C evoked Glu release but has a significant effect on (B) HK5C evoked FM2-10 dye release in diabetic nerve terminals.....	106

Figure 18: 400 nM GVIA reduces both (A) HK5C evoked Glu release and (B) HK5C evoked FM2-10 dye release in diabetic nerve terminals	107
Figure 19: Significant decrease in HK5C evoked Glu release upon application of 1µM MVIIC on (A) Control Synaptosomes and (B) Diabetic Synaptosomes ...	109
Figure 20: 10µM KN93 produced a significant decrease in Glu release in Control Synaptosomes stimulated with (A) HK5C, (B) ION5C and but failed to exert an effect with (C) 4AP5C stimulation	109
Figure 21: 10µM KN93 produced no change in the level of $[Ca^{2+}]_i$ obtained in Control Synaptosomes upon stimulation with (A) HK5C, (B) ION5C or (C) 4AP5C	113
Figure 22: 2µM KN92 produced no significant decrease in Glu release in control synaptosomes stimulated by (A) HK5C, (B) ION5C or (C) 4AP5C.....	114
Figure 23: Comparable amounts of Glu release observed in the presence of 10µM KN93 when evoked with HK5C (orange line), ION5C (green line) and 4AP5C (pink line)	115
Figure 24: 10µM KN93 causes an increase in FM2-10 dye release in control terminals stimulated by 4AP5C	116
Figure 25: 50µM Bleb has no effect on HK5C evoked (A) Glu release but this significantly increases (B) FM2-10 dye release in control terminals	117
Figure 26: 50µM Bleb has no effect on HK5C evoked (A) Glu release but this significantly increases (B) FM2-10 dye release in diabetic terminals	118
Figure 27: 1µM Cys A has no effect on HK5C evoked (A) Glu release but this significantly decreases (B) FM2-10 dye release in control terminals.....	120
Figure 28: 1µM Cys A + 50µM Bleb has no effect on HK5C evoked (A) Glu release compared to non-treated cont but this treatment reduces (B) less HK5C evoked FM2-10 dye release compared to control synaptosomes treated with 50µM Bleb alone.....	121

Figure 29: 160 μ M DYN has no effect on HK5C evoked (A) Glu release or (B) FM2-10 dye release in control terminals. (Note this expt was done previously by A. Ashton and colleagues and is included so that one can compare this with subsequent novel experiments) 123

Figure 30: 50 μ M Bleb + 160 μ M Dyn has no effect on HK5C evoked (A) Glu release compared to non-treated cont but this treatment reduces (B) HK5C evoked FM2-10 dye release compared to control synaptosomes treated with 50 μ M Bleb alone..... 125

Figure 31: 160 μ M Dyn has no effect on HK5C evoked (A) Glu release but this significantly increases (B) FM2-10 dye release in diabetic terminals 126

Figure 32: 160 μ M Dyn has no effect on 4AP5C evoked (A) Glu release but this significantly increases (B) FM2-10 dye release in control terminals 128

Figure 33: 160 μ M Dyn has no effect on 4AP5C evoked (A) Glu release or (B) FM2-10 dye release in diabetic terminals 129

Figure 34: Significant increase in FM2-10 dye release observed in control terminals when stimulation with HK5C in the presence of 0.8 μ M OA..... 130

Figure 35: 0.8 μ M OA has no effect on HK5C evoked (A) Glu release but this significantly increases (B) FM2-10 dye release in diabetic terminals (but not as much when compared to Figure 34 for Control Synaptosomes)..... 132

Figure 36: Increase in 4AP5C evoked FM2-10 dye release in diabetic terminals in the presence of 0.8 μ M OA..... 133

Figure 37: Significant increase in HK5C evoked FM2-10 dye release upon application of 1 μ M PMA in control terminal..... 134

Figure 38: 1 μ M PMA has no effect on HK5C evoked (A) Glu release but this significantly increases (B) FM2-10 dye release in Diabetic terminals (but not as much when compared to Figure 37 for Control Synaptosomes)..... 135

Figure 39: Increase in 4AP5C evoked FM2-10 dye release upon application of 1 μ M PMA in diabetic terminals 136

<u>Figure 40:</u> 0.8 μ M OA +1 μ M PMA has no effect on <u>HK5C evoked (A)</u> Glu release but this significantly increases (B) FM2-10 dye release in Diabetic terminals.....	137
<u>Figure 41:</u> Significant difference observed between HK5C evoked FM2-10 dye release in diabetic terminals treated with 1 μ M PMA and 0.8 μ M OA +1 μ M PMA.....	138
<u>Figure 42:</u> Significant difference observed between HK5C evoked FM2-10 dye release in diabetic terminals treated with 0.8 μ M OA and 0.8 μ M OA +1 μ M PMA.....	138
<u>Figure 43:</u> 0.8 μ M OA + 1 μ M increases 4AP5C evoked FM2-10 dye release \pm in diabetic terminals	139
<u>Figure 44:</u> No significant difference observed between 4AP5C evoked FM2-10 dye release in diabetic terminals treated with 1 μ M PMA alone and 0.8 μ M OA +1 μ M PMA.....	140
<u>Figure 45:</u> No significant difference observed between 4AP5C evoked FM2-10 dye release in diabetic terminals treated with 0.8 μ M OA alone and 0.8 μ M OA +1 μ M PMA.....	140
<u>Table II.1:</u> Proposed difference in Control and diabetic nerve terminals.....	151
<u>Figure II.2:</u> Proposed difference in Control and Diabetic terminals.....	152
<u>Figure II.3:</u> Role of VGCCs, protein kinases and protein phosphatases in defining the mode of exocytosis in Control and Diabetic terminals.....	153
<u>Table II.4:</u> Difference in the mode of release evoked by HK5C in Control and Diabetic terminals following application of Dyn	155
<u>Chapter III: Monitoring Behavioural Changes in Diabetic Rats using LABORAS</u>	
<u>Figure V.</u> The LABORAS behaviour registration system	158
<u>Figure W.</u> Vibration patterns corresponding to individual behaviours are represented pictorially.....	160

<u>Table III.A.</u> Positional and vibrational parameters used in the behaviour classification algorithms	161
<u>Figure 46:</u> Diabetic rats gain significantly less weights than the Control rats over the period over 12 weeks after the STZ injection in (A) Expt 1 (B) Expt 2	164
<u>Figure 47:</u> (A) No significant difference in the amount of weight gain observed in CRs from Expt 1 and 2(B) Significant difference in the amount of weight gained observed in DRs from Expt 2 when compare to DRs from Expt 1 after 40 days post-STZ injection	166
<u>Figure 48:</u> DRs displaced significantly less duration of LMA than CRs for (A) 12hrs dark cycle (B) 24hrs and (C) No significant difference observed in 12hrs light cycle for the Average of Expts 1 and 2.....	168
<u>Figure 49:</u> DRs frequency of LMA was significantly less than CRs for (A) 12hrs dark cycle (B) 24hrs and (C) No significant difference observed in 12hrs light cycle for the Average of Expts 1 and 2.....	169
<u>Figure 50:</u> When the average speed of DRs and CRs was compared for 24hrs it was found that in (A) Expt 1 DRs travelled with significantly more speed than CRs from Week 5-10, however for (B) Expt 2 and (C) Average of Expts 1 and Expt 2 no significant difference observed between DRs and CRs	171
<u>Figure 51</u> No significant difference in the average speed of DRs and CRs was observed in the average of Expts 1 and Expt 2 in (A) 12hrs dark cycle and (B) 12hrs light cycle.....	172
<u>Figure 52:</u> No significant difference in the distance covered by DRs and CRs was observed in the average of Expts 1 and Expt 2 for (A) whole 24hrs (B) 12hrs dark cycle and (C) 12hrs light cycle	173
<u>Figure 53:</u> DRs display significantly less duration of immobility than CRs in Average of Expts 1 and 2 for (A) 24hrs, (B) 12hrs dark cycle and (C) 12hrs light cycle.....	175
<u>Figure 54:</u> No significant difference in the frequency of immobility observed in CRs and DRs for the average of Expts 1 and 2 in (A) 24hrs, (B) 12hrs dark cycle and (C) 12hrs light cycle.....	176

Figure 55: DRs display significantly less duration of rearing in comparison to than CRs in Average of Expts 1 and 2 for (A) 24hrs, (B) 12hrs dark cycle and (C) No Significant difference observed between DRs and CRs for 12hrs light cycle..... 178

Figure 56: The frequency of rearing in DRs was significantly less than CRs in Average of Expts 1 and 2 for (A) 24hrs, (B) 12hrs dark cycle and (C) No Significant difference observed between DRs and CRs for 12hrs light cycle 179

Figure 57: No significant difference in the duration of grooming observed in DRs and CRs in Average of Expts 1 and 2 for (A) 24hrs, (B) 12hrs dark cycle and (C) DRs groomed significantly more than CRs for 12hrs light cycle.....181

Figure 58: DRs groom significantly more than CRs in Average of Expts 1 and 2 for (A) 24hrs, (B) 12hrs dark cycle and (C) 12hrs light cycle..... 182

Figure 59: DRs display significantly more duration of drinking in comparison to than CRs in Average of Expts 1 and 2 for (A) 24hrs, (B) 12hrs dark cycle and (C) 12hrs light cycle 184

Figure 60: DRs drink more frequently than CRs in Average of Expts 1 and 2 for (A) 24hrs, (B) 12hrs dark cycle and (C) 12hrs light cycle 185

Figure 61: DRs consume significantly more amount of water than CRs in 24hrs for Average of Expts 1 and 2 186

Figure 62: DRs display significantly more duration of eating in comparison to than CRs in Average of Expts 1 and 2 for (A) 24hrs, (B) 12hrs dark cycle and (C) 12hrs light cycle 187

Figure 63: DRs eat frequently than CRs in Average of Expts 1 and 2 for (A) 24hrs, (B) 12hrs dark cycle and (C) 12hrs light cycle 188

Figure 64: Increase amount of food consumed in DR than CR for 24hrs the Average of Expts 1 and 2..... 189

Figure 65 DRs display significantly more duration of undefined behaviour in comparison to than CRs in Average of Expts 1 and 2 for (A) 24hrs, (B) 12hrs dark cycle and (C) 12hrs light cycle 190

Figure 66: Similar frequency of undefined behaviour observed in DRs and CRs for Average of Expts 1 and 2 for (A) 24hrs, (B) 12hrs dark cycle and (C) 12hrs light cycle..... 191

APPENDIX

Table VI.1.1: Tecan GENios ProTM microtitre plate reader's settings for the measurement of glutamate release.....228

Table VI.1.2: Tecan GENios ProTM microtitre plate reader's settings for the measurement of FM2-10 dye release 228

Table VI.1.3: Tecan GENios ProTM microtitre plate reader's settings for the measurement of the changes in intracellular $[Ca^{2+}]_i$ 229

Table VI.1.4: Homogenization Buffer (pH 7.4).....230

Table VI.1.5: L0 Buffer (pH 7.4).....230

Acknowledgments

I would like to give my unprecedented thanks to my Research Supervisor, Dr. Anthony Ashton, for his unlimited enthusiasm, dedication and support. I would also like to express my appreciation to Professor Jaipaul Singh & Abdelbary Elhissi, for their undying help and direction in making this research a success. I cannot thank enough, all the staff and technicians at the Animal House of the University of Central Lancashire, particularly Paul Knight and Rose Clee, for giving me the opportunity to perform such interesting experiments and for making me feel truly welcome.

I would like to acknowledge a debt of gratitude to my parents, Harish & Surekha; the references of my life, and my brother, Mitul, for their unfading support and encouragement during my studies. This study would have never been possible without their love and prayers, and I am much fortunate to have such beautiful people as my family.

Finally, a special thanks to my colleagues and friends Dilip Bhuvra and Navin Changrani, for their love and inspiration throughout my research and personal life.

Note to Readers

This study aims to explore two main areas in extensive detail, namely biochemical and behavioural changes. Due to the nature and scope of this study, it has been necessary to include many important and pioneering results and analyses, which has led to this thesis being very detailed. Although every effort has been made to keep the information as concise as possible, the extensive nature of the research undertaken and its novel findings have meant this thesis is comparatively extensive, to preserve the flavor of the research and present its findings in a manner in which it is best understood.

Abbreviations

4-Aminopyridine	4AP
A-amino-3-hydroxy-5-methylisoxazole-4-propionate receptor	AMPA
Active zone	AZ
Action potential	AP
Adaptor Proteins	AdP
ω -Agatoxin IVA	Aga TK
Adenosine-5'-triphosphate	ATP
Alzheimer's disease	AD
Blebbistatin	Bleb
Calcium	Ca ²⁺
Calmodulin	CaM
Ca ²⁺ /calmodulin- dependent protein kinase II	CaMKII
Calcineurin	CaN
cAMP dependent protein kinase A	PKA
Centimetres	cm
Central nervous system	CNS
Clatharin-coated vesicles	CCVs
Control Rats	CR
Cyclosporine A	Cys A
ω -conotoxin GVIA	GVIA
Dense core vesicles	DCVs

Dicaylglycerol	DAG
Diabetic mellitus	DM
Diabetic Rats	DR
dihydropyridines	DHPs
Dynasore	Dyn
Full fusion	FF
Glutamate	Glu
High Potassium with 5mM Ca ²⁺	HK5C
High-voltage activated	HVA
Hours	hrs
Hypothalamic-pituitary-adrenal	HPA
Insulin receptors	IRs
Intracellular Ca ²⁺ concentration	[Ca ²⁺] _i
Ionomycin	ION
Kiss-and-run	K&R
Laboratory Animal Behaviour Observation, Registration and Analysis System	LABORAS
Locomotor Activity	LMA
Long-term potentiation	LTP
Long term memory	LTM
Low voltage-activated	LVA

Millivolts	mV
Millimolar	mM
milli seconds	ms
Micro seconds	μ s
Myosin light-chain kinase	MLCK
Neurotransmitters	NTs
Nifedipine	Nif
Nanomolar	nM
Okadaic acid	OA
Plasma membrane	PM
Postsynaptic density	PSD
Post transitional modification	PTM
Phorbol 12-myristate 13-acetate	PMA
Protein Kinase C	PKC
Protein phosphatases 2A	PP2A
Protein phosphatases 2C	PP2C
Readily releasable pool	RRP
Reserve pool	RP
Soluble N-ethylmaleimide-sensitive factor attachment protein receptor	SNARE
Synaptic vesicles	SVs
Synaptosome-associated protein of 25 kd	SNAP-25

Short term memory	STM
Type 1 diabetes mellitus	T1DM
Type 2 diabetes mellitus	T2DM
Voltage-gated Ca ²⁺ channels	VGCCs
Streptozotocin	STZ

1. Introduction

The human body is very complex and various systems work in synchrony for the normal functioning and well-being of an individual. The distinct systems that work together are the musculoskeletal system, the cardiovascular system (circulatory system), the digestive system, the endocrine system, the integumentary system, the urinary system, the immune system, the respiratory system, the reproductive system and the nervous system (Widmaier et al., 2006).

The nervous system co-ordinates all the other mentioned systems. It consists of the central nervous system (CNS) and the peripheral nervous system. The CNS consists of the brain and spinal cord, and the peripheral nervous system consists of the nerves and ganglia that are outside the brain and spinal cord. The peripheral nervous system is further sub-divided into the autonomic and the somatic nervous system (Widmaier et al., 2006). The CNS, mainly brain, is discussed further in this thesis. The nervous system is exceptional in the numerous complexes of thought processes and control of the activities that it performs.

1.1 Brain Cells/ Neurons

Neurons are the core components of the nervous system (Widmaier et al., 2006). It is believed that the human brain has 10^{11} neurons. A typical brain neuron will have connections with at least 1,000 other neurons (Widmaier et al., 2006; Lodish et al., 2008). Various kinds of neurons can be found in the nervous system. Their effect can be excitatory, inhibitory or modulatory; and their functions can be motor, sensory or secretory (Siegel et al., 1999). A large range of neurotransmitters (NT) and hormones can influence the properties of neurons. This enormous repertoire of functions, associated with various developmental influences on different neurons, is largely reflected in the variation of dendritic and axonal outgrowth (Lodish et al., 2008).

A neuron is a polymorphic cell with the cell body, the perikaryon or soma, with broad dendrites emerging from one pole and a fine axon emerging from the opposite pole (Siegel et al., 1999). The signal that flows between two neurons

originates from the dendrite or soma, and propagates to the axon (Lodish et al., 2008). An axon of one neuron passes the information to the dendrites of the neighbouring neurons (Siegel et al., 1999). A synapse is a specialised structure that permits a neuron to pass a signal to another cell (Giagtzoglou et al., 2009). Sir Charles Scott Sherrington and colleagues conceived word "synapse" from the Greek work "synaptein" ["syn-" ("together") and "haptein" ("to clasp")]. Individual neurons can form thousands of discrete synaptic connections with their postsynaptic partners (Graf et al., 2009). The neurons communicate with each other, and the electrical movement within synapses is caused by a propagation of nerve impulses. This phenomenon is called synaptic transmission or neurotransmission (Peters et al., 1996), and its propagation is unidirectional (only in the forward direction).

1.2 Synapses and the process of exocytosis

There are two types of synapses: electrical and chemical. Electrical synapses work via gap junctions, thereby allowing the flow of ions freely from one cell to another. Most of the signal transmission that occurs in the nervous system is via chemical substances called NTs (small water-soluble molecules) (Widmaier et al., 2006). This includes acetylcholine, norepinephrine, histamine, gamma-aminobutyric acid (GABA), glycine, serotonin and glutamate. These NTs are synthesized intracellularly in the cytosol and packaged via specific transmembrane protein transporters into synaptic vesicles (SVs) (Park and Kim, 2009; Omiatek et al., 2010), which mediate fast synaptic transmission (Xia et al., 2009). For instance, glutamate is transported into the SVs via proteins that make up *vesicular glutamate transporters* (VGLUTs).

Synapses are composed of presynaptic and postsynaptic compartments (Shupliakov, 2009). Each synapse comprises of tightly apposed pre- and postsynaptic membranes, a postsynaptic cluster of NT receptors, and a presynaptic complex of proteins that promotes NT release (Graf et al., 2009). The excitatory or inhibitory terminal has two important structures for their normal functioning: SVs/dense core vesicles (DCVs) and mitochondria (Xia et al., 2009). Upon stimulation, the SVs containing NTs release their contents into the synaptic cleft, which either leads to excitation or inhibition of the postsynaptic neuron

(Refer Fig A). Adenosine-5'-triphosphate (ATP) from the mitochondria provides energy for the process of neurotransmission (Lodish et al., 2008).

The pre- and postsynaptic events are highly coordinated and are subject to use-dependent changes, which form the basis for plasticity and learning in the CNS. Although, direct electrical connections also occur, these account for transmission of information between nerves only in specialized cases. The release of NTs is of central importance for the normal functioning of the brain. The presynaptic neurons/nerve terminal has highly evolved machinery that is specialized for the release of chemical NTs, and SVs are the organelles that are intimately involved in this process (Siegel et al., 1999). The SVs are small membrane-bounded organelles and serve as the primary intracellular unit for the highly efficient storage and discharge of the NTs during signalling processes (Omiatek et al., 2010). They fuse with the plasma membrane (PM) to release NTs, a key aspect of signalling between neurons (Zhang et al., 2007). These NTs are released from the intracellular compartment of the presynaptic terminals into the extracellular domains by the process of exocytosis, which is a calcium (Ca^{2+}) dependent mechanism (Jackson, 2007; Hosoi et al., 2009). In this process, upon the arrival of the action potential (AP), the voltage-gated Ca^{2+} channels (VGCCs) get activated resulting in the influx of Ca^{2+} ions to the inside of the cells (Sudhof, 1995; Fdez and Hilfiker, 2006; Serulle et al., 2007; Sudhof and Malenka, 2008). This causes localized rise in the cytosolic Ca^{2+} levels which triggers the SVs to migrate to the active zone (AZ) and fuse at the PM, thereby releasing their content into the synapses (Hosoi et al., 2009). These messengers interact with various receptors on target cells to communicate, after which they are recaptured or metabolized (Omiatek et al., 2010). A complex meshwork of actin filaments, tethers, and scaffolding proteins mediates vesicle recruitment at the AZ, where SVs are captured and tethered to presynaptic dense projections, and some are placed in close proximity to Ca^{2+} channels (Giagtzoglou et al., 2009; Kim and von Gersdorff, 2009). The released NTs can then activate receptors on the postsynaptic target cells, thereby allowing the signalling between these cells (Fdez and Hilfiker, 2006; Widmaier et al., 2006) (Refer Figure A for the overview of the process of exocytosis). Transmission electron microscopy determined the size (typically 50–800nm diameter) and morphology of SVs

involved in exocytosis (Omiatek et al., 2010). The fusion of SVs with these electron-dense regions of the presynaptic PM is spatially and temporally regulated (Wasser and Kavalali, 2009). A detailed understanding of how a CNS functions requires analysis of its chemical signalling, which is largely mediated by regulated vesicle exocytosis (Xia et al., 2009).

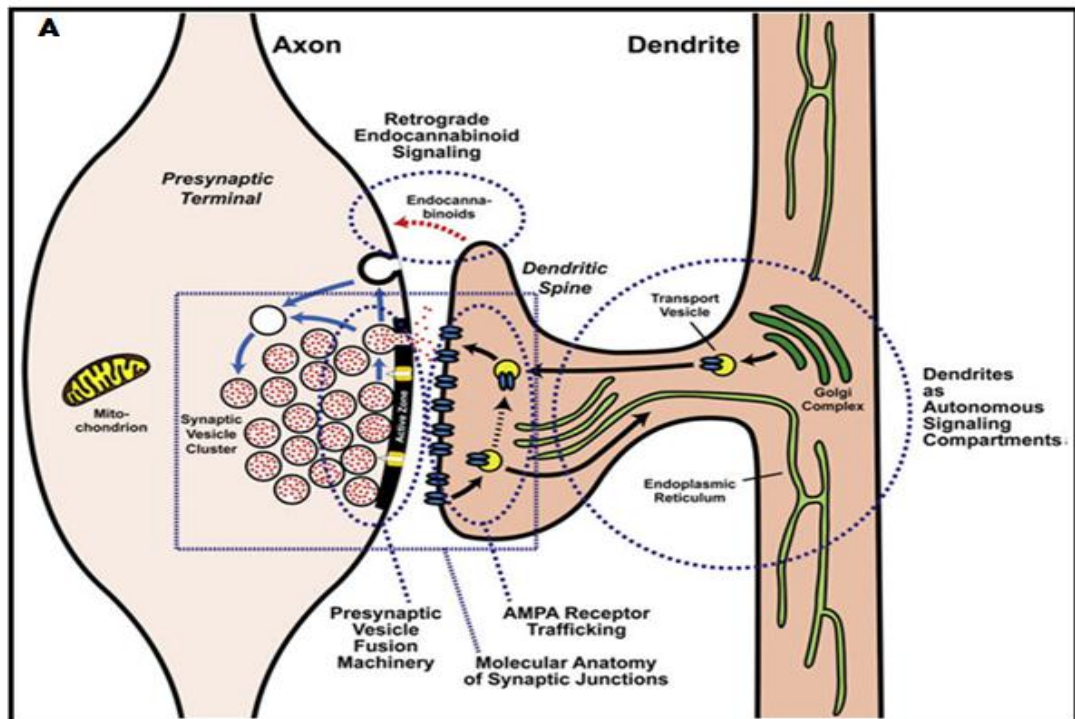


Figure A. Schematic View of an Excitatory Synapse Formed by an Axonal Varicosity (Left) onto a Dendritic Spine (Right): Key elements of the apparatus mediating synaptic transmission are indicated, as is the trafficking of postsynaptic AMPA-type glutamate receptors (Sudhof and Malenka, 2008).

In synaptic terminals, phosphorylation of pre- and postsynaptic proteins is required for basal neurotransmission and synaptic plasticity at both excitatory and inhibitory connections (Munton et al., 2007). Activity-dependent protein phosphorylation is one of the most ubiquitous and vital biochemical processes, which contribute to the regulation and fine-tuning of numerous cellular functions in many cell types (Leenders and Sheng, 2005). At the molecular level, the addition or removal of a phosphate residue can considerably affect the function and/or localization of proteins including enzymes, ion-channels, scaffolding proteins, or signalling molecules.

The events that occur during the synaptic transmissions are detailed in Figure B

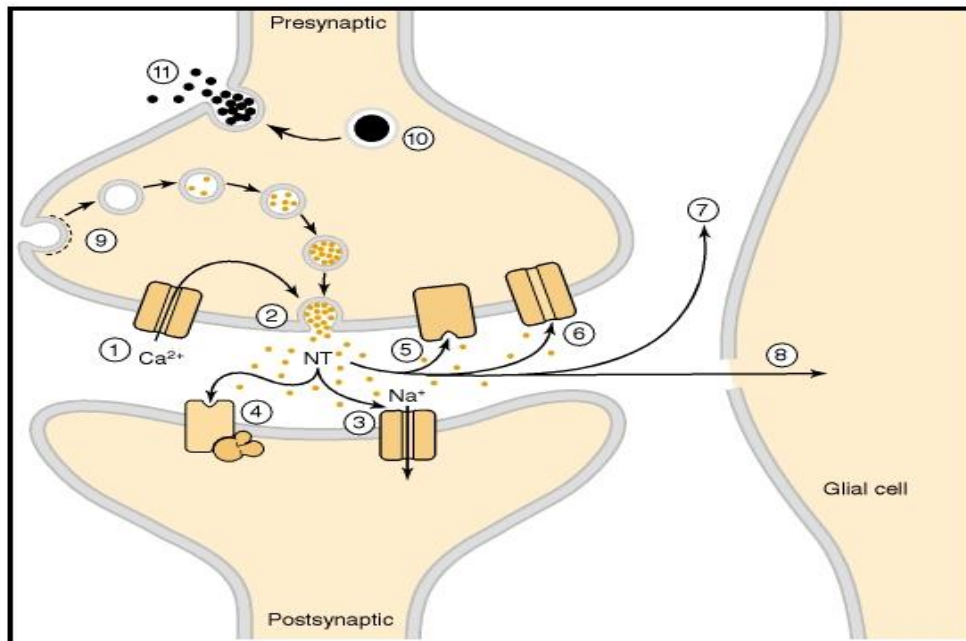


Figure B. Synaptic Transmission: 1. Depolarization opens VGCCs in the presynaptic nerve terminal. The influx of Ca²⁺ and the resulting high Ca²⁺ concentrations at AZ on the PM trigger 2. The exocytosis of small SVs that store NT involved in fast neurotransmission. Released NT interacts with 3. receptors in the postsynaptic membrane, which couple directly with ion channels and with receptors that act through second messengers, such as 4. G-protein coupled receptors. 5. NT receptors, also in the presynaptic nerve terminal membrane, either inhibit or enhance exocytosis upon subsequent depolarization. Released NT is inactivated by reuptake into the nerve terminal by 6. A transport protein coupled to the Na⁺ gradient, for example, dopamine, norepinephrine, glutamate and GABA; by 7. Degradation (acetylcholine, peptides); or by 8. uptake and metabolism by glial cells (glutamate). The SV membrane is recycled by 9. clathrin-mediated endocytosis. Neuropeptides and proteins are stored in 10. larger, dense core granules within the nerve terminal that are released from 11. sites distinct from AZ after repetitive stimulation (Siegel et al., 1999). Note that this is a conventional text book diagram and does not take into account the Kiss-and-run type exocytosis which is the subject of this thesis.

There are mainly two types of synaptic transmitter release: spontaneous and evoked synchronous (Chang and Mennerick, 2010). Presynaptic APs and resulting Ca²⁺ influx cause rapid (within a millisecond) synchronous vesicle fusion (Chung et al., 2010). A third type of release, asynchronous release is believed to complement the phasic release, but this is not yet fully understood.

1.2.1 Initiation and Propagation of Action Potential

The exocytosis of SVs occurs on the arrival of the AP. The neurons maintain an electrical polarized state, by maintaining the voltage difference across the PM (Lodish et al., 2008). Ion-pumps and ion-channels play a major role in maintaining this homeostasis. On an arrival of a stimulus, the ion pumps work in a way to generate depolarization across the membrane upto the threshold, thereby generating AP. In simplistic terms, the proteins of the ion-channel exist in either of two conformations, the open-channel state or closed-channel state. During resting conditions, the channels are closed. Whether an ion-channel is open or closed is controlled by distinct mechanisms, dependent upon the type of ion-channels. The opening and closing of ion-channels either depends on the voltage across the membrane (voltage-gated ion-channels) or on some controlling chemical (chemically-gated ion-channels). Axons have voltage-gated ion-channels, whereas synapses contain both voltage-gated and chemically-gated ion-channels. Dendrites typically have more chemically-gated than voltage-gated ion-channels (Siegel et al., 1999).

The voltage-gated channels that play an important role in the transmission of APs are sodium (Na^+) and potassium (K^+) channels. Na^+ channels are more sensitive to voltage change than K^+ channels, and open more rapidly. Thus, in a depolarization, the Na^+ ions will rush into the axon faster than the K^+ ions will rush out. This sudden depolarization (called an AP) will briefly result in a +30 mV potential difference (Lodish et al., 2008). This process of positive feedback continues until all the Na^+ channels are activated. Within milliseconds (ms), the rising membrane potential results in the closure of the Na^+ channels and opening of the K^+ channel thereby, restoring the negative potential across the membrane, and terminating the AP (Widmaier et al., 2006).

1.3 Role of Calcium ions in the process of exocytosis

Once the AP reaches the presynaptic terminal, it causes a third kind of voltage-gated ion-channel to open (Wykes et al., 2007): Ca^{2+} channels (Giagtzoglou et al., 2009). VGCCs are a diverse family of molecularly and pharmacologically distinct ion-channels underlying various forms of synaptic plasticity (Fourcaudot et al., 2009). In several mammalian synapses such as hippocampus, cerebellar, calyx of Held, it has been shown that NT release requires Ca^{2+} entry into the presynaptic terminals via numerous VGCCs (Bucurenciu et al., 2010). The VGCCs are clustered at the AZ (Giagtzoglou et al., 2009). It is well established that Ca^{2+} influx through VGCCs, following arrival of APs to the nerve terminal, results in a rapid and localized Ca^{2+} signal that interacts with Ca^{2+} sensors on the exocytotic apparatus and initiates various membrane trafficking events (Zhu et al., 2010) that trigger SV fusion with the PM, thus releasing NT (Sudhof, 1995). In the CNS, Ca^{2+} influx plays an essential role for the exocytosis of NT release (Wright and Angus, 1996; Fourcaudot et al., 2009; Atlas, 2010), process outgrowth and synaptic plasticity (Nachman-Clewner et al., 1999). Voltage-activated and receptor-operated Ca^{2+} channels are located on the PM and on the internal membrane of cytosolic organelles of neurons in most brain areas. Ca^{2+} also plays a crucial role in regulating various cellular processes such as; synaptic transmission, muscle contraction, gene transcription, synaptic plasticity (Verma et al., 2009), and even neurotoxicity and neuronal death (Bertolino and Llinas, 1992; Bucurenciu et al., 2010). VGCCs are essential elements of fast stimulus-secretion coupling in presynaptic terminals of the neurons (Zhu et al., 2010). Under resting conditions, the Ca^{2+} concentration of the extracellular fluid is in the millimolar (mM) range, whereas the intracellular free Ca^{2+} concentration is 100 nanomolar (nM). Vesicular fusion may occur at 10–25 μM Ca^{2+} , but during normal synaptic activity intracellular Ca^{2+} concentration ($[\text{Ca}^{2+}]_i$) may exceed 200 μM locally (Omiatek et al., 2010). Two major consecutive Ca^{2+} binding events characterize the dynamics of the release process: first, Ca^{2+} binds at the selectivity filter, the polyglutamate EEEE motif of the VGCC and subsequently following a brief and intense Ca^{2+} inflow; Ca^{2+} binds to synaptotagmin, a vesicular protein (Atlas, 2010). The effect of the NT on the postsynaptic membrane (on the subsequent neuron) will depend on the nature of the NT, the

nature of the postsynaptic receptors, and whether the postsynaptic ion-channels are voltage-gated (Wright and Angus, 1996) or chemically-gated.

Ca^{2+} also acts as a secondary messenger to co-ordinate the release of enzymes, opening/closing of the ion-channels, the expression of genes that are responsible for cellular responses such as long-term potentiation (LTP) (Bertolino and Llinas, 1992). Additionally, the coupling between presynaptic Ca^{2+} channels and Ca^{2+} sensors of exocytosis is of fundamental importance for the timing and efficiency of synaptic transmission (Bucurenciu et al., 2010).

VGCCs play a crucial role in the normal functioning and in various pathological processes that occurs in neuronal, neurosecretory and muscle cells (Dolphin, 2006). An interesting property of the VGCCs in the transmembrane Ca^{2+} entry is the fact that multiple Ca^{2+} channels coexist within the same cell (Serulle et al., 2007). The study done by Bucurenciu et al., (2010) concluded that, opening of a large number of Ca^{2+} channels is necessary for exocytosis at mammalian synapses (Bucurenciu et al., 2010). These channels can be distinguished by their particular pharmacological and biophysical properties (Bertolino and Llinas, 1992). Various classifications of Ca^{2+} channels are a simplification and do not reflect the structural heterogeneity of these heterooligomeric integral membrane proteins. Progress in molecular biology has revealed that VGCCs are formed as a complex of several different subunits: α_1 , $\alpha_2\delta$, β_{1-4} , and γ (Catterall and Few, 2008). The α_1 subunit forms the ion-conducting pore while the associated subunits have several functions including modulation of gating (Dolphin, 2006). The multiple VGCCs are subdivided into two classes by the pattern of channel activation; 1) low voltage-activated (LVA) or low threshold and 2) high-voltage activated (HVA) or high threshold channels. Researchers have showed that LVAs conductance is situated in the soma whilst HVA Ca^{2+} conductances are localized in the dendrites and terminals of the neurons. LVA channels are also called "T" (for transient), and HVA channels are further divided into three subclasses: "L" (for long-lasting), "N" (for neither T nor L or neuronal) and "P" (for Purkinje cell) (Bertolino and Llinas, 1992; Wright and Angus, 1996). Many of these channels appear to have a complex structure comprising the ionophore and multiple ligand binding sites that regulate the activity of the channel. Among various VGCCs, N-

type and P/Q-type Ca^{2+} channels play a major role in regulating the presynaptic NT release (Zhu et al., 2010).

The HVA Ca^{2+} channels are composed of five polypeptide subunits with different molecular masses. They are α_1 subunit (~175 kd), which form the ion-channel and may contain the 1,4 dihydropyridine (DHP) and the phenylalkylamine binding site. The α_2 subunit (~143 kd) is associated with α_1 and does not contain any high-affinity binding site; and the three low molecular weight subunits, β (~54 kd), γ (~30 kd) and δ (~27 kd) in an approximately stoichiometric ratio (Dolphin, 2006). The α_1 and β subunits contain phosphorylation sites for cyclic AMP-dependent protein kinase (Bertolino and Llinas, 1992).

The α_1 subunit is believed to be the principle structure of the Ca^{2+} channels, which has four homologous domains that are predicted to criss-cross the cell membrane and form channel pore. Each of these domains is composed of six transmembrane segments (Bertolino and Llinas, 1992). The α_1 subunit forms the Ca^{2+} selective pore, which contains voltage-sensing machinery and the drug/toxin-binding sites. Ten distinct α_1 subunits have been identified in humans (Nachman-Clewner et al., 1999).

Hydropathy analysis indicated that, the α_1 subunits have 24 putative transmembrane segments that are arranged into four homologous repeated domains, with intracellular linkers and N- and C-termini. The four members of the Ca_v1 family are all L-type channels. $\text{Ca}_v1.1$ is skeletal muscle isoform, and $\text{Ca}_v1.2$ is prevalent in cardiac muscle, $\text{Ca}_v1.3$ and 1.4 are activated at lower voltage thresholds, and have restricted distribution. $\text{Ca}_v2.1$ is the molecular counterpart of P/Q-type Ca^{2+} channels $\text{Ca}_v2.2$ or $\alpha_1\text{B}$ is the molecular counterpart of the neuronal N-type Ca^{2+} channels (Fourcaudot et al., 2009). $\text{Ca}_v2.3$ or $\alpha_1\text{E}$ was initially thought to be a LVA channel, but it is now thought to contribute to the molecular counterpart of the R-type Ca^{2+} current (Dolphin, 2006).

Various combinations of the L-type Ca^{2+} channel subunits gives rise to a variety of Ca^{2+} channels that differ in their Ca^{2+} permeation properties and characteristics of their DHPs binding sites. The α_1 - β combination results in greater number of DHPs binding sites (Nachman-Clewner et al., 1999).

The β -subunit is believed to contribute in the activation and inactivation properties of the channel. Gating of the channel is accelerated when the β -subunit is present and helps in stabilizing the α_1 subunit (Bertolino and Llinas, 1992).

The α_2 is the extracellular glycosylated subunit that interacts with the α_1 subunit. The δ subunit has a single transmembrane region with a short intracellular portion, which serves to anchor the protein in the PM (Dolphin, 2006).

The γ subunit glycoprotein (33 kDa) is composed of four transmembrane spanning helices. The γ_1 subunit does not play a role regulating the channel complex. However, γ_2 , γ_3 , γ_4 and γ_8 are also associated with AMPA glutamate receptors (Dolphin, 2006).

1.3.1 T-type calcium channels

These types of VGCCs are activated with a weak depolarization and carry a transient current at negative membrane potentials that inactivates rapidly during a prolonged pulse. The experiments carried out on the rat dorsal root ganglion cells demonstrated that, the T currents are activated at approximately -50mV, reaches its maximum value between -40 to -10mV, and is inactivated by holding the potential more positive than -60mV. However, interestingly these experiments found that the inactivation is eliminated if the potential decreases from -60mV to -100mV (Bertolino and Llinas, 1992). The precise structure of the T-type channel has not been elucidated, due to the lack of selective ligands.

As the T-type VGCCs are activated at a negative potential close to the membrane resting potential, it is responsible for neuronal oscillatory activity, that is, spontaneous membrane potential fluctuations that are not mediated by synaptic activity. These oscillatory activities may play an important role in various brain functions, such as regulation of wakefulness, motor coordination, and neuronal circuit specification during ontogenesis via oscillatory electrical activity (Bertolino and Llinas, 1992). The studies carried out on the thalamic neurons, confirmed that tonic-firing activity is most commonly recorded in wake animals and phasic firing corresponds to slow-wave sleep. It is believed that, phasic firing is dependent on Ca^{2+} entry through T-type Ca^{2+} channels. The experiments on inferior olivary nucleus neurons in brain stem slices showed that, intrinsic phasic

oscillatory activity occurs due to the activation of a low-threshold Ca^{2+} conductance, which produces an after depolarization responsible for the initiation and maintenance of the oscillatory activity (Bertolino and Llinas, 1992).

1.3.2 L-Type (long lasting) Calcium channels

As mentioned earlier, L-type VGCCs are classed under HVA channels, as they require large depolarization to be activated, and they inactivate slowly (Nachman-Clewner et al., 1999). They are present in muscle, heart, smooth muscle and neurons (Dolphin, 2006). The L-type channels are sensitive to DHPs. The L-type Ca^{2+} channels play a role in the generation of AP, signal transduction events at the cell membrane (Bertolino and Llinas, 1992), neuronal differentiation, neurite outgrowth and NT release (Nachman-Clewner et al., 1999).

One of the striking features of the L-type VGCCs is that the channels open during the membrane depolarization only when phosphorylated (Bertolino and Llinas, 1992). L-type channels generally regulate Ca^{2+} influx into the soma and dendrites (Yang et al., 2009), whereas other VGCCs control presynaptic activities (Verma et al., 2009), although some of this data is based on the lack of effect of inhibition of L-type channels on NT release from nerve terminals. This question has been addressed in this thesis. Existence of L-type Ca^{2+} channels have been confirmed in many regions of the CNS, such as the hippocampus, cerebral cortex, cerebellum, spinal cord, and retina. The microfluorometric imaging studies on brain slices demonstrated that, L-type channels are located on the cell bodies and proximal dendrites of neurons, and are clustered at high density at the base of the major dendrites i.e. they represent a major postsynaptic channel. The wide distribution of the L-type Ca^{2+} channel, both at the level of the CNS and of a single neuron, reflects the multiple cellular functions of this channel (Bertolino and Llinas, 1992). However, L-type channels are also presynaptic and can be localized at the nerve terminal e.g. experiments on ribbon synapses concluded that, L-type Ca^{2+} channel activity on nerve terminals stimulates neurotransmission and contributes to presynaptic structural plasticity (Nachman-Clewner et al., 1999).

Albrecht Fleckenstein coined the term Ca^{2+} antagonist for any drug that blocked excitation-contraction coupling in the same way as removal of external Ca^{2+} ions. He later discovered nifedipine (Nif) as a Ca^{2+} antagonist, the first molecule of many in the therapeutically important class of DHPs. The various classes of Ca^{2+} antagonists were found to block Ca^{2+} currents with differential selectivity in cardiac and smooth muscle in a state-dependent manner, and this forms the basis of their therapeutic role as antihypertensive and antianginal drugs (Dolphin, 2006; Yang et al., 2009). Nif binds to a specific recognition site associated with the α_1 subunit (Dolphin, 2006). Bay K 8644 selectively increases the current generated by L-type channels. Single-channel analysis has demonstrated that DHP Ca^{2+} antagonists affect the activity of the channel by favouring particular modes of gating rather than by blocking the pore of the channel. It has been exhibited that, these pharmacological agents can either up- or down-regulate the DHP binding sites (Bertolino and Llinas, 1992).

Dolphin, (2006) indicated that in neurons some HVA Ca^{2+} current was not L-type, as it was not blocked by DHPs (Dolphin, 2006). This current was inferred to be particularly prevalent at presynaptic terminals, as synaptic transmission was generally found to be DHP insensitive (but see experiments performed in this thesis). The additional non-L-type current component was then subdivided according to its biophysical properties, and subsequently explored with the aid of several invaluable toxins (Bertolino and Llinas, 1992).

1.3.3 N-Type (for Non-L and Neuronal) channels

N-type Ca^{2+} channels are predominantly expressed on presynaptic terminals (Verma et al., 2009). In dorsal root ganglion neurons, the N-type channel was distinguished by range of inactivation between -120 and -30mV. The N-type Ca^{2+} channel was insensitive to DHPs and seemed to have slow inactivating component and a sustained long-lasting component, and the same N-type channel seems to be responsible for both of these two components (Bertolino and Llinas, 1992).

N-type channels are blocked by toxic peptides isolated from the fish-eating marine cone shell mollusc snail, *Conus geographus*, termed ω -conotoxin GVIA

(Bertolino and Llinas, 1992; Wright and Angus, 1996; Dolphin, 2006; Verma et al., 2009). Thus, GVIA can inhibit NT release from the nerve terminals by a pre-junctional action (Wright and Angus, 1996). GVIA blocks highly selectively N-type channels, and does not affect any other neuronal VGCCs, or post-junctional L-type Ca^{2+} channels (Wright and Angus, 1996). This N-type channel blocker is potent, rapid, and rapidly reversible (McDonough et al., 1996). GVIA irreversibly blocks stimulus-evoked release of acetylcholine at the frog neuromuscular junction by inhibiting the presynaptic Ca^{2+} channels. Furthermore, studies performed on isolated frog dorsal root ganglion neurons showed that synthetic GVIA selectively caused depression of Ca^{2+} current without an effect on the Na^+ current or affecting the L-type channels (Bertolino and Llinas, 1992). Allodynia and hyperalgesia due to neuropathic pain has also been observed to be causally related to the N-type VGCCs (Verma et al., 2009).

1.3.4 P/Q-type Calcium channels

A very slowly inactivating Ca^{2+} channel was identified in many mammalian central neurons such as cerebellum granule (Wright and Angus, 1996) and Purkinje cells (Dolphin, 2006). Such cells were highly resistant to responses to both DHP and GVIA following nerve depolarization (Dolphin, 2006). The P/Q-type channel is thought to be a widely distributed Ca^{2+} channel in the mammalian CNS (Bertolino and Llinas, 1992). They are present in Purkinje cells (particularly in the dendrites and presynaptic terminals), the inferior olivary nucleus, several nuclei in the brain stem, olfactory bulb, entorhinal cortex, the hippocampus and the neocortex. They are also detected in retina, the hypophysis, and developing granule cells in the cerebellum. Additionally, the P/Q-type channel appears to be the channel responsible for the high-threshold Ca^{2+} current (Dolphin, 2006).

The P/Q-type Ca^{2+} channel contains a pore-forming α_{1A} subunit and several regulatory subunits, including intracellular β subunits ($\text{Ca}_v\beta_{1-4}$) that bind to the intracellular loop between transmembrane domains I and II of α_{1A} (see Figure C for an illustration of the channel complex). The effect of the regulatory subunits is essential for increasing the expression levels and modulating the voltage-dependent activation and inactivation of P/Q channels (Serra et al., 2010). It is believed that, deletion of both alleles of the P/Q-type VGCCs $\text{Ca}_v2.1$ (α_{1A})

subunit gene in mouse leads to severe ataxia and early death (Lonchamp et al., 2009).

Initially, these channels were called P-type (for Purkinje), and were found to be sensitive to a component of the venom from the American funnel-web spider, *Agelenopsis aperta*. Eventually it was established that a peptide, ω -Agatoxin IVA (Aga TK) isolated from the venom of the funnel web spider was a selective antagonist (at concentration <100 nM) and blocked P-type channels (Wright and Angus, 1996; Serulle et al., 2007).

Another Aga TK-sensitive current (blocked at high concentration of ≥ 100 nM), that was also blocked by the toxin ω -conotoxin MVIIC (MVIIC) from the venom gland of the snail *Conus magus*, (McDonough et al., 1996; Wright and Angus, 1996), showed more rapid inactivation and had a lower affinity for the Aga TK and was identified in cerebellar granule cells. Aga TK actions was slow in onset, but it was very slowly reversible (McDonough et al., 1996). This current was originally thought to represent a different channel, and it was termed the Q-type channel (Dolphin, 2006). These two distinct current components are now usually combined and labelled as the P/Q channel, and the differences probably arise due to different splicing of the same molecular entity or association with different β -subunits (Dolphin, 2006). N-, P- and Q-type Ca^{2+} channels are inhibited by MVIIC, with differences in relative potency and kinetics (Wright and Angus, 1996). It is established that, MVIIC binds to N-type Ca^{2+} channels with an affinity of 10-100 fold lower than GVIA (Randall and Tsien, 1995). It also blocks P-type Ca^{2+} channels at concentrations 100-1000 fold higher than Aga TK with very slow on/off kinetics. It is believed that, MVIIC and Aga TK are equipotent at inhibiting Q-type channels (Wright and Angus, 1996).

There is also a Residual or R-type Ca^{2+} channel component that is resistant to DHPs and the N- and P/Q-type Ca^{2+} channel toxins (Randall and Tsien, 1995). R-type VGCCs are blocked by Ni^{2+} (Fourcaudot et al., 2009).

Previous studies have suggested that N-type and P/Q-type but not L-type Ca^{2+} channels are involved in presynaptic transmission. Furthermore, N-type VGCCs regulate NT release at both peripheral and central synapses, whereas the P/Q-type

VGCCs play a primary role only at the central synapses (Zhu et al., 2010). Both P/Q- and N-type VGCCs play a role in glutamate release, while the P/Q-type is essential in GABA exocytosis in the cerebellum (Lonchamp et al., 2009). These VGCCs are critical to stimulus-secretion coupling in the nervous system; feedback regulation of such channels by Ca^{2+} is therefore predicted to profoundly influence neurotransmission (Wykes et al., 2007; Watanabe et al., 2010). They play a prominent role in NT release at most synapses; and coexist at most release sites but are not uniformly distributed (Lonchamp et al., 2009).

Inactivation of the VGCCs is also important to determine its function as it helps to define the temporal properties of Ca^{2+} signals. There are two factors that control the VGCCs inactivation; voltage and Ca^{2+} . Both of these are regulated by multiple domains within the pore forming α and auxiliary β subunit. It is believed that calmodulin (CaM), a calcium sensor, plays an important role in mediating Ca^{2+} dependent inactivation (Wykes et al., 2007).

VGCCs are also thought to play an additional role in SV exocytosis through direct interactions with syntaxin, SNAP-25, and synaptotagmin (Syt) (see later on for my information on these particular proteins) at the synprint site in a large intracellular loop between transmembrane domains II and III (L II-III) of the VGCC α_1 subunit (Refer Figure C) (Watanabe et al., 2010). VGCC synprint sites anchor a fraction of AP-2 complex, which is likely linked to the PM via interactions with phosphatidylinositol 4,5-bisphosphate [PI(4,5)P₂]. This synprint-AP-2 interaction occurs for both N- and P/Q-type VGCCs (Watanabe et al., 2010).

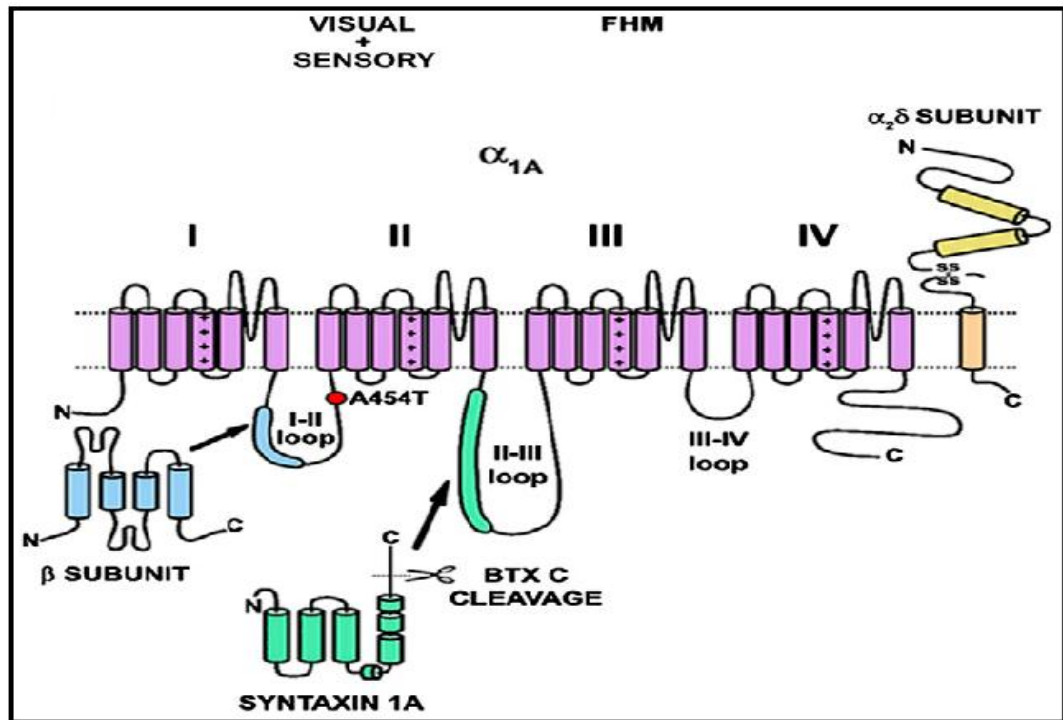


Figure C. Pedigree segregating the A454T mutation and protein location of the amino acid change: Location of the alanine-tothreonine mutation at position 454 (A454T) in the I-II intracellular loop of the P/Q channel α_{1A} subunit (Serra et al., 2010).

1.4 Synaptic vesicles and their various pools

In a typical synapses, the presynaptic terminal contain copious amounts of SVs (approximately 40 nm in size); an AZ at the presynaptic PM, at which the numerous SVs are clustered (Fdez and Hilfiker, 2006); and in front of the presynaptic AZ, the postsynaptic cell also forms a thickening in the PM, which is referred to as postsynaptic density (PSD) (Sudhof, 1995). Such vesicle clusters, together with local vesicle recycling events, allow nerve terminals to regularly convert APs into secretory signals over a large firing range. There are about 200-500 SVs per nerve terminal. However, there are no more than 30 SVs bound to the AZ at a synapse, and most SVs are free in the cytosol of the nerve terminal (Peters et al., 1991).

In a classic presynaptic nerve terminal, various pools of SVs are observed. These vesicles can be subdivided into distinct pools based on their morphology and physiology. Morphologically these pools are distinguished according to their proximity to the PM. The pools that are situated closely to the PM (at AZ) are

called the docked vesicle pools (5-10%) and those that are away are called the reserve pool (Fdez and Hilfiker, 2006). The docked vesicles are generally thought to be ready for release since they can be fused by rapid uncaging of intrasynaptic Ca^{2+} , a 10ms Ca^{2+} current pulse, a brief high-frequency train of APs or by hypertonic stimulation (Wasser and Kavalali, 2009).

Physiologically the pools are divided by the vesicles' ability to be released. These were readily releasable pools (RRP), reserve pool (RP) and silent pool (Refer Figure D) (Santos et al., 2009; Cheung et al., 2010). This release-ready pool of vesicles is referred to as the immediately releasable pool or the RRP, are primed for release and thought to be docked to the AZ (Fernandez-Busnadiego et al., 2010). RRP are the pool from which the vesicles are recruited by low-frequency stimulation (Igarashi and Watanabe, 2007). In addition to the morphological docking, a "priming" step is required to make vesicles fully release competent (Wasser and Kavalali, 2009). Direct association between the morphological and physiological pools are not defined however, the RRP feeds from both docked as well as non-docked vesicles and the recycling pool/also called the RP (in this thesis this term is preferred as the RRP is also included as part of a recycling pool), defined as vesicles that are capable of entering the exocytic/endocytic cycle under normal conditions corresponds to around 20% of the total vesicle pool. The RP is believed to be spatially distant from the release sites and replenishes the vesicles in the RRP that have exocytosed. The number of vesicles contained in the RRP is a critical parameter that regulates the probability of release, which is defined as the probability that a presynaptic AP can result in an exocytotic event (Wasser and Kavalali, 2009). Another pool of vesicles are thought to exist, who do not play a role in the synaptic transmission and are called 'silent' or 'reluctant' or 'resting' pool of vesicles. Their role is still to be elucidated (Fdez and Hilfiker, 2006; Wasser and Kavalali, 2009). This functional allocation of SVs into pools aims to account for the properties of evoked NT release during activity (Wasser and Kavalali, 2009).

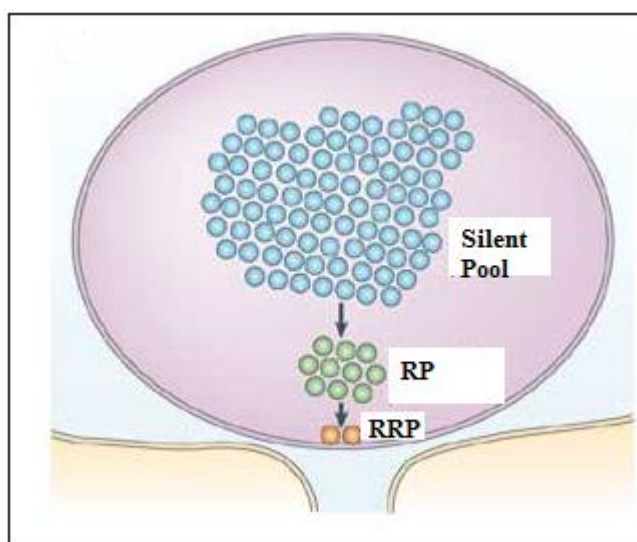


Figure D The classic three-pool model of synaptic vesicle: The silent/resting pool makes up ~80–90% of the total pool, and the recycling pool consisting of the RRP and the RP is significantly smaller (~15–20%). The RRP consists of a few vesicles (~1%) that seem to be docked and primed for release (Rizzoli and Betz, 2005).

1.4.1 Synaptic Vesicle cycle

The relationship between APs and release is regulated by intracellular signal transduction cascades, and can be drastically altered by the repeated use of a synapse (Fdez and Hilfiker, 2006). NT release involves specialized pathway of intracellular trafficking. SVs go through a cycle of processes before the NT is released (Details in Figure E) (Fernandez-Busnadiego et al., 2010). To serve the special needs of synaptic secretion, the SV cycle differs from many other intracellular trafficking pathways (Lodish et al., 2008). The major differences are in the high degree of regulation of intracellular trafficking in the nerve terminal, the exclusive targeting of SVs exocytosis to AZ, the high speed with which Ca^{2+} can trigger release, the tight coordinate regulation of all steps of the cycle and the restriction of SV exocytosis in any given nerve terminal to one SV at a time. In spite of these differences, however, the SV cycle has all of the basic characteristics of other intracellular trafficking pathways and shares the same fundamental mechanisms (Siegel et al., 1999). Details of this cycle explained in supplementary introduction.

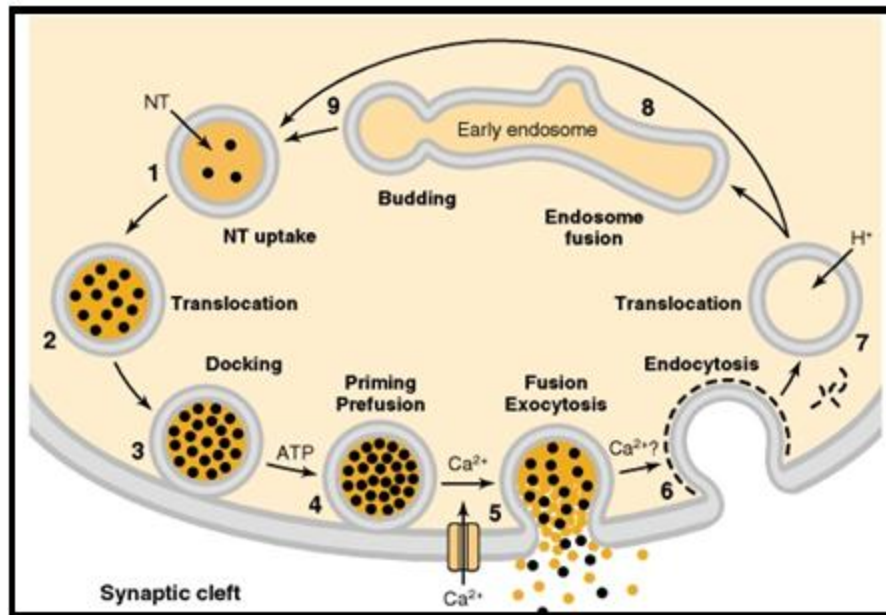


Figure E. The classical synaptic vesicle cycle (Full Fusion): The pathway of SVs in the nerve terminal is divided into 9 stages. **1:** Empty SVs take up NTs by active transport into their lumen using an electrochemical gradient that is established by a proton pump activity. **2:** Filled SVs are translocated to the AZ. **3:** SVs attach to the AZ of the presynaptic plasma membrane but, to no other component of the presynaptic PM, in a targeted reaction (docking). **4:** SVs are primed for fusion in order to be able to respond rapidly to a Ca²⁺ signal later. Priming probably is a complicated, multicomponent reaction that can be subdivided further into multiple steps. **5:** Ca²⁺ influx through voltage-gated channels triggers NT release in less than 1ms. Ca²⁺ stimulates completion of a partial fusion reaction initiated during priming. **6:** Empty SVs are coated by clathrin and associated proteins in preparation for endocytosis. Ca²⁺ may be involved in this process. **7:** Empty SVs shed their clathrin coat, acidify via proton pump activity and retranslocate into the backfield of the nerve terminal. **8:** SVs fuse with early endosomes as an intermediate sorting compartment to eliminate aged or mis-sorted proteins. **9:** SVs are freshly generated by budding from endosomes. Although some SVs may recycle via endosomes (steps 8 and 9), it is likely that the endosomal intermediate is not obligatory for recycling and that SVs can go directly from step 7 to step 1 (Siegel et al., 1999). (Further note that this cycle does not include the non-clathrin dependent Kiss-and-run recycling of SVs that is discussed in detail in this thesis.)

1.5 Modes of Exocytosis

The aqueous compartment inside a vesicle makes its first connection with the extracellular fluid through an intermediate structure termed the exocytotic fusion pore (Jackson and Chapman, 2006). Lipidic fusion pores are fusion intermediates with highly curved membrane, and deforming membranes into such an hourglass shape requires a substantial amount of energy. Distinctly, fusion pore composed of protein can connect two membranes without bending them (Zhang and Jackson, 2010). Ca^{2+} is one of the major factors that affects the opening and dilation of the fusion pore. In DCVs fusion pore openings and re-closures were regulated by Ca^{2+} levels selectively mediated by L-type Ca^{2+} channel entry (Xia et al., 2009). Ca^{2+} -triggered exocytosis membrane bending opposes fusion pore dilation rather than fusion pore formation. Ca^{2+} -triggered exocytosis begins with a proteinaceous fusion pore with less stressed membrane, and becomes lipidic as it dilates, bending membrane into a highly curved shape. A Ca^{2+} -induced shift of exocytic modes to kiss-and-run has been reported for endocrine cells. L-type Ca^{2+} channels exclusively mediate the Ca^{2+} influx that triggers DCV exocytosis in the soma of hippocampal neurons. Previous work indicated that L-type Ca^{2+} channels are localized to somatodendritic regions, where they mediate depolarization-induced entry of Ca^{2+} , which regulates gene transcription. The distribution of L-type Ca^{2+} channels might also underlie the differences in release probability and fusion pore kinetics observed above for DCVs in the cell body and neuritis (Xia et al., 2009). Therefore, the appearance of the SVs at rapid synapses is such that least energy is used and NTs are released with a greater speed.

1.5.1 Full Fusion

In the full fusion (FF) mechanism, the fusion pore expands such that the SV membrane collapses on the PM and fuses completely with it via an “ Ω ” figure to permit the absolute release of the NTs (Zhang et al., 2007; Lynch et al., 2008; Aoki et al., 2010). Thereafter, the excess of membrane is retrieved by endocytosis. In the classical model of SV recycling after neurotransmission, the membrane retrieval occurs at a distant location from AZ, and fusion of the internalized membrane with an endosome-like compartment (Alés et al., 1999). A major pathway for SV recycling is endocytosis by clathrin-coated vesicles (CVVs) (Henkel et al., 2001; Rizzoli and Jahn, 2007). It is mediated by complex

protein machinery that controls membrane lipid composition, cargo recognition, clathrin coat assembly, membrane invagination, membrane fission, and coat disassembly (Brose and Neher, 2009). It has been proposed that fast and slow endocytosis represent clathrin-independent (Shupliakov, 2009) and clathrin-dependent membrane retrieval, respectively (Figure F) (Lou et al., 2008b). Both are initiated by CaM and require GTP hydrolysis and dynamin (Wu et al., 2009).

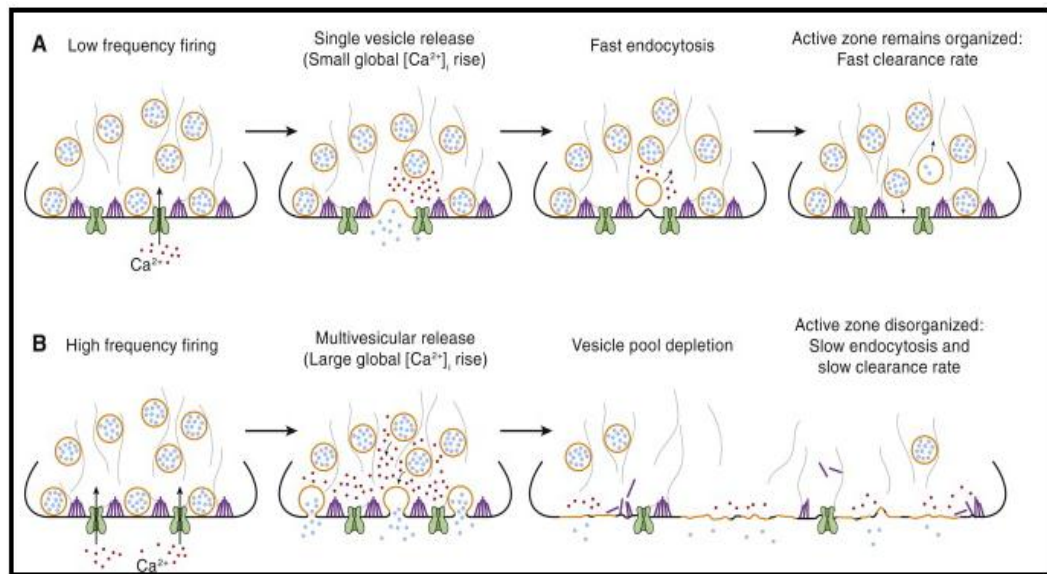


Figure F. Neurotransmitter Release at Active Zones under Low- and High-Stimulation Frequencies: (A) SVs (orange) in nerve terminals are tethered to a filamentous cytoskeleton. A small subsets of SVs are in close physical contact with the PM (depicted as three docked vesicles). Postsynaptic dense projections (purple) on the PM tether docked vesicles and Ca^{2+} channels (green). At low-stimulation frequencies, a single docked vesicle near a Ca^{2+} channel may undergo exocytosis and release NT into the synaptic cleft. The local Ca^{2+} -microdomain that triggers vesicle fusion dissipates quickly and global levels of $[\text{Ca}^{2+}]_i$ remain low. Fast endocytosis allows for the rapid clearance of the fused vesicular membrane from the AZ, so that empty docking sites may be quickly reused. The AZ remains organized and suffers minimal disruption. Vesicles retain their identity and recycle back to the RP.(B) At high firing frequencies several Ca^{2+} channels open at the AZ and multiple vesicles may fuse with the PM. Global $[\text{Ca}^{2+}]_i$ levels are now high, and more time and energy is needed to reduce $[\text{Ca}^{2+}]_i$ levels. The large increase in AZ area may temporarily disrupt the organization of the AZ and vesicle pool depletion may contribute to synaptic depression. In addition, as proposed by, slow endocytosis may be triggered by local Ca^{2+} -microdomains to promote recovery from short-term synaptic depression (Kim and von Gersdorff, 2009).

1.5.2 Kiss-and-run

An alternative model, the ‘kiss-and-run’ (K&R), proposes that the fusion pore (either a lipophilic pore or proteinaceous pore) either abruptly closes or the fusion pore dilates but subsequently recloses and the SVs may transiently fuse with the PM (Henkel et al., 2001; Richards, 2009), without losing its shape and possibly other aspects of their identity (Elhamdani et al., 2006; Zhang et al., 2007); thereby releasing their contents through a partially open fusion pore without merging with PM (Rizzoli and Jahn, 2007; Aoki et al., 2010) (Figure G). As the fusion pore of the SVs is resealed before complete dilation, this transient mode of vesicle exocytosis leads to the partial release of NTs depending on the size and diffusibility of the cargo (Lynch et al., 2008; Aoki et al., 2010). As glutamate is a small molecule, it can all be released during the transient opening of the fusion pore whilst other NTs such as NA need to de-complex from the vesicle core containing chromogranins and so not all may be released, if the fusion pore only has a finite lifetime. However, the molecular mechanism(s) that regulate and maintain the transient fusion pore are still unclear (Aoki et al., 2010). This type of mechanism is highly Ca^{2+} dependent and is thought to occur during fast endocytosis and is believed to be completely independent of clathrin-dependent endocytosis (Graham et al., 2002; Elhamdani et al., 2006; Lou et al., 2008b). Although K&R is accepted as a mode of transmitter release both in central neurons and neuroendocrine cells, the prevalence of this mechanism compared with FF is still in doubt (Elhamdani et al., 2006). The existence of both dynamin-dependent i.e clathrin-dependent and dynamin-independent pathways for fast K&R contributes to the determination of quantal size released by the nerve terminals (Graham et al., 2002). The K&R mechanism is thought to be occurring at the AZ, whilst clathrin-mediated endocytosis and bulk endocytosis occur at the periaxial zone surrounding the sites of release. Note it has been suggested by some that dynamin plays a role in the K&R mode and this thesis provides evidence for this.

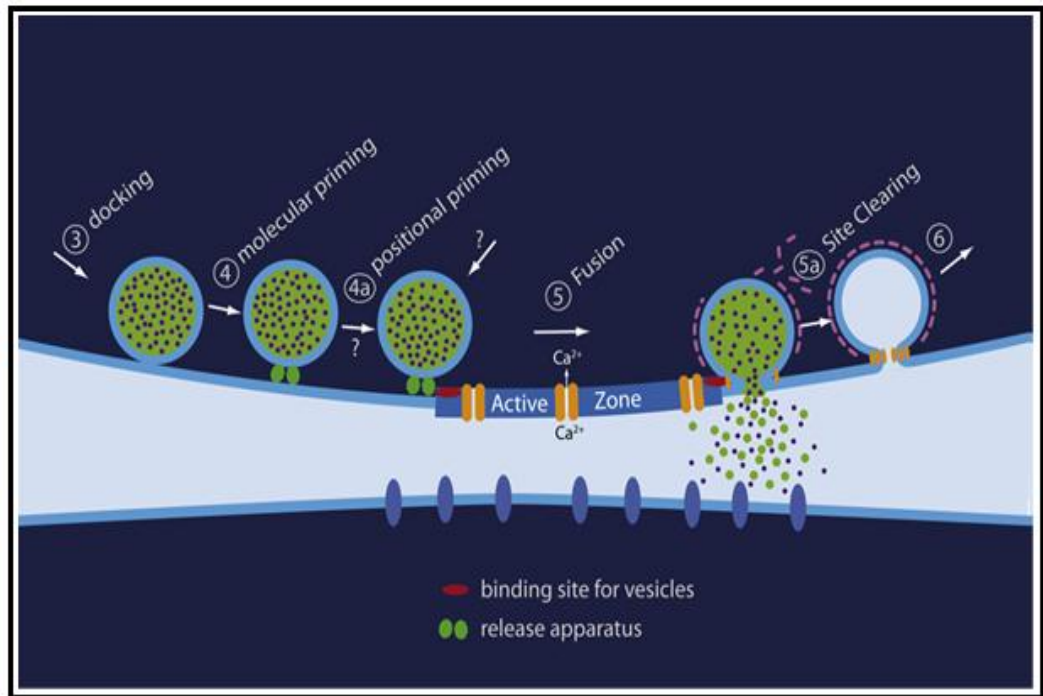


Figure G. Part of the ‘Vesicle Cycle’ of Exo and Endocytosis: For simplicity, the case of K&R exo-endocytosis is depicted on the right side. However, the argument about rate limitation of the site-clearing step 5a would also hold for classical endocytosis, if it is assumed that the interaction between an AZ component and some component of the vesicle or release machinery has to be reversed before another vesicle can dock (Neher and Sakaba, 2008).

Ca^{2+} may modulate the mode of exocytosis–endocytosis by regulating the rate at which fusion pores re-close following fusion (Lynch et al., 2008). At low Ca^{2+} concentrations, vesicles incorporate completely into the PM, whilst with increase in Ca^{2+} accumulation from 10 to 200 μM , increases the probability and rate of re-closure of the fusion pore, leading preferentially to K&R events (Alés et al., 1999). Additionally, the phosphorylation of certain proteins regulates the mode of exocytosis by affecting the conductance and stability of the pore (Henkel et al., 2001). Blocking rapid endocytosis that normally terminates transient fusion events also promotes FF events. Thus, $[\text{Ca}^{2+}]_i$ controls the transition between transient and FF, each of which is coupled to different modes of endocytosis (Elhamdani et al., 2006).

Recent experiments using styryl-FM fluorescent dyes (explained in detail later) have provided evidence that SVs can be internalized much faster than was previously thought, in the order of few seconds, and that SVs are recycled

without passing through an endosomal compartment (Alés et al., 1999). Evidence is provided that fusion pore mediated release (K&R) gives rise to different concentration profiles of glutamate in the synaptic cleft (Rizzoli and Jahn, 2007). The result of this is very weak activation of alpha-amino-3- hydroxy-5-methyl-4-isoxazolepropionic acid (AMPA) receptors, which gives rise to a predominant receptor desensitization, while (under conditions where the magnesium blockade is lifted) the NMDA receptors are activated at levels equivalent to those elicited by FF (Richards, 2009).

1.6 Process of Endocytosis

After exocytosis, the granular membrane has to be recycled in order to avoid infinite growth of the PM (Henkel et al., 2001). Central nerve terminals have a limited supply of SVs, which must be quickly and reliably recycled to maintain NT release, this is particularly important during high stimulation period (Cheung et al., 2010). In order to sustain high-frequency NT release, SVs must be recaptured rapidly with high fidelity, for regenerating release-competent vesicles, such that the newly exocytosed lipid constituents are quickly removed to prevent expansion of the presynaptic membrane (Zhu et al., 2009).

There are three known mechanisms of SVs endocytosis: (1) clathrin-dependent endocytosis after full collapse of the fusing vesicle (which a principle mechanism of exocytosis) (Elhamdani et al., 2006), (2) bulk endocytosis via large membrane invaginations, and (3) K&R fusion and retrieval, during which only a transient fusion pore is formed (Brose and Neher, 2009) (Figure H). Experiments have demonstrated that K&R is the major mechanism of vesicle exocytosis under moderate stimulation conditions; sustained stimulation favours the incidence of FF events at the expense of transient events. Stimulation frequency controls the open time and the conductance of the fusion pore; high $[Ca^{2+}]_i$ favours FF, not K&R. Rapid endocytosis is associated with K&R events. When RE is abrogated, FF takes place and vesicles are recovered by SE, a process that was previously shown to be similar to CCVs endocytosis (Elhamdani et al., 2006). In the results, it is shown that these statements are not exactly correct as they do not take into account the different pools of SVs and these statements are re-worded in the discussion.

Endocytosis allows the internalization of these vesicles to undergo another round of secretion. A characteristic property of presynaptic terminals is their high endocytic capacity. This property enables synapses to function reliably even during high frequency axonal firing (Lou et al., 2008b). It is believed that exocytosis and endocytosis are coupled (Richards, 2009). It is, however, uncertain whether exocytosis and endocytosis are tightly coupled, such that secretory vesicles fuse only transiently with the PM before being internalized (the K&R mechanism), or whether endocytosis occurs by an independent process following complete incorporation of the SV into the PM (FF) (Alés et al., 1999; Zhu et al., 2009).

Bulk endocytosis is the process in which nerve terminals retrieve large amounts of SV membrane during episodes of strong stimulation intensity. Bulk endocytosis invaginates large areas of presynaptic membrane from which SVs can be generated over time. These large endosomes can remain attached to the PM for a considerable amount of time, and these allow SVs to bud from them (Figure H). Alternatively, the large endosome enters into the terminal where budding of SV subsequently occurs. The process is rapidly activated and is thought to be Ca^{2+} dependent in a similar manner to SVs exocytosis (Clayton et al., 2007). Additionally, different forms of bulk membrane retrieval can be recruited in central synapses during intense stimulation (Ales et al., 1999). It has been suggested that clathrin-mediated endocytosis (CME) is dominant during mild neuronal activity, and activity dependent bulk endocytosis (ADBE) is dominant during intense neuronal activity. ADBE is a fast, high capacity SV retrieval mode that invaginates large regions of PM, creating bulk endosomes from which SVs can bud (Cheung et al., 2010).

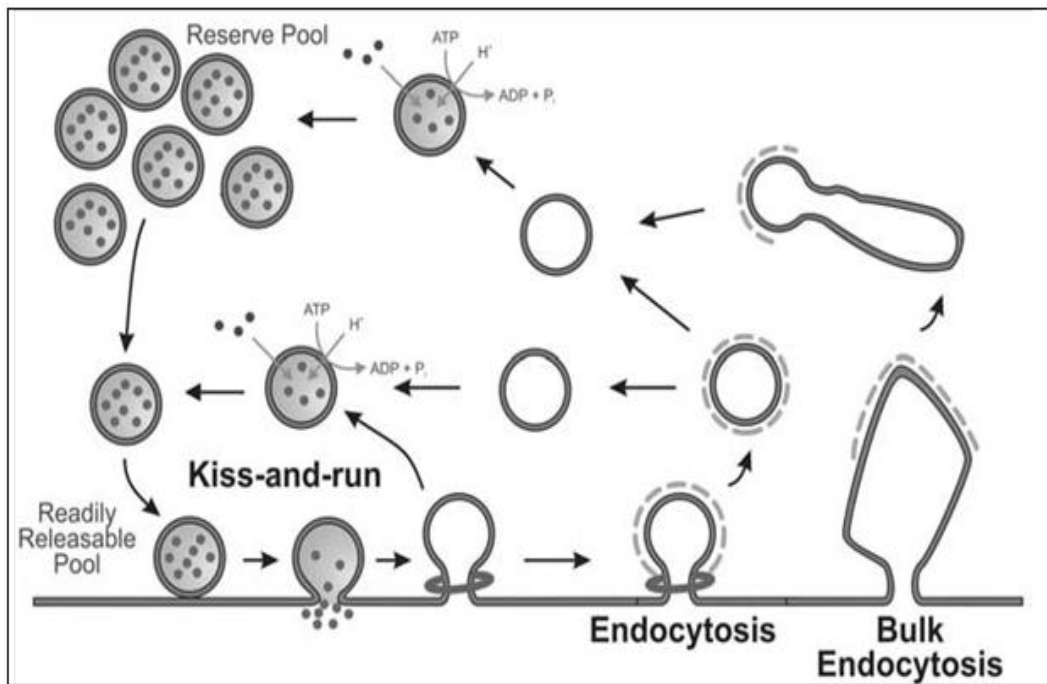


Figure H. Multiple SV retrieval pathways in central nerve terminals: Three different mechanisms are proposed to retrieve SV membrane after exocytosis in nerve terminals. K&R is a mechanism where the SV never fully fuses with the PM and is retrieved intact. Classical clathrin-dependent endocytosis involves the invagination of a single clathrin-coated bud from the PM before its fission and uncoating. Bulk endocytosis is the process where large areas of nerve terminal membrane are invaginated to produce endosomes from which SVs can bud (Clayton et al., 2007).

1.7 Proteins that participate in the process of exocytosis and endocytosis

1.7.1 Synapsin

Existence of synapsins is confirmed in all vertebrates and organisms with a nervous system. Synapsins are a multigene family of neuron-specific phosphoproteins and these represent the most abundant SV proteins (Fdez and Hilfiker, 2006). They are encoded by three distinct genes; synapsin I, II and III, and alternative splicing generates further variants containing distinct C-termini. Most neuronal synapses express synapsins I and II whereas; the levels of synapsin III are less abundant. Highly systemic arrangements of cytoskeletal fibers in the axon terminals help localize SVs in the AZ (Figure I step 9).

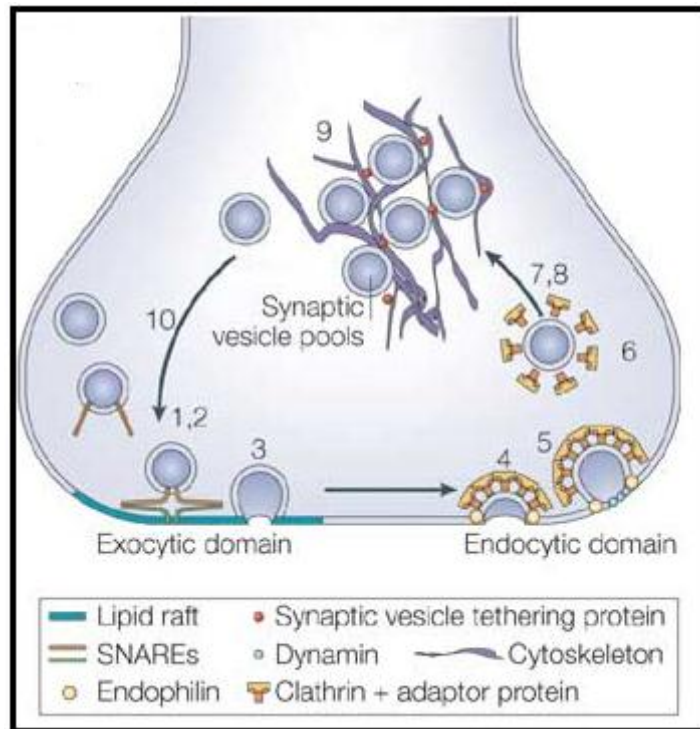


Figure I: Presynaptic terminal depicting the main stages of the SV cycle, characterized by complete fusion and clathrin-mediated endocytosis: Ten stages can be defined: (1) SV docking to the PM, (2) vesicle priming for fusion, (3) Ca^{2+} -triggered vesicle fusion, (4) clathrin-mediated budding and SV formation, (5) fission of a new vesicle, (6) clathrin uncoating, (7) NT loading, (8) vesicle trafficking, (9) **tethering in RP** and (10) mobilization and targeting to the PM release site. Cytoskeletal and tethering proteins interact with vesicle lipids to traffic and sequester SVs (Rohrbough and Broadie, 2005).

The SVs are linked to each other by synapsins that bind the fibrous proteins actin and spectrin, and these proteins are associated with the cytosolic surface of all SV membrane. Additionally, synapsin filaments radiate from the PM and attach to vesicle-associated synapsin. These interactions may allow the SVs to face in the right direction, i.e. towards the PM. Synapsins are preferentially located near the RPs at the ultrastructural level i.e near the vicinity of the AZ (Figure J). Thus, synapsin play a crucial role in recruiting the SVs to the AZ. Such a role is supported by the observation that, disruption of synapsin function leads to a depletion of the RP of vesicles and an increase in synaptic depression (Fdez and Hilfiker, 2006). Mice lacking synapsin, although viable, are prone to seizures during a train of stimulations.

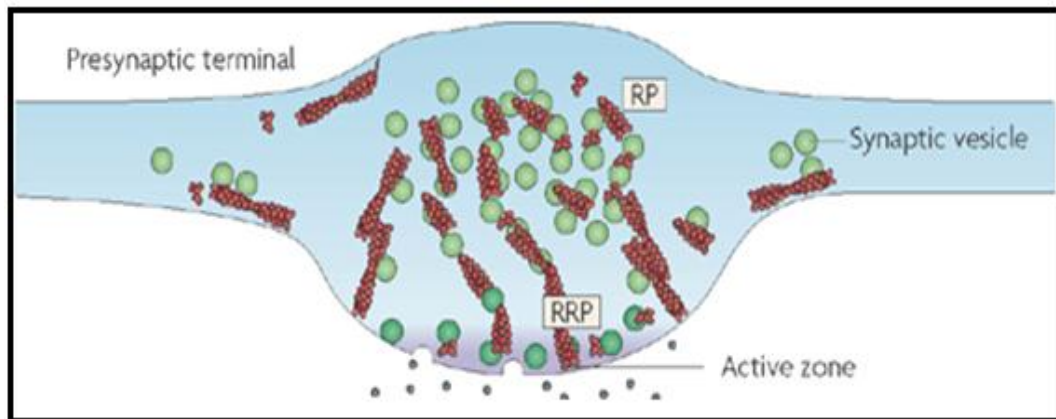


Figure J: Synapsins located near the reserve pools at the ultrastructural level i.e near the vicinity of the AZ: At the presynaptic terminal, some SVs (those belonging to the RRP (dark green) are found docked at the AZ, where they undergo exocytosis to release NTs. Numerous vesicles that presumably belong to the RP(light green) are located centrally, where they are interlinked to each other by short actin filaments (shown in red) and by synapsin (not shown). The subgroups are linked to longer filaments that extend from the PM, some of them from the AZ(Leenders and Sheng, 2005).

It appears that phosphorylation of synapsins is responsible for an important functional regulatory switch involved in vesicle mobilization. Synapsins are dependent on phosphorylation by a variety of protein kinases. All synapsins are substrates for phosphorylation by cAMP dependent protein kinase A (PKA) and Ca^{2+} /calmodulin-dependent protein kinase II (CaMKII) (Shupliakov, 2009). Thus, a rise in cytosolic Ca^{2+} triggers their phosphorylation. Additionally, synapsins are differential targets for phosphorylation by CaMKII, with synapsin I (but not synapsin II being regulated). Subtle changes in the biochemical properties of synapsins are observed due to phosphorylation. Phosphorylation of synapsins by PKA/CaMKII drastically decreases their affinity for SVs (Fdez and Hilfiker, 2006). This appears to cause the release of SVs from the cytoskeleton, thereby increasing the number of vesicles available for fusion. It is generally believed that synapsins and actin are largely responsible for the clustering of the distal pool of vesicles not associated with the scaffolding proteins of the AZ. In addition, synapsin migrates to the periaxial zone upon stimulation and plays a role in promoting actin filament formation at the periaxial zone of the synapse, most probably aiding in the proper organization in order to promote efficient vesicle recycling (Shupliakov, 2009).

By altering actin dynamics, activity that elicits synaptic plasticity could remodel pre- and postsynaptic actin scaffold, the organization of SV pools or the organization of the postsynaptic receptors that are supported by the scaffold. In addition, altered actin dynamics could modulate steps of the SV cycle and postsynaptic receptor activity or traffic, which are directly regulated by actin turnover. Overall, these changes would affect the efficacy of synaptic transmission and, thus, synaptic plasticity (Cingolani and Goda, 2008).

1.7.2 Clathrin

The composition of lipids and lipid modifications play a critical role in various cellular internalization mechanisms, including SV endocytosis (Shupliakov, 2009). In a typical neuron, there is plethora of SVs, many with a protein coat on the cytosolic surface and their membrane, which are formed by reversible polymerization of an explicit set of protein subunits under precise regulated conditions. This coat subunit protein polymerizes around the cytosolic face of a budding vesicle during the vesicle formation. This is crucial, as these coats help the vesicle to pinch off from the parent organelle. Clathrin coat is responsible for transporting the SVs from the PM and the *trans*-Golgi network to late endosomes. In this process, some coat-protein subunits or associated adapter proteins (AdPs) select which membrane and soluble proteins will enter the transport vesicles as cargo proteins. These cargo proteins contain short signal sequences, which direct them to the precise type of transport vesicle (Siegel et al., 1999). Thirdly, the final pinching off requires the GTP-binding protein, dynamin that regulates the rate of the vesicle formation (Min et al., 2007).

The clathrin coat and its AdPs enable internalization of specific cargo proteins or SVs. Once internalized, coat rapidly disassembles, thereby allowing the clathrin to recycle while the vesicle is transported to a variety of locations. After the formation of the bud, only a narrow membrane neck remains, which connects the SVs to the PM. The separation of this is carried out by large GTPase dynamin. It overcomes the energy for bilayer fusion barrier and membrane separation (Lundmark and Carlsson, 2009). Two other proteins have been identified as essential for the formation of CCVs: amphiphysin, which binds to dynamin and assembly particles (Hosoi et al., 2009), and synaptojanin, which binds to

amphiphysin and dynamin. Amphiphysin interacts with dynamin and links clathrin-coats to dynamin (Lu et al., 2009). Amphiphysin is believed to recruit dynamin to the neck of budding vesicles but the actual function of these two proteins to pinch off the SVs with dynamin is still to be elucidated. Additionally, Ca^{2+} and amphiphysin may modulate the release of vesicle contents by controlling the duration of the open “ Ω ” shape rather than by selecting between K&R and FF modes of fusion (Llobet et al., 2008). Another protein that plays an important role in sorting is nexin 9 (SNX9). It strongly binds to dynamin, stabilizes the assembled dynamin oligomer and is partially responsible for the recruitment of GTPase to sites of endocytosis. SNX9 stimulates GTPase activity of dynamin, facilitates the scission reaction, and destabilizes the membrane bilayer (Lundmark and Carlsson, 2009).

CCV-based endocytosis (including receptor-mediated endocytosis) depends on intracellular K^+ (Artalejo et al., 2002). The CCVs are known to be stable at the pH and ionic composition of the cell cytosol. The SVs lose their clathrin coat and the assembly particles after their formation. Cytosolic Hsc70, a chaperone protein is believed to catalyze depolymerization of the clathrin coat into triskelions. These triskelions can then be recycled and reused in the formation of additional pits and vesicles. The formation and the depolymerization of the CCVs are highly regulated, as both these processes occur concurrently (Lodish et al., 2008).

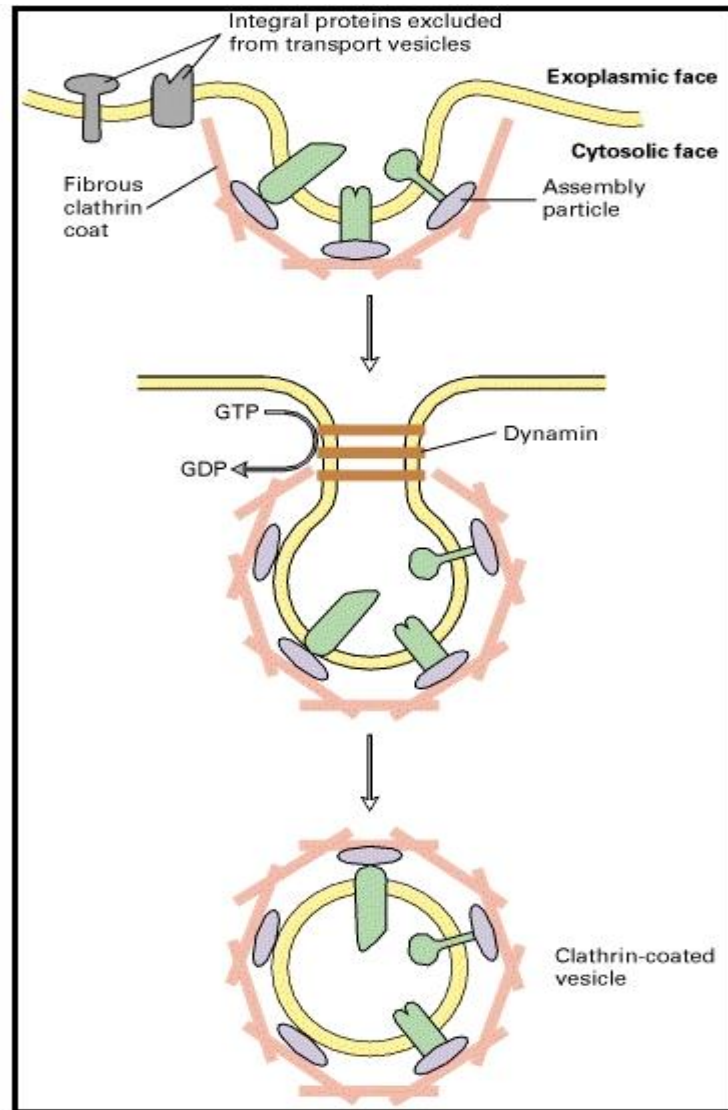


Figure K. Model for the formation of a clathrin-coated pit and the selective incorporation of integral membrane proteins into clathrin-coated vesicles: The cytosolic domains of certain membrane proteins bind specifically to assembly particles that, in turn, bind to clathrin as it polymerizes spontaneously over a region of membrane. Proteins that do not bind to assembly particles are excluded from these vesicles. Dynamin then polymerizes over the neck of the pit; regulated by dynamin-catalyzed hydrolysis of GTP, the neck pinches off, forming a clathrin-coated vesicle (Lodish et al., 2008).

1.7.3 Dynamin

Dynamins (approximately 900-amino-acid cytosolic protein) are a family of proteins that are involved in vesicular fission reactions at various membranes (Artalejo et al., 2002) and in *Drosophila melanogaster*, these proteins are encoded by *shibire* (Kramer and Kavalali, 2008). Dynamin has been implicated in both rapid endocytosis and receptor-mediated endocytosis (Artalejo et al., 2002). It plays a crucial role in the complete formation of clathrin-coated pit, but its role in bulk endocytosis is controversial (Lou et al., 2008b).

There are two types of dynamin: dynamin 2, which is ubiquitously expressed, and dynamin 1 that is brain-specific (Artalejo et al., 2002). Expression of dynamin 1 is essential to allow slow, clathrin-mediated endocytosis to function efficiently over wide range of activity (Lou et al., 2008b; Hosoi et al., 2009). It enables the presynapse to accommodate high levels of slow endocytosis in response to a strong endocytotic load (Lou et al., 2008b). Dynamin1-deficient cortical neurons display a large attenuation in evoked responses with no change in the frequency of spontaneous events (Fdez et al., 2008). Dynamin2 may mostly control receptor-mediated endocytosis in all somatic cells, as it is ubiquitously distributed and this form of endocytosis is universal. Whereas, dynamin1 has a much more restricted expression and is especially concentrated at nerve terminals, where it might participate in rapid endocytotic events governing rapid SV recycling (Artalejo et al., 2002).

Dynamin 1 assembles and polymerizes around the neck of an invaginated pit (Bashkirov et al., 2008), like a spring (Robinson, 2007). As dynamin 1 expands and twists, it pinches off the membrane from the rest of the PM and this can reform the SVs (Robinson, 2007). It binds and hydrolyses GTP to regulate contraction of the polymeric dynamin until the vesicle pinches off (Kramer and Kavalali, 2008). Hydrolysis of dynamin GTP by the GTPase activity is essential for the pinching of the fused CCVs (Fdez et al., 2008). It is thought that, a concerted nucleotide dependent conformational change such as a GTP binding dependent constriction, hydrolysis-dependent longitudinal expansion of a pre-assembled dynamin scaffold generates the force required to separate membranes (Bashkirov et al., 2008; Pucadyil and Schmid, 2008). The cellular expression of

mutant dynamins that cannot bind GTP blocks the formation of CCVs, resulting in accumulation of long-necked pits covered with polymerized dynamin. Dynamin is designed to selectively target highly curved membrane necks and probe their mechanical stability by repetitive squeezing (Bashkirov et al., 2008). Dynamin 1 normally becomes activated during the arrival of AP, when it becomes dephosphorylated and is inhibited immediately after stimulation by re-phosphorylation (Robinson, 2007). Dynamin I has two major interactions: one which is phosphorylation-independent (i.e. will occur regardless of stimulation intensity) and is essential for clathrin-dependent endocytosis (amphiphysin), and the other which is phosphorylation-dependent (i.e. will occur only during strong stimulation) and is therefore implicated in bulk endocytosis (syndapin). The phosphorylation-dependent recruitment of syndapin by the activity-dependent dephosphorylation of dynamin I may be the key molecular event in bulk endocytosis, a process which is important to nerve terminal function (Clayton et al., 2007). It should be noted that dynamin is required for rapid replenishment of the RRP of SVs (Lu et al., 2009) and has been implicated in regulating K&R exocytosis and this is the subject of some of this thesis.

Dynasore is a small membrane-permeable compound that functions as a non-competitive and specific inhibitor of dynamin 1 and dynamin 2 GTPase activity *in vitro* and blocks endocytic functions previously shown to require dynamin (Refer Figure L) (Thompson and McNiven, 2006; Kramer and Kavalali, 2008; Xu et al., 2008; Hosoi et al., 2009; Chung et al., 2010). Dynasore provides a means to rapidly block the formation of CCVs. It blocks SV endocytosis completely, without an immediate effect on exocytosis; thereby suggesting an essential role of dynamin in all forms of compensatory SV endocytosis, including K&R events (Newton et al., 2006). Clathrin-coated pits were blocked at two stages of vesicle formation, an early phase representing shallow pits and a later phase that seemed to represent late-stage vesicles that were unable to undergo the final scission (Thompson and McNiven, 2006). Dynasore may also act at a downstream step involving dynamin activity and subsequently provide constitutive inactivation of dynamin across the endocytic cycle (Lu et al., 2009). It inhibits PI(4,5)P₂-stimulated dynamin 1 activity in a dose-dependent manner (Chung et al., 2010). In the study by Newton et al, (2006) it was concluded that dynasore did not have

any effect on exocytosis, suggesting that acute and rapid block of dynamin function does not have an immediate effect on SV exocytosis. This observation also rules out any effect of dynasore on AP propagation, Ca^{2+} channel function, or exocytic machinery (Newton et al., 2006).

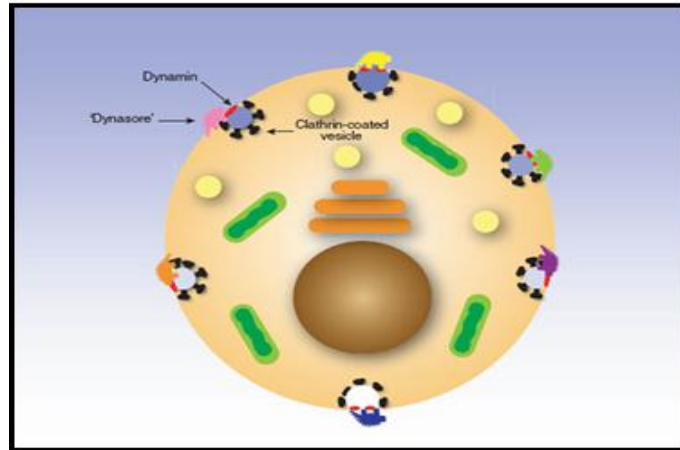


Figure L. Dynasore-reversible inhibitor of dynamin: Clathrin-coated pits (black) trapped at the PM as a result of inhibition of dynamin (red) by dynasore (colored dinosaurs) are shown (arrows highlight an example). Also shown are endosomes (yellow), mitochondria (green), the Golgi (orange) and the nucleus (brown) (Thompson and McNiven, 2006). **1.8 Soluble N-Ethyl-maleimide-sensitive factor (NSF) attachment protein receptors (SNAREs)**

Exocytosis involves the fusion of secretory vesicles with the PM and is governed by complex protein machinery that includes SNARE proteins as central components (McEwen and Kaplan, 2008; Rizo, 2010). Priming is the process that occurs after docking and before SVs fusion (Fdez et al., 2008). SV fusion is mediated by the formation of SNARE (SNAP receptor, where SNAP is defined as soluble NSF attachment protein) complexes (Vrljic et al., 2010) from the SNARE proteins synaptobrevin/VAMP, syntaxin-1 and SNAP-25 (Verona et al., 2000; Fdez and Hilfiker, 2006; McEwen and Kaplan, 2008; Darios et al., 2009; Hosoi et al., 2009). There is specific v-SNARE for specific types of vesicles, which direct them to their respective membrane fusion partner (Jackson and Chapman, 2006). Similarly, every cell's target membrane has t-SNARE as an integral membrane proteins and SNAP25, a ubiquitous fusion protein. The t-SNARE on the target membrane and SNAP25 work together and specifically bind a particular type of

v-SNARE on the cargo vesicle to form the core complex (Vrljic et al., 2010; Xue et al., 2010). t-SNARE complex would recruit synaptotagmins and change the conformation of synaptotagmin with Ca^{2+} -binding loops of both C2 domains positioned in the vicinity of the same membrane (Refer Figure M) (Vrljic et al., 2010). All eukaryotic cells express several related v-SNARE and t-SNARE proteins, thus permitting each type of transport vesicle to be targeted correctly (Igarashi and Watanabe, 2007).

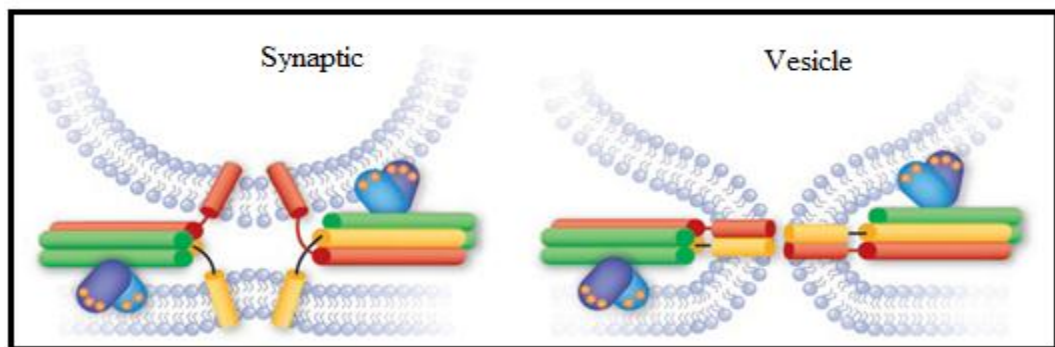


Figure M. Diagram summarizing the main features of the model of how synaptotagmins and SNAREs cooperate in Ca^{2+} -dependent membrane fusion: Syntaxin is shown in yellow (without its N-terminal region), synaptobrevin in red and SNAP-25 in green. The synaptotagmin C2A domain is shown in purple and the C2B domain in blue, with bound Ca^{2+} ions shown as orange circles. The relative orientation between the two C2 domains is meant to reflect the orientation observed in a synaptotagmin crystal structure, with their Ca^{2+} -binding loops located on the same side so that they can bind to the same membrane. The synaptotagmin–SNARE complex interaction is based on the smFRET model built for the synaptotagmin-1–SNARE complex⁵ and involves the bottom side of the C2B domain. The two membranes may be hemifused before Ca^{2+} influx, but this feature is not essential. As an alternative, the model shown here assumes that there is no hemifusion before Ca^{2+} influx. The left panel represents the two membranes before fusion, with some bending in the middle that is induced by the mechanical action of the assembled SNARE complex. This effect, together with perturbations caused by binding of synaptotagmin to one or both of the membranes, would lead to membrane fusion (Rizo, 2010).

In neurons, the process of fusion is tightly regulated by Ca^{2+} concentration, but SNARE complex assembly does not have any Ca^{2+} sensitivity. Other proteins interacting with the core of the SNARE complex, such as VGCCs and synaptotagmin (a putative Ca^{2+} sensor), are considered crucial for the Ca^{2+}

dependence of release and also molecular mediators of synaptic plasticity (Verona et al., 2000; Xue et al., 2009; Rizo, 2010; Vrljic et al., 2010).

The Ca^{2+} -sensing proteins, the synaptotagmins, are a large family of SV proteins that, among other functions, act as Ca^{2+} regulators of exocytosis. They have a hierarchy of Ca^{2+} affinities (Johnson et al., 2010). Synaptotagmin, is believed to be a key Ca^{2+} sensor protein that triggers the SVs exocytosis (Hosoi et al., 2009; Opazo et al., 2010) and is a vesicular protein (Lynch et al., 2008). Ca^{2+} sensing triggers for vesicle fusion are synaptotagmins I and II, which are found throughout the CNS and visual system (Johnson et al., 2010).

Synaptotagmins are comprised of a short intraluminal or extracellular sequence, a single transmembrane helix (N-terminal transmembrane domain) that anchors to the protein to the SV, a linker and two Ca^{2+} -binding domains termed C2A and C2B (Jackson, 2007; McMahon et al., 2010; Opazo et al., 2010; Vrljic et al., 2010). The C2A domain may bind the vesicle/granule membrane, while the C2B domain may bind the PM (McMahon et al., 2010). These two C2 domains can bind to phospholipids and Ca^{2+} (Igarashi and Watanabe, 2007; Lee et al., 2010). Severe loss of Ca^{2+} dependent synchronous release is observed during the genetic deletion of synaptotagmin. In response to Ca^{2+} binding, synaptotagmin may promote the completion of SNARE-complex, and this brings the SVs and the PM into close proximity and that may promote the two lipid bilayers (Refer Figure N). This is achieved by inducing a high positive curvature in target membranes following C2 domain membrane insertion (Lee et al., 2010). The association of VGCC proteins with synaptotagmin and t-SNARE proteins has been suggested to be important for the formation of SNARE complexes at AZ (Zhu et al., 2010).

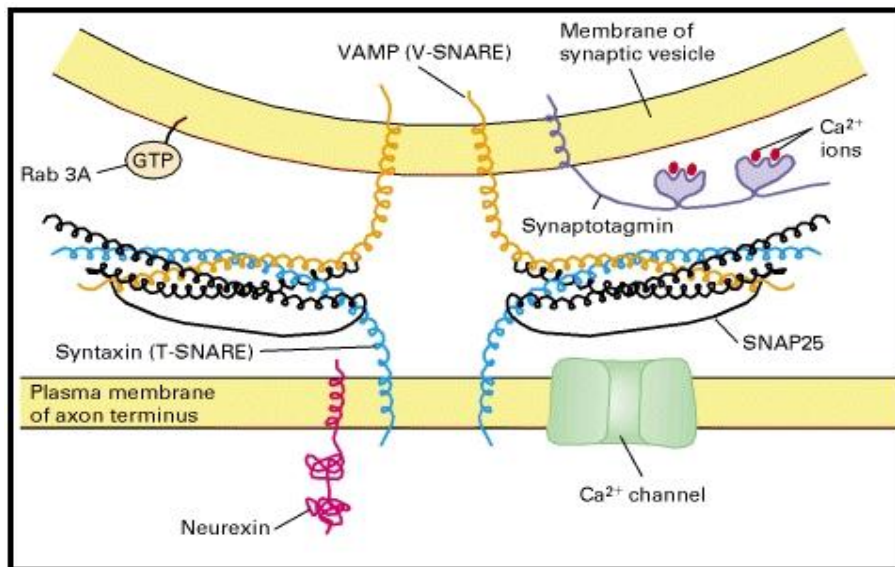


Figure N. Synaptic vesicle and plasma membrane proteins important for vesicle docking and fusion: Interaction of the t-SNAREs syntaxin and SNAP25 with the v-SNARE VAMP is aided by Rab3A. Neurexin, Ca^{2+} channels, and other PM proteins localized to the synaptic region may also interact with SV proteins. The vesicle protein synaptotagmin is the major Ca^{2+} sensor that triggers vesicle fusion (Siegel et al., 1999).

1.8.1 Role of SNAREs and SNAPs

Various biochemical studies have established that v-SNARE, t-SNARE, and SNAP25 are sufficient to mediate vesicle fusion. *Vesicle-associated membrane protein* (VAMP)/synaptobrevin on SVs is an essential component for exocytosis (Igarashi and Watanabe, 2007; Kim and von Gersdorff, 2009). During the exocytosis of the SVs, the v-SNARE VAMP/synaptobrevin is transiently incorporated into the PM (Igarashi and Watanabe, 2007). VAMP/synaptobrevin in SVs does not readily react with syntaxin or SNAP-25 (Darios et al., 2009). *Syntaxin* the t-SNAREs, an integral membrane protein, and SNAP-25, which is attached to the PM by a hydrophobic lipid anchor, palmitoylated cysteines (Fdez et al., 2008).

Repeating heptad sequence is present in the cytosolic regions of these four SNAREs i.e. one from VAMP/synaptobrevin, one from syntaxin, and two from SNAP-25; which allows them to form four α helices (Fdez and Hilfiker, 2006; Xue et al., 2010). These helices coil around each other to form a four-helix bundle. It is believed that the four-helix bundle helps the SVs and the PM to come

into the proximity of the embedded transmembrane domains of the VAMP/SYNAPTOBREVIN and syntaxin, thereby mediating fusion of SVs into the PM (Ohyama et al., 2002). SNARE complexes are thought to assemble by “zippering” in an N- to C-terminal direction, thereby forcing their resident membranes closely together (Fdez et al., 2008).

After the fusion of the SVs occurs, the SNARE complexes need to dissociate in order for them to be available for additional fusion events. As the SNAREs are highly stable molecules, additional proteins and energy are required for its dissociation. One of the cytosolic proteins required is NSF, a tetramer of identical subunits that binds and hydrolyzes ATP (Sudhof and Malenka, 2008). Other proteins, called α -, β -, and γ -SNAPs (*soluble NSF attachment proteins*) are required for NSF to link to the SNARE proteins. It is now the consensus that NSF and α -SNAP are not necessary for the vesicle fusion but are required for the regeneration of free SNARE proteins following the conversion of a trans-SNARE complex (where v and t-SNAREs are in distinct membranes) to a cis-SNARE complex (where v- and t-SNAREs are in the same membrane) (Refer Figure O). SNARE proteins not only provide sufficient energy to initiate exocytosis, but also to accelerate merger of membranes (Kesavan et al., 2007).

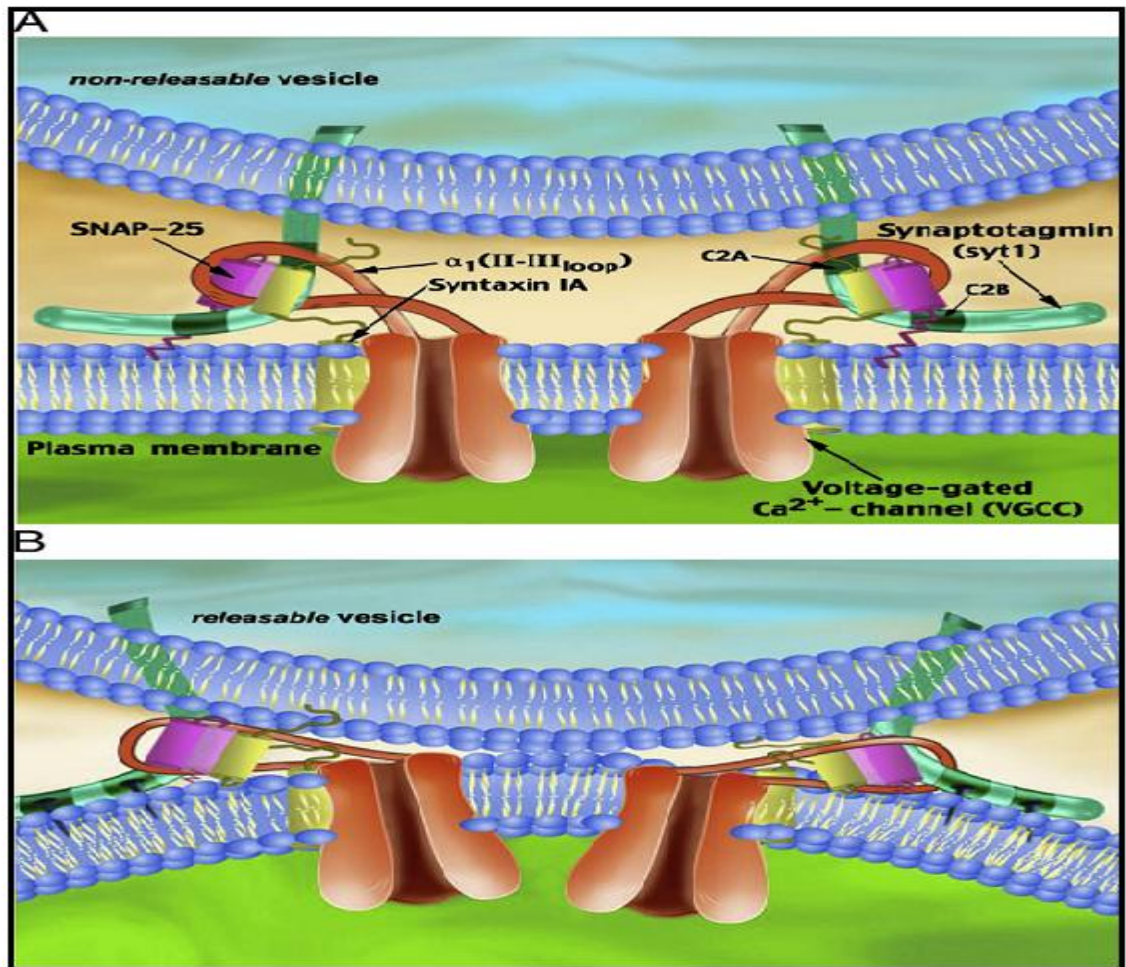


Figure O. Schematic model depicting the organization of the non-releasable and releasable vesicles vis-à-vis the voltage-gated calcium channel, syntaxin 1A, SNAP-25, and synaptotagmin: (A) At rest, Ca^{2+} -independent interactions between the calcium channel with the SNARE binary-complexes (syntaxin 1A, SNAP-25) and synaptotagmin (syt1), assembled into the heteroprotein excitosome complex, hold the vesicles close to the channel. These vesicles cannot fuse in part, due to the repulsion between the negative charges of the syt1 C2 Ca^{2+} -binding site and the negatively charged phospholipids, which prevent syt1's conserved basic residues from interacting with the membrane. Prior to Ca^{2+} binding to syt1 insertion at the membrane there would be no buckling of the vesicle to the membrane. (B) The final structural configuration of the excitosome, prior to the fusion event, is accomplished when Ca^{2+} is bound to the syt1 C2 domains. Subsequent to a transient elevation in the $[\text{Ca}^{2+}]_i$ concentration, the Ca^{2+} binding loops of the C2B domain rapidly insert into the target membrane, pinning the vesicle at the bilayer (black pins). Consequently, the Ca^{2+} -dependent changes in syt1 orientation vis-à-vis the membrane, modify the interplay within the excitosome proteins and transform the vesicle to a releasable state. As depicted, the PM is bent towards the vesicle membrane due to concerted actions of multiple C2B domains that could serve to bring the two membranes

into closer proximity. The excitosome complex is now associated with a releasable vesicle that underwent significant changes at the membrane, including minimizing the repulsive hydration force, and significantly lowering the energy barrier for bilayer merger (Atlas, 2010).

For a synapse to function, the proper balance of proteins must localize to the presynaptic release machinery, and the protein composition at the release site is a likely determinant of its synaptic efficacy. While the general properties of synapses formed by a single axon are similar, the release probability of such synapses can vary dramatically. This heterogeneity of presynaptic terminals is possibly due to mechanisms that control synapse specific plasticity and may represent one aspect of the molecular basis of learning and memory (Graf et al., 2009).

1.9 Secondary messengers

1.9.1 Calcium/calmodulin dependent kinase

Rise in the $[Ca^{2+}]_i$ ions induces complex formation with calmodulin (CaM: a cytosolic Ca^{2+} binding protein) and this can help regulate SV fusion. The activity of PM ATPases is regulated by CaM (Pang et al., 2010). CaM is composed of 148 conserved amino acids and has four Ca^{2+} -binding sites (Igarashi and Watanabe, 2007). Small changes in the level of $[Ca^{2+}]_i$ give rise to a variety of cellular responses (Ohyama et al., 2002). When the level of Ca^{2+} increases above 0.1-0.2 μ M during stimulation it binds to the four sites on CaM, which results in a complex that interacts and alters the activity of various enzymes and other proteins (Lodish et al., 2008). CaM is the Ca^{2+} sensor for Ca^{2+} -triggered endocytosis. Data by Wu et al., (2009) suggests that Ca^{2+} /binding with CaM initiates endocytosis. CaM forms a physical complex with VGCCs and its N and C lobes may sense different Ca^{2+} concentrations, allowing CaM to mediate multiple forms of endocytosis. Additionally, fused vesicle membrane is the substrate used by Ca^{2+} /CaM to initiate endocytosis (Wu et al., 2009).

CaMKII is one of the most abundant proteins in neurons, expressed both in the pre- and postsynaptic density (Sunyer et al., 2008). CaMKII has α , β , γ , and δ , isoforms. The α and β isoforms are dominant in neurons, whereas the γ and δ

isoforms are distributed among various tissues. Both α and β isoforms of CaMKII bind syntaxin *in vitro*. CaMKII α is mainly expressed in glutamatergic neurons (Pang et al., 2010).

Neuronal CaMKII regulates important neuronal functions, including NT synthesis, NT release, modulation of ion channel activity, cellular transport, cell morphology and neurite extension, synaptic plasticity, learning and memory, and gene expression (Yamauchi, 2005). Stimulation of CaMKII, which endogenously phosphorylates synaptotagmin in SVs, increased the interaction of syntaxin and SNAP-25 with synaptotagmin suggesting that, Ca²⁺/CaMKII can increase the synaptotagmin–t-SNARE interactions after phosphorylation (Verona et al., 2000). VAMP-2 binds to CaM in a Ca²⁺-dependent manner and this can regulate the phospholipid-binding activity of VAMP/synaptobrevin. Additionally, CaM binding can prevent VAMP/ synaptobrevin from participating in the formation of the SNARE complex (Igarashi and Watanabe, 2007). CaMKII may also play some scaffolding roles in addition to its kinase activity. It was proposed that CaMKII regulates presynaptic short-term plasticity in the absence of its kinase activity (Pang et al., 2010). Figure P shows a schematic representation of the activation of CaMKII and of the regulation of neuronal functions.

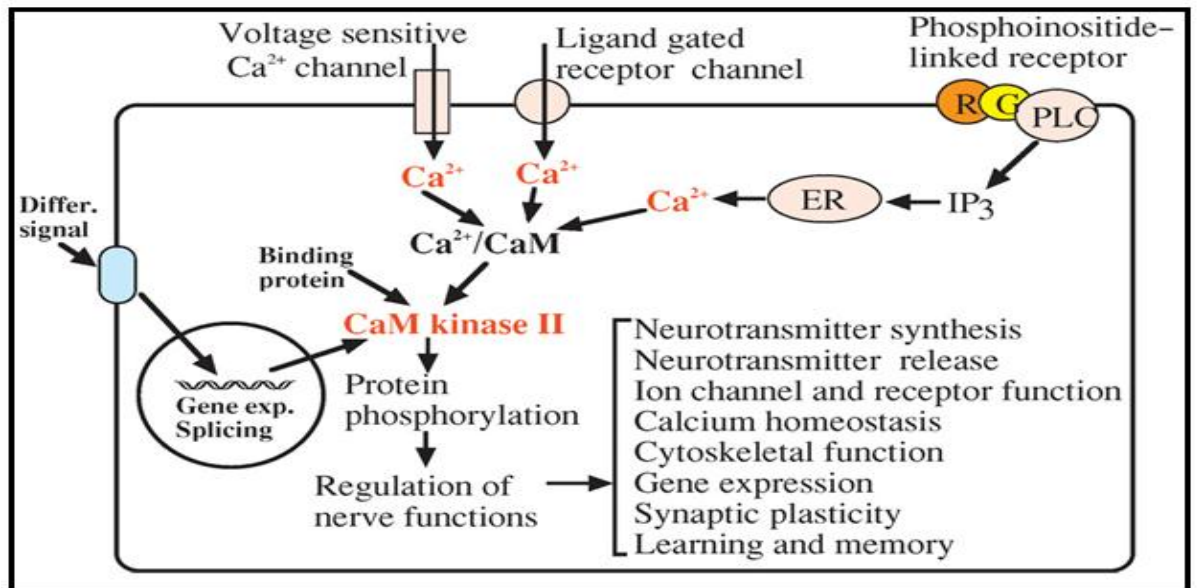


Figure P. Schematic Representation of Activation and Role of CaM Kinase II in Neuronal Cells: $[Ca^{2+}]_i$ is increased by extracellular stimuli, binds to calmodulin, and activates CaMKII. CaMKII phosphorylates various kinds of proteins and regulates physiological processes. CaMKII protein is induced by the stimuli of differentiation. (Yamauchi, 2005).

Hyper-activation of $Ca_v1.2$ L-type VGCCs by CaMKII is associated in Timothy Syndrome, a multi-organ human genetic disorder whose symptoms include mental retardation and cardiac disease (Yamauchi, 2005). Phosphorylation of the N-type Ca^{2+} channel by CaMKII or PKC decreases its interaction with syntaxin and SNAP-25, providing a possible regulatory mechanism that may decrease an inhibitory constraint of SNAREs on channel function and facilitate release (Verona et al., 2000).

All the CaMKII isoforms are believed to have syntaxin 1A-binding ability and these interactions may induce $Ca_v2.1$ channels presynaptic regulation (Pang et al., 2010). CaMKII is a key downstream effector of L-type VGCC signals. CaMKII may bind to and/or phosphorylate the $Ca_v1.2$ α_1 subunit to support multiple forms of L-type VGCC facilitation. CaMKII was also shown to regulate excitation-transcription coupling in neurons (Abiria and Colbran, 2010).

CaM is thought to regulate the asynchronous release, which is not mediated by synaptotagmin. It may also play a role in refilling the RRP and/or modulate presynaptic release by activating CaMKII α and CaMKII β (Munton et al., 2007).

CaM is also thought to control pre- and postsynaptic Ca²⁺-channel function, mediates postsynaptic long-term plasticity by activating CaMKII α and calcineurin, and alters neuronal gene expression (Pang et al., 2010).

CaM regulates NT release by multiple mechanisms, including a direct modulation of Ca²⁺ channels, activation of protein kinases, regulation of SV priming via the cytoskeleton and a process involving binding to the Munc13-1 and Munc13-2 isoforms (Shin et al., 2010).

The CaMK inhibitor 2-[*N*-(2-hydroxyethyl)]-*N*-(4-methoxybenzenesulfonyl)]amino-*N*-(4-chlorocinnamyl)-*N*-methylbenzylamine, KN93, (but not its inactive congener M2-[*N*-(4-methoxybenzenesulfonyl)]amino-*N*-(4-chlorocinnamyl)-*N*-methylbenzylamine, phosphate, KN92) blocked signalling in Sprague-Dawley superior cervical ganglion neurons (Wheeler et al., 2008). KN93 exerts its effect by competing for the CaM binding site of CaMKII (Rezazadeh et al., 2006).

Ca²⁺ influx also recruits an adenylyl cyclase, which activates the cAMP-dependent PKA leading to its translocation to the nucleus, where it phosphorylates the cAMP response element-binding (CREB) protein. CREB activates targets that are thought to lead to structural changes leading to the late phase of LTP (Sunyer et al., 2008).

1.9.2 Protein Kinase C

The second-messenger diacylglycerol (DAG) activates PKC, and this activation can take place when PKC attaches to the cell membrane. Physiological activation of PKC is normally associated with rise in presynaptic [Ca²⁺]_i through inositol triphosphate receptor activation and increase in DAG (Chang and Mennerick, 2010). These two secondary messengers are produced when phospholipase C is activated normally through G-protein coupled receptor activation. PKC can be activated either by Ca²⁺ binding to PKCs C2 domains and/or by binding of DAG to C1 domains. However, the signalling pathways leading to an increase in DAG by presynaptic activity are unclear (Wierda et al., 2007). DAG is responsible for activating PKC function by increasing its affinity for phosphatidylserine (PS)-containing membranes. Upon activation, PKC enzymes are translocated to the PM, where it activates various other signal transduction pathways (Wierda et al.,

2007). Activated PKC may phosphorylate a target protein in the vesicle fusion machinery, like munc-18, which in turn may result in an increase in the Ca^{2+} sensitivity of vesicle fusion (Rizo and Rosenmund, 2008). Other presynaptic proteins, like SNAP25 and synaptotagmin-1, also have PKC phosphorylation sites (Korogod et al., 2007; Wierda et al., 2007). PKC activation changed release kinetics and decreased quantal size by shortening the release period (Graham et al., 2002).

Studies have shown that stimulating chromaffin cells in elevated $[\text{Ca}^{2+}]_i$ increases the quantal size, and pharmacological activation of PKC increases the rate of catecholamine release. Additionally, the physiological stimulation is competent enough to raise cytosolic Ca^{2+} to levels adequate to activate conventional isoforms of PKC, causing its translocation to the cell membrane, where it acts to alter the kinetics and magnitude of exocytosis (Fulop and Smith, 2006). Data by Graham et al., (2002) suggests that during PKC activation, a dynamin-independent fusion pore closure limits release (Graham et al., 2002). PKC also play important roles in spatial memory.

Phorbol 12-myristate 13-acetate (PMA) is an active phorbol ester that activates presynaptic PKC-dependent and independent mechanisms to potentiate transmitter release. PMA are amphiphilic molecules and have tendency to bind to biological phospholipid membrane receptors. They are functional analogues of the lipid-signalling molecule DAG that activates C1-domain of PKCs (Lou et al., 2008a). PMA by activating PKC can enhance the Ca^{2+} sensitivity of vesicle fusion (Korogod et al., 2007) and results in increase of the fusion probability of RRP (Lou et al., 2008a).

Fulop & Smith, (2006) proposed a cellular mechanism whereby increased cell firing increases cytosolic Ca^{2+} and this or the PMA activation of PKC may result in the dilation of fusion pore, thereby switching from K&R to FF mode of exocytosis. This may depend upon the model of exocytosis being studied and also the level of $[\text{Ca}^{2+}]_i$ achieved. This mode shift forms the basis for activity-dependent differential transmitter release (Fulop and Smith, 2006).

1.9.3 Protein Phosphatases

The serine/threonine protein phosphatase family members include protein phosphatases 1 (PP1), 2A (PP2A), and 2C (PP2C). These phosphatases are essential for a number of signal transduction pathways in eukaryotic cells (Rusnak and Mertz, 2000). A difference in divalent metal ion dependence lead to the resolution of the type 2 enzymes into PP2A, PP2B (calcineurin), and PP2C. PP2A was originally described as having no requirement for divalent metal ions, calcineurin is regulated by CaM, and PP2C is Mg²⁺ dependent.

1.9.3.1 PP2A

PP2A is a heterotrimer consisting of three unrelated subunits, the catalytic subunit (C), a 65kDa regulatory subunit (A), and a variable regulatory subunit (B). The A and C subunits are tightly associated and are generally present in the cell as an invariable holoenzyme; substrate specificity and subcellular localization are conferred by the binding of one of a wide variety of related B subunits (Hill et al., 2006).

Okadaic acid (OA) is a widely used small-molecule phosphatase inhibitor that under some circumstances can be regarded as a selective inhibitor of PP2A (Hill et al., 2006). OA, a polyether fatty acid isolated from the black sponge *Halichondria okadai* and under particular conditions is a potent inhibitor of both type-1 and type-2 phosphatases (Morimoto et al., 2000; Rusnak and Mertz, 2000). The phosphatase inhibitor OA, alters the phosphorylation state of synapsin and increases vesicle mobility and NT release under certain stimulation conditions (Fernandez-Busnadiego et al., 2010).

1.9.3.2 PP2B/Calcineurin

Calcineurin (CaN) is a heterodimer consisting of a catalytic subunit, CaN A, and a “regulatory” subunit, CaN B. The active site of CaN is located on the A subunit (Rusnak and Mertz, 2000).

CaN can be phosphorylated by PKC, casein kinase I, and casein kinase II *in vitro*. Even though phosphorylation can be blocked by CaM, the kinetic properties of the phosphorylated and dephosphorylated forms are similar. CaN is a Ca²⁺-dependent protein phosphatase, which has been implicated in the regulation of

endocytosis (Igarashi and Watanabe, 2007), due to the fact that CaN dephosphorylates various synaptic proteins (Kumashiro et al., 2005). Ca^{2+} influx in nerve terminals activates CaN and enzyme dephosphorylates a set of proteins involved in endocytosis: these are called the dephosphins. The dephosphins are grouped together by their capacity to be dephosphorylated by CaN upon nerve terminal stimulation, and by the fact that they are all essential for SV endocytosis. The dephosphins include; dynamin I (Kumashiro et al., 2005), the AdP AdP180, and the accessory proteins amphiphysin I/II, synaptojanin, epsin, esp15 and phosphatidylinositol phosphate kinase type I γ (PIPKI γ). After the stimulus-dependent dephosphorylation, the dephosphins are then rephosphorylated by their individual protein kinases e.g. cyclin-dependent kinase 5 (cdk5) rephosphorylates dynamin I, synaptojanin and PIPKI γ *in vivo* (Clayton et al., 2007). CaN mediates downstream effect on CaM (Yamashita et al., 2010) on vesicle endocytosis in mammalian neurons (Kumashiro et al., 2005). Kumashiro et al., (2005) also demonstrated that CaN was required for endocytosis to the RP, but not for the RRP under particular recycling conditions (Kumashiro et al., 2005).

Cyclosporine A:

CaN is specifically inhibited by the immunosuppressant drug cyclosporine A (Cys A). Cys A binds to cyclophilin (C $_y$ P), a ubiquitous intracellular protein, and undergoes a conformational change. The Cys A-C $_y$ P complex binds to CaN and inhibits its serine/threonine phosphatase activity (Batiuk et al., 1995).

1.9.4 Myosin Family

Myosins are a family of molecular motors that bind to actin (Bhat and Thorn, 2009). Experiments have indicated that members of this protein family account for some vesicle dynamic properties. E.g.1 myosin Va contributes in DCV transport and plays a role in the docking process. E.g.2 Myosin VI is involved in endocytosis by associating with CCVs and is the only known motor protein that transports cargoes to the minus ends of the actin filament (Bhat and Thorn, 2009).

1.9.4.1 Myosin-II

Myosin II is a conventional myosin enriched in neurons, where it is thought to play a role in exocytosis (Igarashi and Watanabe, 2007). Myosin II can control regulated secretion in certain tissues (Bhat and Thorn, 2009). There is extensive evidence that myosin II plays a role in the secretory processes of a variety of cells, including: mast cells, natural killer cells, hippocampal and sensory neurons, chromaffin cells, β -cells, exocrine cells, and oocytes (Bhat and Thorn, 2009). It is thought that myosin II contributes to earlier exocytotic steps, such as vesicle transport in a motor activity-dependent manner.

Myosin II is an ATP-driven molecular motor forming an essential part of the motile machinery of most eukaryotic cell (Kovacs et al., 2004). In sympathetic neurons, inhibiting myosin II decreases synaptic transmission (Tokuoka and Goda, 2006) by inhibiting SV transport. Additionally, it has been shown in PC12 cells that myosin II plays important roles under certain conditions in shifting the exocytotic mode from K&R to FF and increases the speeds of release of the catecholamine (Aoki et al., 2010). Additionally, CaM regulates myosin light-chain kinase (MLCK), which in turn regulates the motor activity of myosin II. CaM may contribute to vesicular recycling by interacting with actomyosin (Igarashi and Watanabe, 2007). Ca^{2+} signalling in presynaptic terminals, therefore, may serve to regulate SV mobility along actin filaments via MLCK (Tokuoka and Goda, 2006; Bhat and Thorn, 2009).

Structurally myosin II has two functional domains; the head domain, which has ATPase activity and is required for motor activity and the other, a long-rod domain, which is required for the assembly of myosin II monomers into bipolar filaments (Aoki et al., 2010). In the research carried out by Aoki et al., (2010), it was found that under the conditions of their experiments myosin II was involved in the modulation of internalization kinetics rather than in the release kinetics. Additionally, they concluded that, the co-localization of myosin II with PM-docked vesicles was retained even with myosin II that lacked ATPase activity, as it was still able to bind actin filaments and bundle them, and the rod domains of myosin II could still interact with the lipid membrane. Thus, myosin II could participate in the transport step of exocytosis via its adaptor function rather than

through its ATPase motor activity (Aoki et al., 2010). However, a study by Bhat and Thorn (2009) on pancreatic cells suggests that inhibition of myosin II ATPase activity affects post fusion events, slowing the opening of the fusion pore and plays a role in promoting vesicle FF (Bhat and Thorn, 2009).

Blebbistatin is permeable to cell membranes. It is a potent inhibitor of skeletal muscle and non-muscle myosin II isoforms (Kovacs et al., 2004). Blebbistatin (Bleb) has a high affinity and selectivity to inhibit class-II myosin ATPase activity and is used to identify and study myosin II-dependent processes in cells (Shu et al., 2005). It preferentially binds to the ATPase intermediate with ADP and phosphate bound at the active site, and slows down phosphate release. Bleb does not interfere with binding of myosin to actin or with ATP-induced actomyosin dissociation. Instead, it blocks the myosin heads in a products complex with low actin affinity. Bleb binding site of the myosin head is within the aqueous cavity between the nucleotide pocket and the cleft of the actin-binding interface. Bleb binds to a nucleotide-bound enzyme intermediate with highest affinity and does not compete with substrate for binding sites on the enzyme. It blocks ATP hydrolysis and motor activity (Doreian et al., 2009).

1.10 Synaptic plasticity

Synaptic plasticity is defined as an activity-dependent change in synaptic transmission. Transient modifications of synapses have been associated with short-term memory (STM) and more lasting changes have been associated with long-term memory (LTM) in the mature neuron (Yamauchi, 2005). Learning can be described as the mechanism by which new information about the environment is acquired; memory represents the mechanism by which that knowledge is retained (Sunyer et al., 2008). Learning and memory rely upon the molecular mechanisms associated with the protein machinery. Stable synaptic changes involve post-translational modification (PTM) of proteins during STM and gene transcription, while the LTM requires the synthesis of protein and synaptic growth. Short-term synaptic plasticity has two mechanistic elements: (1) the source and regulation of the residual Ca^{2+} that initiates the process and (2) the effector mechanism(s) that respond to residual Ca^{2+} and enhance NT release (Catterall and Few, 2008).

Also the study of LTP and long-term depression (LTD) reveal that, the forms of activity-dependent synaptic plasticity in the mammalian CNS play a role in the mechanisms underlying learning and memory (Sunyer et al., 2008). LTP is the long-lasting strengthening of the connection between two nerve cells, which is typically caused by high-frequency stimulation of excitatory input leading to rapid elevation of Ca^{2+} in postsynaptic dendritic spines (Sudhof and Malenka, 2008). Whilst, LTD comprises of persistent activity-dependent reduction in synaptic efficacy, that typically occurs following repeated low frequency afferent stimulation (Sunyer et al., 2008).

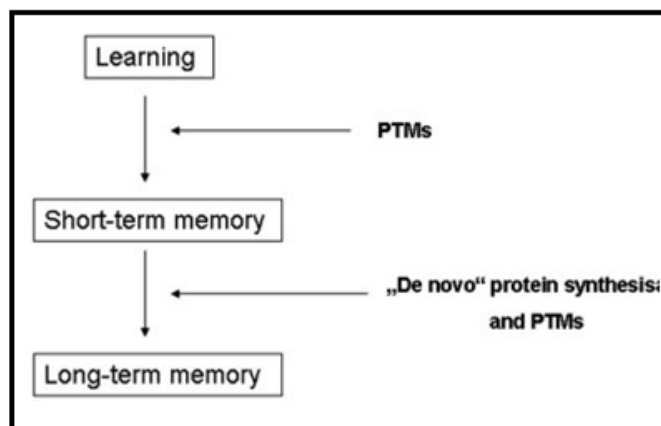


Figure Q. Memory consolidation needs PTMs and protein synthesis (Sunyer et al., 2008)

1.10.1 Post-Translational Modification of Endocytotic Proteins

The change in protein phosphorylation helps in the initiation of endocytosis. Protein phosphorylation is required for the induction of many forms of synaptic plasticity, including LTP and LTD. Various protein kinases play important roles in the regulation of NT release, and candidates for protein substrates essential for the regulation have been identified (Sunyer et al., 2008). Recent research have suggested that PTMs like phosphorylation of serine, threonine, and tyrosine play a major role in the cognitive processes such as synaptic plasticity in the brain, release of NT, vesicle trafficking and synaptosomal or synaptosomal-associated proteins that are substrates of a series of specific protein kinases and their counterparts, protein phosphatases (Sunyer et al., 2008). The serine-threonine kinase that phosphorylates the μ -subunit of AP2 and possibly other accessory factors is considered to promote coat assembly (Hosoi et al., 2009; Shupliakov,

2009). Intriguingly, dephosphorylation of several accessory proteins (Sunyer et al., 2008) also known as dephosphins after the Ca^{2+} influx, is also responsible for promoting the clathrin mechanism in the synapses (see earlier discussion about the dephosphins). It is believed that dephosphorylation triggers the interaction of these proteins with the other components of the endocytotic machinery (Shupliakov, 2009).

Researchers have demonstrated that the risk of neurodegenerative disorders increases with age. The major changes seen in aging neurons include increased Ca^{2+} release from intracellular stores through inositol (1,4,5)-trisphosphate receptors (InsP_3R) and ryanodine receptors (RyanR), increased Ca^{2+} influx through L-type VGCCs, reduced contribution of N-methyl D-aspartate receptor (NMDAR)- mediated Ca^{2+} influx, reduced cytosolic Ca^{2+} buffering capacity and activation of CaN and calpains. The resulting changes in neuronal Ca^{2+} dynamics lead to augmented susceptibility to induction of LTD and an increase in the threshold frequency for induction of LTP in aging neurons (Breukel et al., 1997).

The factors responsible for the age-induced alteration may be defects in mitochondrial function due to cumulative oxidative damage or mitochondria are depolarized and less competent in handling Ca^{2+} load.

1.10.2 Neurotoxicity

In brain, unregulated enhanced release of excitatory NTs can lead to neuronal damage and death. This excitotoxic neuronal death induced by increased synaptic glutamate is implicated in the pathology of multiple neurodegenerative diseases including Alzheimer's and Huntington's diseases along with ischaemia and epilepsy (Fdez et al., 2008). NMDARs are believed to play a crucial role in the process of excitotoxicity and neuronal degeneration. A continuous increase in the $[\text{Ca}^{2+}]_i$ concentration is considered to trigger a series of events (including persistent activation of Ca^{2+} -dependent enzymes, production of toxic metabolites, and disruption of the cytoskeletal network) that results in cytotoxicity and cell death. It has been demonstrated that, several pathological states, such as anoxia, ischemia, or chronic degenerative diseases such as epilepsy, amyotrophic lateral sclerosis are associated with modified glutamate levels (Bertolino and Llinas, 1992).

Extraneuronal concentrations of glutamate in injured brains are dramatically increased because of an abnormal release of the transmitter from damaged nerve terminals and because of reduced glutamate reuptake. These increased extraneuronal glutamate concentrations cause paroxysmal stimulation of NMDARs thereby, destabilizing neuronal Ca^{2+} homeostasis (Bertolino and Llinas, 1992).

Chronic blockade of AP firing in neuronal cultures increases trafficking of the AMPA receptor subunits GluR1 and GluR2 to postsynaptic sites, thus increasing sensitivity to released glutamate (Fdez et al., 2008). Researchers have also demonstrated that as NMDAR channels are highly permeable to Ca^{2+} ions, the receptor channel has considered being the central pathway for the Ca^{2+} entry in the presence of glutamate (Bertolino and Llinas, 1992). Ca^{2+} influx followed by PTMs may also serve as an important signal for the accumulation of key endocytic proteins at the periaxonal zone and serve as an important mechanism to initiate endocytosis in synapses.

Activity-dependent long-term changes in the efficacy of glutamatergic synaptic transmission are important in many forms of learning (Fourcaudot et al., 2009). The LTP studies of glutamatergic synaptic transmissions in different brain areas like cortex, hippocampus, and amygdala unfolded that synaptic strength is enhanced by two mechanisms, both dependent on the rise in $[\text{Ca}^{2+}]_i$. The first is by continual increase in the postsynaptic response to a fixed amount of glutamate released and the other is due to the dependence of NT release on the Ca^{2+} influx, the LTM in the presynaptic Ca^{2+} entry or sensing could cause a persistent increase in the release probability (Fourcaudot et al., 2009).

In a study done by Fourcaudot et al., (2009), it was concluded that LTP expression can be mediated by a persistent development of L-type VGCC efficacy. This might involve a PKA-dependent mechanism and/or proteins interacting with L-type VGCC such as the presynaptic AZ component RIM1 α (Rizo and Rosenmund, 2008). They also concluded that the L-type VGCC is responsible for presynaptic LTP in LTM formation (Fourcaudot et al., 2009).

For an efficient NT release, the formation of SNAP receptor (SNARE) complex is necessary. This process involves: (1) binding of the synprint sites on N-type or P/Q-type Ca^{2+} channels with presynaptic membrane proteins synaptotagmin and t-SNARE (i.e. SNAP25 and syntaxin 1A) (Jackson and Chapman, 2006; Serra et al., 2010), (2) dissociation of Syb/ VAMP2 from synaptophysin I, a small SV protein that interacts with Syb's transmembrane domain (Darios et al., 2009; Hosoi et al., 2009), and (3) association of Syb with t-SNARE, all of which are tightly regulated by $[\text{Ca}^{2+}]_i$ and the phosphorylation of the synprint sites on N-type and P/Q-type Ca^{2+} channels located within the intracellular loop-connecting domains II and III ($L_{\text{II-III}}$) (Refer Figure C) (Rizo and Rosenmund, 2008; Serra et al., 2010).

CaMKs and PP2B also act as mediators in this regulation (Shupliakov, 2009). Reverse phosphorylation is predominantly accomplished by the cdk5. However, the step at which the PTM occurs in the SVs recycling still remains unclear. Recent research have suggested that some of the enzymes are compartmentalized at the synapse, which further implies that PTMs predominantly occur at specific synaptic compartments (Shupliakov, 2009).

The balance of activities of such protein kinases and protein phosphatases contribute to the control of synaptic strength and plasticity underlying LTP, learning and memory. An imbalance in the regulation of protein kinases and protein phosphatases in the affected neurons can cause disease such as Alzheimer's disease.

Old neurons are sensitized to cytosolic Ca^{2+} toxicity because Ca^{2+} -buffering capacity declines with advancing age. The supranormal cytosolic Ca^{2+} signals might cause excessive Ca^{2+} handling by mitochondria and induction of apoptotic cell death (Bezprozvanny, 2009).

The regulation of presynaptic Ca^{2+} channels by effectors and regulators of Ca^{2+} signalling depicts that Ca^{2+} channel play a critical role in regulating neurotransmission and presynaptic plasticity. Failure of function and regulation of presynaptic Ca^{2+} channels leads to migraine, ataxia, and potentially other forms of neurological disease (Peretz et al., 1998). Recent evidence indicates that

neuronal Ca^{2+} signaling is abnormal in many of the neurodegenerative disorders like, Alzheimer's disease (AD), Parkinson's disease (PD), amyotrophic lateral sclerosis (ALS), Huntington's disease (HD) and spinocerebellar ataxias (SCAs) (Bezprozvanny, 2009).

As protein phosphorylation has also been shown to be involved in regulating the mode of SV exocytosis, the role of CaMKII in this process has also been studied (Catterall and Few, 2008).

1.11 Background Results

Studies in a model of type 1-diabetes whose exocytotic activity may involve various processes that have been discussed above: Very excitingly, it has been discovered by Dr A. Ashton that diabetic nerve terminals behave differently to control terminals. Diabetic terminals release exactly the same amount of glutamate (Glu) as controls when release was evoked by HK5C (Fig i.A). Intriguingly, HK5C induced a larger change in $[\text{Ca}^{2+}]_i$ in diabetic synaptosomes than in control synaptosomes (Fig i.C). This result suggests that, there is a difference between control and diabetic terminals in the mechanisms that contribute to this stimulus induced change in Ca^{2+} levels. Remarkably, whilst there is no change in HK5C evoked Glu release, there is a reduction in the amount of HK5C evoked FM2-10 dye release in diabetic terminals when compared to control synaptosomes (Fig i.B). This result indicates that HK5C evokes a greater amount of K&R exocytosis in diabetic synaptosomes. These results led to the hypothesis that it is the higher $[\text{Ca}^{2+}]_i$ induced by HK5C in diabetic terminals that leads to a larger proportion of exocytosis by the K&R mode and this could be due to the diabetic preparations possessing differences in components that contribute to this raised $[\text{Ca}^{2+}]_i$ levels.

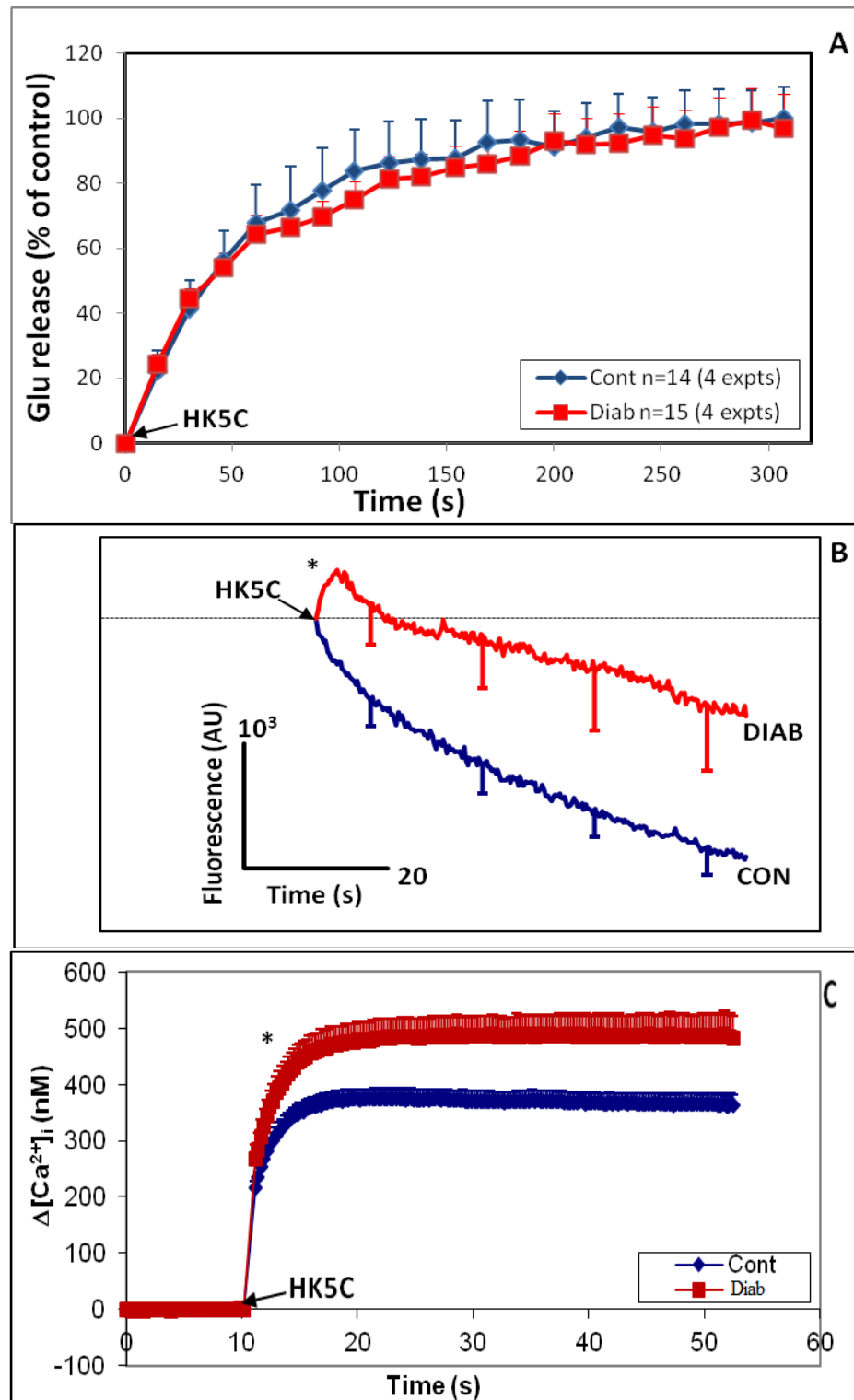


Figure i. Comparison between control and diabetic synaptosomes: A) No significant difference observed in the amount of glutamate released B) FM2-10 dye study confirms that the diabetic terminals undergo more K&R mode of exocytosis in comparison to the control C) Fura-2AM study reveals that application of HK5C induces a larger change in $[Ca^{2+}]_i$ in diabetic synaptosomes compared to control synaptosomes.

Since the above biochemical differences were observed in diabetic terminals, further studies on other biochemical and behavioural changes were carried out on such diabetic rats.

1.12 Diabetes Mellitus

Diabetes is from the Greek word meaning "siphon," and "mellitus" comes from melliferous, meaning "of or relating to honey." Diabetes has been recognized for centuries and was originally diagnosed by testing the urine and finding it sweet (melliferous). The World Health Organisation (WHO) defines diabetes mellitus (DM) as "a chronic disease, which occurs when the pancreas does not produce enough insulin, or when the body cannot effectively use the insulin it produces. This leads to an increased concentration of glucose in the blood (hyperglycaemia)" (Donath et al., 2005). In diabetes, the patient has a high blood glucose level either due to the body being unable to produce sufficient amount of insulin (type 1 diabetes) or due to the cells in the body becoming insulin resistant (type II diabetes) (Donath et al., 2005).

The pancreatic islet β -cell regulates cellular fuel metabolism and glucose homeostasis by secreting the hormone, insulin (Min et al., 2007). Insulin promotes anabolism, and inhibits catabolism in muscle, liver, and fat cells. Its functions include the increase in the rate of synthesis of glycogen, fatty acids, and proteins. Thus, insulin plays a crucial role in the process of digestion (Donath et al., 2005). Abnormal insulin secretion or usage results in DM. Several pathogenic processes are involved in the deficiency of insulin (Romero-Aroca et al., 2010). These include, autoimmune destruction of the β -cells of pancreas. Also can include the tissues/cells (mainly muscle, liver and/or fat cells) becoming insulin resistant. Another possibility is a defect in cellular signalling such that there is inadequate insulin secretion or inadequate response to insulin secretion. The first type is called type 1 diabetes mellitus (T1DM) and the second is called type 2 diabetes mellitus (T2DM). Liver is an important insulin dependent tissue and plays a pivotal role in glucose and lipid metabolism, and is severely affected during diabetes (Moller, 2001). In diabetes the levels of hepatic enzymes increases (Farswan et al., 2009).

1.13 Symptoms for both types of DM include; marked hyperglycaemia (rise in blood glucose level), polyuria (frequent urination), polydipsia (increased thirst), weight loss sometimes with polyphagia (excessive hunger), and blurred vision (Kirpichnikov and Sowers, 2001; Latham et al., 2009). The reason for increased amount urine and thirst is because, glucose leaks into urine which 'pulls out' extra water through the kidneys. Uncontrolled diabetes leads to acute and life-threatening consequences like hyperglycaemia with ketoacidosis (a state of metabolic dysregulation characterized by the smell of acetone) or the non-ketotic hyperosmolar syndrome (due to dehydration). Other symptoms include Kussmaul breathing (a rapid, deep breathing), nausea, vomiting and abdominal pain, and an altered state of consciousness (Anderson, 2008). Frequent infections, especially around genitals such as recurring thrush and, other infections such as developing boils are indication for the development of T2DM.

The late-stage diabetic complications can occur in both types of diabetes. In T1DM late stage complications usually develop after 10-15 years after the diagnosis of the disease, whereas in T2DM, symptoms may appear close to the time of actual diagnosis because the disease may go undetected for longer (Tfayli and Arslanian, 2009). Studies show that proper control in glucose level (as close to normal level) can significantly reduce or even stop complications.

Although the pathogenesis of diabetes-related vascular complications is composite and multifactorial, they are associated with the level of glycaemia (Kirpichnikov and Sowers, 2001). Uncontrolled glucose regulation can result in the development of hyperglycaemia (Roy et al., 2010). If persistent and untreated, hyperglycaemia can damage many of the body's tissues, particularly the vasculature. As a result, diabetes-associated microvascular and macrovascular complications occur at advanced stages (Cooper et al., 2001). The major microvascular complications are nephropathy, retinopathy, and peripheral neuropathy, whereas the macrovascular complications in diabetes is manifested by accelerated atherosclerosis, clinically resulting in premature ischemic heart disease, increased risk of cerebrovascular disease, and severe peripheral vascular disease (Feener and King, 1997). Further, the thesis concentrates on the effects of diabetes on the nervous system.

1.14 Cognitive Dysfunction

In addition to its well known adverse effects on the cardiovascular and peripheral nervous systems, diabetes appears to negatively affect the brain, increasing the risk of depression and dementia. Along with diabetes, cognitive dysfunction is also a serious problem and its prevalence is rising worldwide, especially among the elderly (Thomas et al., 2001). Diabetes associated cognitive dysfunction, first described nearly a century ago (Zhou et al., 2010), occurs in both types of diabetes. Recent studies have also confirmed the link between the cognitive dysfunction and diabetes, i.e. DM could also be the risk factor for the development of cognitive diseases (Allen et al., 2004). Human subjects with either T1DM or T2DM typically show impaired cognitive function compared to age-matched non-diabetic subjects (Desrocher and Rovet, 2004; Greenwood and Winocur, 2005). Latest observations have concluded that, compared to people without diabetes, people with diabetes are at a greater rate of decline in cognitive function (a 1.5-fold greater risk of cognitive decline; and a 1.6-fold greater risk of future dementia). Compared to non-diabetic individuals, diabetes increased the risk of vascular dementia and Alzheimer's dementia 1.3 and 4.4-fold, respectively (Cukierman et al., 2005). In T1DM, the effect on the brain structure and function occurs at the extremes of age, i.e. during childhood and during old age (Wessels et al., 2007; Biessels et al., 2008; Kloppenborg et al., 2008). Studies have concluded that, neuronal deficits may be associated with impaired neurotrophic support, inflammation and oxidative stress. Some studies have also demonstrated that, poorly controlled T1DM and fatal brain oedema of ketoacidosis is associated with a decreased presence of insulin and IGF-1 receptors and accumulation of nitrotyrosine in neurons of affected areas and the choroid plexus leading to neuronal deficits (Hoffman et al., 2010). Cognitive deficits have also been documented in rodent models of diabetes (Biessels et al., 2008).

DM has negative impacts on the CNS leading to diabetic encephalopathy and concomitant augmented incidence of cognitive problems (Brands et al., 2006), which are particularly associated with atrophy of the hippocampal formation that is involved in learning and memory processing (Gold et al., 2007). It is also associated with other moderate cognitive deficits and neurophysiological and structural changes in the brain (Satoh and Takahashi, 2008). A recent study

carried out by Stranahan, et al., (2008) confirmed that, diabetes deteriorates hippocampus-dependent memory, perforant path synaptic plasticity and adult neurogenesis in both insulin-deficient rats and insulin-resistant mice (Stranahan et al., 2008).

It has been observed that, the peripheral nerves in diabetes have an additional pathway by which insulin acts on the brain and sends messages via the nervous system to exert a higher level of control on glucose output from the liver (van Duinkerken et al., 2009). Experimental studies in animal models and in humans without diabetes have shown that, poor glucose regulation after a glucose challenge test was associated with poorer performance on a variety of cognitive tests, the effect being more pronounced in the older age group (Messier, 2004; Stranahan et al., 2008).

Neurons have a constantly high glucose demand. Neuronal glucose uptake depends on the extracellular concentration of glucose, and cellular damage can ensue after persistent episodes of hyperglycaemia; a phenomenon referred to as glucose neurotoxicity (Tomlinson and Gardiner, 2008). Even though quite a few studies have found the link between the brain alteration and changes in the level of insulin, the role of insulin in the brain is still to be elucidated. It is postulated that insulin and its signalling play an important role in neuronal, glial, and overall cognitive and memory functioning. Also, recent researches have shown that insulin does penetrate the cerebral spinal fluid, probably via receptor-mediated transport and reach the rest of the brain. Autoradiography (*Autoradiography* is the use of X-ray (or occasionally photographic) film to detect radioactive materials) studies have shown that insulin can cross the blood-brain barrier (BBB), penetrating to the circum-ventricular organs, including the arcuate and ventromedial nuclei of the hypothalamus (Bingham et al., 2002). For insulin-stimulated glucose metabolism to occur in the brain; insulin, IRs and insulin-sensitive glucose transporters are required. Recently studies have proved that, insulin receptors (IRs) are present on the endothelium of the BBB, which allow receptor-mediated active transport of insulin into the brain (Banks et al., 1997). It has also been assumed that, insulin can be synthesised in the brain (Bingham et al., 2002); however, most of the brain insulin is thought to originate from the systemic circulation.

Some studies have also identified IRs in central neurons, astrocytes, synapses, and other glia (Zhao et al., 2004). The presence of IR has been confirmed throughout the human brain, with particularly high concentrations in the hypothalamus, cerebellum, cortex (Hopkins and Williams, 1997) olfactory bulb, hippocampus, amygdala and septum (Unger et al., 1991).

Additionally, before glucose can be delivered to CNS neurons, it must cross the BBB (Tomlinson and Gardiner, 2008). Although, brain glucose uptake seems to be independent of insulin action, insulin sensitive glucose transporters have also been found at the BBB and on glial cells in various studies of animal brain. These include both insulin-sensitive GLUT4 and a partially insulin-sensitive GLUT1 (Ngarmukos et al., 2001). GLUT1 is expressed in the microvessels of brain (Tomlinson and Gardiner, 2008). The regional distribution of GLUT4 suggests that insulin-dependent glucose uptake might occur in specialized neuronal phenotypes but, in general, vascular barriers offer neurons the only protection against glucose toxicity during hyperglycaemia. The highest expression of GLUT1 and GLUT4 is in the hippocampus, the cerebellum and the olfactory bulb; lower expression is reported for the lateral hypothalamus, the arcuate nucleus and the globus pallidus (Tomlinson and Gardiner, 2008). mRNAs coding for accessory molecules, such as glucokinase and the IRs, are also expressed in some of these brain regions, but insulin-regulated glucose uptake has not yet been proven to occur in the brain. Recently, GLUT8 has also been identified in the brain, localized specifically to the hippocampus, the cerebral cortex and the hypothalamus. Studies in hippocampus suggest that it does not respond to insulin, but that it is activated by glucose itself, which recruits GLUT8 to the PM (Tomlinson and Gardiner, 2008). Even though the regional distribution of GLUT4 suggests that insulin-dependent glucose uptake might occur in specialized neuronal phenotypes, there is no strong evidence that these systems provide protection against hyperglycaemia. Positron emission tomography studies in humans, however, have shown no effect of increasing insulin levels on global brain glucose uptake (Hasselbalch et al., 1999), and based on the lack of effect of hyperinsulinemia, it has been concluded that in human brain glucose metabolism is not insulin sensitive. This contrasts with the clear evidence for an effect of insulin on brain function mentioned above. The study conducted by Duarte et al., (2009) suggested that the neurochemical alterations in the hippocampus of male

diabetic Sprague–Dawley rats (tested 4 weeks after STZ administration), are not related to defects in glucose transport in the brain, but is likely to reflect osmoregulatory adaptations caused by hyperglycaemia (Duarte et al., 2009). The published studies testify inconsistent effects of hyperglycaemia on substrate transport into the brain. Particularly, glucose transport into the brain was suggested to be reduced, augmented (Duelli et al., 2000) or unaffected (Simpson et al., 1999) by chronic hyperglycaemia. As mentioned before, hyperglycaemia may cause deregulation of brain metabolism involving inadequate glucose utilization, the hallmark of diabetic conditions in peripheral tissues. Also, hyperglycaemia-induced hippocampal dysfunction and damage may be because of the disruption of osmotic balance, which is of fundamental importance for the viability of cells, in particular of neurons (Tomlinson and Gardiner, 2008). In one study, it was found that chronic hyperglycaemia, induced by STZ administration, caused a plethora of metabolic alterations in the hippocampus, most of which were normalized upon restoration of euglycemia (Duarte et al., 2009).

In a recent review, a number of possibilities were considered for the association between diabetes and cognitive decline.

1. Hypoglycaemia may also affect cognitive function; however, it is not fully established. Studies have confirmed that intensive treatment regimens that were associated with increased hypoglycaemic episodes in individuals with T1DM did not adversely affect cognition (Reichard and Pihl, 1994).

2. Hyperglycaemia may also be a factor for development of chronic cognitive impairment (Huang et al., 2002).

Depression occurs more frequently in people with diabetes (Anderson et al., 2001) and is difficult to differentiate clinically from dementia and early cognitive decline (Swainson et al., 2001).

1.14.1 Hypoglycemia and brain

The brain is a very vulnerable organ to any changes in the glucose level. If both higher and lower level of glucose persists in the circulatory system, it can lead to severe alteration in the brain. In uncontrolled DM, the only treatment is insulin therapy. Rise in the level of insulin in the circulatory system, can lead to increase the risk of both moderate and severe hypoglycaemia (Puente et al., 2010) and can thereby result in the alteration of the brain function (Bingham et al., 2002).

Severe and recurrent episodes of hypoglycaemia results in the brain getting deprived of glucose, causing brain damage in animal studies, and leading to long-term impairments in learning and memory (Suh et al., 2005). Severe hypoglycemia has been shown to alter brain structure and cause significant cognitive damage in many but not all studies (Puente et al., 2010).

1.14.2 Hyperglycaemia and neuronal deficient

Despite the fact that the underlying neuropathological and biological substrates are still not elucidated, hyperglycaemia leading to microangiopathy in the brain is thought to be the primary reason for the cerebral complications observed in diabetes (Wessels et al., 2007). Hyperglycaemia induces variety of secondary metabolic defects such as, polyol pathway flux, protein glycosylation, oxidative stress, and impaired neurotrophic support. These secondary effects have been identified as main factors for sensory polyneuropathy in diabetes.

Some research has demonstrated that, hyperglycaemia can induce cellular damage through increased glucose metabolism by aldose reductase (Obrosova, 2005), elevated protein glycation (Thornalley, 2002), and increased mitochondrial NADH supply, thereby enhancing electron availability and causing partial reduction of oxygen to superoxide radicals in the proximal part of the electron transport chain (Du et al., 2001). These three mechanisms may combine to trigger large elevations in reactive oxygen species (ROS) that induce oxidative stress and tissue damage (Calcutt et al., 2009). It is assumed that, the ability of diabetic nerves to survive oxidative stress may be impaired because of the suboptimal trophic support from insulin, insulin-like growth factors, and neurotrophic factors (Calcutt et al., 2009). Although increased oxidative stress has become a widely accepted consequence of hyperglycaemia in models of diabetic neuropathy, the source of excessive ROS is not defined. Hyperglycaemia may also responsible for triggering the other cascade of changes, such as glycation end products (Huang et al., 2002), activation of the hypothalamic-pituitary-adrenal axis (HPA), which could have an effect on the brain (Chowdhury et al., 2010). In a research carried out by Messier et al., (2005), it was found that humans with poorly controlled diabetes show hyperactivation of the HPA, resulting in elevated circulating cortisol and cognitive dysfunction in diabetes. The role of glucocorticoids in cognitive dysfunction in diabetes is still unknown but, high levels of cortisol has

been associated with poor cognitive ability in humans subjected to psychosocial stress, during normal aging and in AD (Stranahan et al., 2008). It has also been demonstrated that, hyperglycemia results in increased corticosterone, and impairments in hippocampal neurogenesis, synaptic plasticity and learning (Stranahan et al., 2008).

Post mortem studies of senile plaques from the brains of people with Alzheimer's dementia found metabolic oxidation products associated with hyperglycaemia (Horie et al., 1997). Changes in the strength of synapses between groups of neurons within the hippocampus are critical in certain types of learning and memory (Stranahan et al., 2008). The regulation of synaptic connectivity at the level of the dentate gyrus extends beyond changes in the number and strength of synapses to the de novo addition of new neurons in adulthood (Leuner et al., 2006). Recent studies of animal models suggest impairment of both synaptic plasticity and adult neurogenesis in diabetes. Streptozotocin (STZ)-induced diabetic rats, a frequently used model of T1DM, is characterized by chronic hyperglycaemia associated with impaired hippocampal-dependent learning and memory as well as defective synaptic plasticity in the hippocampus (Biessels et al., 2008; Duarte et al., 2009).

The cellular mechanism of learning and memory depends on LTP of synaptic transmission, is believed to be impaired in the dentate gyrus of rats with STZ-induced diabetes (Kamal et al., 2006).

Duarte et al., (2009) reported that, chronic hyperglycaemia triggers astrocytosis in the hippocampus, and increased glial fibrillary acidic protein immunoreactivity in hippocampal membranes of STZ-induced diabetic rats, when compared to controls (Duarte et al., 2009). It is believed that astrocytic proliferation may be due to the neuronal damage, as observed in other neurodegeneration such as amyotrophic lateral sclerosis, AD (Lauderback et al., 2001) and Lewy-body dementia, and may contribute for diabetes-induced hippocampal deterioration as reactive astrocytes are known to produce free radicals (Chao et al., 1996) and apoptotic factors (Ferrer et al., 2001).

Both pre- and postsynaptic deficits have been associated with impaired LTP in the diabetic hippocampus. Synaptic transmission changes in the pyramidal cells of the hippocampus in STZ-induced DM in rats (Kamal et al., 2006). Short-term replacement of insulin in STZ-treated rats from the onset of diabetes prevents

cognitive decline and protects against hippocampal potentiation deficits (Francis et al., 2008).

The affect of all physiological fates due to the increased glucose level is highlighted in Figure R.

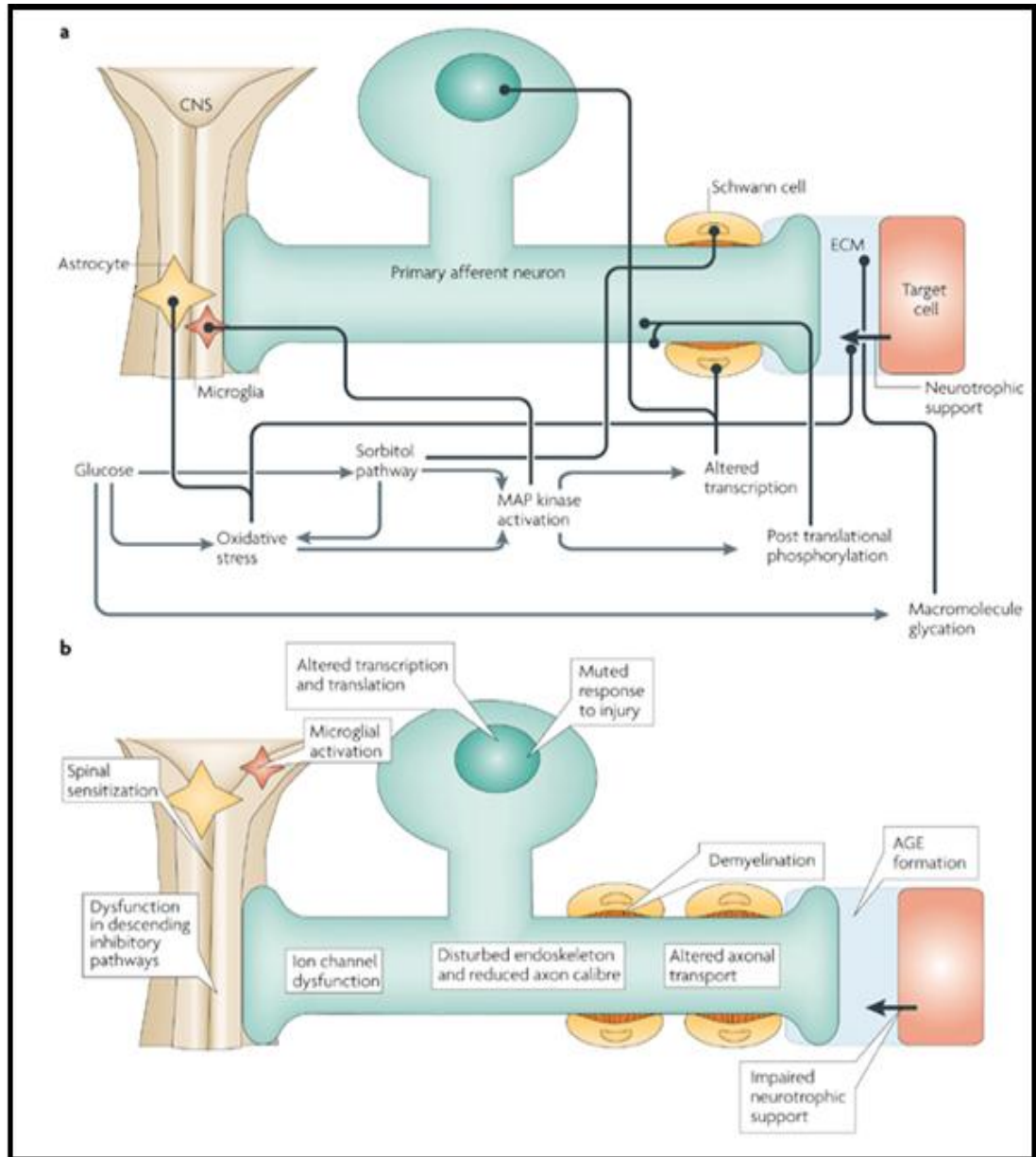


Figure R: Physiological fates due to the increased glucose level: a | The major damaging metabolic pathways driven by raised glucose levels and their damage targets (indicated by the round-ended arrows) in a primary afferent neuron and its accessory cells (astrocytes, microglia and Schwann cells). b | The processes that are disturbed by these metabolic impacts include spinal sensitization, dysfunction of descending inhibitory pathways, muted response to injury, demyelination and altered axonal transport, among

others. (AGE, advanced glycation end-product; ECM, extracellular matrix; MAP kinase, mitogen-activated protein kinase) (Tomlinson and Gardiner, 2008).

1.14.3 Hyperglycaemia and neuronal regeneration

The ability of nerves to regenerate is inversely proportional to the duration of the diabetes (Duarte et al., 2009). Axonal regeneration is impaired after nerve cut or crush injury in the STZ model of diabetes (Tomlinson and Gardiner, 2008).

Experiments have confirmed that, selective synaptic degeneration occurs in diabetic rodents due to reduction of the density of synaptic proteins such as syntaxin, SNAP25 and synaptophysin, in the hippocampus. The number of the postsynaptic protein, PSD95 was unaltered in the hippocampus of STZ-treated rats, when compared to the control rats, suggesting that diabetes mainly affects the presynaptic component of the synapse following long-term illness (Duarte et al., 2009). Eventually, these modifications in nerve terminals may be responsible for some of the altered synaptic plasticity in the hippocampus and thus memory impairment observed in STZ-induced diabetic rats (Biessels, 1996).

Experiments using Ca^{2+} ionophore in mouse motor nerve endings have illustrated that synaptic fusion can be directly regulated by the redox state. In these nerve endings, evoked and spontaneous quantal release was reduced by physiological levels of ROS (Giniatullin et al., 2006). When the neuronal proteins were studied to check their sensitivity to the oxidative stress, it was found that, SNARE proteins are sensitive to oxidative stress, with SNAP25 being the most sensitive (Giniatullin, 2006). The redox state is known to affect cysteine residues. Specific cysteine residues in SNAP25 play a role for the disassembly of SNARE and exocytosis and not for membrane targeting. During oxidative stress in motor nerve endings, crucial alterations in SNAP25 structure (cysteine residues) may underlie the lack of SNARE complex assembly and reduced exocytosis. Interestingly, the expression of some exocytotic proteins, including SNARE proteins, is altered in disease-relevant brain areas in neurodegenerative diseases such as AD and HD (Sze, 2000; Morton, 2001; Suh et al., 2005). The redox modulation of SNARE complex formation is therefore another mechanism by which mitochondrial dysfunction occurs early in some neurodegenerative diseases and might reduce synaptic activity (Keating, 2008).

Experiments on STZ-diabetic rat's hippocampus have demonstrated that, neurological dysfunction and impaired learning with diabetes are correlated with reduced expression of the presynaptic protein synaptophysin in the absence of neuronal loss. A decrease in basal synapsin I phosphorylation, which mediates the fundamental initiating event in regulating the release of NT from the cytoskeleton, may hinder the mobilization of vesicles within the presynaptic terminal. This phosphorylation event is affected by CaMKII. CaMKII content and activity are reported to be decreased by diabetes in the hippocampus, which also exhibits electrophysiological abnormalities and synaptic protein loss. Insulin replacement therapy partially rectified CaMKII activity in STZ-diabetic rat brain (VanGuilder et al., 2008). Additionally, it has been found by Ramakrishnan et al., (2005) that diabetes have increase in CaMKII expression and enzyme activity in different brain regions that in most instances are correlated with increased serotonin levels, thereby suggesting that CaMKII may be involved in the regulation of indolamines in diabetic animals (Ramakrishnan et al., 2005).

As explained earlier, as ageing in the brain takes place, various changes in numerous aspects of NT signalling occurs. Recent researches have indicated gross imbalances in NTs occurring during brain aging and age-related diseases of the brain (Uranga et al., 2010). For instance, the levels and density of key NTs such as dopamine have been demonstrated to be decreased in the aging brain (Meng, 1999). Moreover, the levels of NTs such as acetylcholine decreases and is accepted in the aging brain and age-related neurodegenerative disorders such as AD (Terry and Buccafusco, 2003; Hynd, 2004). Along with the changes in the level of NT, changes in the levels of key NT receptors have also been reported. The glutamate receptor subunits NR1, NR2A, and NR2B; and the AMPAR decline with age (Adams, 2008; Newton, 2008). There is also significant age-related decrease in the levels of dopamine receptors D1, D2, and D3 (Kaasinen, 2000). The effects of aging on the levels of cholinergic receptors, however, are still unclear (Uranga et al., 2010).

1.15 Behavioural Studies

In all the living organisms, natural actions are due to the synchronized coordination of various complex sequences of patterns such that, each pattern must be connected to another in a well-organised fashion (Berridge, 1989). Behaviour is one of the most important properties of animal life. It plays a critical role in biological adaptations, and is believed to be the bridge between the molecular and physiological aspects of biology. Experiments on learning, memory and perceptual processes are revealing new insights into neural plasticity and developmental influences on the brain. Today the behavioural study is not only important to understand how the brain works but also is significant to elucidate the neural disorder during diseases like AD. Cognitive neuroscience, a discipline aimed at understanding the functioning of the brain, encompasses approaches ranging from behaviour to molecular.

Studies monitor animals' behavioural patterns in order to gain comprehensive understanding of their behaviour and also to determine the effects of the environmental changes, drugs or to have a detailed insight in the neuronal regulation of the behaviour (Van de Weerd et al., 2001). Each species-specific behaviour provides basic understanding of how the brain organizes elemental actions into patterned sequences. These actions allow syntactic processes of sequence control to be isolated and examined, without the use of training procedures, and relatively independent of the learning and memory processes on which trained action sequences depend.

This laboratory investigates the molecular mechanisms of NT release and its perturbation in diseased states. However, after examining the diabetic synaptosomes, it has been established that the basic neuronal machinery is affected. Therefore, the present behavioural study was undertaken with the intention of establishing the biochemical changes and the behavioural changes that occurs in the diabetic animals in order to elucidate the co-relation between the behavioural patterns to the biochemical changes that occurs in these animals.

1.16 Rationale Behind the methods used

Experiments reported herein used the well-established model system consisting of pinched off nerve terminals (synaptosomes) prepared from the cerebral cortex of rat brain. These allow the study of the various pools of SVs from adult tissue.

1.16.1 Synaptosomes

Synaptosomes are a well-established model for NT release and are susceptible to pharmacological manipulations (Fernandez-Busnadiego et al., 2010). They were first isolated by Whittaker in 1958 (Breukel et al., 1997). Synaptosomes are intact nerve terminal particles with small, clear vesicles, signifying their presynaptic origin. Clearly, synaptosomes contain all the components necessary to store, release, and retain NTs. They also contain viable mitochondria with ATP and active energy metabolism. They maintain resting $[Ca^{2+}]_i$ concentrations of 100-200 nM in the presence of 2 mM $[Ca^{2+}]_e$. Resting membrane potential (which is regulated by a Na^+/K^+ -ATPase) is maintained and they express functional uptake carriers and ion-channels in their PM. On application of diverse depolarizing stimuli (e.g. potassium and 4-aminopyridine), Ca^{2+} enters synaptosomes via VGCCs or one can use ionomycin which allows Ca^{2+} entry due to its ionophore transport properties and these three stimuli triggers exocytosis of docked vesicles, thereby releasing various NTs (Breukel et al., 1997) .

1.16.2 Glutamatergic synaptic transmission

Glutamate is the main NT present in mammalian synaptosomes (Nicholls et al., 1987). It plays a critical role in many neuronal functions (as discussed above) (Sato and Takahashi, 2008). Various types of glutamate receptors are present in the CNS. Ionotropic glutamate receptors (iGluR), i.e. NMDA, AMPA and kainate, are responsible for mediating fast synaptic transmission, whereas activation of metabotropic receptors (mGluRs) modulates neuronal excitability and transmission (Woolley et al., 2008). About eight mGlu types of receptors have been identified so far. It is believed that, mGlu2 receptors are located presynaptically at the periphery of the synaptic area, where they function to

monitor excessive glutamate that has escaped from the synaptic space and provide negative feedback to prevent excessive glutamate release (Woolley et al., 2008). It was demonstrated that, physiological concentrations of transmitter in the synaptic cleft were insufficient to activate all the postsynaptic receptors suggesting that glutamate concentrations during synaptic transmission could possibly be the regulatory function of synaptic strength. Because of its role in synaptic plasticity, glutamate is involved in cognitive functions like learning and memory (Meldrum, 2000). Glutamatergic vesicles are defined by their ability to pack glutamate (Glu) for release, a property conferred by the expression of a VGLUT. VGLUTs are subject to regional, developmental, and activity-dependent changes in expression.

Since >80% of all cerebral cortical synaptosomes are glutamatergic, the release of endogenous Glu at 22°C (determined using a glutamate dehydrogenase coupled assay and measuring fluorescence of NADPH product) was studied in this thesis.

1.16.3 FM2-10 dye assay to study the modes of exocytosis

Applications of styryl dye staining and destaining during endocytotic and exocytotic processes have been used to study the kinetics of vesicle cycling and the prevalence of different exocytotic modes of release i.e FF versus K&R exocytosis (Omiatek et al., 2010). Fluorescent styryl dyes (e.g. Fei Mao), enduring both lipophilic and divalent cation groups, are widely used to label membranes for fluorescence microscopy investigations of vesicular exocytosis. Styryl dyes like Fei Mao (FM) fluoresce brightly when harboured in the hydrophobic vesicle membrane, but not in aqueous solution, and thereby report vesicle fusion events (Zhang et al., 2007). Upon stimulation, when the SVs that undergo exocytosis in the presence of the styryl dye, the dye molecules are subsequently integrated into the vesicular domain following endocytosis. This dye molecule partition easily and reversibly inside of the cell membrane, and increases the fluorescence intensity significantly by 20 fold (Omiatek et al., 2010). This dye cannot escape through a flickering proteinaceous pore (Henkel et al., 2001). FM dye can leave the vesicle membrane by lateral diffusion away from fused membrane upon FF (Zhang et al., 2007). Zhang et al., (2009) hypothesized that the nanoparticles of the styryl dye are small, which allows them

to be transported into the vesicle (interior lumen space estimated as about 24 nm diameter), but are spatially excluded from the narrow fusion pore (1-5 nm diameter) formed during K&R (Zhang et al., 2009).

To remove non-specific binding of FM dye to the PM, Advasep-7 is utilized. Advasep-7 has a higher affinity for the dye than membranes. The dye inside the membrane is not disturbed as advasep-7 cannot cross the PM. Upon a subsequent stimulation, the SVs re-exocytose and depending on the mode of exocytosis, the dye will or will not de-partition from the membranes. The FM dye should be discharged during FF mode of exocytosis and the membrane will completely lose its fluorescence. This would allow direct interrogation of the mechanism of release (Figure S). Whilst in K&R mode of exocytosis, the SVs do not fully collapse and so the FM dye is still trapped within the luminal domain of the SV. Previous studies have suggested that the K&R mode of exocytosis dominates at the onset of stimulation, and that FF prevails following continuously repeated stimulation. The results in this thesis re-inteprets the significance of this finding since it relates to the pools of SVs. The use of lipophilic FM dyes to follow vesicle cycling has also suggested the existence of fast K&R exocytosis in synaptosomes (Graham et al., 2002; Richards, 2009).

Optimal stimulation conditions that produce maximum NT release will enable all releasable SVs to be loaded with FM dye, and subsequently such SVs can be released upon the application of a stimulus. Sub-optimal conditions for dye loading will make it difficult to compare endogenous NT release because dye free vesicles will still be able to release NT. Maximum stimulus is required to be applied for the study of the FM dye release as all the vesicles (RRP and RP) needs to be labelled. Drugs that perturbed Glu release, and therefore reduce the number of SV exocytosing cannot be used for such experiments.

In FM dye studies, the application of a depolarizing stimulus with 30mM K⁺ plus 5mM Ca²⁺ (HK5C) produced maximal synaptosomal NT release, and the inclusion of a 5min post-stimulus incubation, both carried out in the presence of 100µM FM2-10 dye, ensured that all releasable vesicles were fully labelled. All loading of FM dyes, washing and release were performed at RT (22°C). Exocytosis was studied by measuring the decrease in fluorescence in response to

optimal concentrations of secretagogues and Ca^{2+} known to induce maximal release. The size of the releasable pool(s) is reflected by the terminals' response to a single application of the strongest release stimulus.

Such conditions have been established herein and furthermore all three stimuli employed only induce one round of release of the SV pools such that one can correlate release of Glu with FM dye.

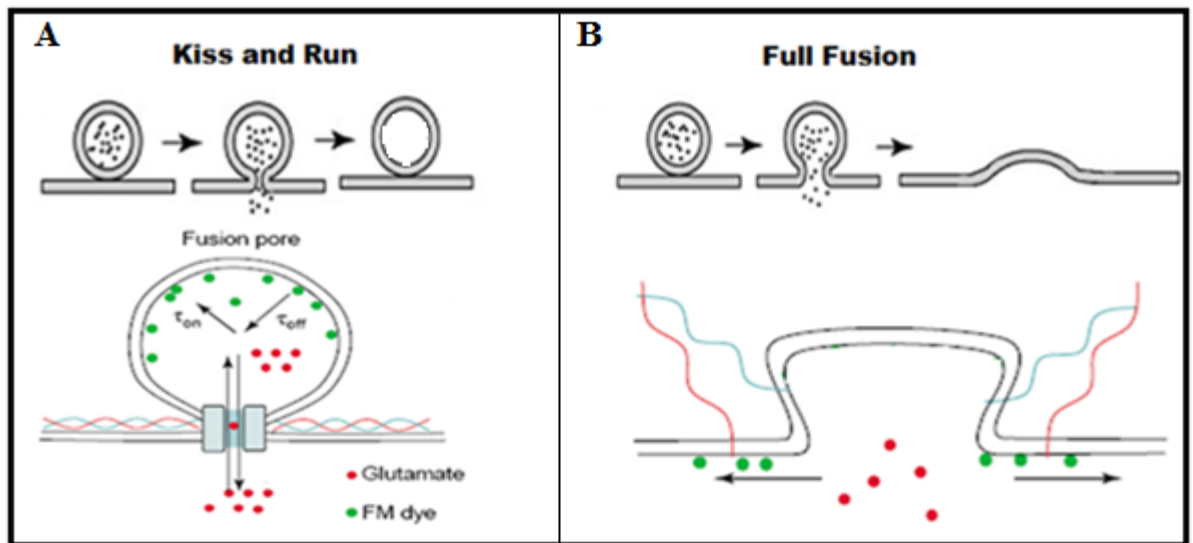


Figure S. Dynamics of FM-dye terminal staining in the two models of NT release: A. K&R mode of exocytosis where the FM dye (green spots) do not dissociate when glutamate (red spots) are released. B. FF mode of exocytosis where both the FM dye and Glu is released as the vesicle completely fuses with the PM (Krupa and Liu, 2004).

I.16.4 Fura-2AM experiments

Fura-2, a Ca^{2+} -indicator is used for measuring of $[\text{Ca}^{2+}]_i$ concentration. Cells are loaded by immersion in a solution of the permeant acetoxymethyl ester form (Fura-2AM), which is fluorescent but Ca^{2+} -insensitive. Following cleavage by intracellular esterases liberates Fura-2AM (the pentacarboxylate Ca^{2+} -indicator), and thereby being trapped into the cell. Measurement of Ca^{2+} -induced fluorescence at excitation wavelength 340 nm and 380 nm allows for calculation of Ca^{2+} concentrations based 340/380 ratios with an emission wavelength 535 nm (here the wavelengths of emission was at 535 nm and excite at 340 nm and 390 nm were measured but for results, it is often referred to the 340/390 ratio as the 340/380 ratio). The use of the ratio automatically cancels out certain variables such as local differences in Fura-2AM concentration or cell thickness that would otherwise lead to artifacts when attempting to image Ca^{2+} concentrations in cells.

$[\text{Ca}^{2+}]_i$ is calculated from the ratio (R) of fluorescence intensities obtained using the formula of Grynkiewicz, et al., (1985):

$$[\text{Ca}^{2+}]_i = Kd\beta(R - R_{min}) / (R_{max} - R). \text{ (Gillis et al., 1994).}$$

where, R_{max} values obtained by permeabilizing PM with 0.3% Triton X-100 in the presence of 7mM Ca^{2+} and R_{min} values measured by permeabilizing PM with 0.3% Triton X-100 in the presence of 15mM EGTA at pH 7.4 to chelate the available Ca^{2+} ions.

Studies by others and by Ashton and Ushkaryov, (2005) illustrate that measuring the 340 nm/390 nm ratio removes artifactual variations in the fluorescence measured due to changes in dye concentration and instrument efficiency (Ashton and Ushkaryov, 2005).

I.16.5 Three stimuli employed in this study: HK5C, ION5C and 4AP5C.

K^+ was raised (with a corresponding reduction in Na^+ ions) to 30mM (HK). This causes clamped depolarization at the nerve terminal membrane which activates various Ca^{2+} channels and causes a large increase in $[Ca^{2+}]_i$ (depending upon the $[Ca^{2+}]_e$ employed) at the AZ and a subsequent generalized lower increase in Ca^{2+} throughout the nerve terminal.

The application of a potent and selective Ca^{2+} ionophore, ionomycin (ION) (Yoon et al., 2008) (in the presence of extracellular Ca^{2+}) to cells leads to influx of $[Ca^{2+}]_e$, and results in a large increase in the $[Ca^{2+}]_i$, which can induce SV exocytosis and triggers secretion. The molecule acts as a motile Ca^{2+} carrier and enhances Ca^{2+} influx by direct cation entry across biological membranes. Please note that ION5C works throughout the nerve terminal (not just at the AZ) and the amount of Ca^{2+} at the AZ is not same as that for HK.

The addition of 1mM 4-aminopyridine (in the presence of extracellular Ca^{2+}) (4AP) causes the prolonged opening of VGCCs at the AZ due to its action on K^+ channels (note others believe that 4AP also has actions that are independent of the K^+ channels). However, this does not cause a clamped depolarization, unlike HK, and so the actual increase in the $[Ca^{2+}]_i$ at the AZ and throughout the nerve terminal will not be as great as that for HK.

1.16.6 STZ as a model

Streptozocin (STZ), which has been proven to be toxic only to the β -pancreatic cells in rodents; and STZ-induced diabetes is a well established model for T1DM. STZ (an alkylating agent) is a naturally occurring chemical, which is derived from the soil microorganism *Streptomyces achromogenes*. It is a cytotoxic glucose analogue, which preferentially accumulates in pancreatic β -cells via low-affinity GLUT2 glucose transporter in the PM causing necrosis of β -cells. However, STZ has no immediate, direct inhibitory effect upon glucose transport or on glucose phosphorylation by glucokinase (Lenzen, 2008).

When STZ enters the β -cells of pancreas, it breaks into its glucose and methylnitrosourea moiety. The alkylating property of methylnitrosourea modifies biological macromolecules, fragments DNA and destroys the β -cells, causing a state of insulin-dependent diabetes (Lenzen, 2008). It works by transferring the methyl group from STZ to the mitochondrial DNA, thereby impairing the signalling function of β -cell mitochondrial metabolism, causing inhibition of glucose-induced insulin secretion. As a result of this, poly (ADP-ribose) polymerase is overstimulated in order to repair DNA. This results in diminishing cellular NAD^+ and ATP stores, which ultimately causing β -cell necrosis. It causes further damage by protein glycosylation. Although STZ also methylates proteins, DNA methylation is ultimately responsible for β -cell death, but it is likely that protein methylation contributes to the functional defects of the β -cells (Lenzen, 2008).

Due to STZ's chemical properties (As presented in Figure T), mainly due to its greater stability, it is the agent of choice for reproducible induction of a diabetic metabolic state in experimental animals (Lenzen, 2008). Significant and rapid hyperglycaemia is observed at 1wk post-STZ (Tomlinson and Gardiner, 2008).

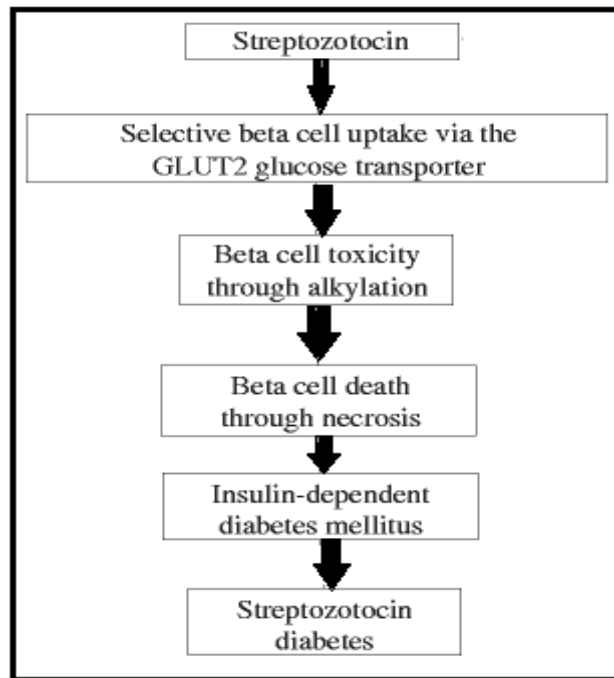


Figure T. Schematic representation of the toxic effects of the glucose STZ in β -cells, which produce chemical diabetes (Lenzen, 2008).

Studies have confirmed that STZ itself does not induce neurotoxicity in insulin-deficient diabetes (Davidson et al., 2009). The mouse/rat model of STZ-induced diabetes has peculiar features that are observed in humans with respect to non-ischemic systolic and diastolic performance and microvascular rarefaction, which are associated with changes in VEGF isoform expression and redox imbalance in the myocardium (Stranahan et al., 2008). Slowing of motor and sensory nerve conduction velocity is a common feature in animal models of STZ-induced diabetes (Thomas et al., 2001). In T1DM rats it has been demonstrated that, impaired vascular reactivity precedes the development of nerve dysfunction as identified by reduced nerve conduction velocity. Reduced conduction velocity develops in motor and sensory nerves in STZ animals (Tomlinson and Gardiner, 2008). In addition to this, studies have demonstrated that 5wk of STZ-induced diabetes caused significant oxidative stress (Han et al., 2009). In an experiment conducted by Davidson et al., (2009), mice displayed hypoalgesia 4-12wks after injection of STZ and subsequent induction of diabetes (Davidson et al., 2009). However, Beiswenger et al. reported that thermal hypoalgesia developed after only 2 weeks of diabetes (Beiswenger et al., 2008).

1.17 Aims and Hypothesis of the Research

Hypothesis

Intracellular Ca^{2+} plays an important role in modifying specific nerve terminal proteins via Ca^{2+} dependent phosphorylation and this determines whether the SVs undergo FF or K&R in nerve terminals prepared from either control or STZ-induced diabetes. Interestingly, higher $[\text{Ca}^{2+}]_i$ levels result in more of the K&R mode of exocytosis and less FF and such conditions prevail in diabetic terminals. It is hypothesized that compared to control animals, diabetic animals may have a larger activation or smaller inactivation of a specific Ca^{2+} channel subtype. Furthermore, this may regulate a larger change in phosphorylation of specific proteins compared to control terminals and this will play a role in the increased amount of K&R in the diabetic terminals. Further correlation of such changes will be compared to the behavioural changes observed in STZ-induced diabetic rats.

Main aim: The main aim of the study is to investigate the role of Ca^{2+} and protein phosphorylation in the switching of mode in control and diabetic nerve terminals. Additionally, to determine the behavioural changes that may occur in diabetic rats.

Specific Aims:

1. To determine the reason for the higher level of $[Ca^{2+}]_i$ present in the diabetic animals by using P-, L-, N- and Q-type Ca^{2+} channel blockers, as these channels may play important physiological roles in the determining the mode of exocytosis.
2. To investigate the role of CaMKII in switching of the exocytotic modes of SVs in both diabetic and control animals by using specific inhibitors.
3. Determining the contribution of dynamin in the switching of the mode of exocytosis in diabetic terminals.
4. Investigating the involvement of PKC in the regulating the modes of SV exocytosis.
5. Determining the role of myosin II in the distinct modes of exocytosis in both diabetic and control terminals by blocking this enzyme with Bleb.
6. Determine the difference in the STZ-induced diabetic rat's behaviour in comparison to the age-matched control rats, thereby finding the link between biochemical and behavioural aspects.

II. Regulation of the Mode of Exocytosis in Control and Diabetic Terminals

II.1 Materials and Methods

All experiments were conducted according to the requirements of the United Kingdom Animals (Scientific Procedures) Act (1986) and approved and supervised by University of Central Lancashire Science and Technology ethical approval committee. The diabetic animals used were under the license of Prof. Jai Paul Singh (License number- PIL 50/824)

II.1.1 Animal house

Male Wistar rats (Charles River, UK) weighing approximately 160-200grams at the time of arrival were used throughout the experiment. The animals were kept in the cage in groups of 2-4, in a temperature ($22\pm 2^{\circ}\text{C}$) and humidity ($55\pm 2\%$) controlled environment, with *ad libitum* access to food pellet and tap water on a 12hour light/dark cycle (lights on 07.00-19.00h). The control animals were housed with wood shaving bedding and the diabetic rats were kept in sawdust bedding in a rectangular wire topped RC2R cages from North Kent Plastics with overall dimensions $56 \times 38 \times 22\text{cm}$ and internal size $1575\text{cm}^2 \times 22\text{cm}$. All the principles for laboratory animals were followed and all the procedures were carried out in accordance with the standard University of Central Lancashire Procedures and Home office guidelines.

The rats rendered to be diabetic (approximately when they were 200-250grams) received single intraperitoneal injection of 150mg/kg of STZ (Sigma, St. Louis, MO, USA) dissolved in 0.05M citrate buffer, pH 4.5. STZ was administered within 10mins after preparation, in the caudal abdominal cavity using sterile 25grams needle by holding the rat in one hand in dorsal position. The injection site was swabbed using povidone-iodine solution and the designated amount of STZ was injected (according to the weight of the animal). During the following four days, the rats were tested for diabetes using glucometer. Animals whose blood glucose level exceeded 200mg/dL after treatment were considered diabetic

(generally, the blood glucose level above 12mM was considered to indicate diabetes but most animals had blood sugar levels averaging about 25mM). Severity of the induced diabetic state was assessed by daily monitoring of blood glucose levels. At the time of the experiments, the diabetic rat brains were the same size as the control and no obvious neuronal dysfunction were observed.

II.1.2 Biochemical Assays

The chemicals that were purchased from Sigma-Aldrich Co. Ltd. (UK) are NaCl, KCl, MgCl₂, hepes, glucose (used for the preparation of the L0 physiological buffers), sucrose, calcium, glutamic acid, dimethyl sulphoxide (DMSO), HCl, dynasore, glutamate dehydrogenase type II, NADPH, advasep-7. Ionomycin, okadaic acid, blebbistatin, cyclosporin A, phorbol-12-myristate-13-acetate were purchased from Tocris Bioscience (UK). FM2-10 dye and Fura-2AM were purchased from Invitrogen Ltd. (UK).

A motor driven Potter homogenizer, specifically designed for synaptosomal preparation was used for the homogenization procedure of the brain tissue. For initial centrifugation Beckman centrifuge with a JA17 rotor was used. Tecan GENios ProTM microplate reader (Figure U) was used for measuring release in the different assays used. XFluorTM software based on Microsoft Excel[®] was used by the plate reader, thereby providing basic instrument handling and display of raw data in an Excel[®] spread sheet. Greiner 96 well, flat (black and transparent) bottom microplates were purchased from Greiner Bio-one (UK).



Figure U. The Tecan GENios Pro: **A)** The Tecan GENios Pro advanced multifunctional injector Reader **B)** Loading of micotitre plate **C)** Compact injector system with high-precision pumps **D)** Patented injector carrier.

Photos courtesy of <http://www.labx.com/v2/adsearch/detail3.cfm?adnumb=367614>

II.1.3 Preparation of Synaptosomes

Following injection with STZ, male Wistar rats were used within 4-12 weeks for all the experimental procedures unless specified. The rats were humanely killed by a blow on the head, followed by cervical dislocation. Thereupon, the skull was carefully cut open and the cerebral cortex was removed and placed in ice-cold sucrose buffer- 0.32M sucrose and 0.1M hepes pH 7.4 (maintained at 1-4° Celcius on ice). The cortex obtained was homogenised in the sucrose buffer and centrifuged in Beckman centrifuge at 4,500rpm [relative centrifugal force (RCF) $2030 \times g$] for 10minutes (mins) at 4°C. The supernatant obtained was subsequently centrifuged at 14,500rpm (RCF- $21,075 \times g$) for 20mins at 4°C and the pellet was discarded. After the centrifugation, the supernatant was removed whilst the pellet was resuspended in L0 buffer (125mM NaCl, 5mM KCl, 1mM

MgCl₂, 10mM glucose, 20mM HEPES; pH 7.4). The homogenized sample was further centrifuged at 14,500rpm at 4°C for 20mins. This step is done to get rid of all the cellular debris and to obtain crude P2 synaptosomes. This P2 synaptosome pellet was used in all the experiments as the contaminating inactive mitochondria and myelin did not interfere with any of the assays, and further purification of synaptosome to remove these contaminants produce synaptosomes that had a shorter time of viability than the P2. The resultant pellet obtained is homogenized in 12ml of ice-cold L0 buffer which was gassed with pure oxygen. The resuspended synaptosomes obtained were kept on ice and continuously gassed with pure oxygen. These synaptosomes were utilized for various different assays such as, glutamate assay, FM2-10 dye assay or Fura-2AM assay. The synaptosomes were used within 6hrs following their preparation. In order to make direct comparisons between the different assays, the synaptosomes were pre-treated identically for the three assays. Relevant controls were carried out in every experiment in order to compare results from different experiments.

The assays for glutamate release, FM2-10 dye release and Fura-2AM measurement of $[Ca^{2+}]_i$, were used with synaptosomes in the presence or absence of nifedipine, ω -agatoxin TK, ω -conotoxin GVIA, ω -conotoxin MVIIC, KN93, KN92, dynasore, cyclosporine A, blebbistatin, okadaic acid and active phorbol ester. Some of these drugs were used in combination (double drug treatment) in certain experiments. In most of the assays, the drug was initially added during a 5min 37°C incubation and was reapplied during the final resuspension step (following washing steps) just prior to the synaptosomes being transferred to the wells of a microtitre plate. However, blebbistatin and dynasore were not added in the last step as mentioned above, but were included in an initial washing step. This procedure was undertaken because preliminary experiments with dynasore and blebbistatin indicated that the presence of the drugs during the measurement stage of the assays interfered with the actual assays. However, both these drugs were known to be still active following their initial removal as indicated by the results. Eventually, such removal of these drugs could lead to reversibility of their effects but this takes longer than the time scale of the experiments conducted. Part of the disturbance may be due to the drugs themselves interfering with the fluorescence signals.

The synaptosomes were stimulated to evoke exocytosis using varying concentration of Ca^{2+} and distinct stimuli; including HK, 4AP, and ION. All the above mentioned assays involve the measurement of fluorescence changes. All these methods are routinely employed in the laboratory of Dr. A. Ashton (see Ashton and Ushkaryov, 2005).

II.1.4 Glutamate Assay

Rat synaptosomes prepared were used in the following procedure for measuring evoked glutamate release under various conditions. $2 \times 1\text{ml}$ aliquots of synaptosomes were added to microcentrifuge tubes and $2 \times 0.25\text{ml}$ of HK and Ca^{2+} (HK5C final) containing buffer (130mM K^+ , 25mM CaCl_2) were added to them. The mixture was incubated at RT for 90seconds (s). Thereafter, the tubes were centrifuged in an Eppendorf bench top centrifuge at $11,500\text{rpm}$ ($\text{RCF } 11,000 \times g$) for 40s. The supernatant was discarded and the pellets obtained were resuspended in gassed $2 \times 0.22\text{ml L0}$ and pooled (final volume 0.5ml as the pellets had some volume) and incubated for 10mins at RT. Thereafter, desired drug or solvent i.e. DMSO (for control samples) was added to the synaptosomes and further incubated for 5mins at 37°C . Then the sample was spun down and the pellet obtained was resuspended in 1ml of L0. Finally, the pellet obtained was resuspended in 1.6ml L0 with the relevant amount of drug or DMSO. Then $0.121\mu\text{l}$ aliquots of synaptosomes samples were added to 12 wells in a row of a Greiner 96 well microtitre plate (black with transparent bottom) after adding $20\mu\text{l}$ of L0 to each well. This was followed by adding $10\mu\text{L}$ of 20mM NADP^+ and $9\mu\text{L}$ of glutamate dehydrogenase (GDH type II: 4 units per mL and so 36mUnits added) to all the wells. Then the plate was incubated for 10mins. In the mean time, synaptosomes for the next part of the experiments were prepared. Following the 10mins incubation, $40\mu\text{l}$ HK or 5mM 4AP or basal buffer without Ca^{2+} was added to wells 6-12 inclusive and wells are thoroughly mixed. $40\mu\text{l}$ of HK with 5mM Ca^{2+} (HK5C) or 4AP with 5mM Ca^{2+} (4AP5C) or $5\mu\text{M}$ ION with 5mM Ca^{2+} (ION5C) are added to wells 1-5 Wells 1-9 are then measured immediately in Tecan GENios ProTM microplate reader. The fluorescence was measured for 21 cycles. The relevant settings for the microplate reader are specified in appendix (table VI.1.1). Following the measurement of glutamate release from the synaptosomes, (as determined by changes in the fluorescence signal), the

response to the addition of a standard amount of Glu was measured. 10 μ L of L0 was added to wells 7-9 and 10 μ L of 1mM (10 nmol) freshly prepared stock glutamate was added to wells 10-12 and following mixing. The change in fluorescence was measured over 15 cycles.

II.1.5 FM2-10 Dye Assay

The assay for FM2-10 dye release was carried out under similar conditions as for the glutamate assay, in order to make a direct comparison between both the assays. However, if a drug was found to perturb Glu release, then it was not tested in the FM2-10 dye assay because one would not be able to interpret results if all SVs were not being released.

Synaptosomes were prepared (See section II.1.3 above) and resuspended in 16mL of L0 buffer. Before the treatment for each set of measurements, 2mL of synaptosomes were oxygenated at RT for 15mins. This step was undertaken to ensure that the terminals had equilibrated properly at this temperature and this would enable maximal FM2-10 dye uptake. After the 15mins incubation 2 \times 1mL of aliquots were spun down in microfuge tubes in an Eppendorf bench top centrifuge at 11,500rpm (RCF 11,000 \times g) for 40s. The pellets obtained were resuspended in 2 \times 0.5mL of L0 buffer and pooled together (final volume was 1.1ml as pellets have some volume). Into this mixture, 2.2 μ L of 50mM FM2-10 dye (100 μ M final concentration) was added and incubated for 60s. Then, 0.275mL HK5C was added and stimulated synaptosomes were incubated for 90s. This step is very important, as this stimulus exposes the luminal membrane domain of exocytosing SVs to FM2-10 dye, which then binds to these membranes and when the SVs re-internalized the dye is also internalized. Following this, the synaptosomes were centrifuged for 40s, and the pellet obtained is resuspended in 1mL of L0 with 2 μ L of 100mM FM2-10 dye and the sample is incubated for 5mins at RT whilst being oxygenated. This is to assure that all the SVs are labelled with the dye as some vesicles take several minutes to internalize and removal of the extracellular dye before this time could lead to wash out of dye from these non-internalized vesicles and as a result not all releasable vesicles would be labelled. Subsequently, specific concentration of drug or DMSO (in case of control samples) was added to the synaptosomes and these were further

incubated for 5mins at 37°C. Following this step, 4µL of 250 nM stock advasep-7 (final concentration 1mM) was added to the terminals. Advasep-7 removes FM2-10 dye from the PM of the synaptosomes; since it has a higher affinity for the dye than the hydrophobic phospholipid bilayer (this reduces the background fluorescence). Such synaptosomes are spun down and the pellet is resuspended in 1ml of L0 buffer. This sample is again centrifuged and resuspended in 1mL of L0 buffer. 5 × 0.2mL of these synaptosomes are prepared and 5 × 1mL of L0 buffer is added to each. This step is done to ensure the maximum amount of dye is removed from the outside of the membrane. These samples are then centrifuged and each aliquoted pellet is resuspended in 0.28ml of L0 containing the desired drug or DMSO. These samples are pooled and 160µL of aliquots were added to each of the 8 wells of Greiner 96 well microtitre plate (flat black bottom). The fluoroimeter measurement settings are specified in appendix VI.1.2. For each row of 8 wells (labelled 1-8), 4 wells were injected with 40µL of either HK5C or 4AP5C or ION5C for evoked FM2-10 dye release measurement, whereas the other 4 wells were injected with 40µL of L0 buffer to produce the values for basal release of dye. Each well was measured separately for 2mins (461 cycles). As the individual wells are being measured separately (unlike for the Glu assay), the first well of the series (well 1) will be measured about 16mins prior to the last sample being measured (well 8). It is essential to take this into account and so each type of experiment was repeated twice within the same experiment, such that in one of 8 wells, the first 4 wells were exposed to stimulus and the last four wells had basal buffer added; whilst in the other row, the first 4 wells had basal buffer added whilst the last four wells had the stimulus. The data was averaged for all the 8 wells exposed to the stimulus and for the 8 wells exposed to basal buffer, to avoid the time dependent difference in the measurements. Each experiment was repeated at least four times to allow us to carry out statistical analysis. Furthermore, the experiments were designed such that the order of the particular drugs treatment was varied in between these distinct experiments to ensure that the age of the synaptosomes (since their preparation) did not play a role in the observed action of a particular drug treatment.

II.1.6 Fura-2-acetoxymethyl ester Assay

Following the synaptosomes preparation (Refer Section II.1.3), they were resuspended in 10mL of L0 buffer. 50 μ L of 50mg Fura-2AM in DMSO (1mM stock: 5 μ M final) was added and the sample was incubated for 30mins at 37°C with oxygen. After incubation, 3mL of L0 buffer was added and 12 \times 1mL of aliquots were transferred to microfuge tubes. These were spun down in an Eppendorf bench top centrifuge at 11,500rpm (RCF 11,000 \times g) for 40s. Each of the synaptosomal pellets obtained were further washed in 1mL of L0 buffer (this step was undertaken to remove any extracellular Fura-2AM) and resuspended in 1.1mL of L0 buffer. These samples were then pooled and kept oxygenated on ice until required.

2 \times 0.8mL of aliquots were placed in the Eppendorf tubes and 2 \times 0.2mL of HK5C was added. These samples were incubated for 90s before they underwent centrifugation with the corresponding pellets being resuspended in 2 \times 0.5mL of L0 buffer. The aliquots obtained were pooled together and transferred to test tubes. These synaptosomes were incubated at room RT for 10mins whilst being oxygenated. Thereafter, the required concentration of the selected drug/ DMSO was added and the synaptosomes were further incubated at 37°C for 5mins. Then the sample was transferred to the microfuge tube and was spun down. The pellet was resuspended in 1mL L0 buffer prior to recentrifugation. Finally, the sample was resuspended in 1.6mL of L0 buffer containing the relevant concentration of the desired drug/DMSO. 0.12mL of this synaptosomal suspension were added to each of 12 wells of a Greiner 96 well microtitre plate (black flat bottom) for measuring the Fura-2AM fluorescence. The settings for the measurement of Fura-2AM fluorescence is detailed in Appendix VI.1.3.

Fluorescence measurements were measured from the top of the plate. Each well was measured twice. Firstly, the samples were measured at the excitation wavelength of 340 nm and emission wavelength of 535 nm for 40 cycles without any stimulus or basal buffer being injected by the integral injector present within the plate reader (Refer Figure U). Thereafter, the settings were changed to measure 160 cycles with a 40 μ L injection of either the selected stimulus or L0 (basal buffer). This double measurement procedure was then repeated with the

next adjacent well except that the samples were measured at the excitation wavelength of 390 nm and emission wavelength of 535 nm. The results for these two adjacent wells were lined up and the 340/380 ratios (actually 340/390) for the time courses could be ascertained (e.g. well 1 at 340 and well 2 at 390 were combined). This procedure was then repeated for wells 3, 4, 5, and 6. In one row, wells 1-6 had Ca^{2+} containing stimulus injected whilst wells 7-12 had basal buffer injected. The wells with L0 buffer act as a measure of the basal change in 340/380, which can be utilized to determine the specific change in $[\text{Ca}^{2+}]_i$ induced by the stimulus. This procedure was continued until all the 12 wells were measured. Following this, a maximum and minimum Ca^{2+} signal was calculated, by introducing 16 μL of 33.75mM Ca^{2+} with the detergent - 4.05% Triton X-100 to the synaptosomes with the stimulus (i.e. that already contained extracellular Ca^{2+}) to observe maximum signal for Ca^{2+} . Likewise, 16 μL of L0 buffer was added to the samples with the basal buffer, followed by 24 μL of a solution containing ethylene glycol tetraacetate acid (EGTA) (Ca^{2+} chelating agent; giving a 15mM final concentration) plus 3% Triton X-100 which was used to determine the minimal signal for Ca^{2+} . All the wells were then measured together firstly at 340 nm and then at 390 nm respectively for 40 cycles each. A repeat of this procedure was carried out in a subsequent row except wells 1-6 had basal L0 buffer injected whilst wells 7-12 had the relevant stimulus injected. The results of these two sets of measurements were averaged to take into account any difference due to the age of the synaptosomes in the wells.

II.1.7 Statistical Analysis

Independent experiments carried out in set of 2-4 were averaged and all the calculations and statistical analyses were performed using Microsoft Excel and GraphPad Prism software. The level of significance for the data was obtained by analysing a few points between the two sets of data being compared. The values were statistically analysed using *unpaired student's t-test*. The results are presented as the average and the error bars are the standard error of the mean (SEM) for the data points obtained. The results with probabilities less than 0.05 were considered to be statistically significant for all the experiments.

Many data points were obtained during the FM2-10 dye assay. Therefore, graphs obtained had the data points too close together and the SEM obtained was fused together such that the line appears as a nearly continuous thickened curve. For presentational purposes some SEM are deleted so that distinct points can be visible.

The legends in the graphs indicate the number of independent experiments and the number of times each condition is measured. The glutamate assay results are presented as the percentage of the maximum Glu released in order to compare the experiments performed on different days and with different conditions. It is to be noted that, even though the weight of the diabetic animals used during the experiments were just more than half the weight of the control rats (presented in Chapter III), the weight of the cortex was similar in both the rats. Therefore, direct comparisons could be carried out between the two rat terminals. The yield of synaptosomes was equivalent for both control and diabetic animals.

The wavelengths for the three assays performed are indicated in the table below (table 3.A). The emission fluorescence obtained is that which is used in the Y-axis in all the graphs accordingly.

Table II.A: Wavelengths used for experimental study

Assay	Excitation Wavelength (nm)	Emission Wavelength (nm)
Glutamate assay	340	465
FM2-10 dye assay	485	555
Fura-2AM assay	340 and 390	535

II. 2 Results

As stated in the introduction, the level of the evoked change in $[Ca^{2+}]_i$ was higher in the diabetic nerve terminals in comparison to the control terminals (Figure i.C). It was speculated that this might be because of differences in the properties of the VGCCs between control and diabetic terminals. Therefore, various Ca^{2+} channel blockers were tested to see whether difference in the activity of distinct VGCCs could account for the differences in the two terminals and whether such channels may play a role in the switching of the modes of exocytosis.

II.2.1 Role of P-type VGCCs

ω -Agatoxin TK (Aga TK) is a potent P-type VGCCs blocker (Wright and Angus, 1996; Serulle et al., 2007) at 50 nM and synaptosomes were incubated with this concentration. 50 nM Aga TK failed to block Glu release in both control and diabetic synaptosomes, indicating that all the releasable SVs have been exocytosed (Figure 1).

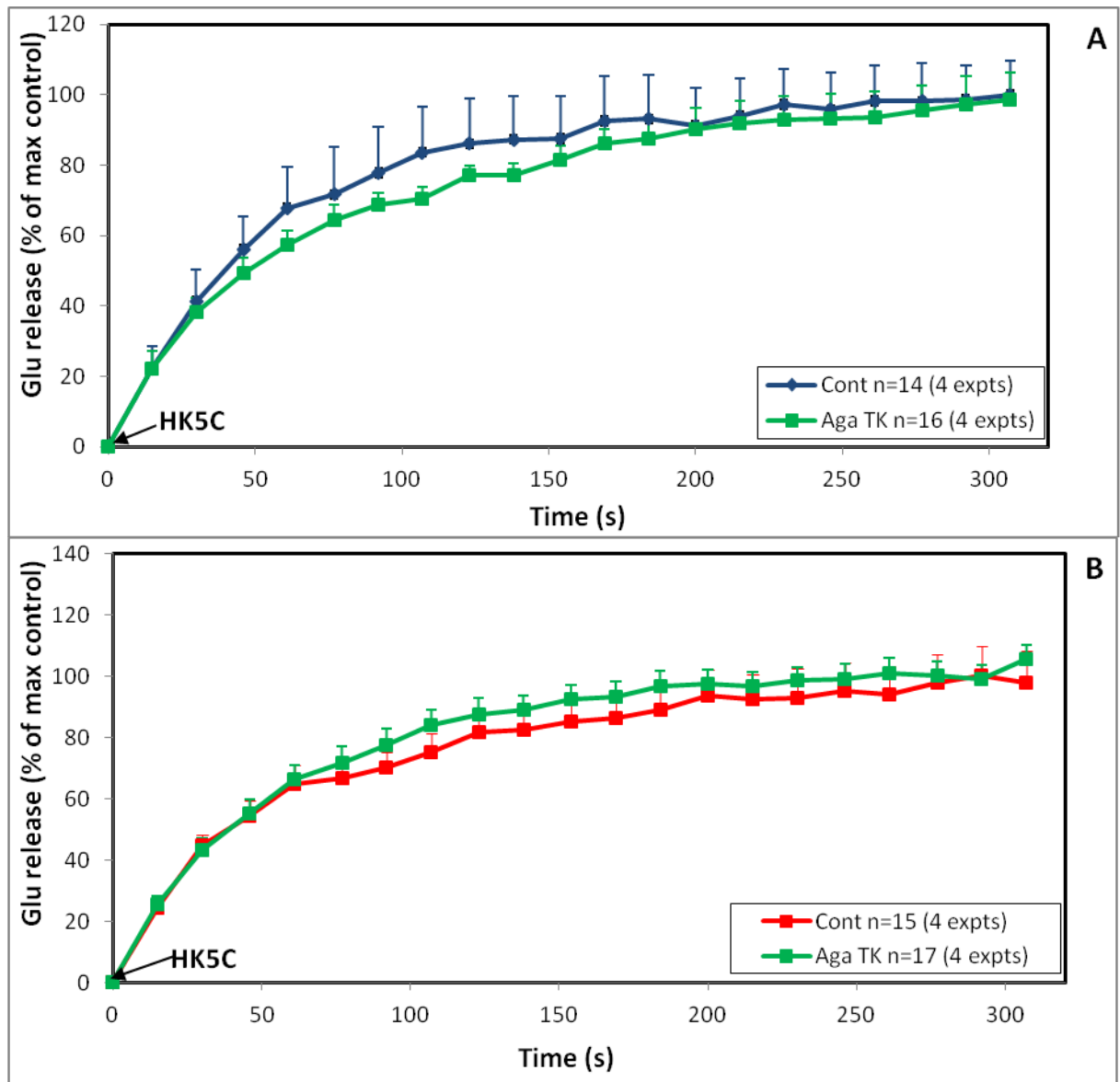


Figure 1: No effect of HK5C evoked Glu release \pm 50 nM Aga TK on (A) Control synaptosomes and (B) Diabetic synaptosomes.

Although, this toxin does not block the Glu release when evoked with HK5C, some of the P-type channels were significantly blocked as when evoked changes in $[Ca^{2+}]_i$ were measured (using Fura-2AM), there was reduced Ca^{2+} entry. This was the case for both the control (Figure 2A) and diabetic synaptosomes (Figure 2B).

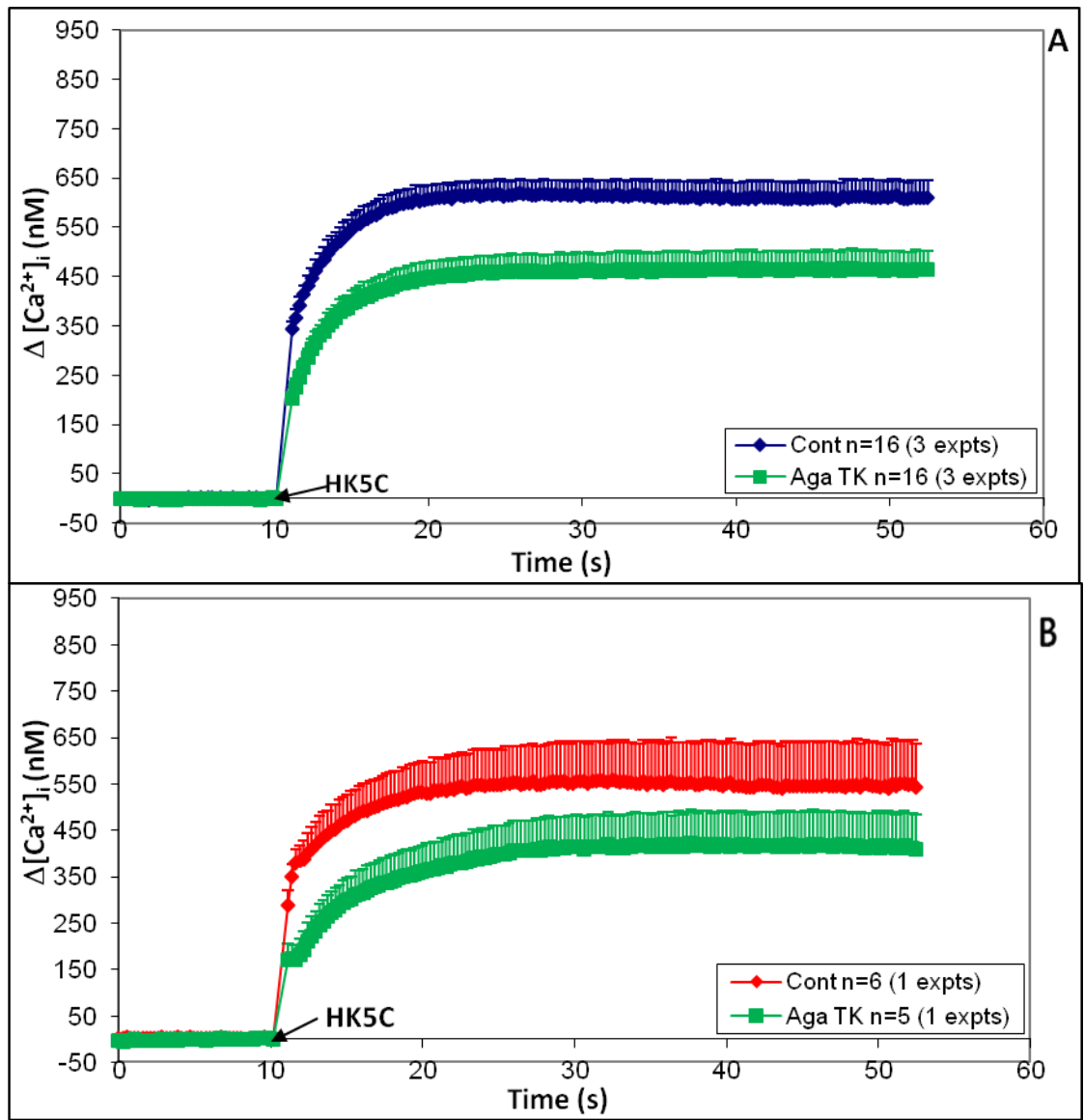


Figure 2: 50 nM Aga TK significantly perturbs HK5C evoked $[Ca^{2+}]_i$ release using Fura-2AM on (A) Control synaptosomes and (B) Diabetic synaptosomes.

Please note that the above experiments were carried out at different times. Further, such measurements were only performed once on diabetic terminals so the actual levels of $\Delta[Ca^{2+}]_i$ for control and diabetic nerve terminals in these figure cannot be compared.

Results observed from Figures 1 and 2 suggest that blockage of P-type VGCCs does not reduce the HK5C evoked changes in $[Ca^{2+}]_i$ sufficiently enough at the AZ to reduce the maximum Glu release. A supra-maximum Ca^{2+} concentration is employed when using HK5C, such that there is more Ca^{2+} entry than is needed to

induce maximum Glu exocytosis, so that even a reduction in this (as seen with treatment with Aga TK) is still sufficient to induce maximum Glu release. This demonstrates that there is sufficient Ca^{2+} entry through other Ca^{2+} channel subtypes for maximum Glu release. At lower $[\text{Ca}^{2+}]_e$ concentration researchers have suggested that P-type channels play a role in Glu release (Wykes et al., 2007; Ladera et al., 2009).

To verify this, the nerve terminals were stimulated with HK in the presence of 1.25mM of Ca^{2+} . Under such conditions, Glu release was significantly decreased in control synaptosomes using 50 nM Aga TK (Figure 3A), thereby proving that P-type channels do play a role in Glu release. However, Figure 3B indicates that 50 nM Aga TK still does not affect the Glu release in diabetic terminals. This data leads us to make an initial conclusion that P-type channels do not appear to contribute to Glu release in the diabetic terminals.

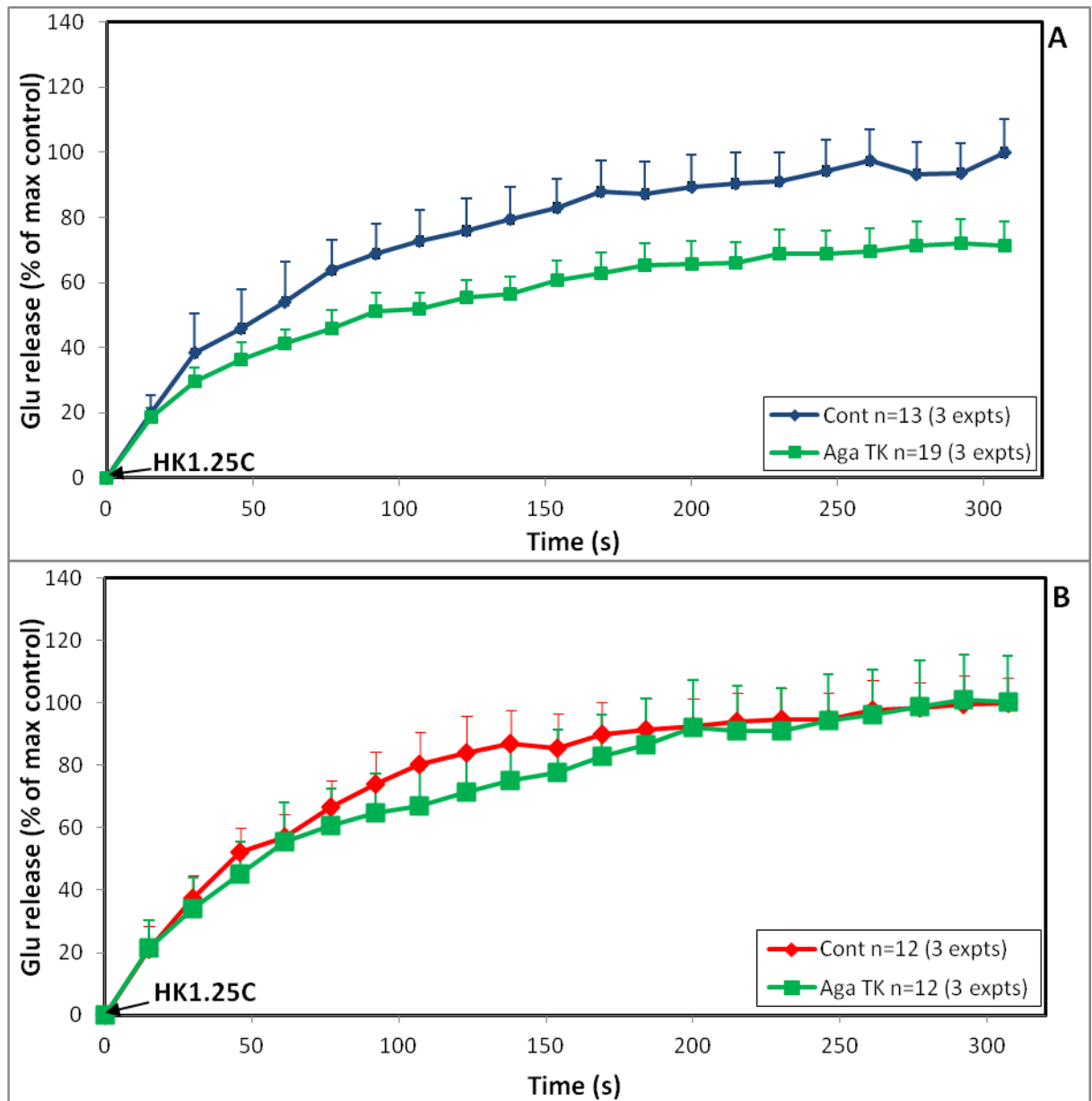


Figure 3: 50 nM Aga TK action on HK1.25C evoked Glu release is significant in(A) Control synaptosomes , but has no effect in (B) Diabetic synaptosomes.

As P-type channel blockade did not affect the total number of SVs exocytosing upon application of HK5C (as Glu release was not perturbed) in control synaptosomes, the role of such channels in switching of the mode of exocytosis was tested using the FM2-10 dye assay. A pre-requisite for relating any changes in FM2-10 dye release to changes in exocytotic mode is that all the releasable SVs must undergo exocytosis (i.e. need maximum amount of Glu release for any particular stimulus).

Figure 4 reveals that blockade of P-type channels with 50 nM Aga TK does not play a role in switching of the mode of exocytosis since there was the same amount of FM2-10 dye release with or without Aga TK treatment.

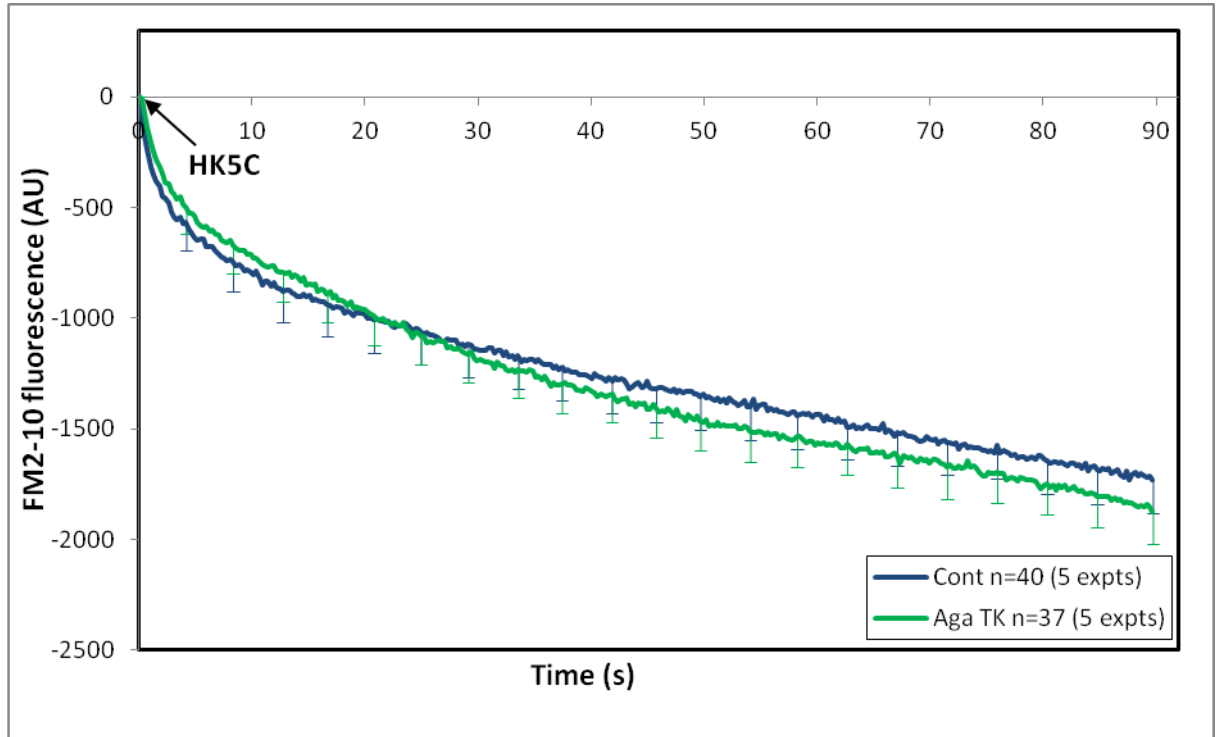


Figure 4: No change in HK5C evoked FM2-10 dye release in control synaptosomes treated with 50 nM Aga TK

II.2.2 Role of L-type channel

Experiments carried out in Dr. Ashton's laboratory show that $1\mu\text{M}$ of the L-type VGCCs blocker nifedipine (Nif) (Dolphin, 2006; Yang et al., 2009) does not affect the HK5C evoked Glu release in control (5A) and diabetic (5B) nerve terminals.

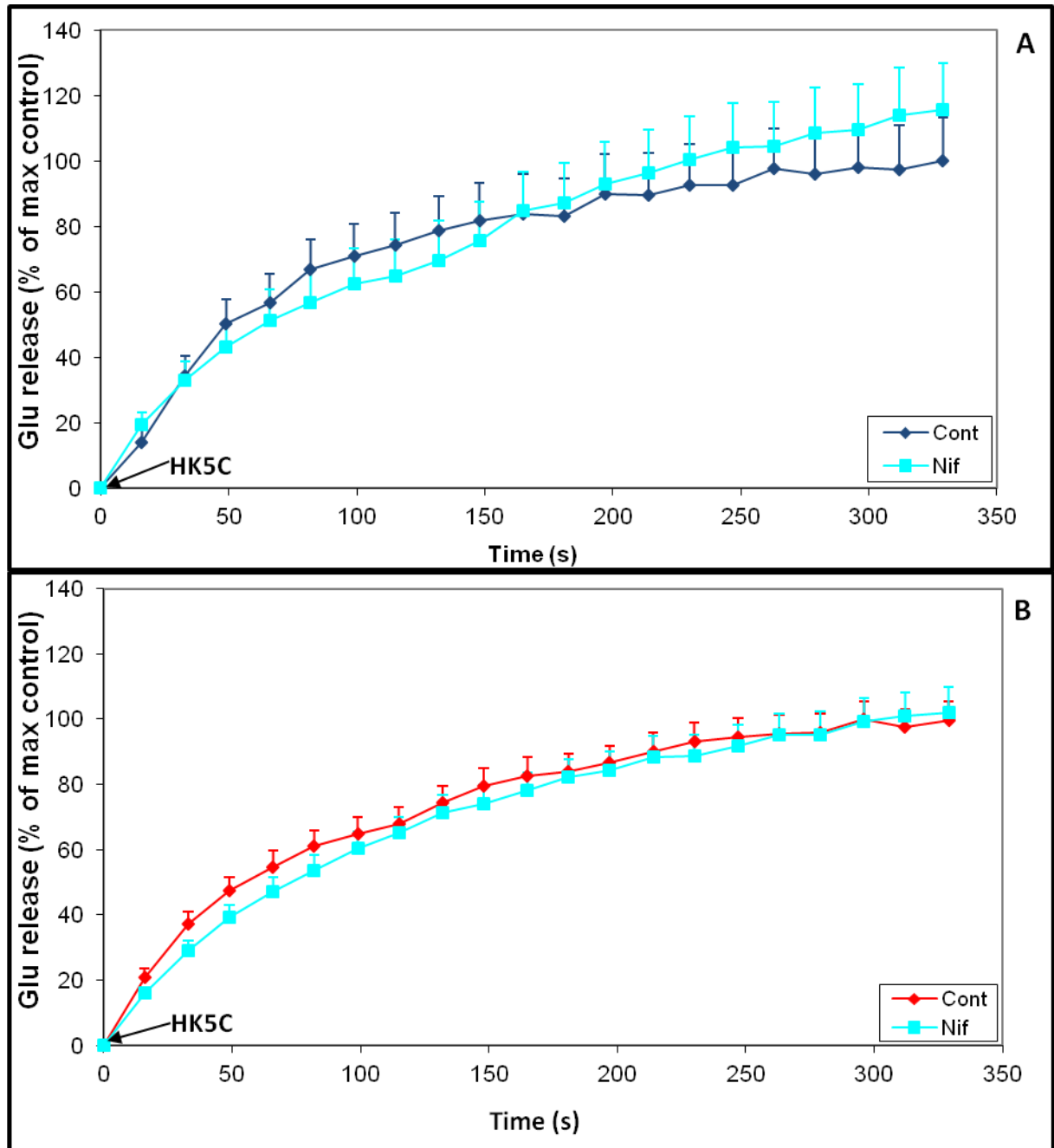


Figure 5: $1\mu\text{M}$ Nif fails to perturb the Glu release evoked by HK5C in (A) Control synaptosomes and (B) Diabetic synaptosomes (Barba, 2010).

Therefore, the role of L-type VGCCs in Glu release was examined using sub-maximal Ca^{2+} concentration i.e. HK with 1.25mM Ca^{2+} (HK1.25C) on control and diabetic synaptosomes. Figure 6A demonstrates that 1 μ M Nif perturbed substantial amount of Glu release in comparison to non-treated terminals in the control synaptosomes. However, like the results with Aga TK, no effect was observed with Nif on the diabetic synaptosomes stimulated with HK1.25C (Figure 6B). Clearly, the contribution of Ca^{2+} channels to evoked release seems to be distinct between control and diabetic terminals.

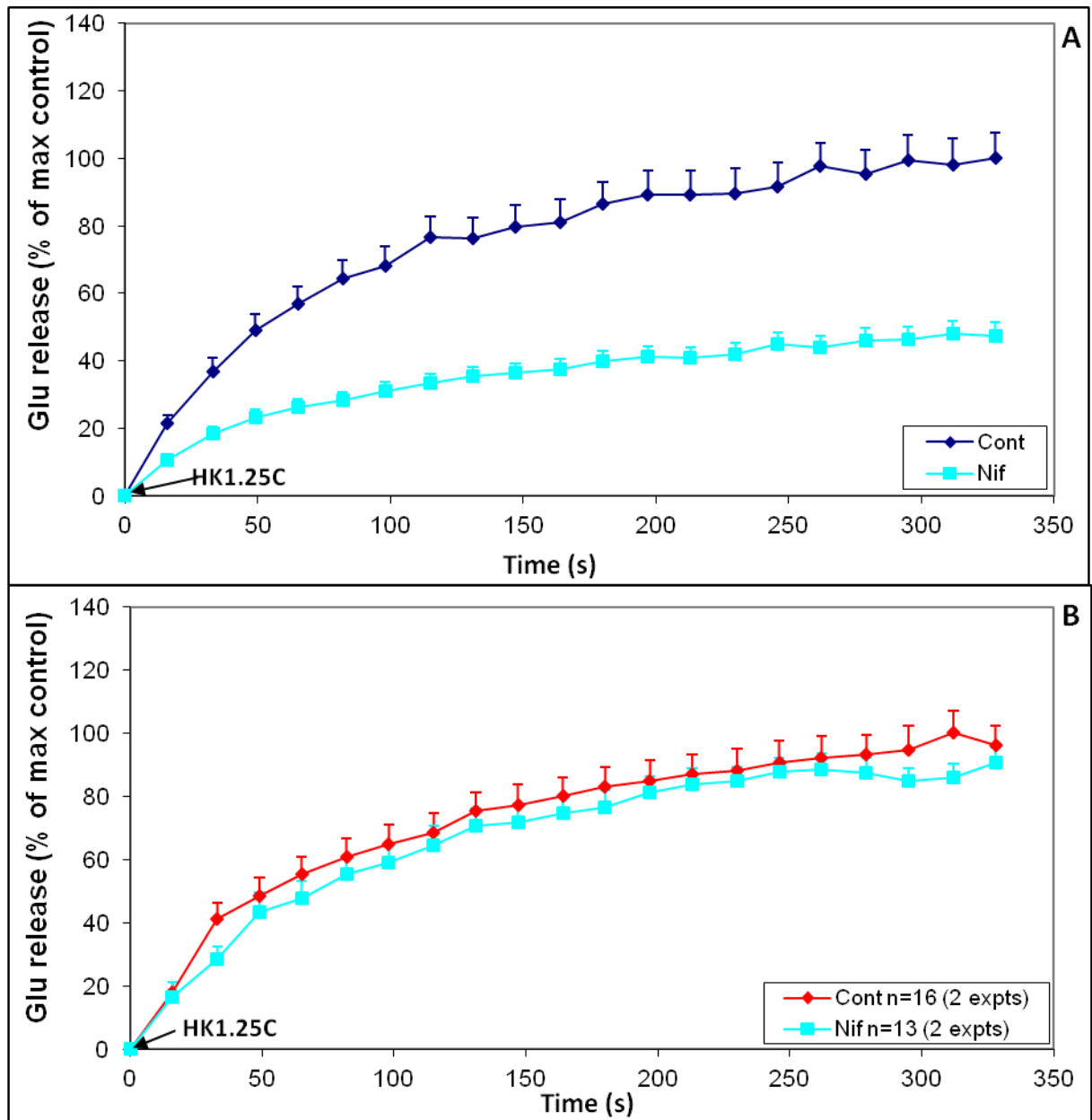


Figure 6: (A) Significant amount of Glu release perturbed when evoked with HK1.25C in control synaptosomes treated with 1 μ M Nif (Barba, 2010) (B) No difference observed when similar treatment applied on Diabetic synaptosomes.

As the amount of Glu released was not perturbed using HK5C evoked release, the FM2-10 dye assay was carried out to study the role of L-type channels in the switching of the modes.

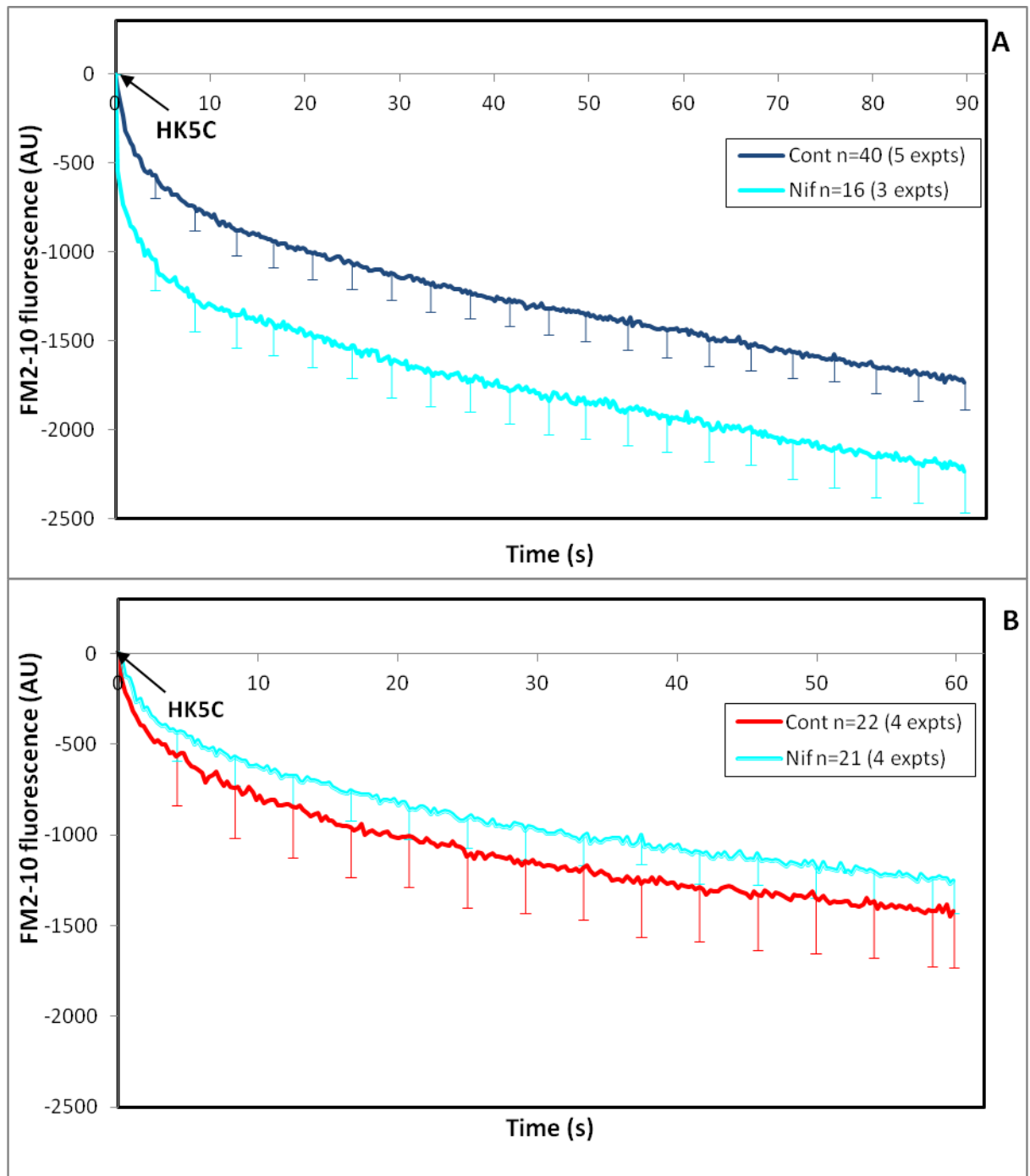


Figure 7: HK5C evoked FM2-10 release is increased in the presence of $1\mu\text{M}$ Nif in (A) Control terminals but is not changed in (B) Diabetic terminals.

Remarkably, $1\mu\text{M}$ Nif exhibits distinct effects on the control and diabetic synaptosomes. Figure 7A demonstrates that the blockage of L-type VGCCs causes a switch in the mode from K&R mode of exocytosis to FF in control nerve terminals. However, Figure 7B shows that $1\mu\text{M}$ Nif does not affect the mode of exocytosis in the diabetic terminals. This suggests that, L-type channels in

diabetic terminals do not play the same role as they play in control terminals. For control terminals, this result is important, as for the first time it is demonstrated that, Ca^{2+} going through specific VGCC, in this case L-type VGCCs, can play a role in the regulating the mode of exocytosis. Therefore, Ca^{2+} going through the L-type channels would allow the RRP to undergo K&R mode of exocytosis, and when this channel is blocked, the mode is switched to FF.

Figure 8 displays the comparison between FM2-10 dye release with $1\mu\text{M}$ Nif and $0.8\mu\text{M}$ OA (okadaic acid), which is known to switch all RRP from K&R mode of exocytosis to FF (Dr. Ashton's unpublished data). The two curves look almost similar, thereby suggesting that Nif also switches all the RRP from K&R to FF mode of exocytosis. Please refer later for more experiments involved with OA.

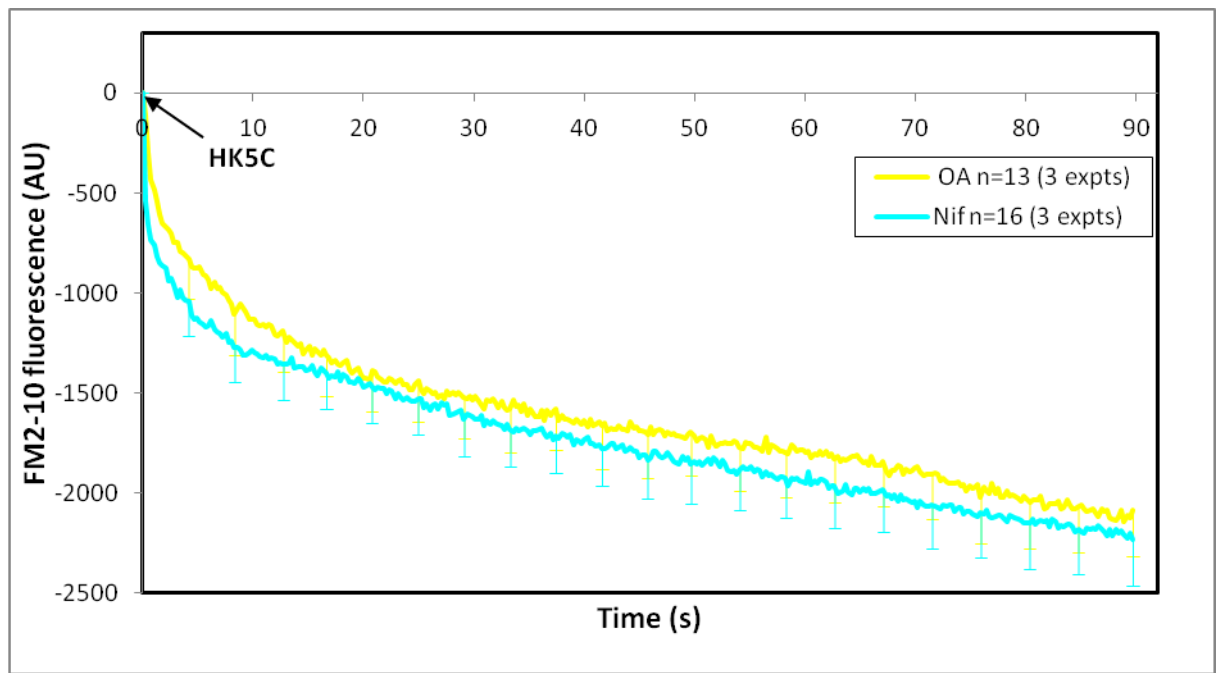


Figure 8: Similar amount of FM2-10 dye release observed in Control terminals evoked with HK5C and treated with $0.8\mu\text{M}$ OA or $1\mu\text{M}$ Nif

Finally, figure 9 show that $1\mu\text{M}$ Nif reduces some Ca^{2+} entry in control synaptosomes stimulated with HK5C. This indicates that, there must be supra-maximum Ca^{2+} present in the extracellular space, such that Ca^{2+} entry through the other VGCCs types, is sufficient to permit maximum Glu release (Figure 5A: see similar arguments above for Aga TK), although blockade of L-type channels does cause a change in the mode of fusion.

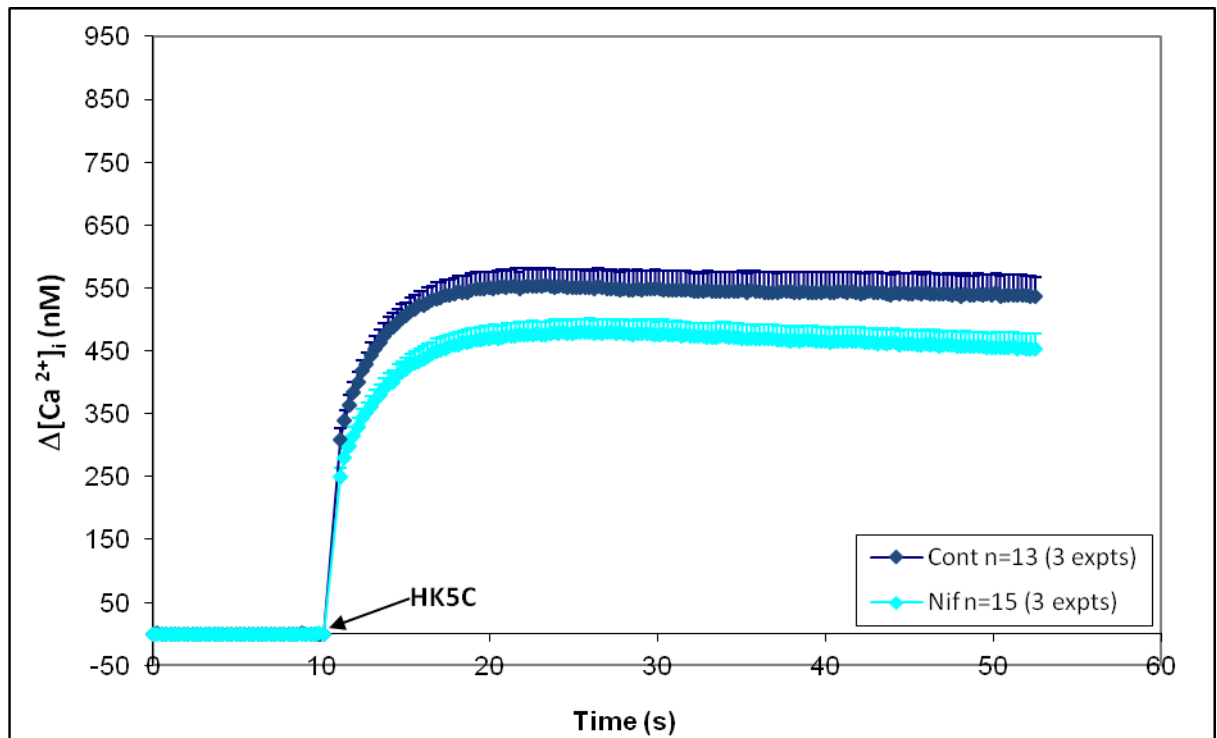


Figure 9: Application of 1 μ M Nif significantly decreases HK5C evoked $[Ca^{2+}]_i$ in control terminals

II.2.3 Role of N-type VGCCs

After studying P- and L-type VGCCs, the role of N-type VGCCs were elucidated by using N-type channel blocker 1 μ M ω -conotoxin GVIA (GVIA) (Wright and Angus, 1996) on the control and diabetic nerve terminals.

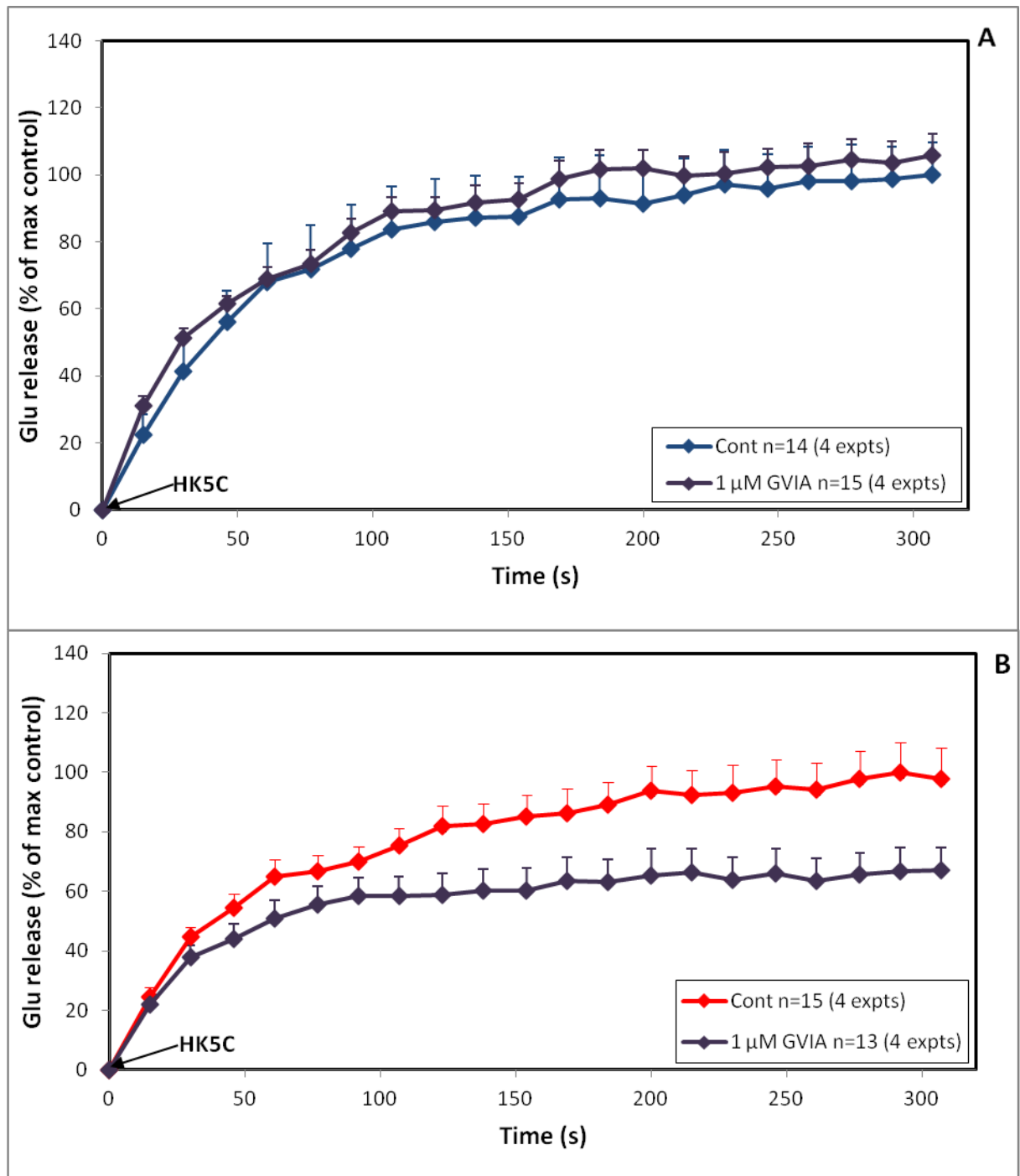


Figure 10: 1μM GVIA has no effect on HK5C evoked Glu release 1μM GVIA in (A) Control synaptosomes but has an effect in (B) Diabetic synaptosomes.

When N-type VGCCs are blocked using 1μM GVIA, the stimulated HK5C Glu release in control nerve terminals is not altered (Figure 10A). Interestingly, however, 1μM GVIA inhibits some of the HK5C Glu release in diabetic terminals (Figure 10B).

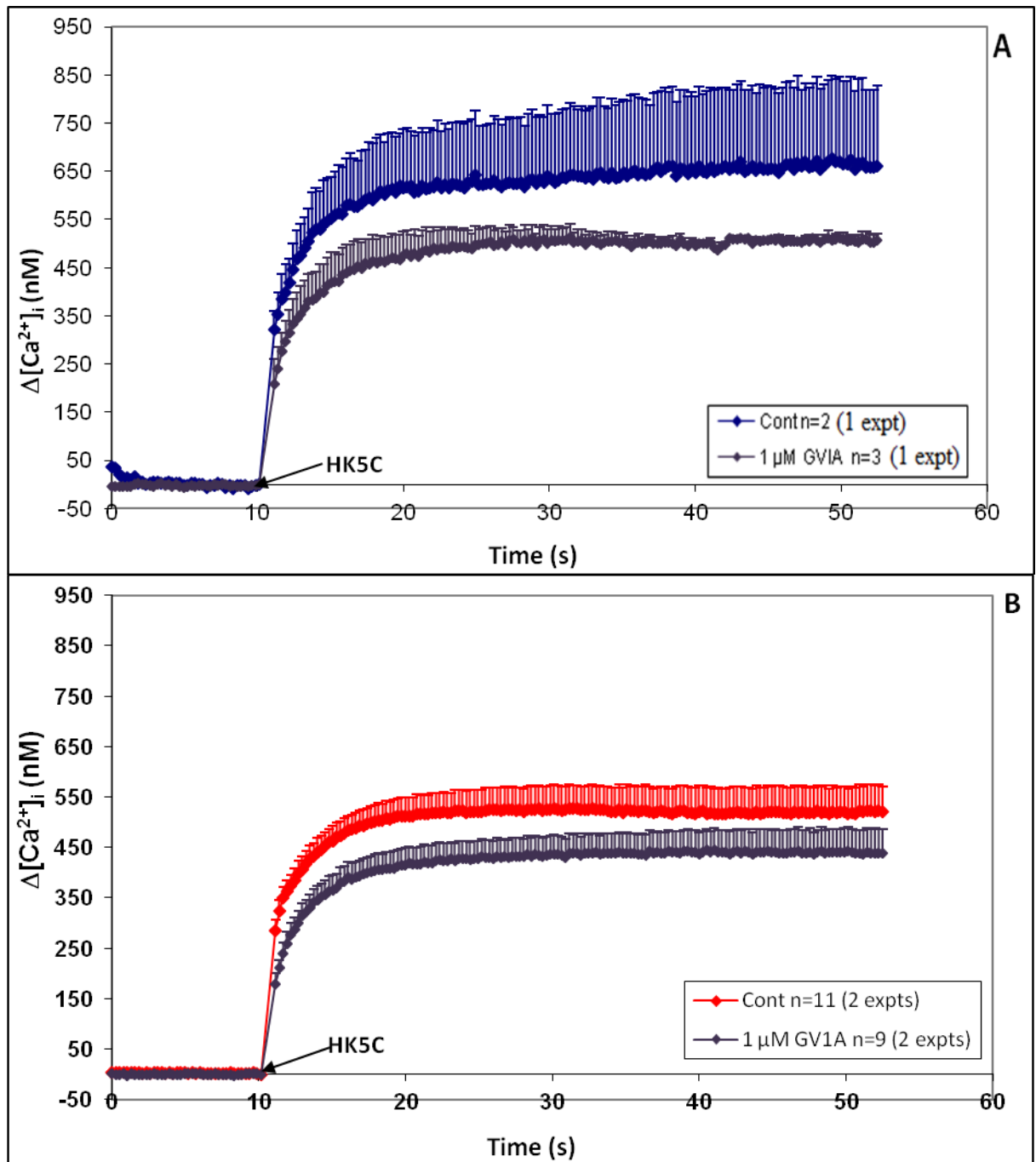


Figure 11: There is a significant decrease in HK5C evoked change in $[\text{Ca}^{2+}]_i$ upon addition of $1\mu\text{M}$ GVIA in (A) Control synaptosomes and in (B) Diabetic synaptosomes.

Figures 11A and 11B indicate that $1\mu\text{M}$ GVIA does perturb the Ca^{2+} entry in both control and diabetic nerve terminals. The result demonstrates that this toxin blocks N-type VGCCs at least to a certain extent.

Previously, researchers have implicated the role of N-type channels in the Glu release in control terminals (Ladera et al., 2009) and this was demonstrated using sub-maximal Ca^{2+} level i.e. HK1.25C (Figure 12) .

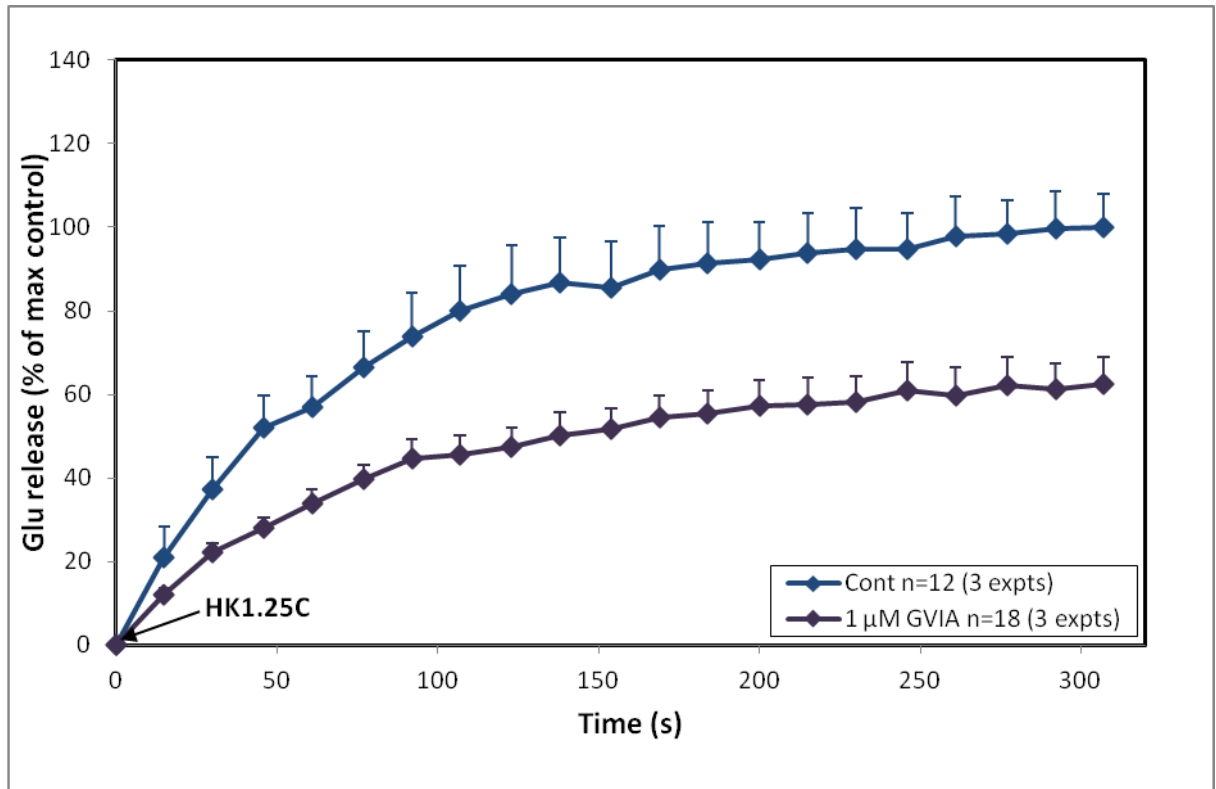


Figure 12: 1 μM GVIA perturbs HK1.25C evoked Glu release in Control synaptosomes.

When FM2-10 dye release was studied with control terminals using HK5C no change in dye release is observed, a result similar to that for Aga TK but different from Nif. These results lead to the conclusion that the N-type VGCCs do not play a role in switching the mode of exocytosis in control nerve terminals.

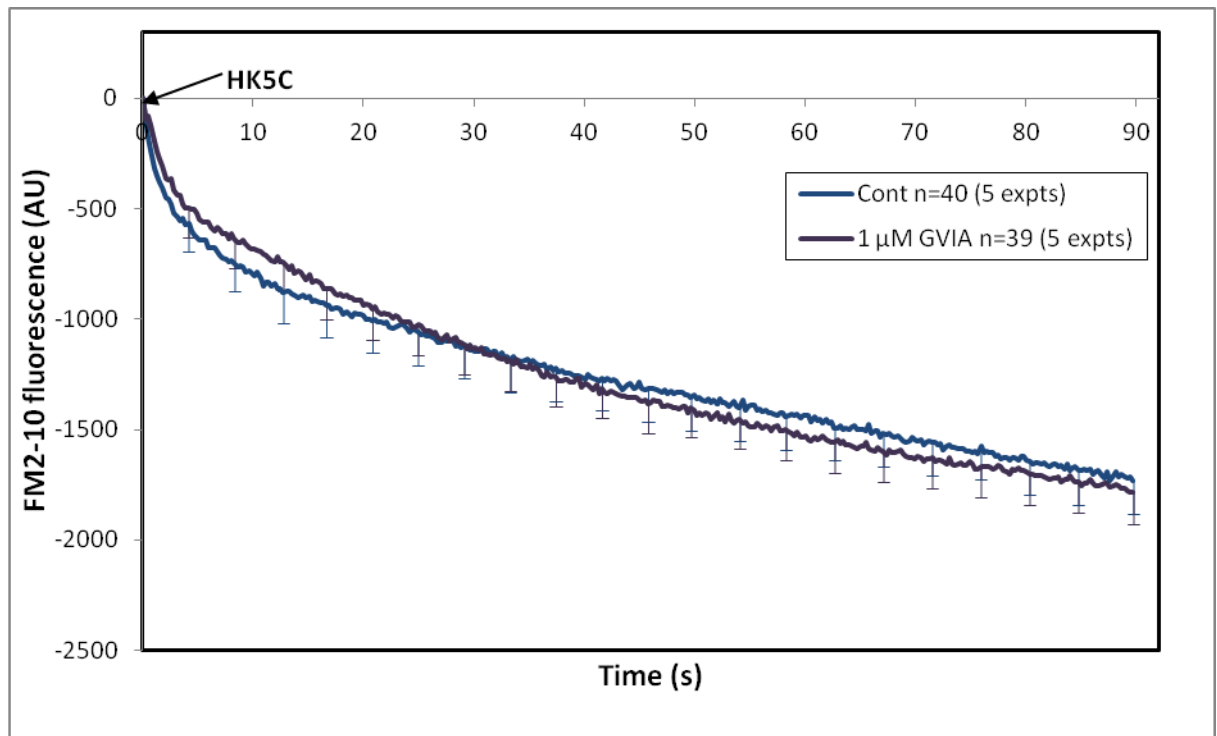


Figure 13: No change in the FM2-10 dye release in control terminals evoked with HK5C following treatment with 1 μ M GVIA

Clearly, 1 μ M GVIA does not affect either the Glu release or the FM2-10 dye release in control terminals, but it appears to inhibit significant amount of Glu release in diabetic terminals (Figure 10B). Therefore, this concentration of GVIA cannot be used to study the FM2-10 dye release in diabetic terminals.

However, as the data suggests that N-type channels do play a role in SV exocytosis in diabetic terminals, further studies were undertaken. Investigations were carried out to ascertain whether the use of sub-maximal dose of GVIA might produce a sub-maximal blockade of N-type VGCCs in diabetic terminals, such that Glu release is not perturbed, but that such a reduction in Ca²⁺ entry may be sufficient to switch the mode of exocytosis. Thus, the concentration of GVIA was varied and its effects were observed. Figures 14-18 demonstrate the effect that increasing sub-maximal concentrations of GVIA have upon HK5C evoked Glu release and FM2-10 dye release from diabetic terminals.

As demonstrated in Figure 14, 100 nM GVIA has no effect on the HK5C evoked Glu release in diabetic terminals (Fig 14A) and negligible effect on FM2-10 dye release (Fig 14B).

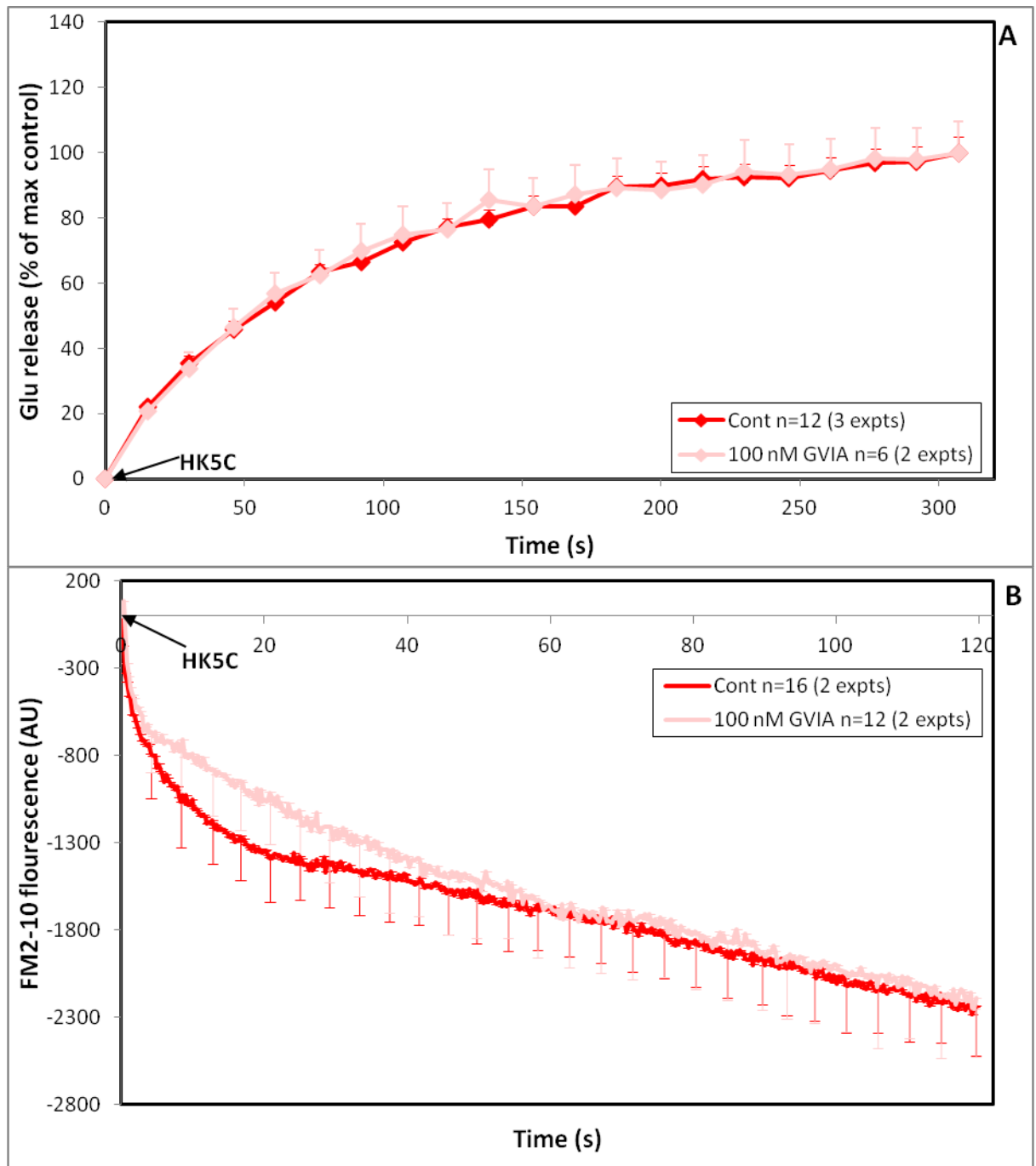


Figure 14: 100 nM GVIA has no effect on HK5C evoked (A) Glu release or (B) FM2-10 dye release on diabetic nerve terminals.

When the concentration of GVIA was increased to 150 nM, there was no effect on Glu release (Figure 15A) although there was a small effect on FM2-10 release but this was not statistically significant (Figure 15B).

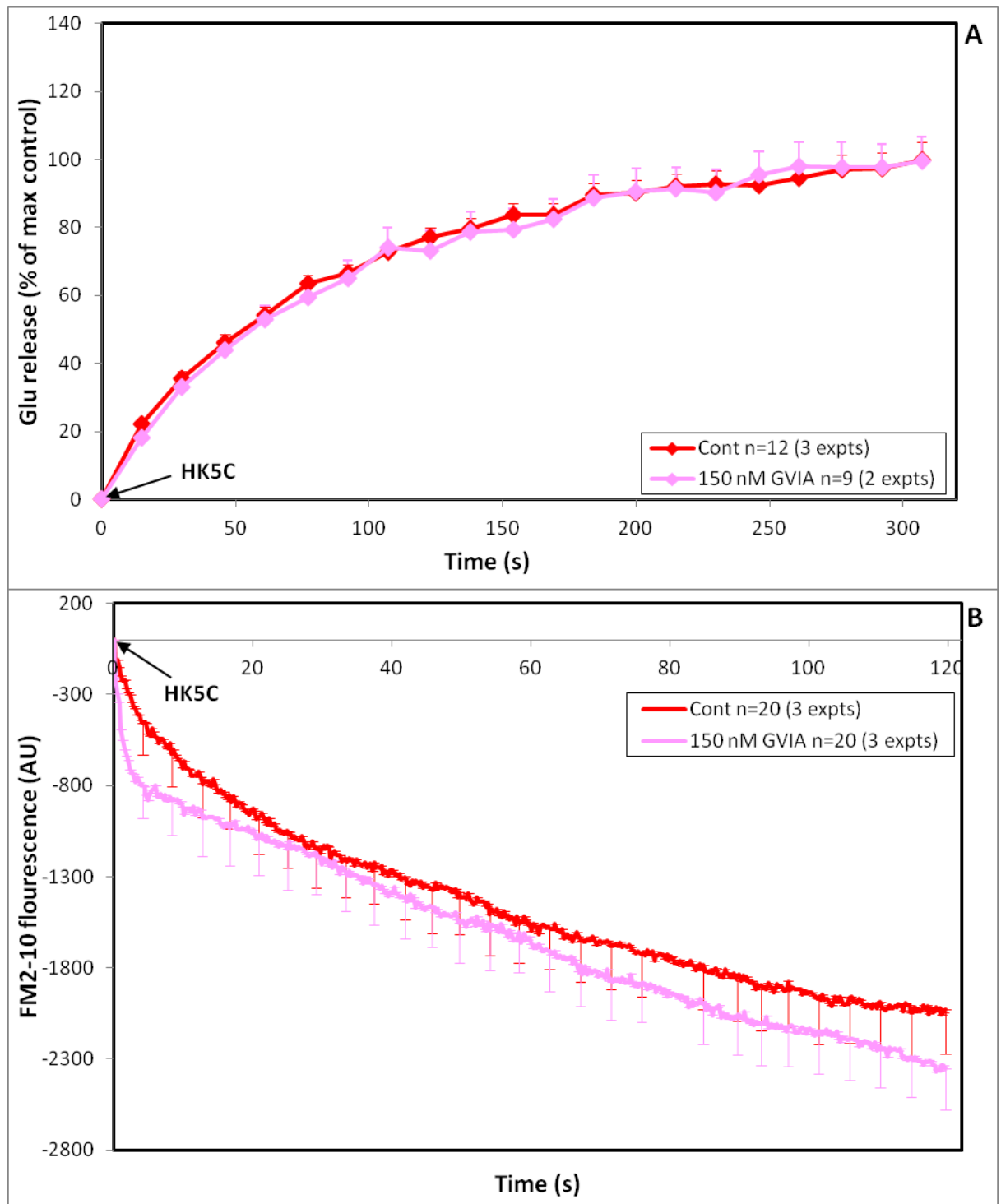


Figure 15: 150 nM GVIA has no effect on (A) HK5C evoked Glu release but has a small but non-significant effect on (B) HK5C evoked FM2-10 dye release in diabetic nerve terminals.

Then the concentration was increased to 200 nM. GVIA failed to have an effect on HK5C evoked Glu release (Figure 16A), but the FM2-10 dye release appears to be increased (Figure 16B) as compared to the effect produced by 150 nM

GVIA. However, the increase in the FM2-10 dye release is still not significant as compared to control nerve terminals.

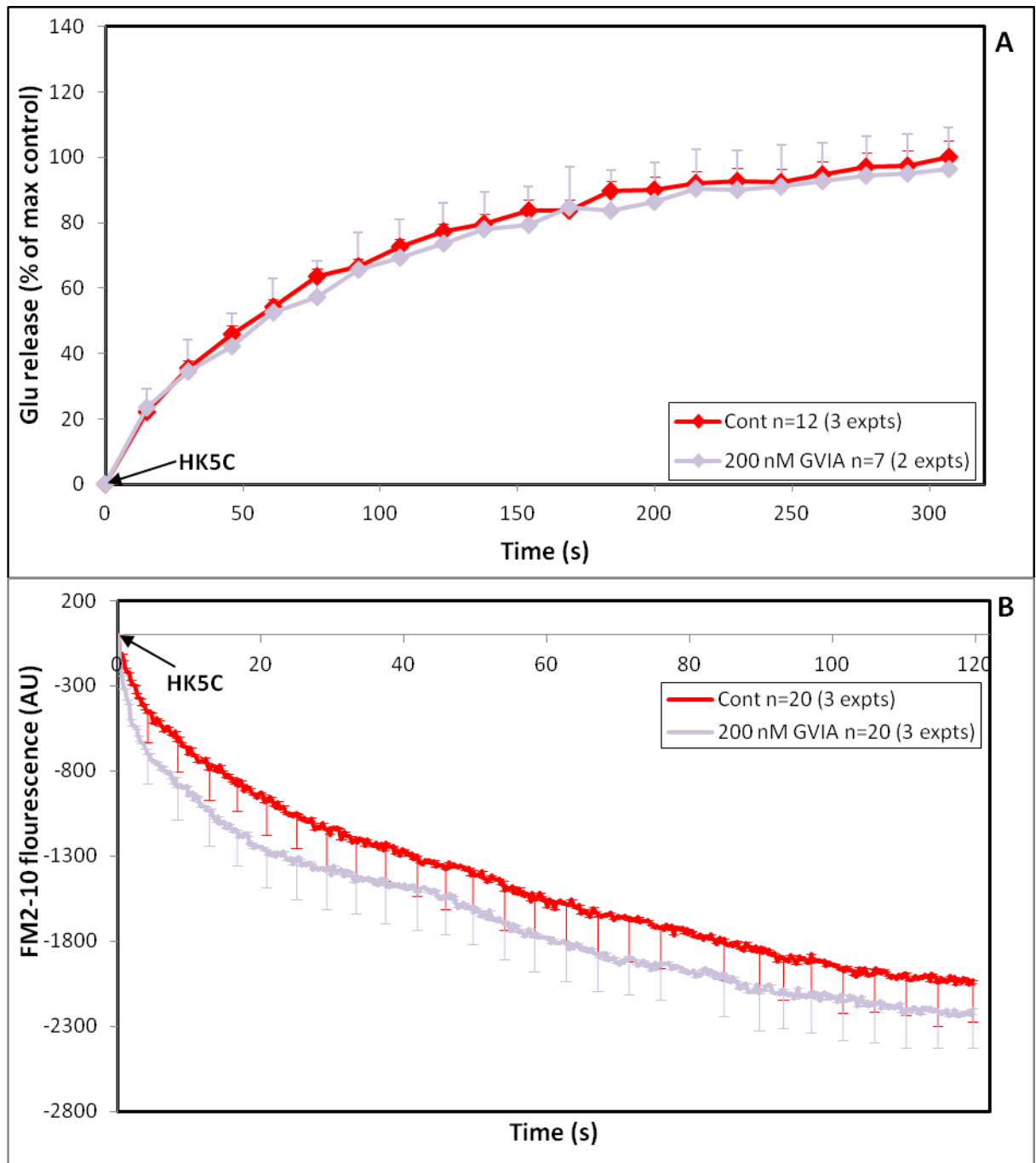


Figure 16: 200 nM GVIA has no effect on (A) HK5C evoked Glu release but has a small but non-significant effect on (B) HK5C evoked FM2-10 dye release in diabetic nerve terminals.

With an increase to 300 nM of GVIA, no effect on Glu release is demonstrated (Figure 17A), but now a significant increase in FM2-10 dye release-for the first 30s out of the 120s measurement cycle-is observed when compared to the control nerve terminals. This is an important result, as a condition has been established such that, this sub-maximal dose of GVIA can be involved in switching of the mode of exocytosis. However, this experiment needs to be carried out more times in order to show the significant difference for the entire time course.

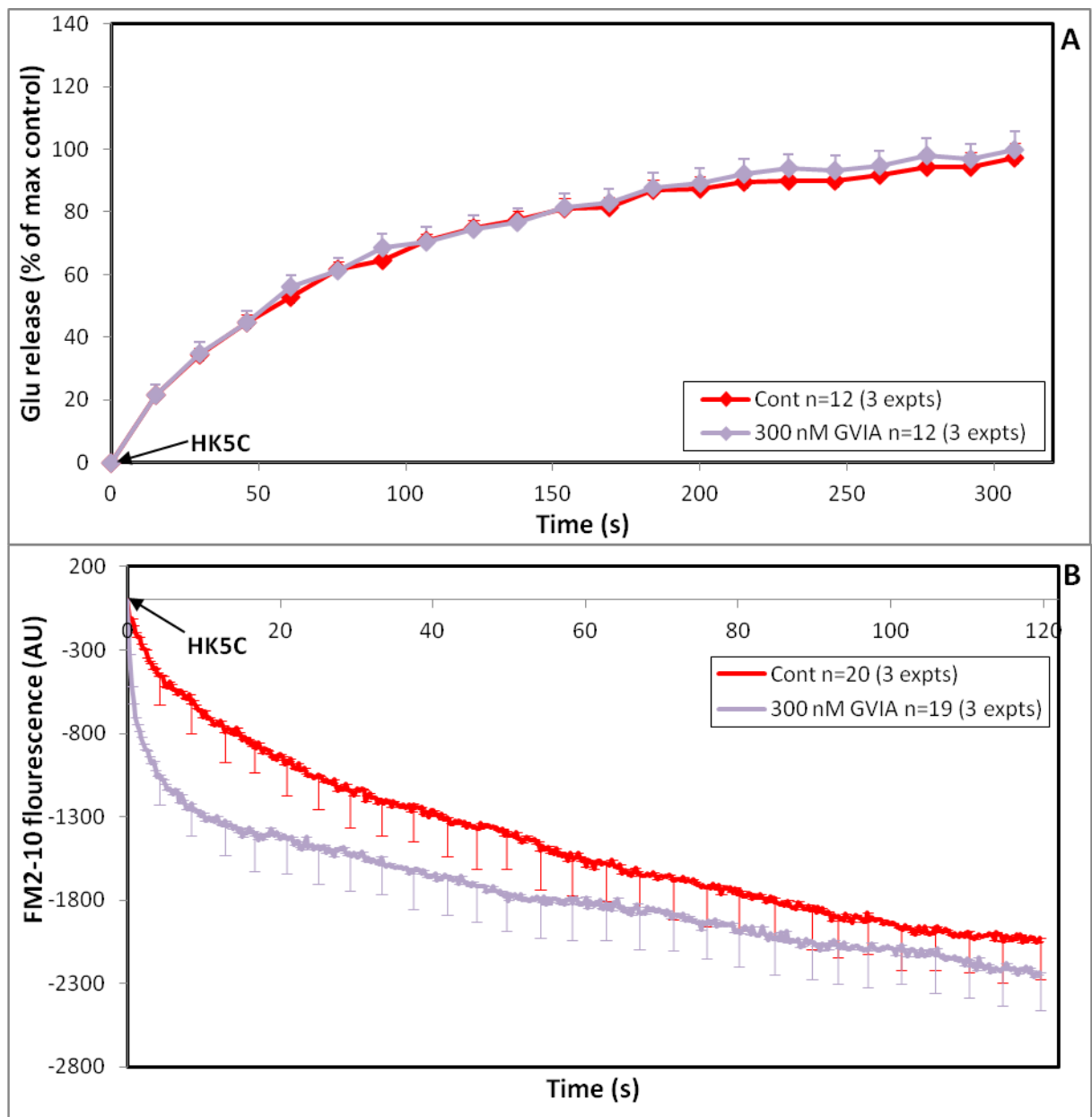


Figure 17: 300 nM GVIA has no effect on (A) HK5C evoked Glu release but has a significant effect on (B) HK5C evoked FM2-10 dye release in diabetic nerve terminals.

The use of a higher concentration of N-type Ca^{2+} channel blocker (400 nM GVIA) actually induced a small blockade in HK5C evoked Glu release (Figure 18A), but this is less than as seen with 1 μM GVIA. Clearly, as this condition causes less SV to exocytose one would expect a reduction in the amount of FM2-10 dye that would be released and this is actually what is found when the effect of 400 nM GVIA on FM2-10 dye release from diabetic terminals is measured (Figure 18B).

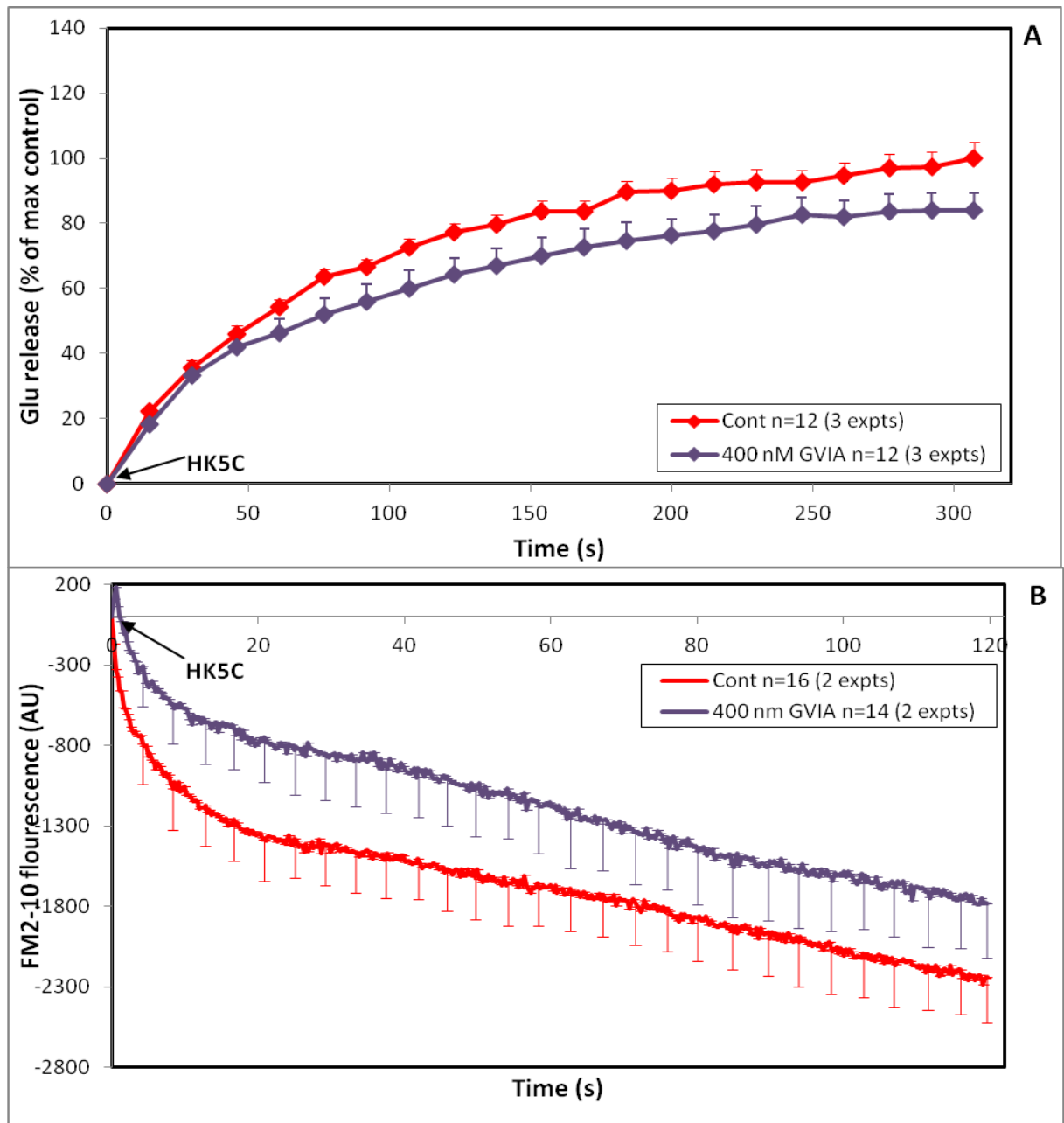


Figure 18: 400 nM GVIA reduces both (A) HK5C evoked Glu release and (B) HK5C evoked FM2-10 dye release in Diabetic nerve terminals.

From the above results obtained with GVIA, there remains a possibility that the best sub-maximal concentration of GVIA to study the role of N-type Ca^{2+} channels in regulating the mode of exocytosis has not yet been established, as this could be between 200 and 300 nM (250 nM) or even between 300 and 400 nM (350 nM). Such concentrations of GVIA need to be tested in the future.

After monitoring the role of individual VGCCs, we conclude that in control terminals L-type channels play an important role in the switching of the mode of exocytosis, whilst in the diabetic terminals N-type channels seem to play distinct role in controlling the fusion of the vesicles and also the mode of exocytosis. The present results support this argument that P- and N-type channels in the control synaptosomes, and L- and P- type channels in diabetic synaptosomes do not play a role in regulating the mode of exocytosis.

II.2.4 Role of P-, Q- and N-type VGCCs

A toxin that blocks several channels together was tested in the following experiments. N-, P- and Q-type Ca^{2+} channels are inhibited by ω -conotoxin MVIIC (MVIIC) (Wright and Angus, 1996).

Figure 19A establishes that $1\mu\text{M}$ MVIIC treatment leads to a reduction in HK5C evoked Glu release from control synaptosomes. However, in diabetic terminals, MVIIC induced a smaller amount of inhibition of HK5C evoked Glu release (Figure 19B) than that seen in the control terminals.

This result obtained is not surprising; as more N-type channels are active in the diabetic synaptosomes in comparison to the control. Also it has been established that MVIIC binds to N-type Ca^{2+} channels with an affinity of 10-100 fold lower than GVIA (Randall and Tsien, 1995) and blocks P-type Ca^{2+} channels at concentrations 100-1000 fold higher than Aga TK with very slow on/off kinetics. It is believed that, MVIIC is potent at inhibiting Q-type channels (Wright and Angus, 1996). Thus, this toxin probably only partially blocks the three distinct channels but as only the N-type channels seems to be important for diabetic terminals, one would expect less blockade in these terminals.

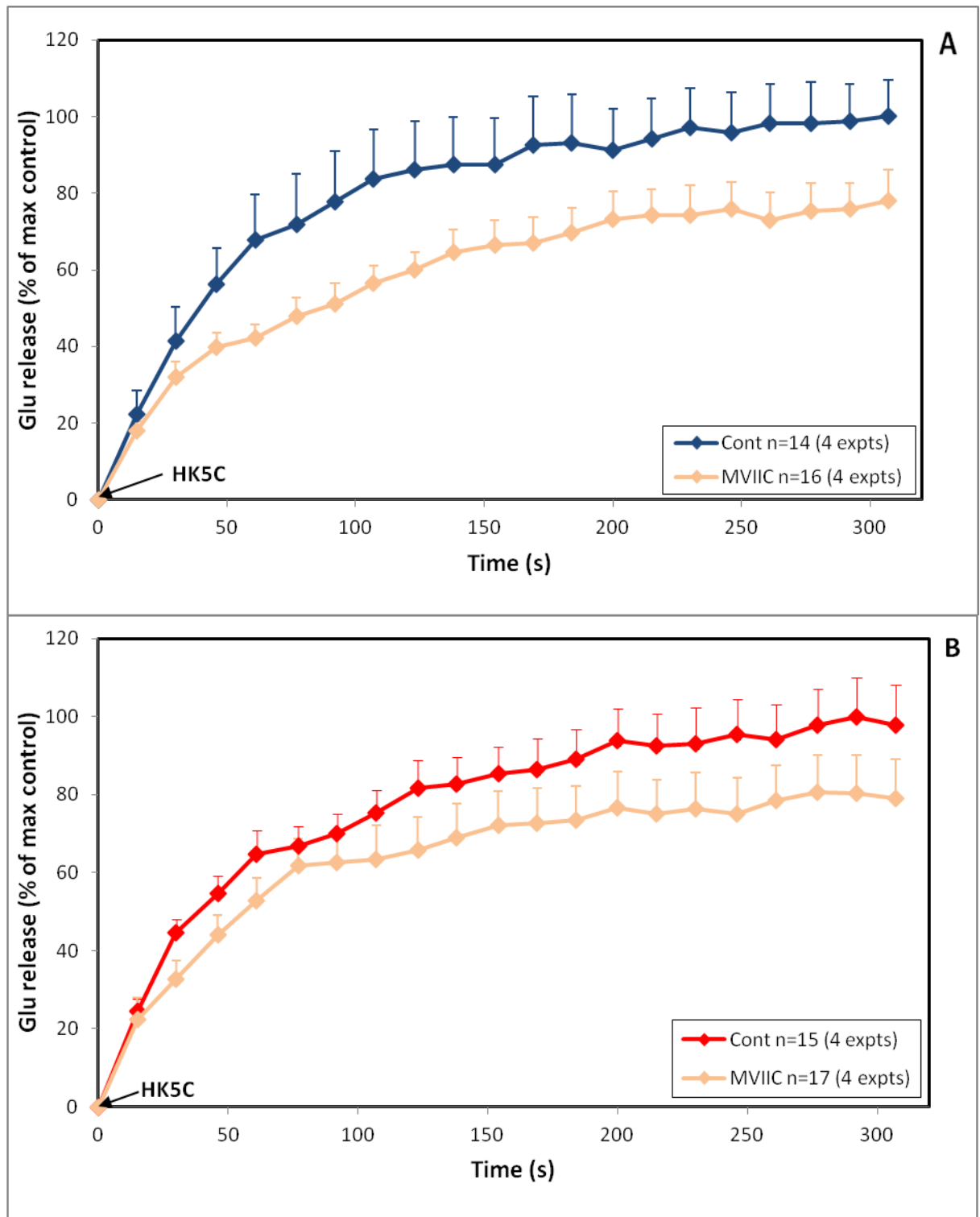


Figure 19: Significant decrease in HK5C evoked Glu release upon application of 1µM MVIIC on (A) Control Synaptosomes and (B) Diabetic Synaptosomes.

II.2.5 CaMKII define mode of exocytosis for RRP

Research was carried out to determine whether CaMKII might play a role in regulating the mode of exocytosis. An increase in the level of $[Ca^{2+}]_i$ during stimulation activates CaMKII and this can regulate SV release by several distinct mechanisms (Pang et al., 2010). This can be tested by using a specific CaMKII inhibitor 10 μ M KN93. This methoxybenzenesulfonamide compound exerts its effect by competing for the CaM binding site of CaMKII, thereby inhibiting CaMKII's effect (Rezazadeh et al., 2006). Importantly, the specificity of KN93 can be assessed by using its inactive homolog, KN92, which is known not to affect CaMKII. To study effect of CaMKII, three stimuli; HK5C, ION5C and 4AP5C were employed.

Remarkably, when the Glu release was studied using the above three stimuli, it was discovered that, 10 μ M KN93 significantly reduced the number of SVs fusing when HK5C (Figure 20A) and ION5C (Figure 20B) were applied whereas interestingly, the Glu release was unaffected with 4AP5C (Figure 20C)

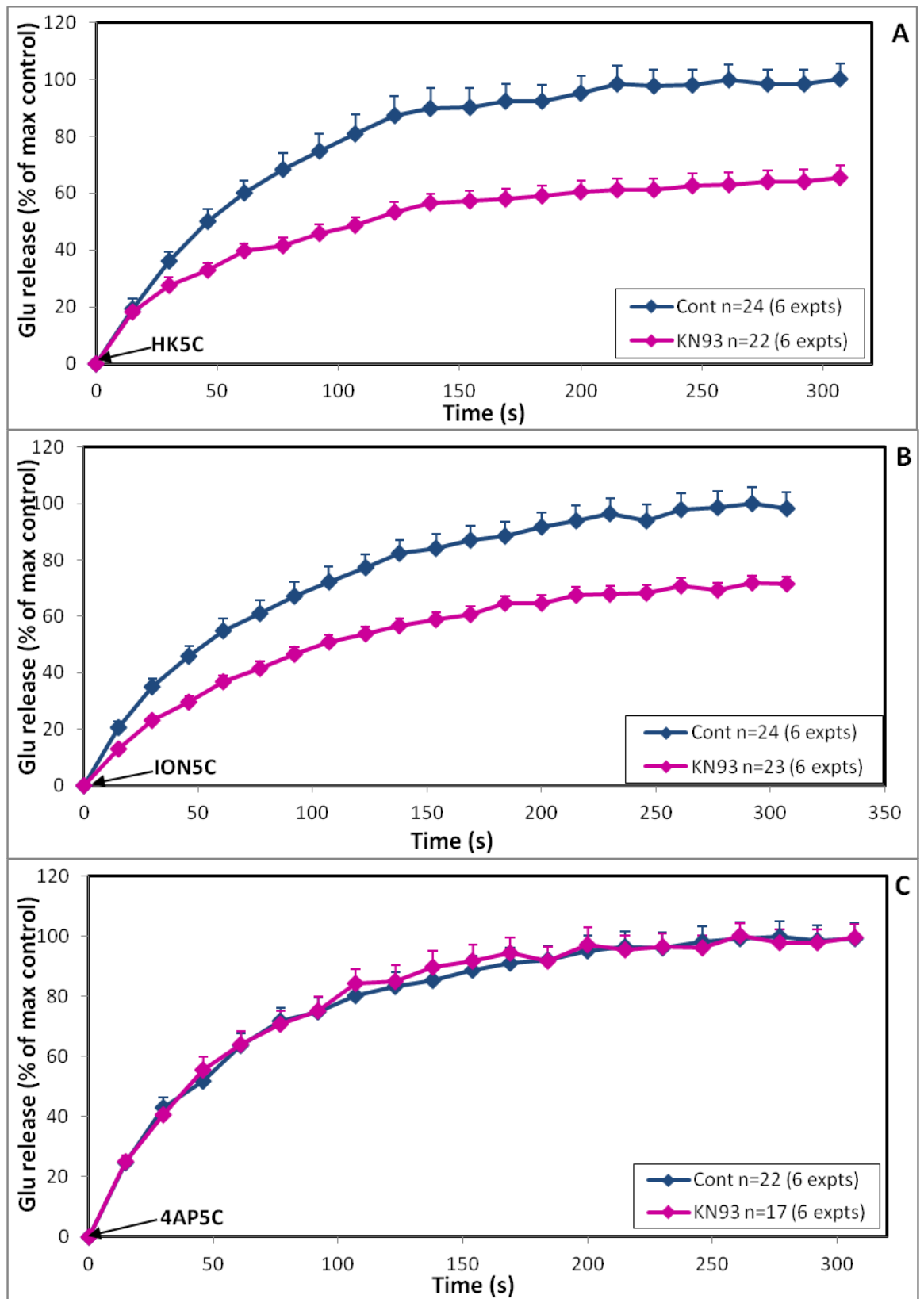


Figure 20: 10 μ M KN93 produced a significant decrease in Glu release in Control Synaptosomes stimulated with (A) HK5C, (B) ION5C and but failed to exert an effect with (C) 4AP5C stimulation.

These effects observed are not due to changes in the evoked increase in the $[Ca^{2+}]_i$, as 10 μ M KN93 does not change the $[Ca^{2+}]_i$ when stimulated by HK5C (Figure 21A), ION5C (Figure 21B) and 4AP5C (Figure 21C).

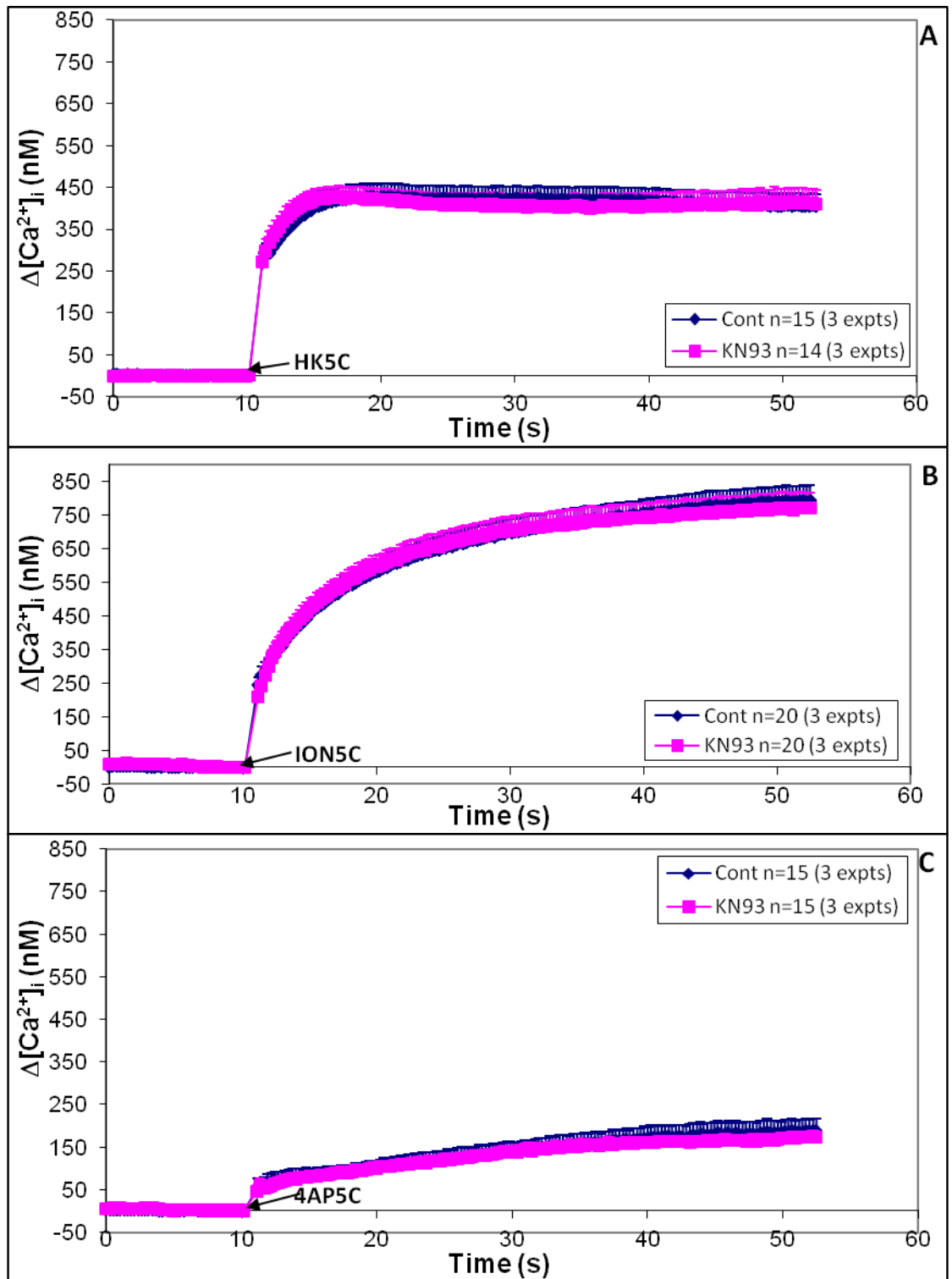


Figure 21: 10 μM KN93 produced no change in the level of $[\text{Ca}^{2+}]_i$ obtained in Control Synaptosomes upon stimulation with (A) HK5C, (B) ION5C or (C) 4AP5C.

The specificity of KN93 was tested using its inactive homolog, KN92 (Wheeler et al., 2008). 2 μ M KN92 failed to affect the evoked Glu release induced by these three distinct stimuli (Figures 22 A, B and C). Note that whilst the experiments with HK5C and ION5C were done thrice, the result with KN92 and 4AP5C was determined only once. However, as KN93 itself failed to affect 4AP5C evoked release (Figure 20C), it was believed that KN92 has no action upon 4AP5C evoked Glu release.

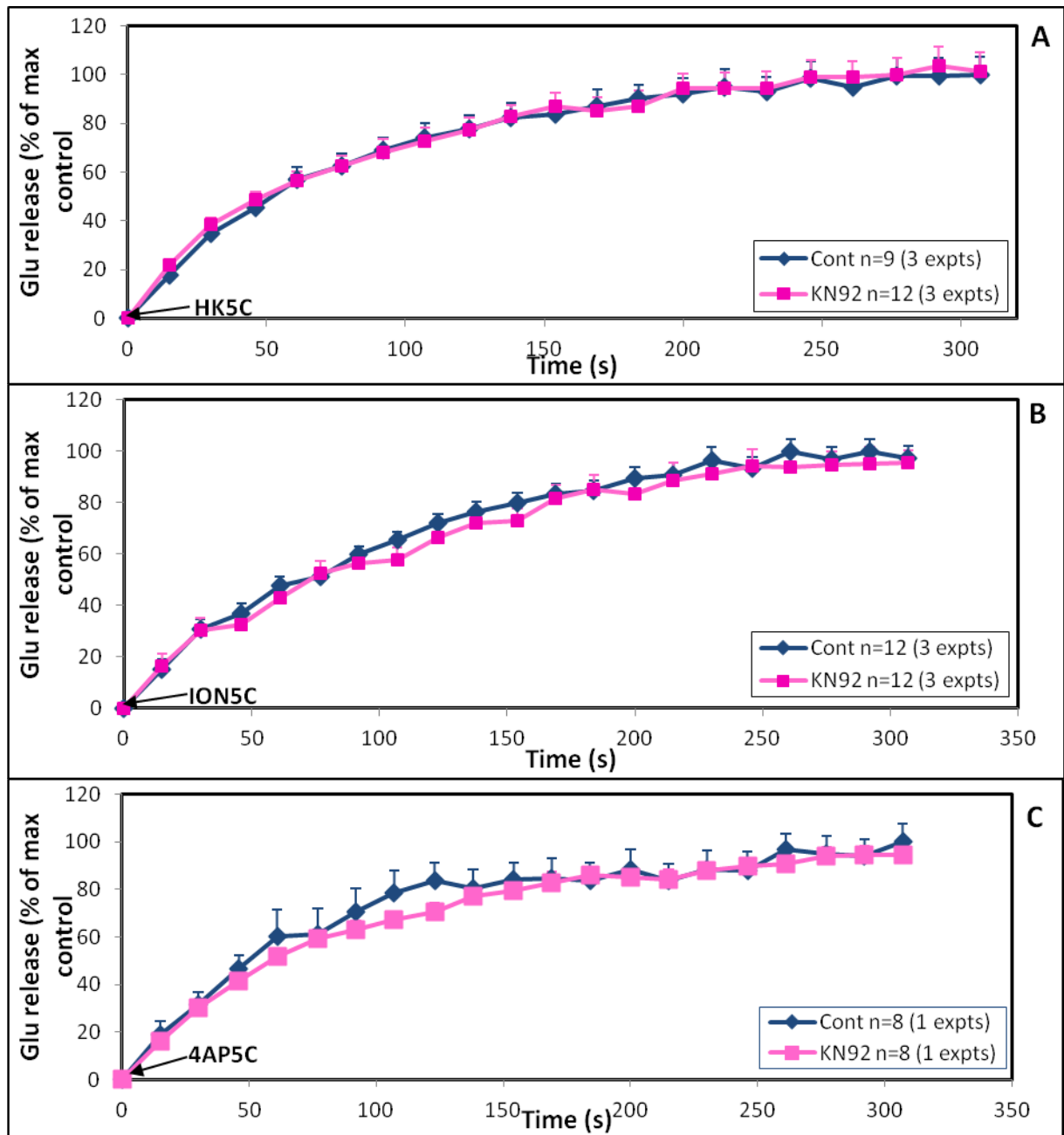


Figure 22: 2 μ M KN92 produced no significant decrease in Glu release in control synaptosomes stimulated by (A) HK5C, (B) ION5C or (C) 4AP5C.

The results following CaMKII inhibition demonstrated in Figure 20 can be explained in terms of the pools of SVs that are being stimulated by the various stimuli. Both HK5C and ION5C cause sufficient $[Ca^{2+}]_i$ increase at the AZ and areas distant from this to induce the release of both the RRP and RP. Whereas, 4AP5C causes an increase in the $[Ca^{2+}]_i$ that is sufficient to evoke the release of the RRP, but it does not induce the RP of SVs to fuse. This information indicates that, 10 μ M KN93 inhibits the release of the RPs but not RRP. This is obvious when the Glu release evoked by the three stimuli in presence of KN93 is compared (Figure 23): all three stimuli release similar amounts of Glu and this represents the release of the RRP.

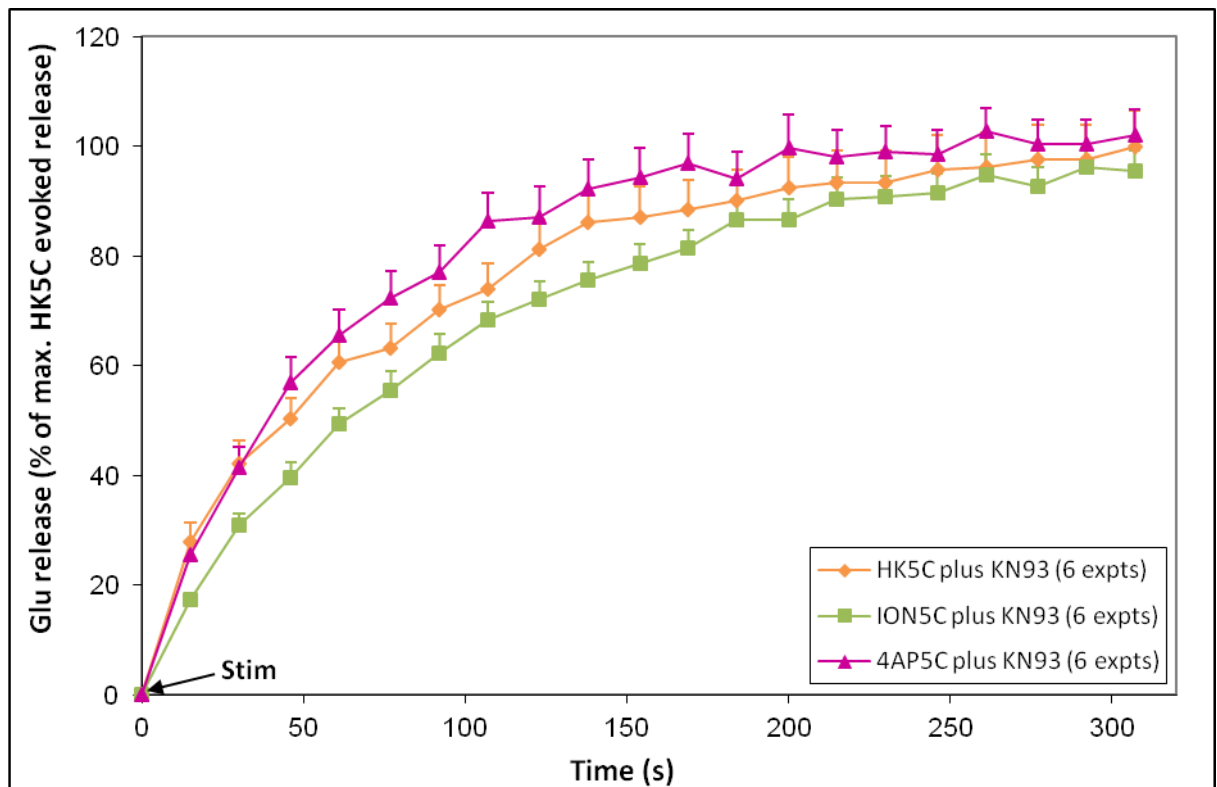


Figure 23: Comparable amounts of Glu release observed in the presence of 10 μ M KN93 when evoked with HK5C (orange line), ION5C (green line) and 4AP5C (pink line).

The data with KN-93 can be explained by the interaction of CaMKII and synapsin I (Refer discussion for details). From these results the role of CaMKII in regulating the mode of exocytosis can only be assessed by studying 4AP5C evoked release of the RRP (Figure 24) as the number of SVs exocytosing is not

changed. One cannot use HK5C or ION5C as there is a difference in the number of SVs exocytosing with or without 10 μ M KN93. Excitingly, Figure 24 demonstrates that CaMKII inhibition with 10 μ M KN93 leads to a larger increase in 4AP5C evoked FM2-10 dye release indicating that active CaMKII induces K&R mode of exocytosis for some RRP of vesicles.

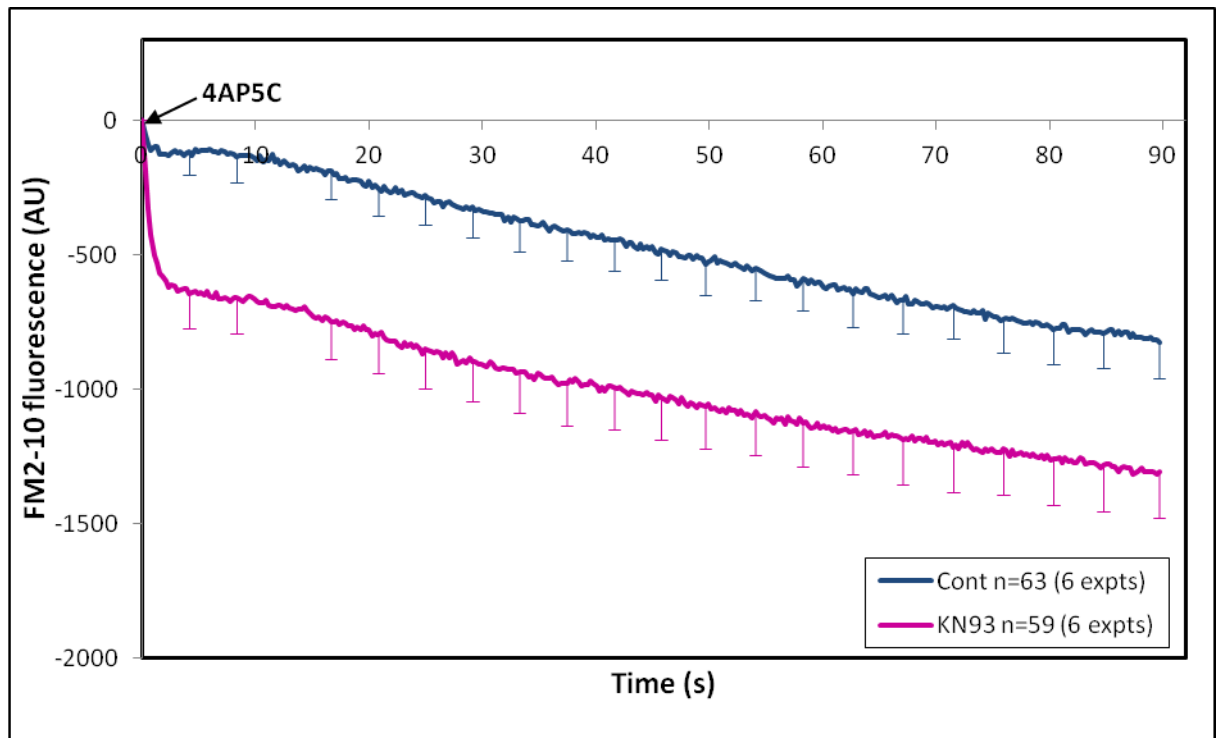


Figure 24: 10 μ M KN93 causes an increase in FM2-10 dye release in control terminals stimulated by 4AP5C.

Having established the role of VGCCs for both control and diabetic terminals, and a role of CaMKII on control terminals (similar studies with KN93 need to be undertaken on diabetic terminals in the future), the role of specific phosphoproteins in defining the mode of exocytosis was investigated.

II.2.6 Myosin II is unaltered in diabetic synaptosomes

Unpublished study by Dr. A. Ashton and colleagues reveal that myosin II may play a role in switching of the mode of exocytosis with a particular stimulus. This question was addressed by comparing control and diabetic terminals.

Figure 25A and 25B is a repeat of previous experiments. It shows that inhibition of myosin II with its potent inhibitor Bleb (Shu et al., 2005) has no effect on the HK5C evoked Glu release whereas, it increases the amount of FM2-10 dye release in control nerve terminals (Figure 25B). This indicates that, myosin II induces K&R mode of exocytosis on RRP with HK5C evoked release.

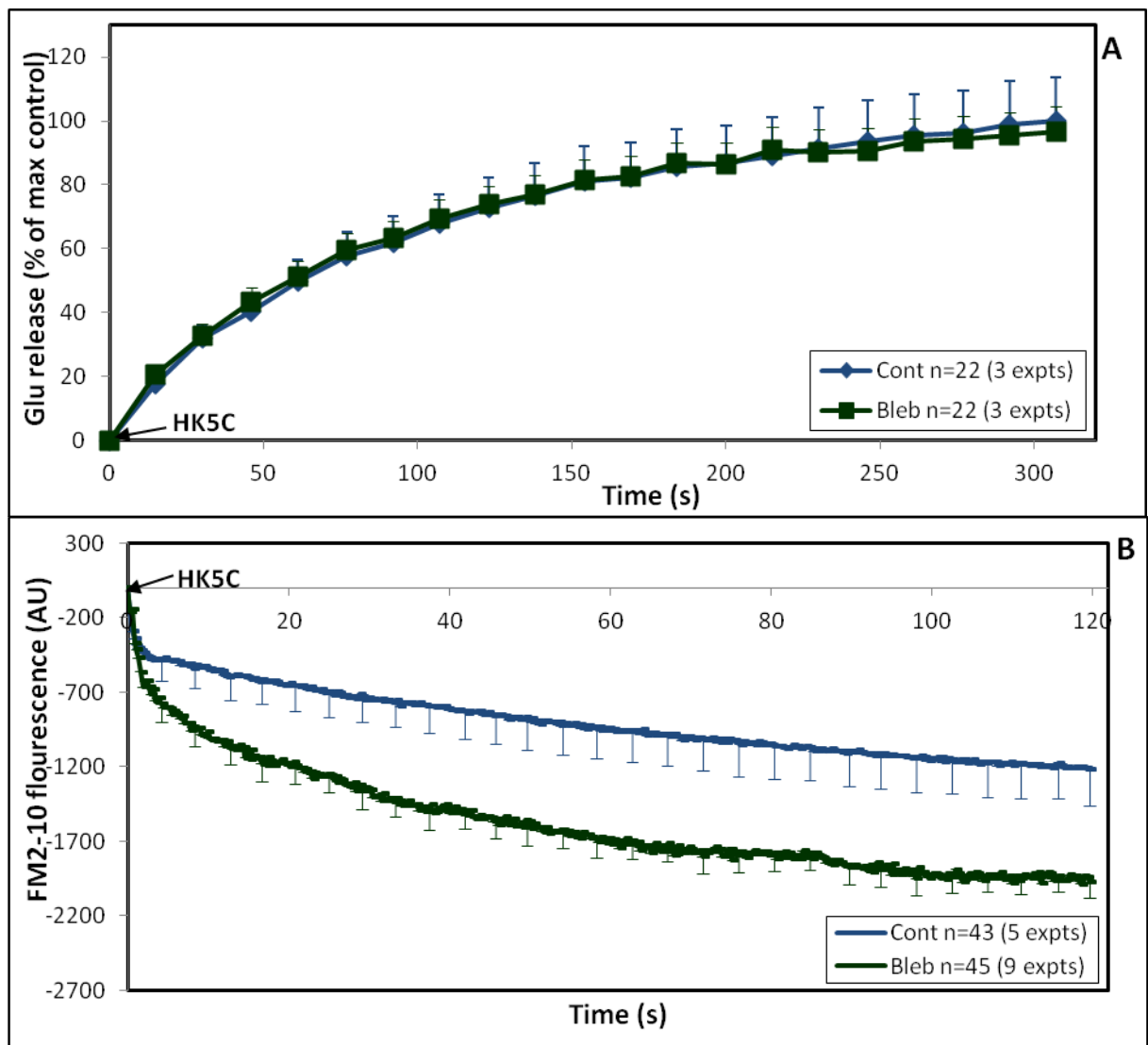


Figure 25: 50 μ M Bleb has no effect on HK5C evoked (A) Glu release but this significantly increases (B) FM2-10 dye release in control terminals. When

equivalent experiments were performed on the diabetic terminals in the presence and absence of 50 μ M Bleb, it was established that the Glu release was not perturbed (Figure 26A). Likewise, it also causes similar increase in the FM2-10 dye release (Figure 26B). Therefore, it can be concluded that no difference in the activity of myosin II is observed in diabetic and control terminals.

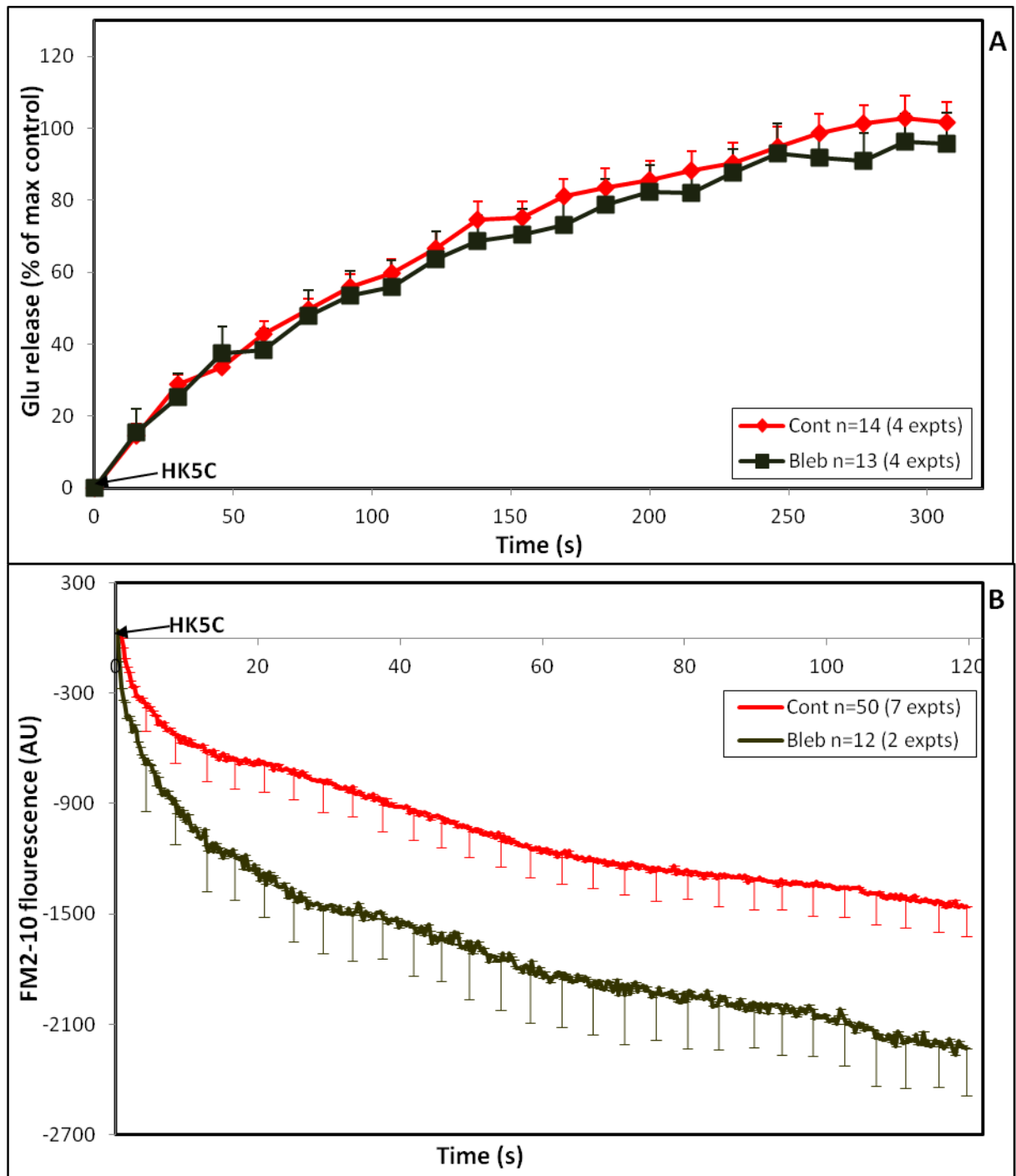


Figure 26: 50 μ M Bleb has no effect on HK5C evoked (A) Glu release but this significantly increases (B) FM2-10 dye release in diabetic terminals.

II.2.7 Inhibition of Protein Phosphatase 2B/Calcineurin increases the kiss-and-run mode of exocytosis in control synaptosomes

The results seen above in which HK5C evoked FM2-10 dye exocytosis was increased in the presence of Bleb suggested that, HK5C induced increase in $[Ca^{2+}]_i$ at the AZ is sufficient to activate myosin II (Tokuoka and Goda, 2006; Bhat and Thorn, 2009), which would normally close the pore quickly (i.e. produce apparent K&R exocytosis). This action of myosin II may override the action of other proteins that might regulate the mode of exocytosis, e.g. role of dynamin (see later). Thus, research was undertaken to investigate the interaction of myosin II with other components of the regulatory machinery including protein PP2B/ CaN in control nerve terminals. The inhibition of CaN with cyclosporine A (Cys A), results in a larger increase in stimulus evoked changes in $[Ca^{2+}]_i$, and so it was speculated as to whether Cys A treatment would lead to a further activation of myosin II, which would then lead to a even larger increase in FM2-10 dye release when myosin II was inhibited by Bleb. Indeed, perhaps myosin II could be a protein whose phosphorylation state was regulated by CaN. In order to compare Bleb action vs Bleb plus Cys A action, it was necessary to repeat earlier experiments (already carried out in Dr. Ashton's laboratory), to monitor the effect of Cys A on control terminals. Figure 27A demonstrates that 1 μ M Cys A does not perturb the Glu release when evoked with HK5C. However, inhibition of CaN decreases the amount of HK5C evoked FM2-10 dye release from control synaptosomes. This is because activated CaN allows the RPs to undergo FF and inhibition by Cys A results in some of the RPs being converted to a K&R mode of exocytosis.

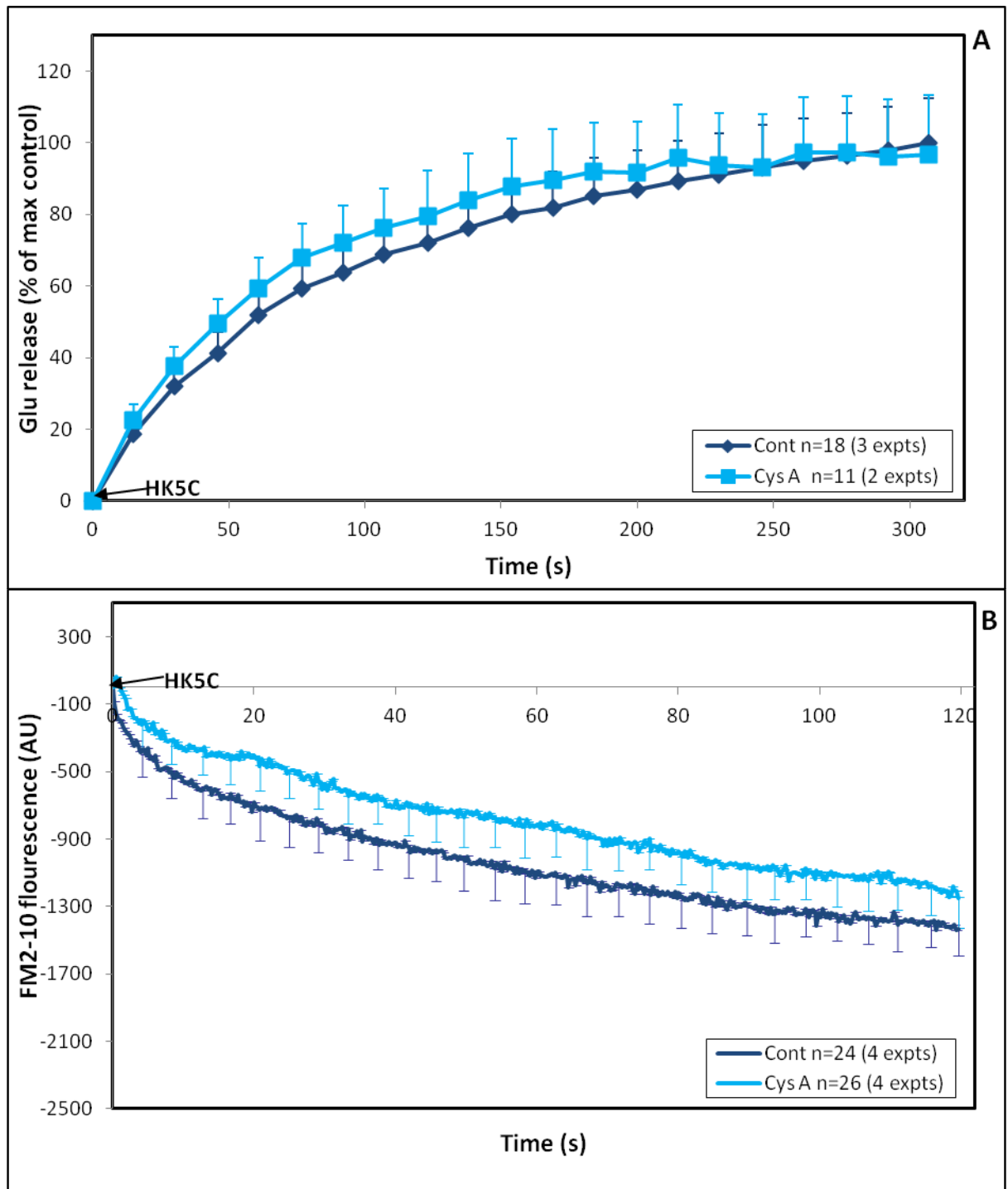


Figure 27: 1 μ M Cys A has no effect on HK5C evoked (A) Glu release but this significantly decreases (B) FM2-10 dye release in control terminals

II.2.8 Dual effect of Myosin II and PP2B inhibitor

Figure 28A demonstrates that, the dual treatment of Cys A plus Bleb does not have any effect on the HK5C evoked Glu release. However, the initial hypothesis was disproven when the effect of Cys A plus Bleb on HK5C evoked FM2-10 dye release was investigated. Rather than observing an increase in FM2-10 dye release, Cys A appear to prevent Bleb from inducing any increase in FM2-10 dye release, such that there is much less dye release in the presence of both drugs than when there was only Bleb present (Figure 28B).

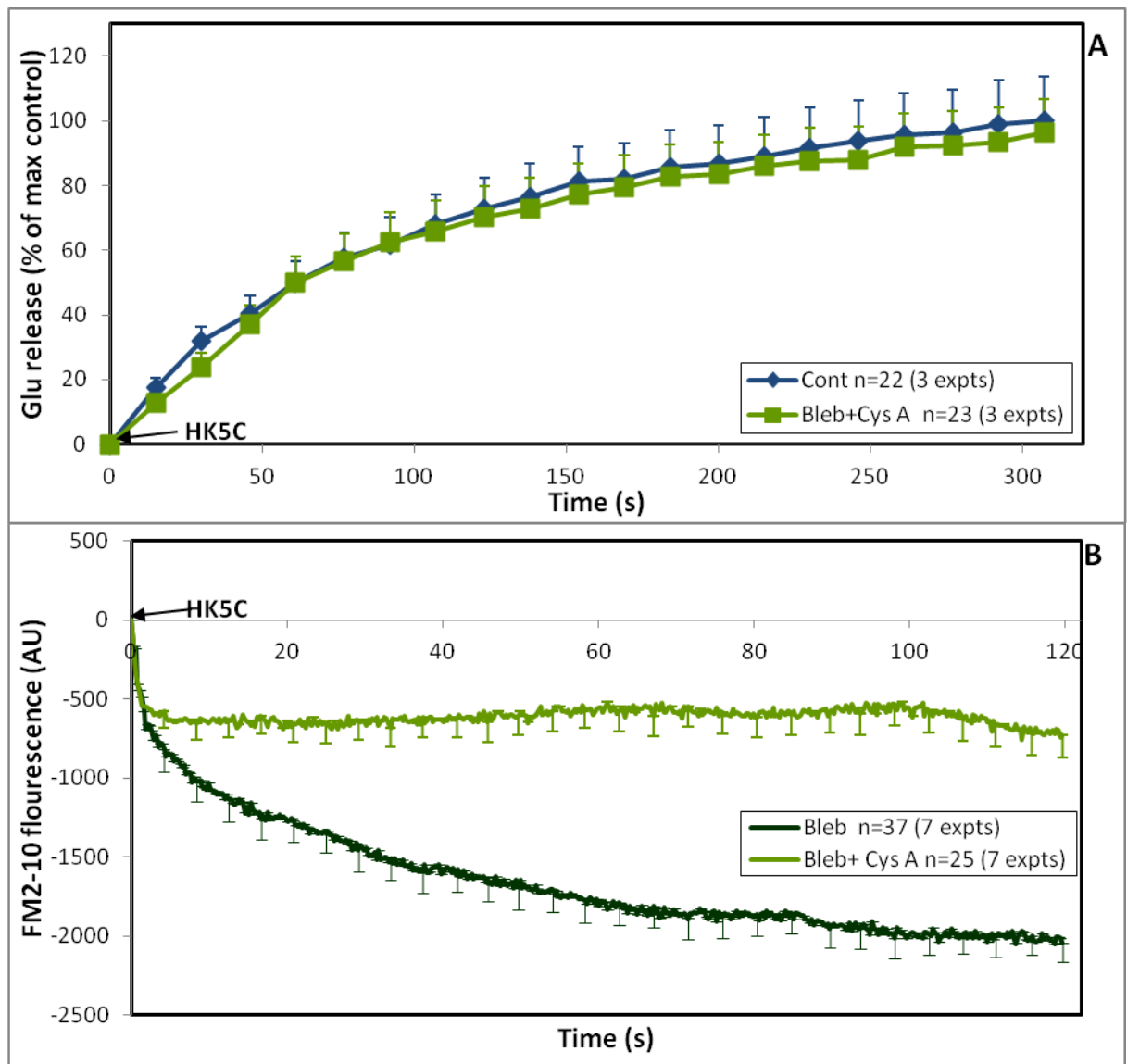


Figure 28: 1 μ M Cys A + 50 μ M Bleb has no effect on HK5C evoked (A) Glu release compared to non-treated cont but this treatment reduces (B) less HK5C

evoked FM2-10 dye release compared to control synaptosomes treated with 50 μ M Bleb alone.

The result obtained in Figure 28B is very significant (explained in details in discussion) as this could help future researches to understand precisely the molecular mechanism that occurs in the switching of the mode of different SVs.

II.2.9 Effect of the inhibition of dynamin on Control Terminals

Figure 29A demonstrates that inhibition of dynamins I and II with 160 μ M dynasore (Dyn) has no effect on the HK5C evoked Glu release on the control synaptosomes. Furthermore, no effect on FM2-10 dye release was also observed in Figure 29B.

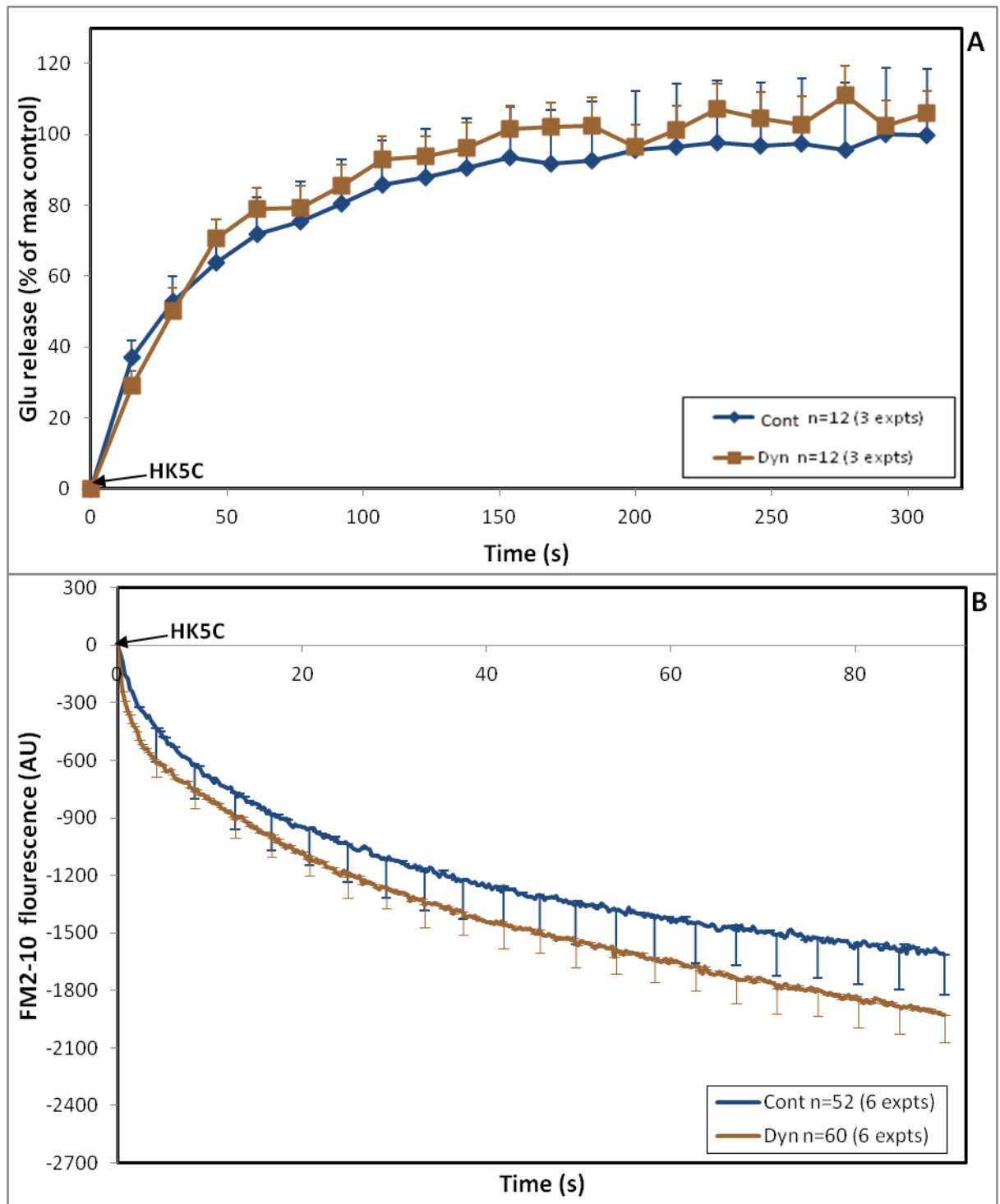


Figure 29: 160 μ M DYN has no effect on HK5C evoked (A) Glu release or (B) FM2-10 dye release in control terminals. (Note this expt was done previously by A. Ashton and colleagues and is included so that one can compare this with subsequent novel experiments)

II.2.10 Dual effect of Dynamin and Myosin II inhibitor

A novel experiment investigating the dual effect of 50 μ M Bleb and 160 μ M Dyn on the SV exocytosis from synaptosomes was carried out. As these drugs do not individually affect the Glu release, it was fully expected that the dual treatment would not affect HK5C evoked Glu release and, therefore, the number of SVs exocytosing. Figure 30A demonstrates that this is the case. From all the current (e.g. Figure 30A) and previous results (e.g. Figure 29) it was anticipated that myosin II was capable of bypassing the role of dynamins, so Bleb should cause an increase in HK5C evoked FM2-10 dye release even when dynamins are inhibited by Dyn. However, again the hypothesis was disproved, as when HK5C evoked FM2-10 dye release was compared following treatment with 50 μ M Bleb alone and the combination of 50 μ M Bleb and 160 μ M Dyn (Figure 30B), it was observed that the action of Bleb was blocked i.e. less dye was released. This result suggests that, all the RRP's were switched back to K&R mode under this dual treatment mode. This result is crucial, as it helps to determine the pathway in mode switching, although currently this result remains difficult to interpret. Clearly, more experiments need to be repeated on this facet to understand this fully.

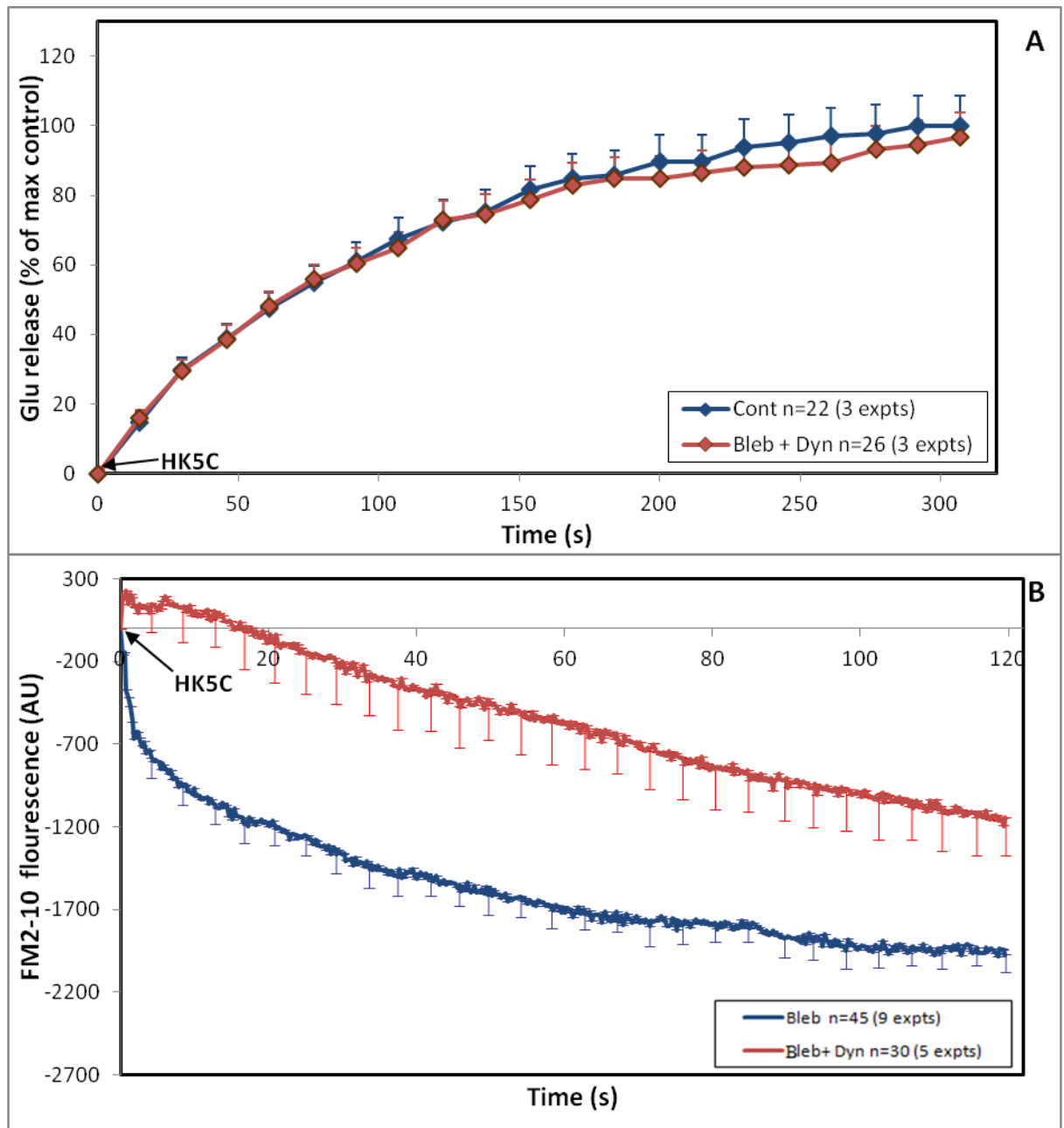


Figure 30: 50 μ M Bleb + 160 μ M Dyn has no effect on HK5C evoked (A) Glu release compared to non-treated cont but this treatment reduces (B) HK5C evoked FM2-10 dye release compared to control synaptosomes treated with 50 μ M Bleb alone.

II.2.11 Dynamin inhibition switches the RPs to full fusion in Diabetic terminals

As differences in the mechanism of VGCCs were obtained in control and diabetic synaptosomes, it was decided to examine if there were differences in the

contribution that dynamins play in HK5C evoked SV exocytosis from diabetic synaptosomes. HK5C evoked Glu release was not affected by the treatment with 160 μ M Dyn (Figure 31A). However, in comparison to control synaptosomes, it was detected that Dyn significantly increased the amount of HK5C evoked FM2-10 dye release from the diabetic synaptosomes, suggesting that dynamins can play a role in defining the mode of exocytosis in diabetic nerve terminals.

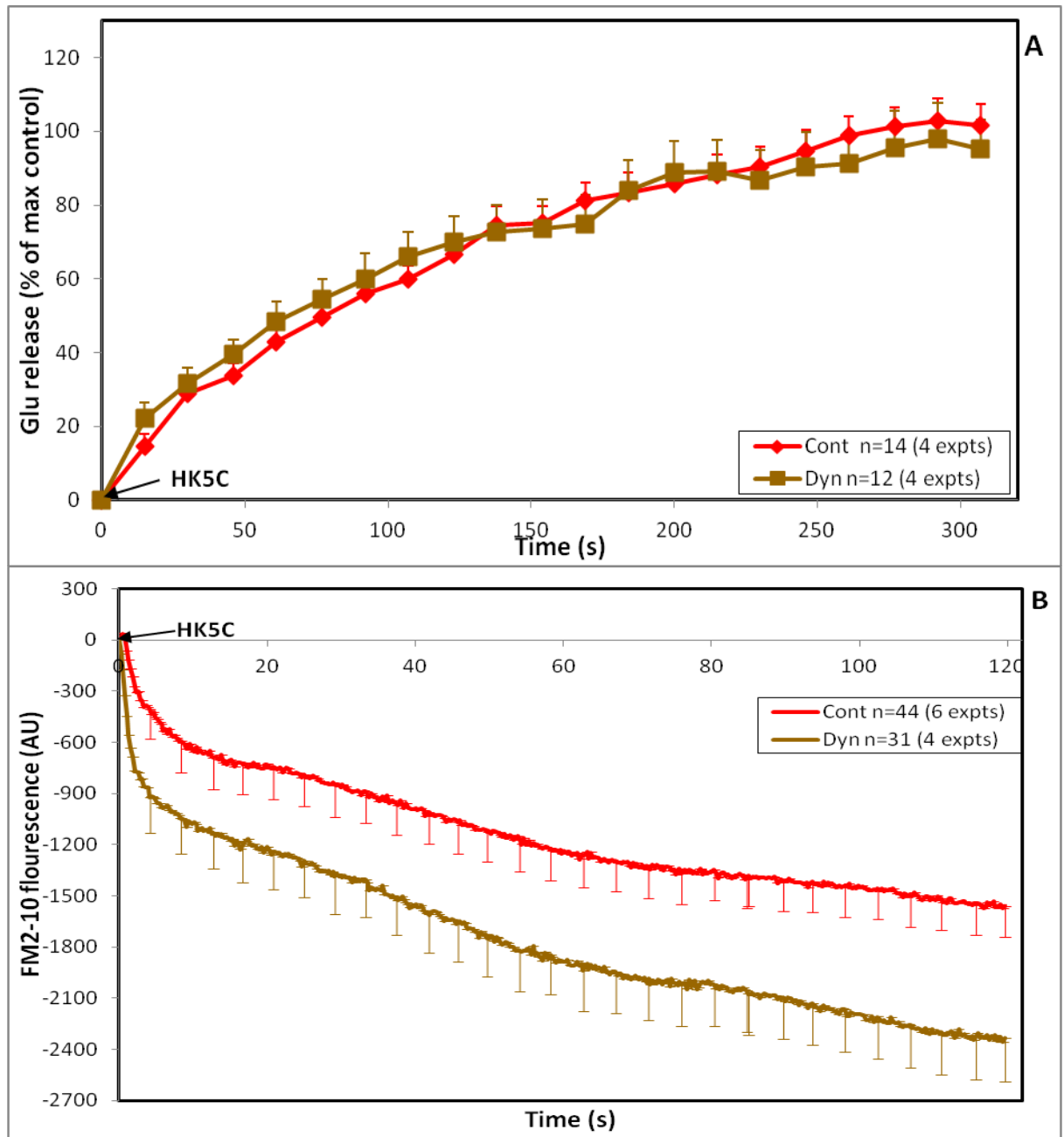


Figure 31: 160 μ M Dyn has no effect on HK5C evoked (A) Glu release but this significantly increases (B) FM2-10 dye release in diabetic terminals.

Clearly, there appears to be a difference in response to HK5C stimulation between control and diabetic terminals following inhibition of dynamins. It was therefore, investigated whether there was a difference in the effect of Dyn between control and diabetic terminals when the SV exocytosis were stimulated using 4AP5C.

Figure 32A demonstrates that Dyn did not affect the 4AP5C evoked Glu release. However, inhibition of dynamins led to a larger amount of FM2-10 dye release evoked by 4AP5C in control terminals. This suggests that dynamins can induce SVs to exocytose by a K&R mode when evoked by 4AP5C but that this is switched to FF when dynamins are inhibited by Dyn (Figure 32B).

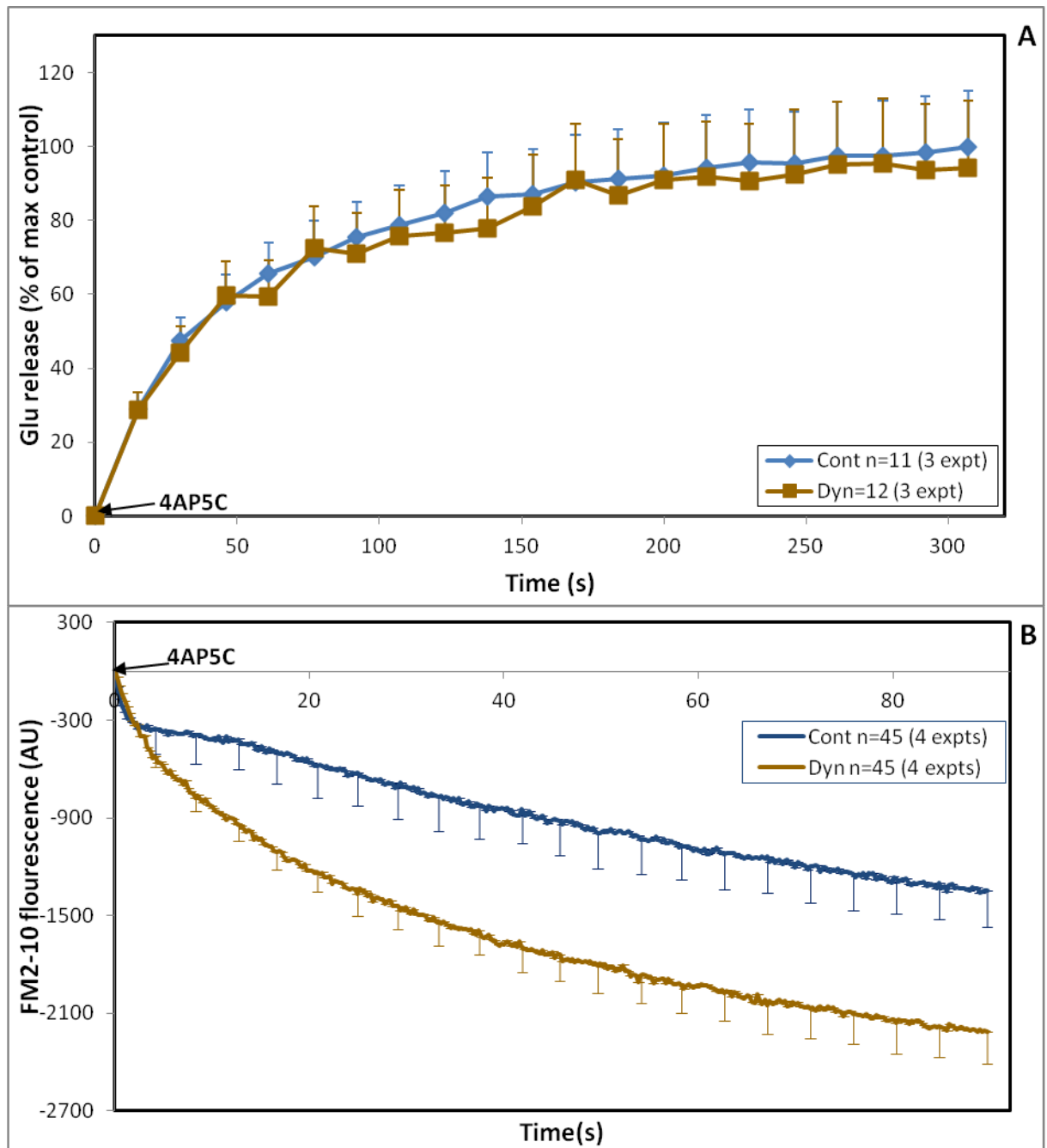


Figure 32: 160 μ M Dyn has no effect on 4AP5C evoked (A) Glu release but this significantly increases (B) FM2-10 dye release in control terminals.

In contrast, when 4AP5C evoked Glu (Figure 33A) and FM2-10 dye release (Figure 33B) was measured in diabetic synaptosomes in the presence of Dyn, neither the Glu or FM2-10 dye was altered compared to the non-treated control. Note that there is a need to do more experiments for release of Glu. These results highlight differences between the control and diabetic synaptosomes, which may help us to elucidate the precise mechanisms occurring. In particular, this could

reveal that the drugs and their target proteins may actually be acting on only one pool of the two pools of SVs. This is considered in more detail in the discussion at the end of this chapter.

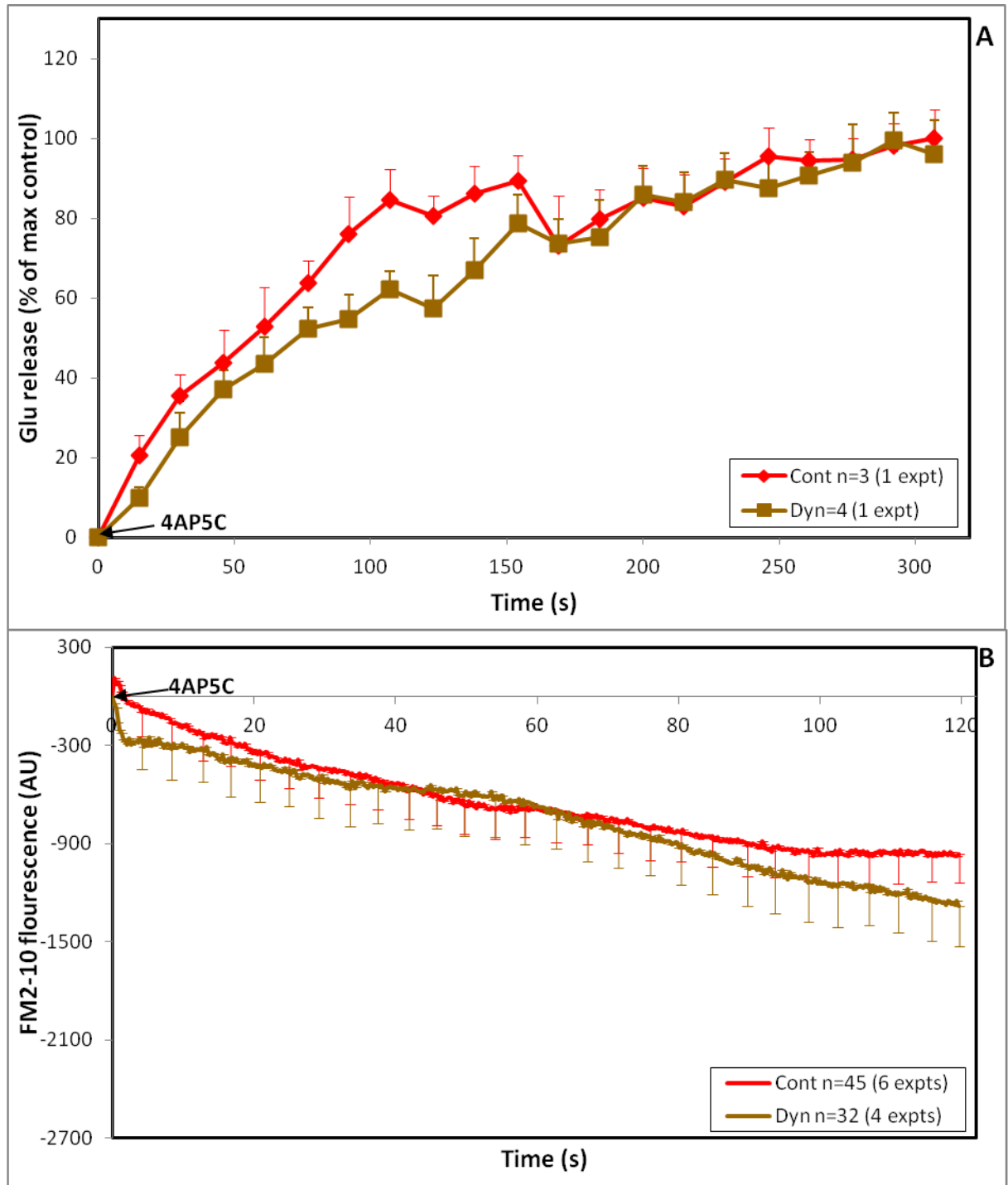


Figure 33: 160 μ M Dyn has no effect on 4AP5C evoked (A) Glu release or (B) FM2-10 dye release in diabetic terminals.

II.2.12 Role of Protein Phosphatase 2A

From the previous experiments, it has been established that the diabetic terminals undergo more K&R mode of exocytosis in comparison to control nerve terminals (Figure iB). In control synaptosomes, RRP of vesicles undergo K&R mode of exocytosis. However, in diabetic terminals as less FM2-10 is released, it is believed that some of the RP of vesicles also undergo K&R mode along with the RRP. In Dr. Ashton's laboratory it is already established that, PP2A inhibitor okadaic acid (OA) plays a role in switching the RRP of vesicles from K&R mode to FF mode of exocytosis in control terminals (demonstrated by Figure 34) when FM2-10 dye release is evoked with HK5C.

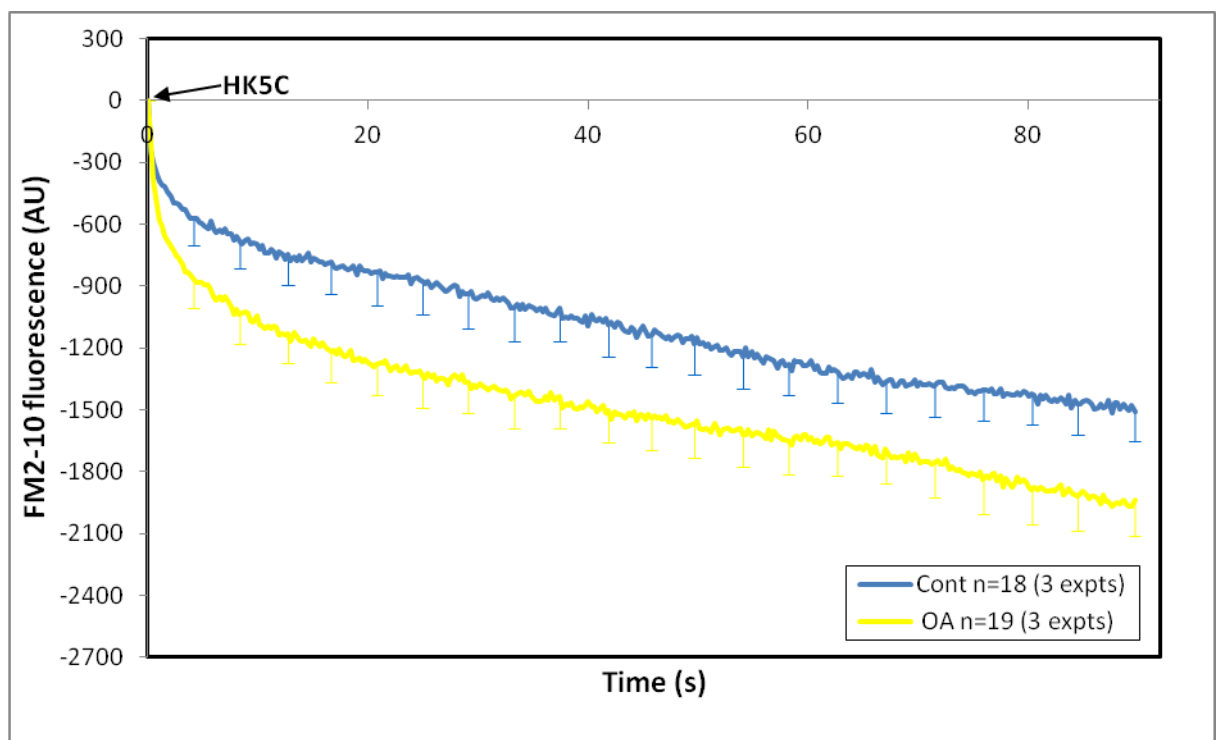


Figure 34: Significant increase in FM2-10 dye release from control terminals upon stimulation with HK5C in the presence of 0.8 μ M OA

The current study was undertaken to establish conditions whereby all those vesicles that are undergoing K&R in diabetic terminals can be switched to FF. Hence, the role of PP2A in the diabetic terminals was studied. Figure 35 demonstrates the effect of 0.8 μ M OA on HK5C evoked release. As Glu release was not perturbed by OA (Figure 35A), FM2-10 dye assay was subsequently

measured. The study revealed that OA increases the amount of dye released from the diabetic terminals significantly. However, careful analysis of all experiments previously carried out with control terminals indicates that, there is less FM2-10 dye being released from the diabetic terminals and so not all the SVs are being switched by OA treatment to FF in the diabetic terminals. This could be explained by the suggestion that, OA just works on the RRP vesicles and fails to switch those RPs that are undergoing K&R in diabetic terminals. In control terminals, only the RRP SVs are undergoing K&R.

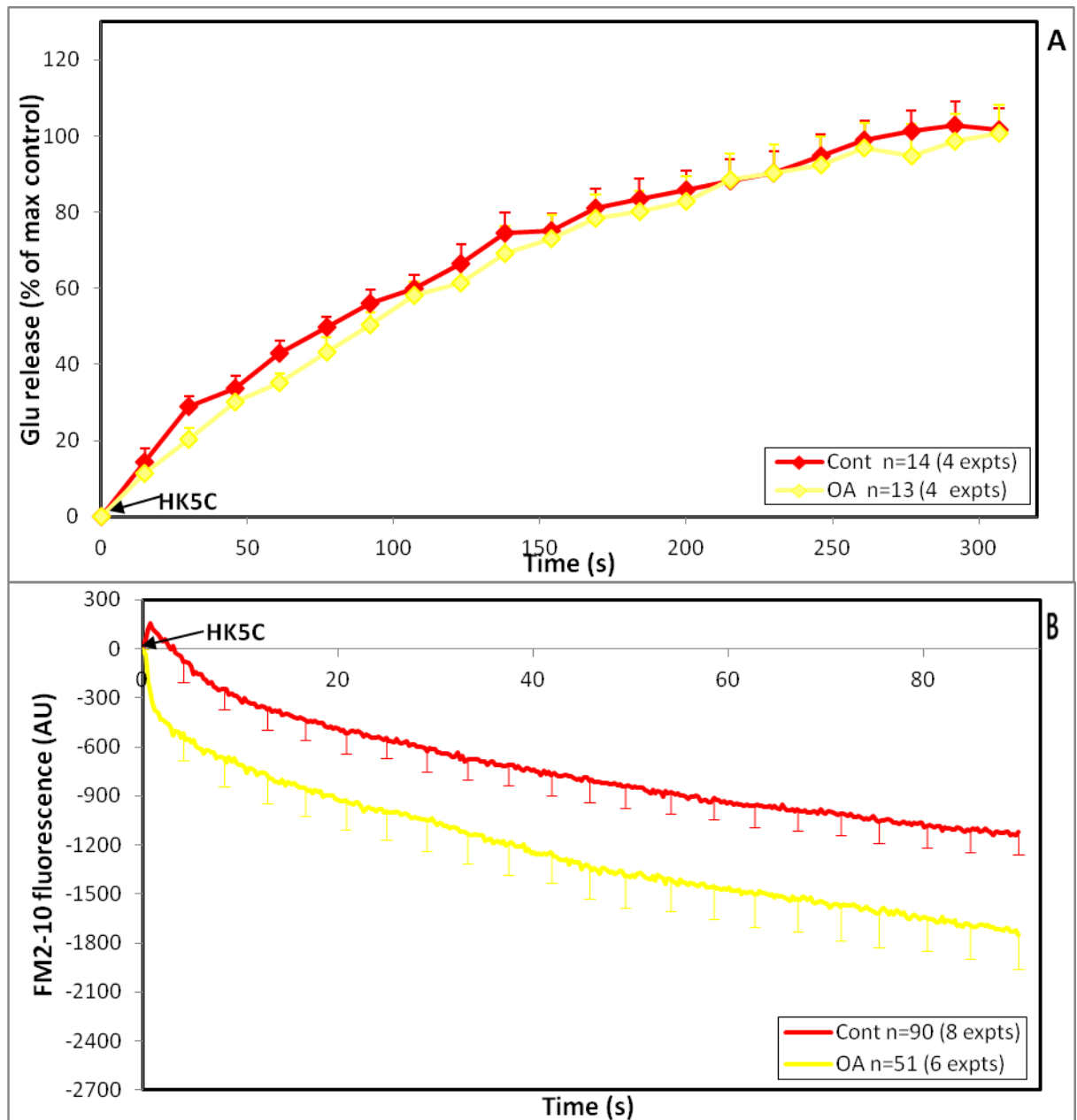


Figure 35: 0.8 μM OA has no effect on HK5C evoked (A) Glu release but this significantly increases (B) FM2-10 dye release in diabetic terminals (but not as much when compared to Figure 34 for Control Synaptosomes).

When the action of OA in diabetic terminals was measured following 4AP5C evoked release, significant amounts of FM2-10 dye was released indicating that, the OA did cause a switch of some RRP of SVs to a FF mode (Figure 36).

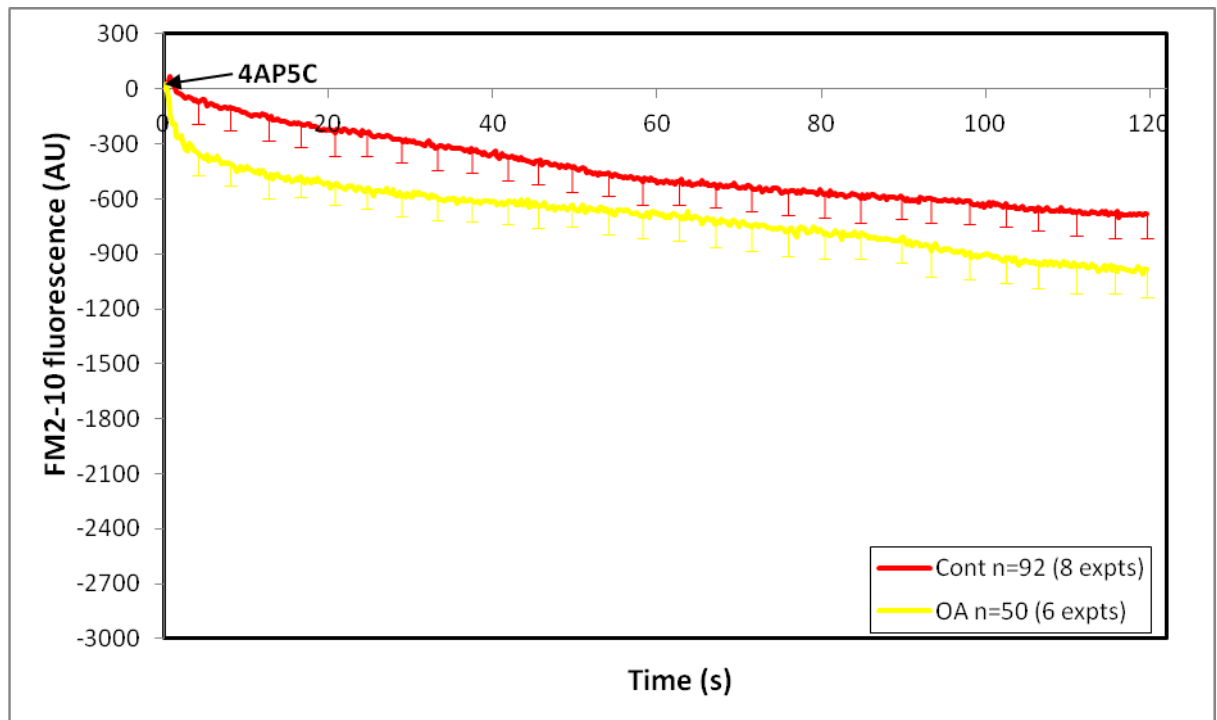


Figure 36: Increase in 4AP5C evoked FM2-10 dye release in diabetic terminals in the presence of 0.8 μ M OA .

II.2.13 Protein Kinase C switches some SVs to full fusion mode of exocytosis in diabetic terminals

The role of PKC was studied by treating the synaptosomes with active phorbol esters (PMA) which activate this kinase (Lou et al., 2008a). 1 μ M of PMA is known to cause switching of the RRPVs to FF, that were normally undergoing K&R, when release is evoked with HK5C (e.g. Figure 37) without affecting the total number of SVs exocytosing, as shown by the lack of effect of PMA on HK5C evoked Glu release.

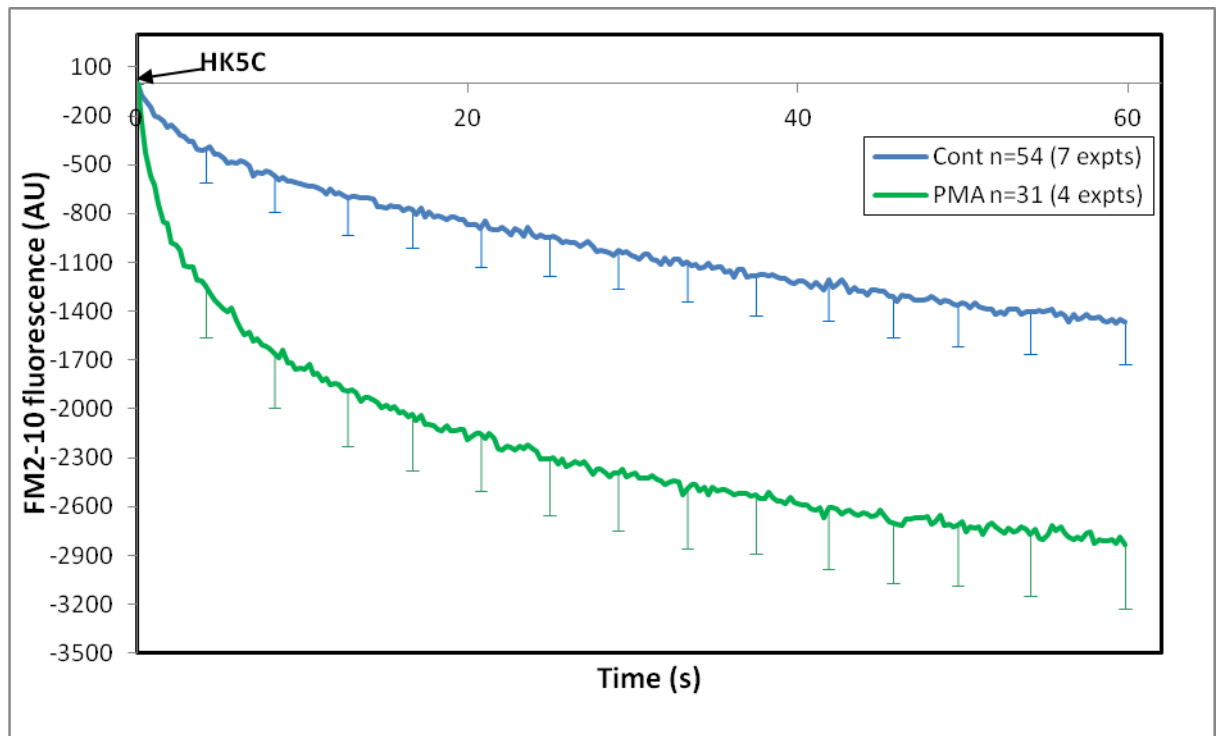


Figure 37: Significant increase in HK5C evoked FM2-10 dye release upon application of 1 μ M PMA in control terminals.

Glu release evoked with HK5C in diabetic nerve terminals was not affected by PMA (Figure 38A). However, the HK5C evoked FM2-10 dye release was significantly increased following PMA treatment on diabetic synaptosomes (Figure 38B), but the amount of release was not as great as that seen in the control terminals (Figure 37). When PMA was added to diabetic terminals and 4AP5C evoked FM2-10 dye release was measured, PKC activation led to an increase in dye release indicating that, some RRP SVs have been switched to a FF mode (Figure 39).

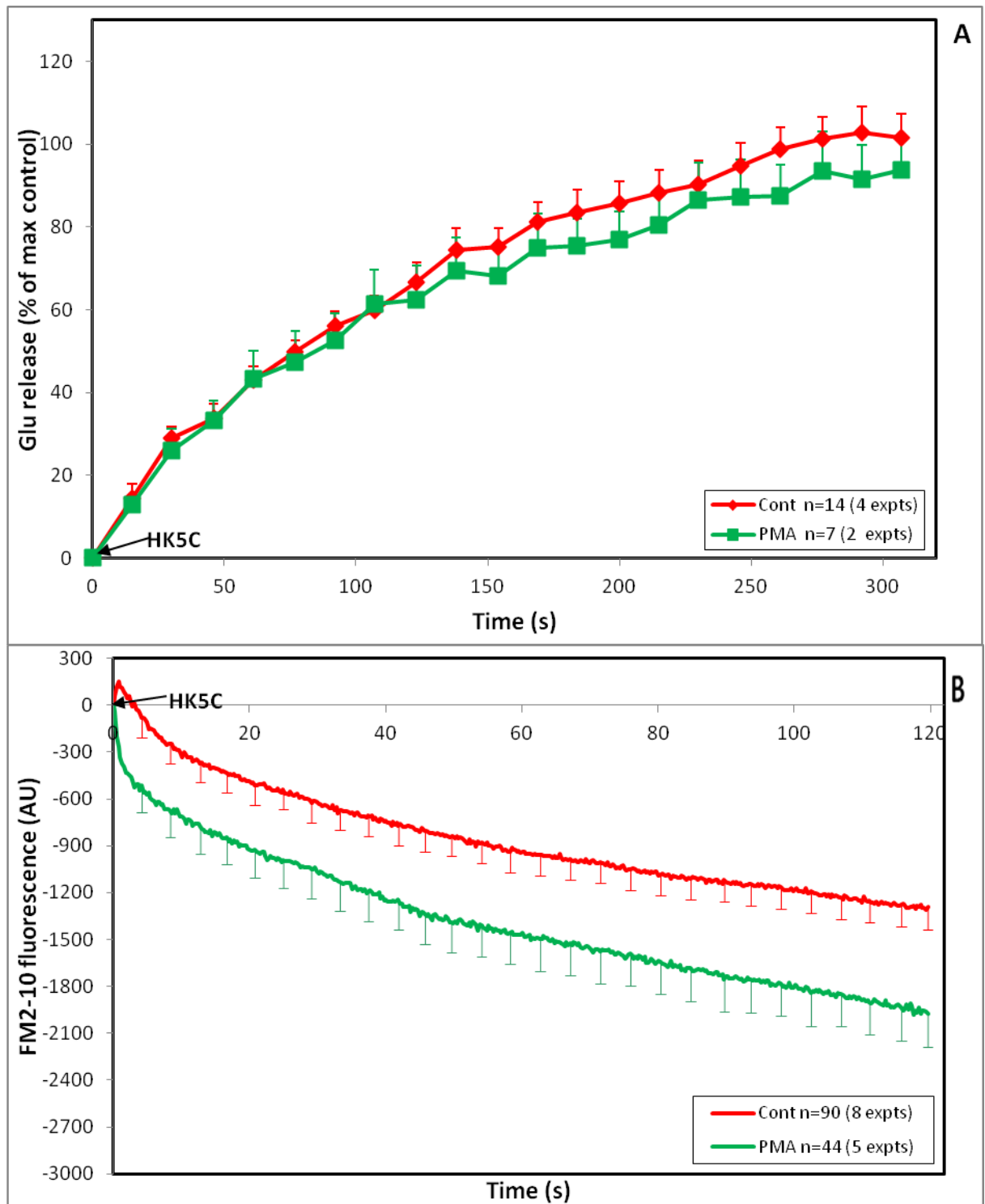


Figure 38: 1 μ M PMA has no effect on HK5C evoked (A) Glu release but this significantly increases (B) FM2-10 dye release in Diabetic terminals (but not as much when compared to Figure 37 for Control Synaptosomes).

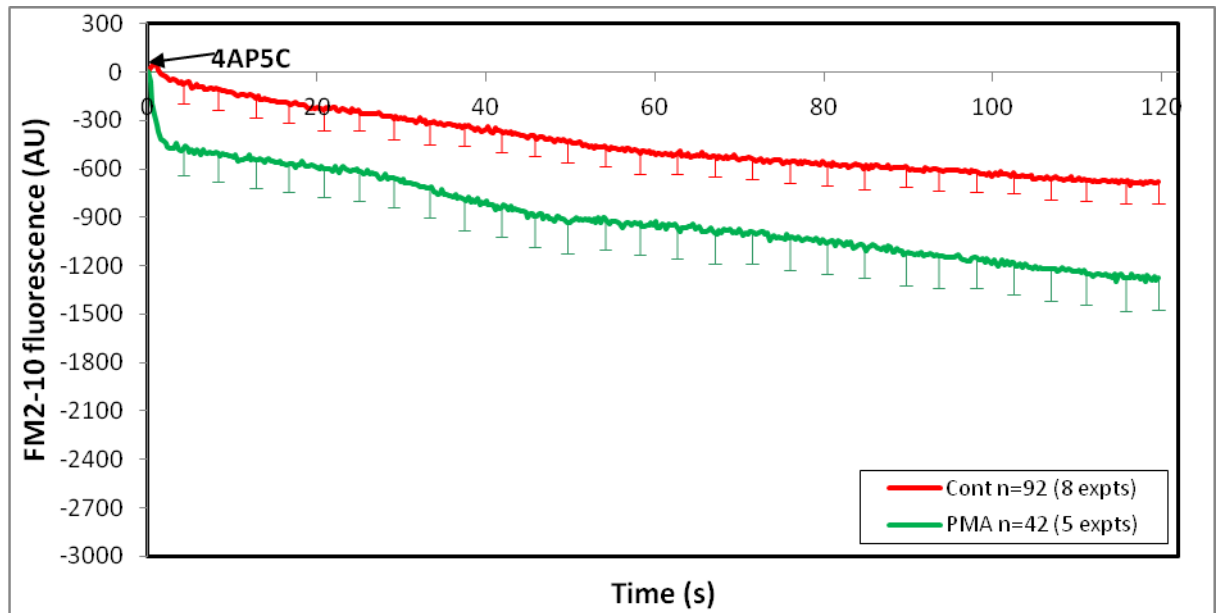


Figure 39: Increase in 4AP5C evoked FM2-10 dye release upon application of 1 μ M PMA in diabetic terminals.

II.2.14 Dual treatment by inhibiting PP2A and activating PKC switches all the pool of SVs to full fusion in diabetic terminals

It would appear from the results with OA or PMA in diabetic terminals that some SVs which were undergoing K&R exocytosis were not switched to FF. Thus, the dual effect of 0.8 μ M OA+ 1 μ M PMA was investigated to observe whether this treatment might produce maximal FM2-10 dye release and therefore complete switching of SVs to FF.

The double treatment had no effect on the amount of HK5C evoked Glu release in diabetic terminals (Figure 40A). However, such dual treatment induced a significantly larger amount of dye to be released from the nerve terminals upon the application of HK5C (Figure 40B) on diabetic terminals. This FM2-10 dye release is larger in comparison to treatment with PMA (Figure 41) or OA alone (Figure 42).

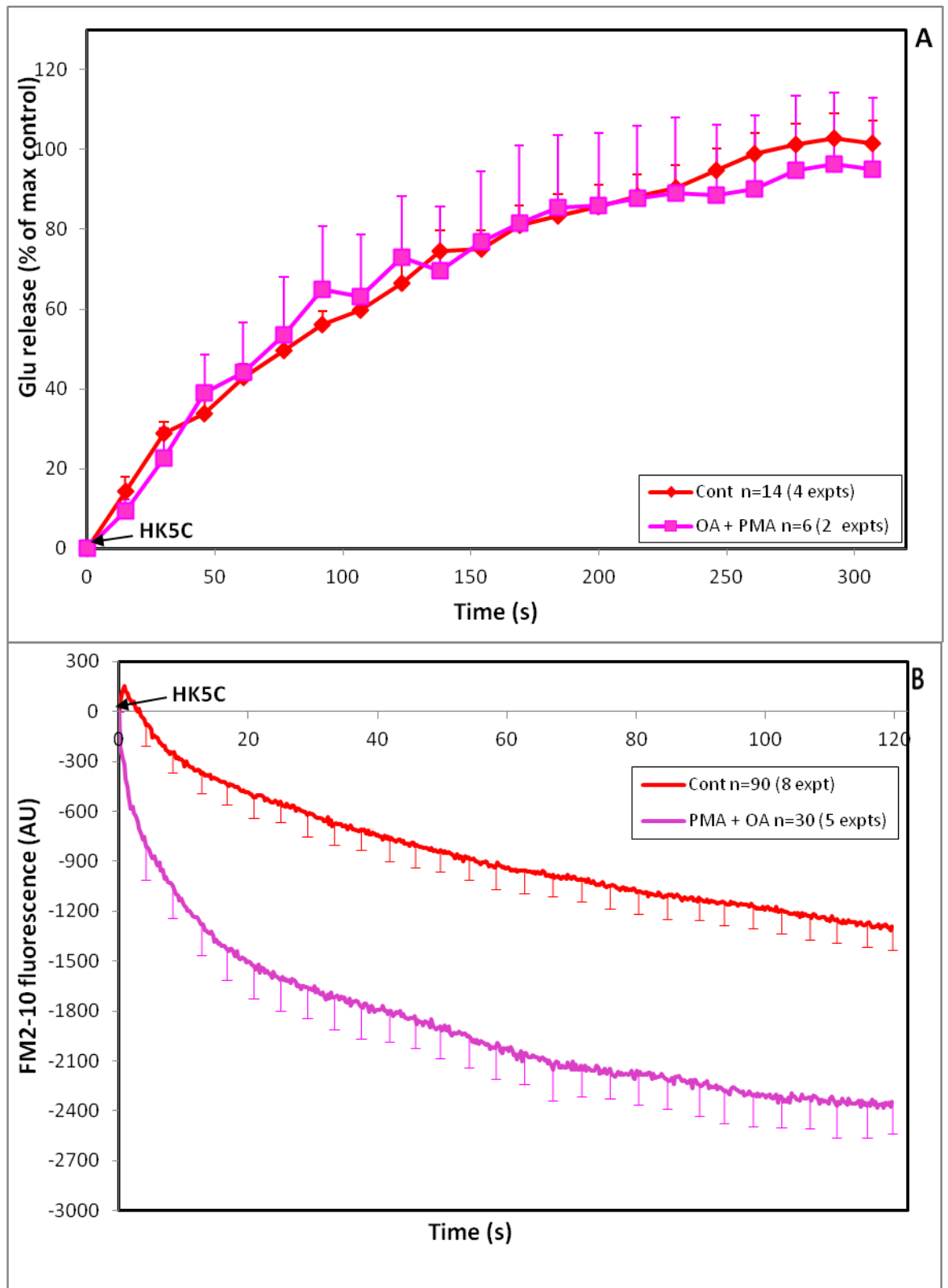


Figure 40: 0.8 μ M OA +1 μ M PMA has no effect on HK5C evoked (A) Glu release but this significantly increases (B) FM2-10 dye release in Diabetic terminals.

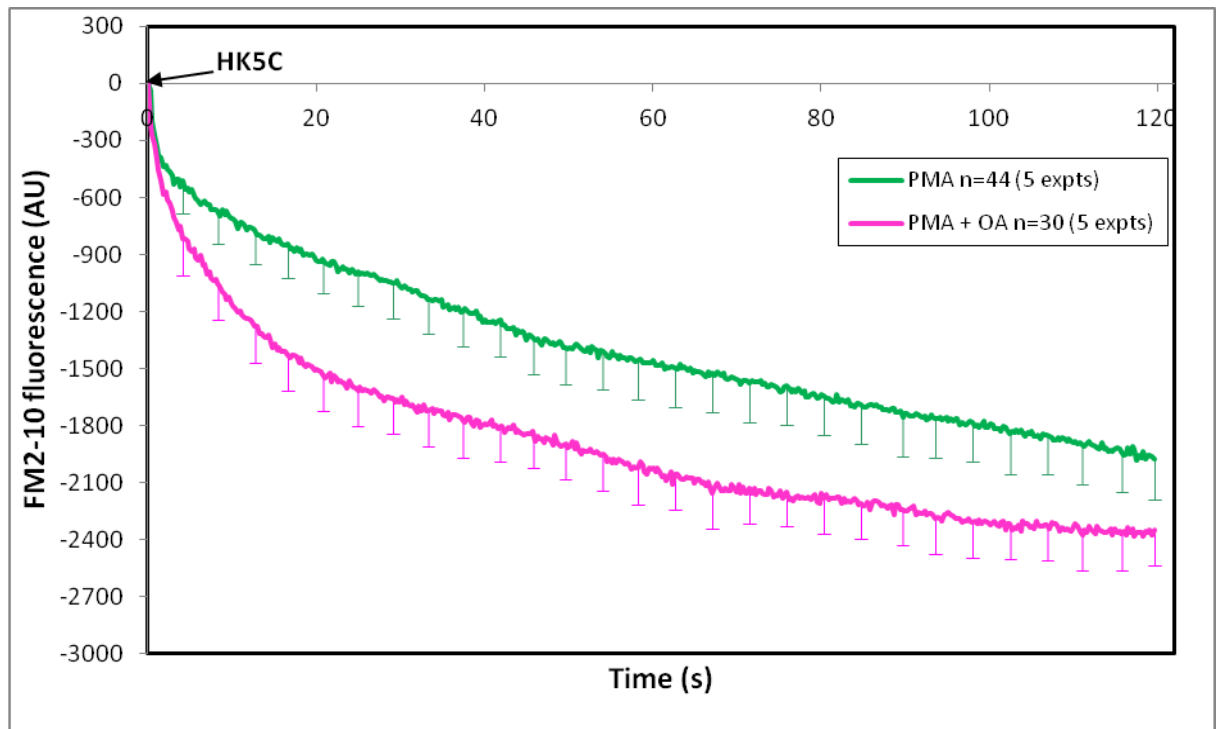


Figure 41: Significant difference observed between HK5C evoked FM2-10 dye release in diabetic terminals treated with 1 μM PMA compared to joint treatment with 0.8 μM OA + 1 μM PMA

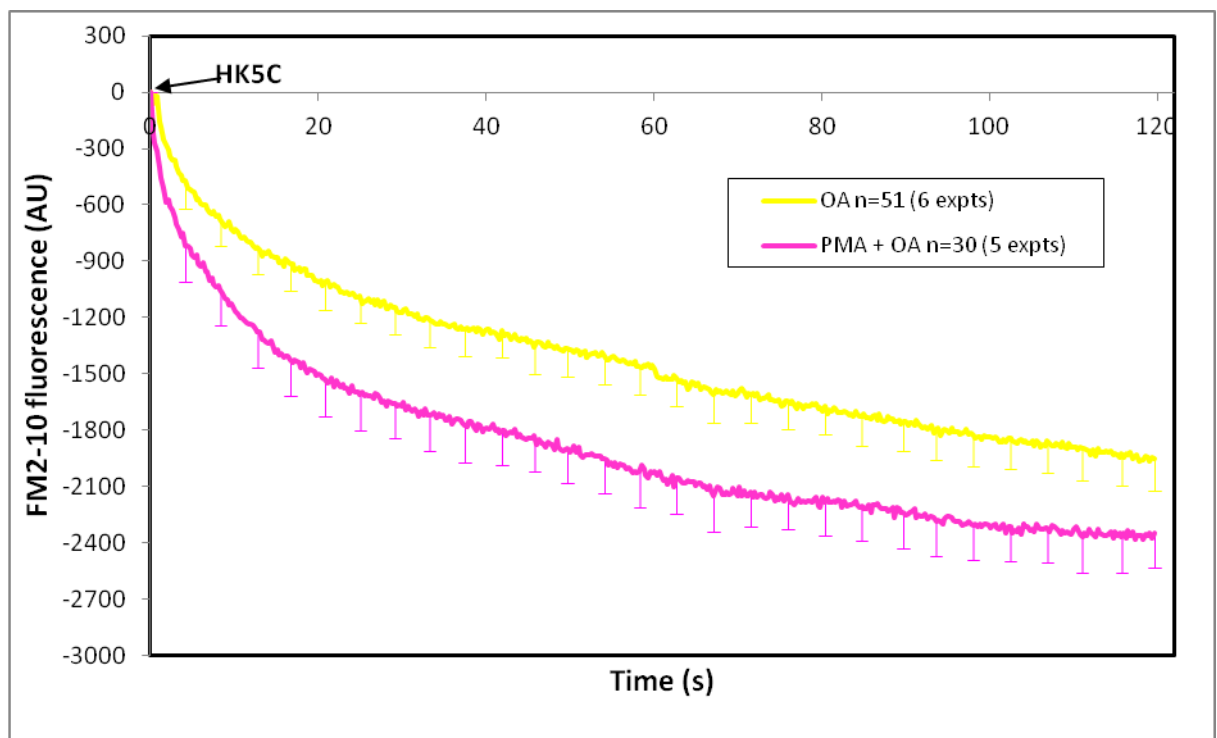


Figure 42: Significant difference observed between HK5C evoked FM2-10 dye release in diabetic terminals treated with 0.8 μM OA compared to joint treatment with 0.8 μM OA + 1 μM PMA.

The 0.8 μ M OA +1 μ M PMA dual treatment also increased the amount of 4AP5C evoked FM2-10 dye release from diabetic terminals, (Figure 43) but this did not produce a bigger difference than treatment with the individual drugs alone i.e PMA alone (Figure 44) or OA alone (Figure 45).

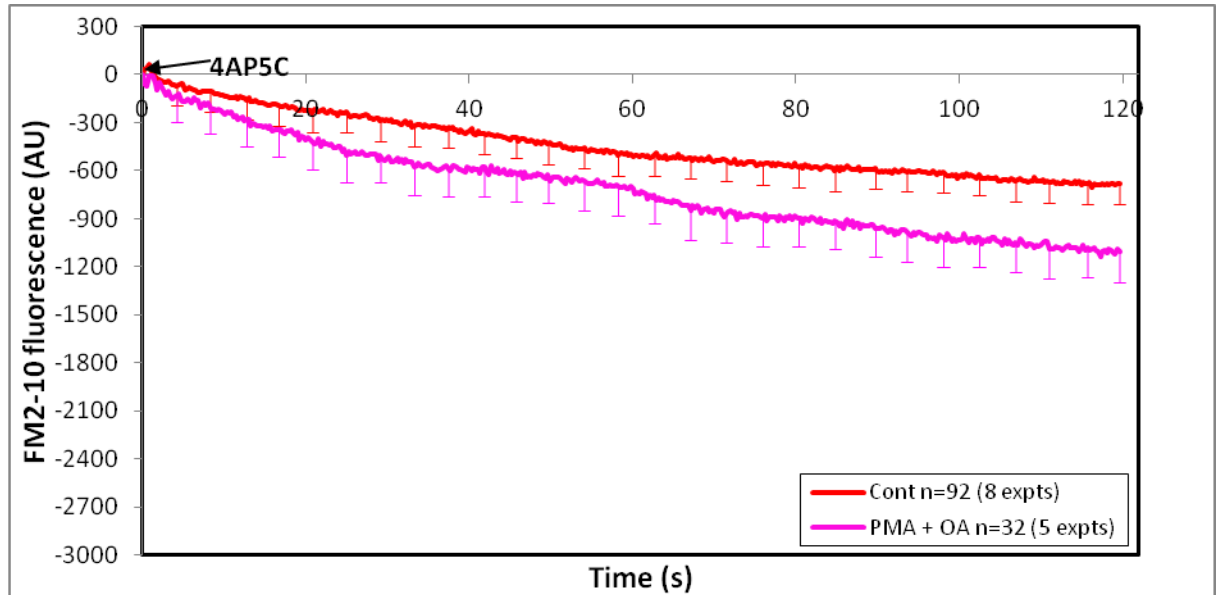


Figure 43: 0.8 μ M OA + 1 μ M increases 4AP5C evoked FM2-10 dye release \pm in diabetic terminals

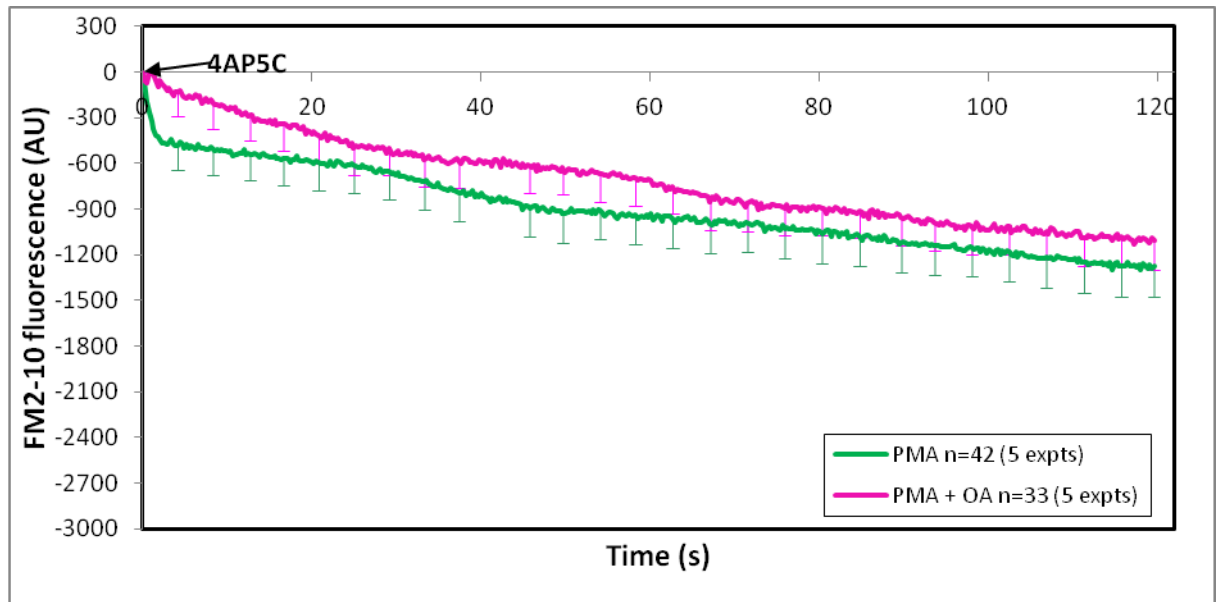


Figure 44: No significant difference observed between 4AP5C evoked FM2-10 dye release in diabetic terminals treated with 1 μ M PMA alone and with 0.8 μ M OA + 1 μ M PMA.

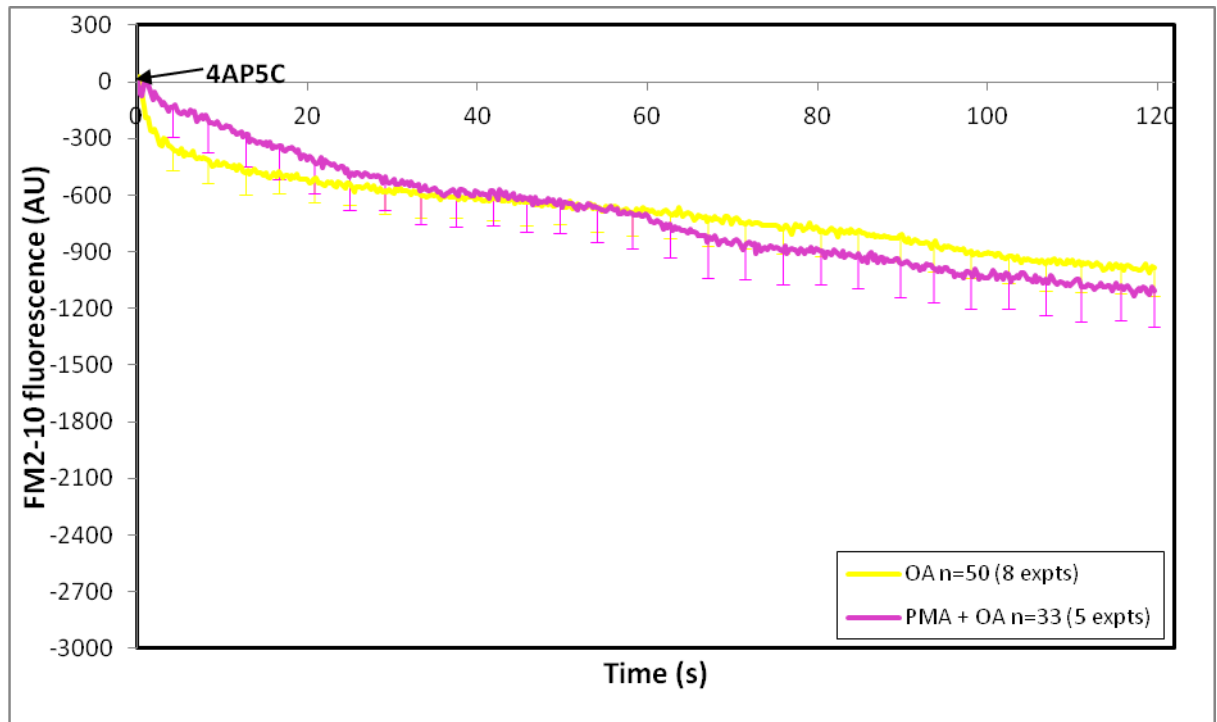


Figure 45: No significant difference observed between 4AP5C evoked FM2-10 dye release in diabetic terminals treated with 0.8 μ M OA alone and with 0.8 μ M OA + 1 μ M PMA.

II.3 Discussion

It was already established in Dr. Ashton's laboratory that the diabetic terminals exhibited a larger stimulus induced increase in $[Ca^{2+}]_i$ levels and a higher proportion of K&R mode of exocytosis as compared to the control terminals (Figure iB and iC). However, the Glu release remained unchanged (Figure iA). The main aim of this study was to establish any biochemical changes that occur in the diabetic terminals that could account for the changes outlined above. The approach employed was to establish role for various VGCCs, Ca^{2+} dependent kinases and protein phosphatases in regulating the mode of exocytosis and to decipher differences between control and diabetic terminals, which could shed light on this process.

II.3.1 Role of VGCCs

The main cause for the difference in the behaviour of diabetic terminals and control terminals was speculated to be due to the level of $[Ca^{2+}]_i$ obtained during stimulation and, therefore role of various VGCCs was examined. The blockade of P-type VGCC with 50 nm Aga TK (Wright and Angus, 1996; Serulle et al., 2007) did not block the Glu release from HK5C evoked diabetic and control synaptosomes (Figure 1A and B). Additionally, no change in the mode of exocytosis was observed in both the terminals (Figure 4). However, it perturbed change in the $[Ca^{2+}]_i$ from HK5C evoked control and diabetic terminals (Figures 2A and B) and also reduced the HK1.25C evoked Glu release in the control synaptosomes (Figure 3A), suggesting that the P-type channels can play a role in the evoked release of Glu in control terminals under certain conditions. However, even under these conditions (e.g. see Figure 3B) 50 nm Aga TK failed to perturb Glu release from diabetic terminals, and so P-type channels probably do not play a role in mode switching in diabetic terminals.

The role of L-type channels was investigated using the blocker 1 μ M Nif (Yang et al., 2009). This VGCC blocker does not affect the HK5C evoked Glu release in control and diabetic terminals (Figures 5A and 5B). When evoked with HK1.25C, 1 μ M Nif treatment blocked Glu release in the control terminals but exhibited no effect on the diabetic terminals. This result may suggest that L-type channels do not play a role in mode switching in diabetic terminals. Furthermore, when FM2-

10 dye study was observed in the control terminals, blockade of L-type VGCCs induced a switch in the mode of exocytosis to FF, (Figure 7A) whilst Nif had no effect upon diabetic terminals. Therefore, L-type channels appear to play a role in defining the mode of exocytosis in the control terminals. Under the appropriate conditions, Ca^{2+} going through the L-type channels would enable the RRP of SVs to undergo K&R mode of exocytosis, but Ca^{2+} fails to flow through this channel due to its blockade by Nif, the mode is switched to FF. This is further confirmed when the FM2-10 curve is compared with OA treated control synaptosomes (Figure 8). However, no such switch was observed in the diabetic terminals (Figure 7B).

It can thus be concluded that, L-type channels can play a role in defining the mode of exocytosis in control terminals. This result is similar to the results obtained by Xia et al., (2009) when studying the exocytosis of DCVs. However, no previous studies have discovered a role for such channels in defining the mode of exocytosis in nerve terminals. Previously, some models of synaptic transmission have revealed a role for L-type VGCCs in NT release under certain conditions (Nachman-Clewner et al., 1999), and such channels have been shown to be important for LTM formation (Fourcaudot et al., 2009). In contrast, it was found that in diabetic terminals, L-type channels do not perform the same roles as in control terminals. This may be due to fact that, in diabetic terminals either the L-type channel are less active, or that other channels are more active such that the role of L-type channels is replaced.

The treatment of the terminals with the N-type VGCC blocker, 1 μM GVIA (Verma et al., 2009) revealed some interesting results. Although, the HK5C evoked Glu release from the control terminals were unaffected (Figure 10A), the release was perturbed in the diabetic terminals (Figure 10B). This result indicates that, N-type VGCC play a major role in Glu release in diabetic synaptosomes relative to their contribution to release in control terminals. Further investigation in control terminals indicated that blockade of N-type channels played no role in regulating the mode of exocytosis (Figure 13).

There are several explanations for the fact that the N-type blocker reduced the Glu release in diabetic terminals. In such tissues, the N-type channels are either

overactive, or the number of these channels are increased through the insertion of additional N-type channels in the presynaptic membrane or such channels remain open for a longer period of time. Any of these explanations would mean that, the roles of other channels are reduced such that most of the Ca^{2+} entry into these terminals will be through N-type channels. There are various phosphorylation cascades that could contribute to this effect, and activation of PKC is an attractive candidate mechanism; as PKC can enhance N-type channel activity directly and antagonize signalling cascades that inhibit N-type channel opening (Ahmed and Siegelbaum, 2009). An additional explanation is that, one might be able to enhance coupling between Ca^{2+} influx through the N-type channels and the release machinery. In many CNS terminals, Ca^{2+} influx through N-type channels is less efficiently coupled to release compared to Ca^{2+} influx through P/Q-type channels (Ahmed and Siegelbaum, 2009). Perhaps it could be possible that, as N-type channels are important in the diabetic terminals, these channels increase the total $[\text{Ca}^{2+}]_i$ load. Interestingly, it has been found in other conditions that one can get upregulation of Ca^{2+} channels e.g. upregulation of N-type channel in the spinal cord is related to inflammation in the hind paw induced after chronic constrictive nerve injury. This condition leads to symptoms of allodynia and hyperalgesia (Verma et al., 2009) and intriguingly, these have often been observed in uncontrolled diabetic rats.

Conditions were established in the diabetic terminals such that Glu release was not perturbed, even though some but not all N-type channels were blocked. This concentration could then be used to study the FM2-10 dye release. 300 nM GVIA did not affect HK5C evoked Glu release but this toxin did induce an increase in FM2-10 dye release. This release was greater at all time points relative to the control but statistically the difference was only significant in the early stages of the time course (Figure 17). This experiment needs to be repeated several more times to establish that there is a significant difference for the whole time course of release. Further study need to measure the 300 nM GVIA induced reduction in HK5C evoked changes in $[\text{Ca}^{2+}]_i$. Likewise, it needs to be established whether 250 or 350 nM GVIA may be a better concentration of toxin to use than 300 nM.

1 μ M MVIIC (which blocks multiple VGCCs) significantly reduced HK5C evoked Glu release in both control and diabetic terminals (Figure 19) but the extent of blockade in diabetic terminals was significantly less than in control terminals. This result is not surprising as, MVIIC is known to block N-, P-, and Q-type VGCCs (Wright and Angus, 1996) and control terminals seem to rely on several channel subtypes for release, whilst N-type channels seem to play the major role in diabetic terminals. As MVIIC has 10-100 times lower affinity for N-type channels than GVIA (Randall and Tsien, 1995) not all the N-type channels in the diabetic terminals will be blocked, no other channels play that much of a role and so more Glu release will be observed than seen in the control terminals.

Overall, all these experiments indicate that L-type channels play a role in establishing the mode of exocytosis in the control terminals, whilst N-type channels play a crucial role in the diabetic terminals. However, the precise concentration of GVIA to be used to study this phenomenon still needs to be established.

II.3.2 Role of Calcium/Calmodulin dependent Kinase II

Previous data indicated that both Ca²⁺ and protein phosphorylation regulate the switch between the two modes of exocytosis. Treatment with 10 μ M KN93 (that specifically blocks the action of CaMKII) (Wheeler et al., 2008) was undertaken to elucidate the role of CaMKII. When three different stimuli were used to study evoked Glu release, it was established that HK5C and ION5C evoked release were perturbed in the presence of KN93, whilst 4AP5C evoked release was not affected in the control terminals. This result can be explained from knowing that 4AP5C induces smaller changes in the amount of Ca²⁺ influx, which is sufficient enough to release the RRP but not the RP. From this data, it can be inferred that; inhibition of CaMKII blocks the release of the RP of SVs but not the RRP (Figure 23). The data with 10 μ M KN-93 can be explained by the fact that, the RP of SVs is associated with the cytoskeleton, and in order for these vesicles to exocytose they need to be dissociated from the cytoskeleton. The SVs are linked to each other by the phospho-protein synapsin 1, that binds the fibrous proteins actin and spectrin and is linked to the cytosolic surface of all SV membranes. Additionally,

synapsin filaments radiate from the PM and attach to vesicle-associated synapsin. These interactions may allow the SVs to face in the right direction, i.e. towards the PM. Synapsins are preferentially located near the RPs at the ultrastructural level i.e near the vicinity of the AZ (Fdez and Hilfiker, 2006). After the arrival of AP, the Ca^{2+} entry results in the activation of CaMKII, which then phosphorylates synapsin 1 (Shupliakov, 2009). Upon phosphorylation, synapsin 1 loses affinity for both the SV membrane and the actin microfilaments (Cingolani and Goda, 2008). This mechanism enables the SVs to detach from the cytoskeleton and such vesicles are then available to contribute to NT release (Fdez and Hilfiker, 2006). The results obtained suggest that, the RPs are attached to the cytoskeleton and that the inhibition of CaMKII by KN93 results in the synapsin 1 remaining in its dephosphorylated form, such that the RPs cannot detach from the cytoskeleton; and are therefore unavailable for exocytosis as is demonstrated by the decrease in the Glu release (Figure 20A and B). This result also emphasizes the fact that, HK5C and ION5C evoke release of not only the RRP but also the RP of vesicles. Likewise, this also provides further evidence of the claim that 4AP5C only acts on the RRP and does not act on the RP of vesicles.

Importantly, the role of CaMKII in regulating the mode of exocytosis could be studied by evoking FM2-10 dye release with 4AP5C. In control terminals, it was found that blockade of CaMKII resulted in the switching of the mode of exocytosis, from K&R to FF (Figure 24). Thus, phosphorylation of certain proteins by CaMKII results in the RRP undergoing exocytosis by a K&R mode, whilst failure to phosphorylate such proteins leads to the vesicles exocytosing by the FF mode. Similar studies needs to be carried out in the future on diabetic nerve terminals.

II.3.3 Role of Myosin II

The inhibition of myosin II by Bleb was responsible for the switch in mode of exocytosis when evoked by HK5C from K&R to FF in control terminals and in the diabetic terminals, indicating that the function of myosin II was unaltered in such synaptosomes. Previous results in chromaffin cells in which catecholamine vesicle fusion was studied demonstrated a similar role of myosin II in regulating the mode of fusion (Aoki et al., 2001). However, it is difficult to directly compare

control synaptosomes (Figure 25B) and diabetic synaptosomes (Figure 26B) as these were done several months apart. To directly compare the exact amounts of FM2-10 dye being released between control and diabetic one actually needs to do these at the same time (i.e. in the same experiment). Whilst one can observe that a drug has an effect upon FM2-10 dye release from either type of synaptosome, the actual absolute amounts sometimes vary and this makes it difficult to assign the change in release to a particular pool of SVs. This argument is put forward because it was speculated that the effect of Bleb on diabetic synaptosomes is probably due to the switch of RRP of SVs to FF, but that there is no switch of those RP of SVs that are undergoing K&R. This is because it has been hypothesized that myosin II acts when activated by the high amount of Ca^{2+} at the AZ following application of HK5C. However, such levels of Ca^{2+} will not be seen by the RP of vesicles as they are exposed to the bulk $[\text{Ca}^{2+}]_i$ which is probably not sufficient enough to activate myosin II. Thus, it is believed that the Bleb treatment in the diabetic terminals induces the RRP to switch to FF, but as myosin II is not activated by the level of Ca^{2+} that activates the RP, those RP of SVs that are K&R will not be switched to FF. This is not so obvious if one compares Figs 25B and 26B.

II.3.4 Role of Calcineurin

1 μM Cys A inhibits CaN, Ca^{2+} -dependent protein phosphatase (Batiuk et al., 1995; Igarashi and Watanabe, 2007). When control terminals were treated with Cys A, there was no effect on HK5C evoked Glu release but, intriguingly, there was a decrease in HK5C evoked FM2-10 dye release. Furthermore, inhibition of CaN with Cys A results in a larger increase in $[\text{Ca}^{2+}]_i$ following application of a stimulus, a result seen previously (Person and Raman, 2010). This treatment was repeated herein, just to compare with the dual treatment involving the inhibition of myosin II and CaN. Such treatment failed to perturb HK5C evoked Glu release but unexpectedly, decreased the HK5C evoked FM2-10 dye release compared with Bleb treatment alone. This disproved the initial hypothesis that, the combination of these two drugs may result in a larger increase in FM2-10 dye release, due to a CaN mediated increase in $[\text{Ca}^{2+}]_i$ upon stimulation. This could possibly activate myosin II further (thus, get greater K&R) but this would be switched to a greater amount of FF due to the fact that Bleb inhibited myosin II.

One possible explanation could be that, all the RP of vesicles are switched to K&R mode of exocytosis with the dual treatment (usually the Cys A only causes a switch of some of the RP of SVs to this mode), whilst Bleb induces the RRP of vesicles to undergo FF. Thus, the two drugs give opposing effects and so compared to Bleb alone there will not be as much FM2-10 dye released following the dual treatment. This might appear to suggest that, Cys A has counteracted Bleb's action but the hypothesis above suggests that the two drugs are acting on different pools of SVs. However, the fact that Bleb treatment may increase the effect of Cys A on the RP of vesicles will need to be further investigated in future. These results and explanation actually add to the knowledge gained in Dr. Ashton's laboratory about the pools of SVs and modes of exocytosis. It now seems apparent that, Cys A may only work on the RP of SVs (remember with HK5C all the RRP of SVs are already releasing via a K&R mode). Indeed, in preliminary experiments Dr. Ashton has found that Cys A fails to have an effect on the mode of exocytosis evoked by 4AP5C and this fits in with the fact that, 4AP5C only evokes exocytosis of the RRP and Cys A does not affect the RRP. Thus, it would appear that dephosphorylation of protein substrates for CaN is required for the RP to undergo the FF mode of exocytosis, and prevention of dephosphorylation by blockade of CaN will lead to the RP of SVs undergoing K&R exocytosis. This argument is supported by the study carried out in *Drosophila* which demonstrated that, CaN was required for endocytosis to the RP but not for the RRP (Kumashiro et al., 2005). Clearly, this effect may involve inhibiting the role of dynamin in clathrin-dependent endocytosis, which is associated with FF as dephosphorylation of dynamin is required for this latter process to occur.

An obvious future study is to carry out an equivalent experiment to Figure 28B where dual treatment of Bleb and CaN are applied on diabetic terminals.

II.3.5 Role of Dynamins

In order to directly study the role of dynamin an inhibitor of its GTPase activity - 160 μ M Dyn was employed (Chung et al., 2010). In the control terminals, Dyn did not affect the amount of Glu or FM2-10 dye release when evoked with HK5C (Figures 29A and B). This result with Glu release also confirms another result that has been established in the Dr. Ashton's laboratory. It has been shown that all three stimuli (HK5C, ION5C and 4AP5C) actually only evoke one round of SV fusions (of either the RRP and the RP or just the RRP) (Ashton, unpublished observation). This is confirmed herein because if there were several rounds of release, those SVs which exocytosed by FF and recycled by the dynamin requiring clathrin-dependent endocytotic pathway would be inhibited by Dyn, and so one should observe a reduction in the amount of Glu released compared to the control; and this is not seen. Likewise, recycling by a dynamin-dependent clathrin-independent mode (possibly K&R, see below) should be perturbed and so less release should occur if there was recycling and re-releasing of SVs during the time of application of these stimuli.

In the diabetic terminals, HK5C evoked release of Glu was not perturbed by Dyn treatment, but it was found that these synaptosomes discharged significantly greater amount of FM2-10 dye than control terminals (Figures 31A and B). This interesting result suggests that, dynamins do play a role in defining the mode of exocytosis of some of the SVs in the diabetic terminals. Active dynamin causes a greater amount of the K&R mode of fusion. However, both the 4AP5C evoked release of Glu and FM2-10 dye were not changed following Dyn treatment on the diabetic synaptosomes. As 4AP5C only releases the RRP, this result suggests that Dyn allows the RPs to undergo FF mode of exocytosis and not the RRP (as no extra release observed with 4AP5C). It can thus be concluded that, dynamins work on the RPs in defining the mode of exocytosis in diabetic terminals and there is no effect on the RRP of vesicles. It should be noted that just as with experiments with Bleb the absolute amount of FM2-10 dye released from Dyn treated terminals cannot be directly compared between the control (Figure 29B) and diabetic synaptosomes (Figure 31B), as both these experiments were not performed at the same time.

The result obtained also suggests that even though dynamins are required for replenishment of RRP in the control synaptosomes (Lu et al., 2009); it works on defining the mode of exocytosis on the RPs in the diabetic terminals.

The last couple of arguments might suggest that Dyn would act on the RPs and switch them to FF, whilst Bleb acts on the RRP to switch them to FF. However, the result for control synaptosomes for 4AP5C evoked Glu and FM2-10 dye release following Dyn treatment also needs to be considered. Whilst inhibition of dynamins has no effect on 4AP5C evoked Glu release, there is more FM2-10 dye release. Thus, with 4AP5C evoked release it would appear that Dyn is inducing the RRP of SVs to switch to a FF mode of exocytosis. This result differs from the findings in control synaptosomes with HK5C evoked release treated. A possible explanation for the difference obtained could be that, HK5C induces a larger change in the Ca^{2+} level at the AZ than 4AP5C, and the former condition can activate myosin II whereas 4AP5C does not (Tokuoka and Goda, 2006; Bhat and Thorn, 2009). Thus, the activated myosin II can close the pore independently of any action of dynamin and so dynamin action can be blocked by Dyn but myosin II if active can still close the pore. However, as myosin II is not activated upon the application of the 4AP5C stimulus but dynamins are, these latter proteins will play a role in closing the pore and when blocked by Dyn, a switch to FF is observed; as demonstrated by the increase in FM2-10 dye release. Such an explanation is borne out by the results with the diabetic terminals. Upon application of the HK5C stimulus, some RP of SVs are undergoing K&R release (as explained previously this may be due to the larger changes in $[Ca^{2+}]_i$ obtained following HK5C application). However, as these RP of SVs is not exposed to levels of Ca^{2+} that could activate myosin II; the mode of these vesicles can be regulated by dynamins (unlike the RRP of SVs). However, with 4AP5C stimulation the increase in $[Ca^{2+}]_i$ level at the AZ in diabetic terminals may now be sufficient to activate myosin II and so Bleb can regulate the mode of exocytosis and this will bypass any role of dynamins.

II.3.6 Dual effect of Dynamin and Myosin II inhibitor

HK5C evoked Glu release in control synaptosomes, was not changed following the dual treatment with 50 μ M Bleb and 160 μ M Dyn. From all the experiments and discussion above, it was expected that such a joint treatment would cause all SVs to switch to FF. However, completely disproving the hypothesis, this dual treatment significantly reduced the amount of FM2-10 dye release. This finding remains unexplained, as it was believed that myosin II bypasses the role of dynamins and therefore, by inhibiting both of these proteins could result in more of the FF mode of exocytosis. Perhaps, the inhibition of both of these proteins causes activation of another protein or these two proteins actually regulate each other in some way, possibly, at some particular stage in the vesicle pathway. Future experiments utilizing this dual treatment on diabetic terminals may help reveal the complex interactions that might be occurring.

II.3.7 Role of Protein Phosphatase 2A and Protein Kinase C

Phosphatases play a crucial role in a number of signal transduction pathways in neurons (Rusnak and Mertz, 2000). Dr Ashton had already established that, inhibition of PP2A with 0.8 μ M OA results in switching of the mode of exocytosis from K&R to FF mode of exocytosis in the control terminals (Figure 34). As there is more K&R exocytosis observed in the diabetic terminals this must be because some RPs along with all the RRP release via this mode. 0.8 μ M OA did switch the mode of exocytosis to FF in such diabetic terminals (Figure 35), but this switch did not produce maximal FF as in control terminals. As a complete switch to FF of the RRP of SVs was apparent with 4AP5C in OA-treated diabetic terminals (Figure 36), such results suggest that, the RP of SVs that were undergoing K&R in the diabetic terminals could not be switched by inhibiting PP2A. These results suggest that, PP2A exclusively acts on the RRPs of SVs, and the RPs in the diabetic terminals that undergo K&R is unaffected.

1 μ M of PMA causes a switch in the mode of exocytosis in the control terminals (Figure 37) and so this was studied in diabetic terminals. It is known that PMA activates the PKC and Munc 13 pathway, but it has been shown by Dr Ashton (unpublished observation) that PMA switches the mode of exocytosis in control

synaptosomes via the PKC pathway, as its action can be blocked by an inhibitor of PKC. Interestingly, similar results to those following OA treatment were observed in the diabetic terminals (Figure 38) This could also suggest that, PKC also acts exclusively on the RRP (as shown with 4AP5C stimulation, Figure 39) and not on the RPs in the diabetic terminals.

However, when diabetic nerve terminals were exposed to OA and PMA together, all the pools of SVs were switched to a FF mode of exocytosis (Figure 40). This was further confirmed by comparing the combined treatment with the individual treatment. It was thus established that, PMA+OA induced more FM2-10 dye release than PMA alone (Figure 41) or OA alone (Figure 42). Thus, whilst each of these treatments seem to work exclusively on the RRP, the joint treatment also allows the switch of the RP. Clearly, there appears to be some extra activity that is acted upon under the dual treatment. This could involve a larger increase in the phosphorylated state of some PKC substrates due to the inhibition of PP2A. Clearly, further studies need to be carried out in order to elucidate the mechanism by which such a joint treatment acts. However, this could be very useful in determining an important PKC substrate that regulates the modes of exocytosis.

II.3.8 Summary of Results obtained

The summary of the results obtained are depicted in the Figures and Tables below. The proposed difference in the Control and Diabetic nerve terminals are summarized in Table II.1 and Figure II.2 below:

Table II.1: Proposed difference in Control and Diabetic terminals using HK5C.

	Control Terminals		Diabetic terminals	
	RRP	RP	RRP	RP
K&R	✓	x	✓	✓ (some)
FF	x	✓	x	✓ (some)
Increase in $[Ca^{2+}]_i$	✓ ✓	✓	✓ ✓ ✓	✓ ✓

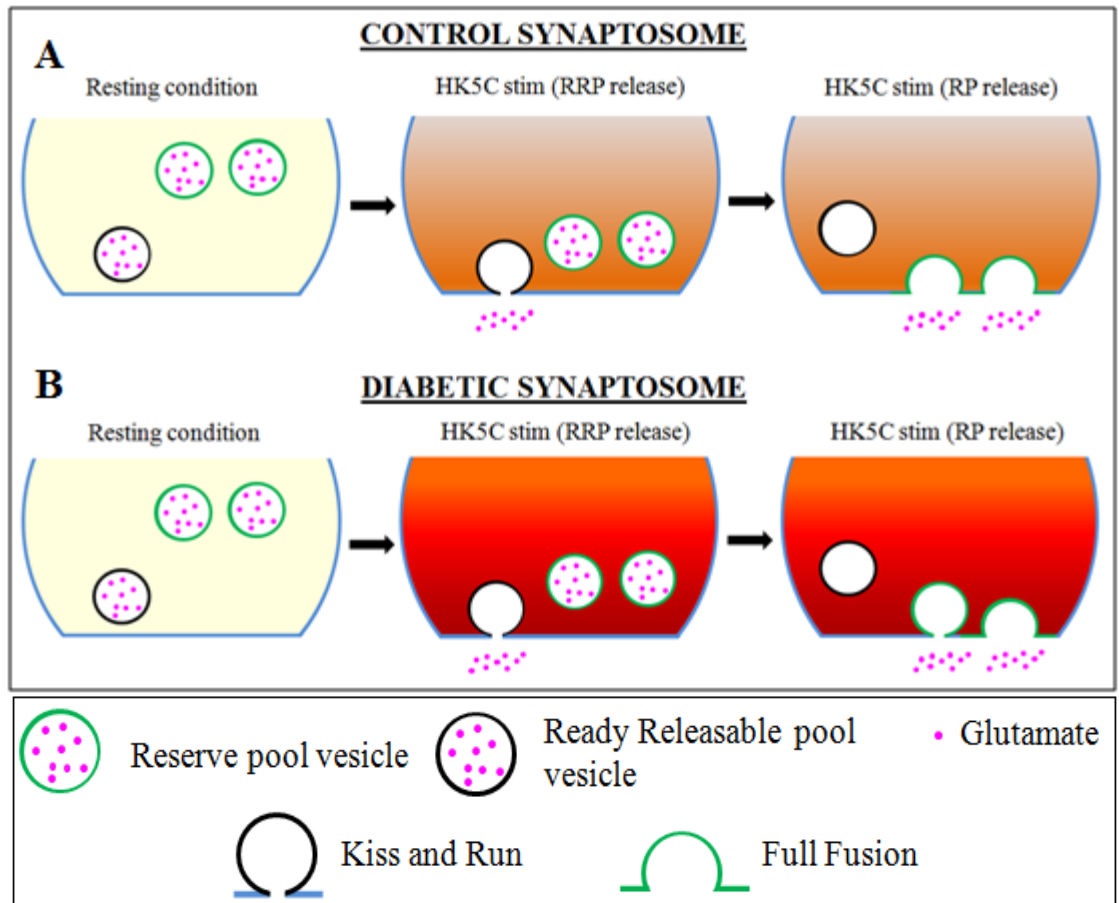


Figure II.2: Proposed difference in Control and Diabetic terminals: (A) The Left panel depicts a typical Resting nerve terminal (when no stimulus is applied) with black vesicles representing the RRP and the green ones signifying the RPs. Note that just one RRP of SV and two RP vesicles have been illustrated as this reflects that usually the RP is larger than the RRP but this does not indicate the actual number of SVs in the RRP and the RP. The middle panel represents a typical increase in the $[Ca^{2+}]_i$ upon application of stimuli (HK5C in this case). The orange colour represents the level of Ca^{2+} and the level drops as you go further away from the AZ of the terminal (the intensity of the orange colour decreases). First the RRP are released by K&R mode of exocytosis as soon as the stimulus is employed. Thereafter, the RPs are released by FF seconds after the arrival of stimulus (represented by the Right panel). (B) In the diabetic terminal upon the arrival of stimulus (represented by the middle panel), the $[Ca^{2+}]_i$ level is increased to a higher level than in the control terminal (Red colour). Herein, the RRP are released similar to that of the control terminal. However, subsequently some RPs are released by K&R mode of exocytosis (due to the higher level of $[Ca^{2+}]_i$) and the rest of the RPs are released by FF mode of exocytosis.

Upon application of various drugs to such terminals to elucidate the role of the VGCCs, the protein kinases and phosphatases are summarized in Table II.3.

Table II.3: Role of VGCCs, protein kinases and protein phosphatases in defining the mode of exocytosis in Control and Diabetic terminals.

Role in defining of the mode of exocytosis	Control Terminals			Diabetic terminals		
	HK5C		4AP5C	HK5C		4AP5C
	RRP	RP	RRP	RRP	RP	RRP
P-type VGCCs	x	x	Not Tested	x	x	Not Tested
L-type VGCCs	✓	x	Not Tested	x	x	Not Tested
N-type VGCCs	x	x	Not Tested	✓	Not known	Not Tested
CaMKII	Cannot be tested	Cannot be tested	✓	Not Tested	Not Tested	Not Tested
Myosin II	✓	x	x	✓	x	✓
Calcineurin	x	✓	Not tested	Not tested	Not tested	Not tested
Dual effect of blocking	x	✓	Not	Not	Not	Not

Myosin II and Calcineurin			tested	tested	tested	tested
Dynamins	x	x	✓	x	✓	x
Protein Phosphatase 2A	✓	Possibly	Not tested	Possibly	Possibly	x
Protein kinase C	✓	x	Not tested	✓	x	✓
Dual effect of blocking Protein Kinase C and Protein Phosphatase 2A	Not tested	Not tested	Not tested	✓	✓	✓

✓ Plays a Role in Defining the mode of exocytosis.

x Does not play a Role in Defining the mode of exocytosis

An example of such drug action is illustrated in the change in the mode of exocytosis upon application of Dyn in Figure II.2 below:

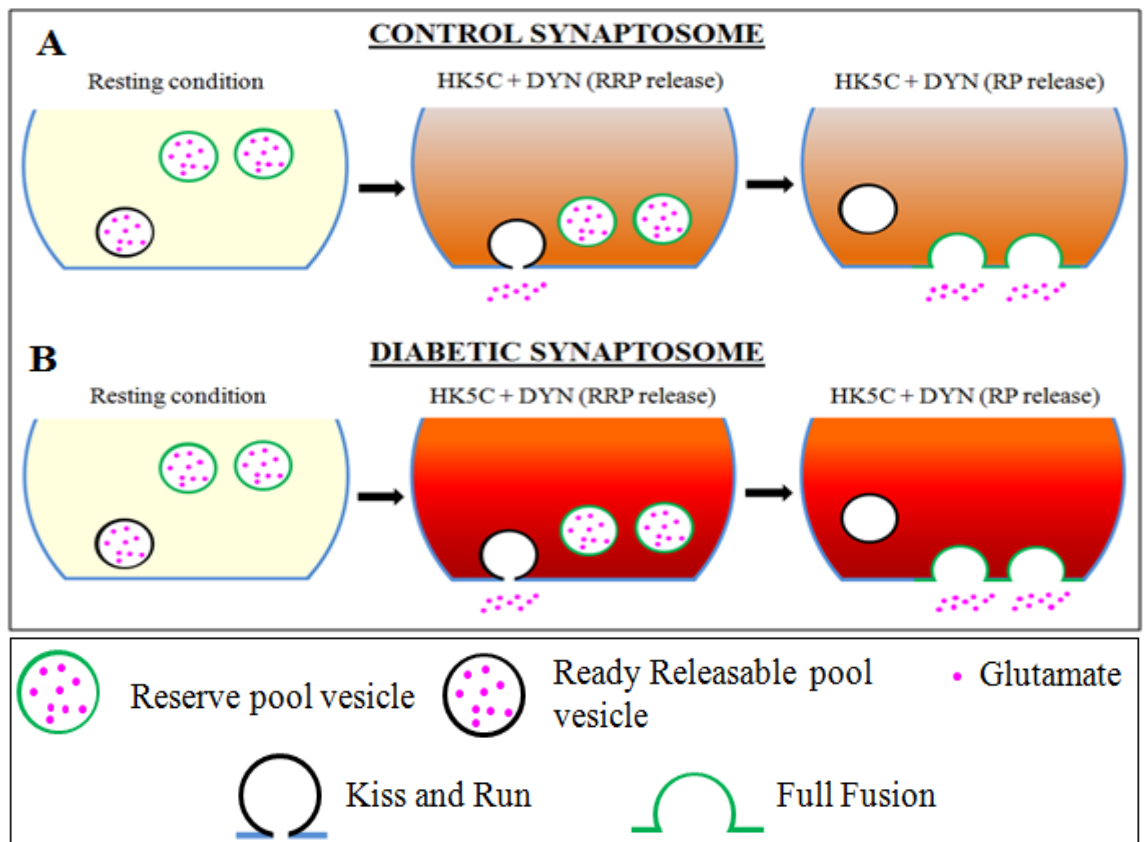


Figure II.4: Difference in the mode of release evoked by HK5C in Control and Diabetic terminals following application of Dyn: **(A)** There is no difference in the control terminal upon application of Dyn. The panel is replica of the panel A in Figure II.1, and this indicates that dynamins do not play a role in the mode switching (with HK5C) in the Control terminals. **(B)** In the diabetic terminal, however, upon application of HK5C in presence of Dyn, the RRP are still undergoing the K&R mode of exocytosis (represented by the middle panel) but those RPs undergoing K&R mode of exocytosis are switched to FF. This signifies that Dynamins play a role in defining the mode of exocytosis of RPs in Diabetic terminals.

II.4 Conclusions and Future Studies

It can be concluded that, L-type channels play a role in the switching of the mode of exocytosis in control terminals. However, N-type channels play a significant role in the diabetic terminals and more experiments with the optimal sub-maximal concentration of ω -conotoxin GVIA need to be performed.

Activated CaMKII can induce a K&R mode of exocytosis of RRP in control synaptosomes, as the mode is switched to FF following KN93 induced inhibition of this enzyme. Additionally, these experiments confirmed that, 4AP5C exclusively releases the RRP whilst HK5C and ION5C release both RRP and RP of SVs. A role for CaMKII in mode switching in diabetic terminals needs to be established.

There was apparently not much difference in the role of myosin II in regulating the mode of exocytosis in control and diabetic synaptosomes when HK5C was employed, but 4AP5C activated myosin II, and thereby bypasses an effect of dynamin, in diabetic terminals. The dual blockade of myosin II and CaN led to the idea that, CaN only regulates the fusion mode of the RP of SVs in control terminals. Thus, by using diabetic terminals and comparing these to control terminals, it was established that, active PP2A regulates the mode of exocytosis of the RRP of SVs whilst active PP2B (CaN) regulate the mode of exocytosis of the RPs. The inhibition of both dynamins and myosin II resulted in many SVs undergoing a K&R mode of fusion via an unexplained mechanism. An explanation may be revealed in the future by repeating this study on diabetic synaptosomes.

Finally, the dual treatment of OA and PMA led to a switch of all SVs to a FF mode by a mechanism that is not fully understood. More research needs to be carried out to understand the underlying mechanism of the changes observed.

III. Monitoring Behavioural Changes in Diabetic Rats using LABORAS

As demonstrated in Chapter II, the diabetic rat terminals exhibit different biochemical changes when compared to control nerve terminals. Consequently, it was suspected that these changes affect the synaptic plasticity in the long-term and may result in some behavioural changes. Thus, some initial observations involving studying various aspects of behaviour was carried out. A newly developed behaviour registration system, Laboratory Animal Behaviour Observation, Registration and Analysis System (LABORAS) for the automatic registration of different behavioural elements of individually housed mice and rats was validated.

III.1.1 Laboratory Animal Behaviour Observation, Registration and Analysis System

LABORAS is a powerful system that fully automates the behavioural scoring of small laboratory rodents, like rats and mice. LABORAS not only provides tracking related data, but also provides you with data on a large number of real behaviours, unlike many other systems, such as photo-beam trackers and video tracking. It is a sophisticated and extensive technique rather than the conventional use of video systems or 'infrared beam breaking' systems, as LABORAS measures vibrations. It thereby does not have the problems of reflections, poor resolution or large data files. LABORAS is independent of light conditions i.e. it can measure in dark and under all light conditions. It automates the behaviour scoring of up to eight solitary housed animals at the same time. This home-cage system can monitor behaviour of rats for over a 24hrs activity period for up to 7 days. Van de Weerd et al., (2001) compared the conventional observation methods with LABORAS and showed that LABORAS is a reliable system for the automated registration of eating, drinking, grooming, climbing, resting and locomotor activity (LMA) of rodents during a prolonged period of time. Thus, this system can reduce observation labour and time considerably (Van de Weerd et al., 2001) and can be reliable and free of inter- and intra-observer bias or anticipated scoring, thereby providing a standard behavioural measurement

worldwide. LABORAS enables the researcher to carry out more and increasingly effective experiments in less time using fewer animals and less equipment. It is this unique functionality, which enables LABORAS to perform behavioural research faster, more consistently and more efficiently than human observations or other automated systems can achieve.

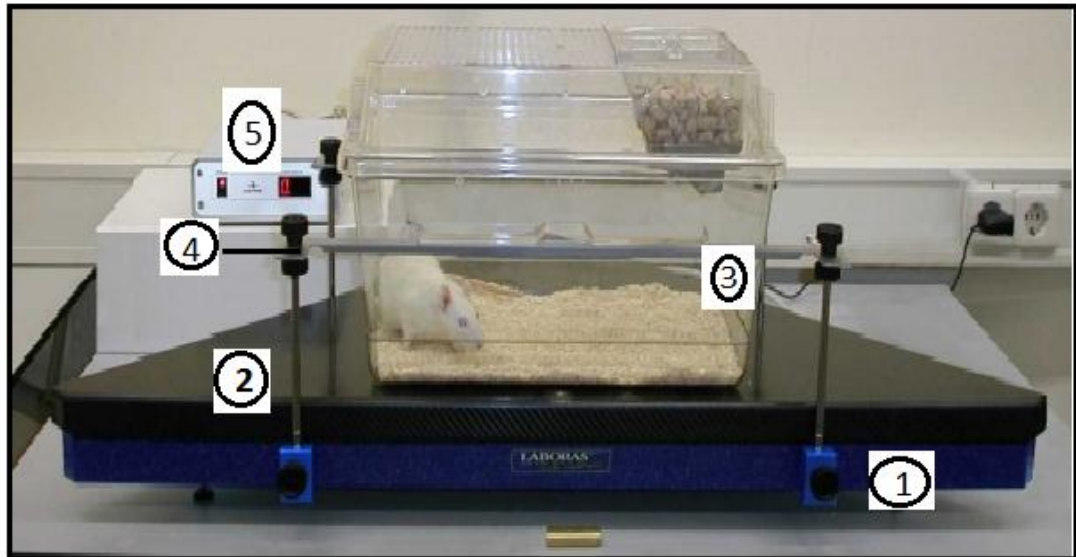


Figure V: The LABORAS behaviour registration system: Sensor platform 1. Corian baseplate 2. Carbon Fibre measurement plate 3. Clear polycarbonate cage 4. Construction that holds upper part of the cage 5. LABORAS Control Unit (http://www.metris.nl/en/products/laboras/laboras_information/)

LABORAS is based on vibration and force signal analysis to determine both the behaviour and the position of the animal. This system (Figure V) is made up of a triangular shaped sensor platform consisting of a heavy "Corian" baseplate where the force transducers are accumulated, a very lightweight and firm Carbon Fibre measurement plate (Carbon Fibre Plate $700 \times 700 \times 1000 \times 30$ mm, Metris b.v.) which is positioned on the top of the transducers (Van de Weerd et al., 2001). These are positioned on two orthogonally placed sensors (SPS Load cell, 1 kg, AE-sensors BV, Dordrecht, The Netherlands) and a third fixed point, attached on a bottom plate ($690 \times 690 \times 976 \times 13$ mm, Aeroweb Honeycomb material, CIBA-Geigy, Switzerland). The whole structure is positioned on three poles, which have rubber feet to adjust height and to absorb external vibrations (Quinn et al., 2005). The rats are positioned in clear polycarbonate cages (floor area 840cm^2 , height

25cm/height to food hopper 15cm, cage: UNO Roestvaststaal, Zevenaar, The Netherlands, Hopper and Bottle: Lab Products Inc., Seaford, USA) with beddings (either wood shavings for control rats or sawdust for diabetic rats), which is placed on the sensor platform (Quinn et al., 2003). The upper part of the cage (including the top, food hopper and drinking bottle) is suspended in a high adjustable frame and is free from the sensing platform (As shown in Figure V). Four platforms are connected to the hardware and computer. The resultant mechanical vibration caused by the movements of the rats are picked up by the carbon fibre measuring plate and is transformed by each force transducer into electrical signals by each sensor (Quinn et al., 2005). These signals are amplified to a fixed signal and filtered to eliminate noise by the pre-amplifier. According to the weight of the rats entered during the commencement of the experiment, the gain and offset of the pre-amplifier are adjusted. The software through a simple calibration practice regulates this. The output signals of the amplifiers are sent to the LABORAS Control Unit (LCU), which converts the analogue signals into a digital format. The LCU can handle the signals of up to eight measurement platforms. The LCU sends the data over a serial line and digitally stores on a computer for further processing. In this system, each movement pattern has a unique frequency and amplitude and can be differentiated by the computer into separate behavioural categories (Quinn et al., 2003). This is illustrated in the Figure W. The LABORAS software (Metris B.V., Hoofddorp, The Netherlands) consists of an administration module that registers information on the experiment and test conditions. The data acquisition and storage module controls the hardware and handles the storage of the sampled signals. The software then processes the stored data using several signal analysis techniques to classify the signals and registers the duration and frequency into multiple behavioural categories of eating, drinking, rearing, climbing, immobility, undefined, LMA, and grooming (Van de Weerd et al., 2001; Quinn et al., 2005).

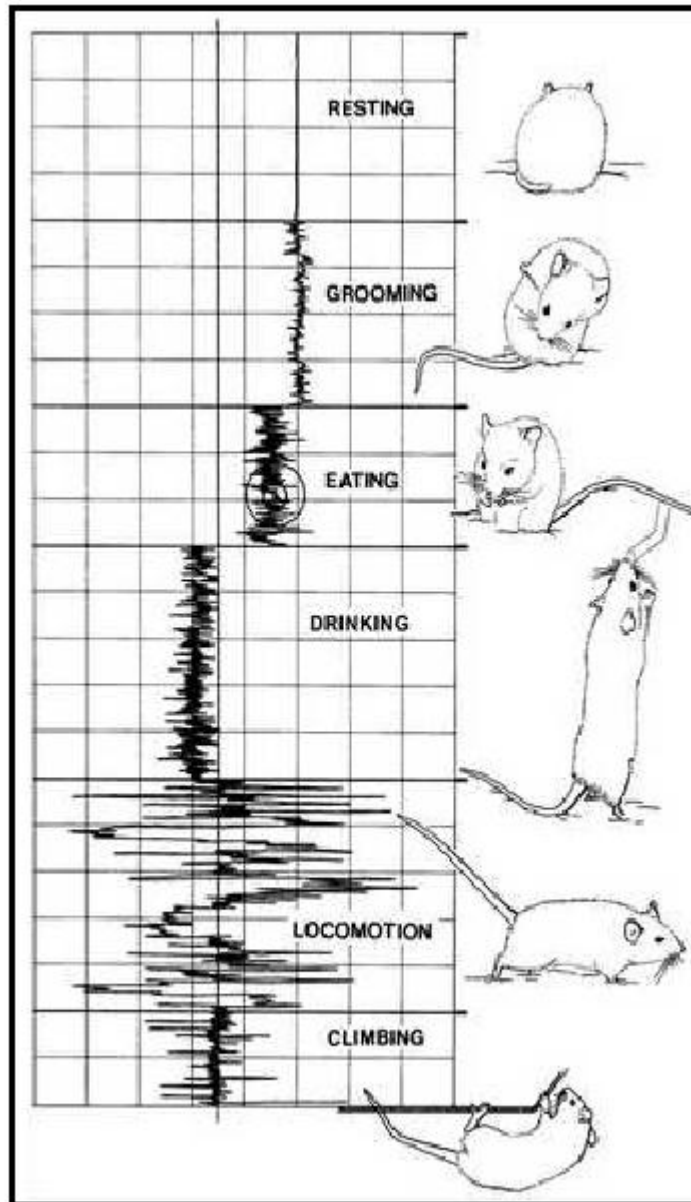


Figure W: Vibration patterns corresponding to individual behaviours are represented pictorially (Van de Weerd et al., 2001)

Table III.A: Positional and vibrational parameters used in the behaviour classification algorithms

Behaviour	Description for LABORAS
Drinking	The animal stands upright to lick water from the water bottle
Eating	The animal eats food pellets while standing upright, gripping the bars of the food hopper with its front paws and gnaw the food between the bars. It also includes gnawing a particle of food clasped between the front paws
Grooming	Shaking, scratching, wiping or licking its fur, snout, ears, tail or genitals
Motionless/Immobility	Movements are absent while the animal is in a sitting position
Locomotor activity	Activities such as walking, running, or jumping.
Rearing	Standing on the hind legs without touching the cage walls with the forepaws
Undefined	All behaviours that do not fit in one of the previous categories

The time resolution for behavioural sampling was 0.25s and the measures based on changes of gravity of the rats. Changes in gravity that exceeded 1.45cm/ 0.25s were recorded as LMA. Immobility was registered when the animal moved less than 0.75mm/0.25s (Augustsson et al., 2003). The behaviour that dominates is scored. In addition, it also provides tracking parameters such as position, speed, maximum speed, average speed, travelled distance and position distribution.

III.2.1 Materials and methods

For the validation study, 4 male Wistar rats either control or diabetic were used. At the time of the arrival, rats were about 160-200grams in weight. The animals were kept in same conditions as mentioned in section II.1.1 when not used for studies.

During the 24hrs monitoring period, 4 rats were singly housed with *ad libitum* access to food and water in a temperature and humidity controlled environment. Prior to the study, the rats were weighed, along with the amount of food and water given during the study. The weight of the food and water after 24hrs of monitoring was also recorded. The instrument was calibrated and then the rats were transferred into the respective cages and monitored for 24hrs. Each batch of rats (i.e. either the control or the diabetic cohort) was monitored every alternate day (4 days in a week); 2 days for diabetic and 2 days for control.

Most animals have circadian rhythm in their behaviour. Therefore, night-time tests would be more appropriate for rats since they are nocturnal animals, as they have high levels of activity after the beginning of darkness, thereafter periods of rest and activity alternate. Before dawn they have another (lower) activity peak. During the day, they mostly sleep (Borlongan et al., 1995). Consequently, the data presented has showed both the whole 24hrs period and the graphs for active period (Night time 19.00- 7.00). The active period is henceforth addressed as dark cycle. Additionally, 12hrs light cycle (7.00-19.00) was analyzed.

III.2.2 Statistical Analysis

The results were obtained by averaging each 2.24hr time point data obtained during the two independent experiments carried out on the same week and with the age-matched data obtained during the next set of experiment performed. The data was plotted using Microsoft Excel and *unpaired student t-test* was used to obtain statistical significance. The results with $p \leq 0.05$ were considered to be statistically significant for all the experiments.

The results presented compared the difference in each behavioural pattern found in each experiment and an average of the two independent experiments performed during different times of the year. The behavioural patterns were plotted as the total duration for which each were carried out and the frequency of the patterns. Additionally, the data is presented for the entire period of study (24hrs), for the dark cycle and light cycle. Each day the experiments were commenced at slightly different times (as following the 24 hours of measurements LABORAS takes 2 hours to calculate the data), so the precise start time for each experiment were noted and then the time courses were adjusted accordingly e.g. so that the time points in the 24 hour period were the same.

III.3 Results

As described earlier, LABORAS is capable of measuring various behavioural parameters at the same time.

III.3.1 Comparison of weights

The weights of the rats were monitored on daily basis along with the amount of food and water consumed. Figure 46 and 47 illustrates the comparison of weight gained by control (Cont) and diabetic (Diab) animals over the whole experiment, two independent experiments that were carried out.

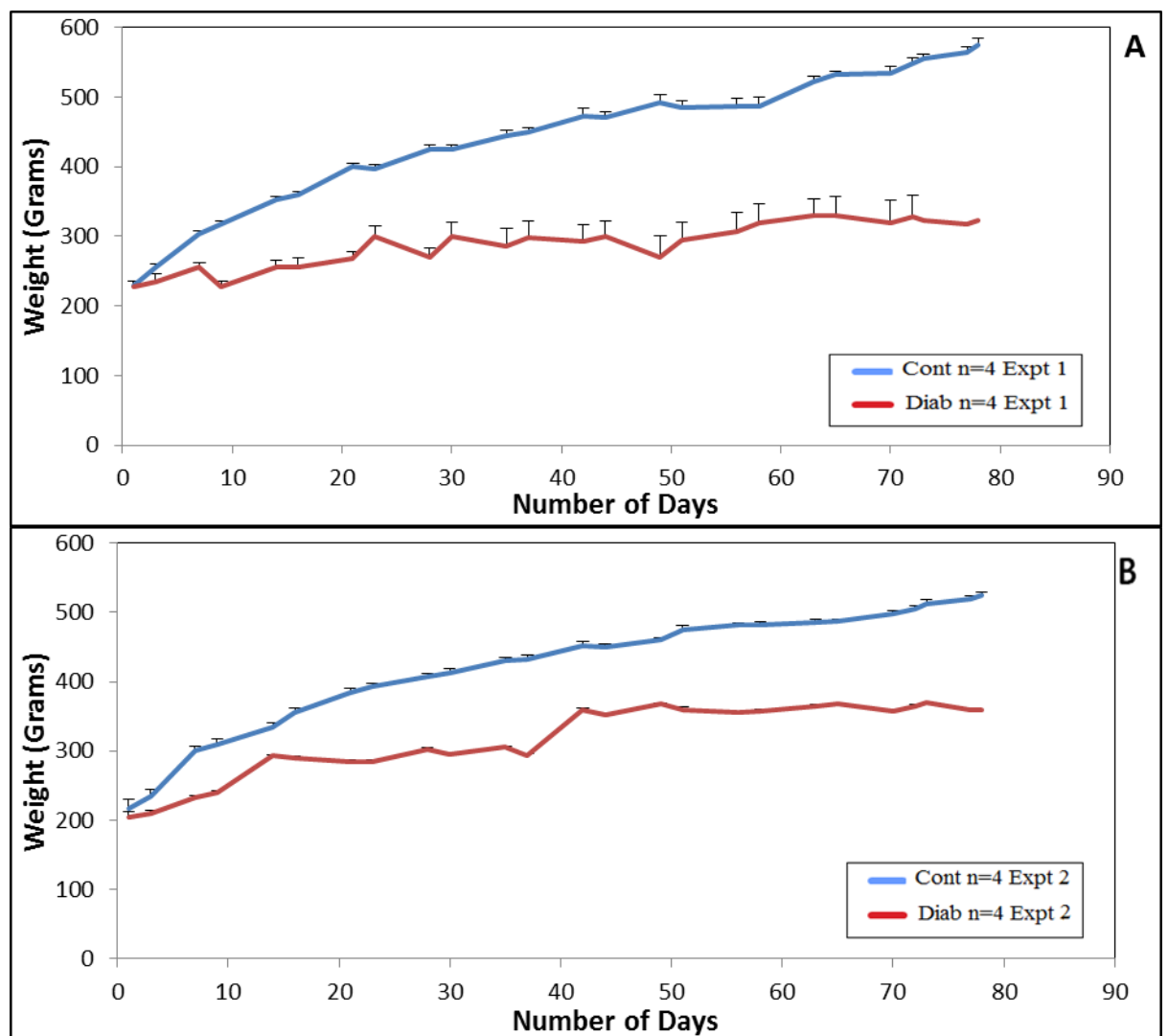


Figure 46: Diabetic rats gain significantly less weights than the Control rats over the period over 12 weeks after the STZ injection in (A) Expt 1 (B) Expt 2

It is clear from Figure 46 that the diabetic rats (DR) put on a little more than half the weight of the control rats (CR), for both the experiments (Figure 46A and Figure 46B). However, when the CR and the DR were compared against the two experiments, it was found that the amount of weight the DR gained in experiment 2 (Expt 2) was significantly more than the DR from experiment 1 (Expt 1) (Figure 47B). However, no significant difference for the weight gained was observed in the CR (Figure 47A). Many factors could be responsible for the difference observed in the two experiments. It could be possible that the amount of STZ injected would be slightly different for the two experiments, and as a consequence the animals from expt 2 do not develop as severe diabetic condition as the rats in expt 1. Alternatively, the rats in expt 1 may have been more sensitive to the STZ treatment, or the rats from expt 2 might have become resistant to STZ treatment. These could possibly explain some of the discrepancies that were observed in the results from the two experiments. However, it should be noted that at the end of 12 weeks, the rats used in expt 2 were still diabetic and this was checked by measuring their blood glucose levels, which was $> 20\text{mM}$ for all the rats.

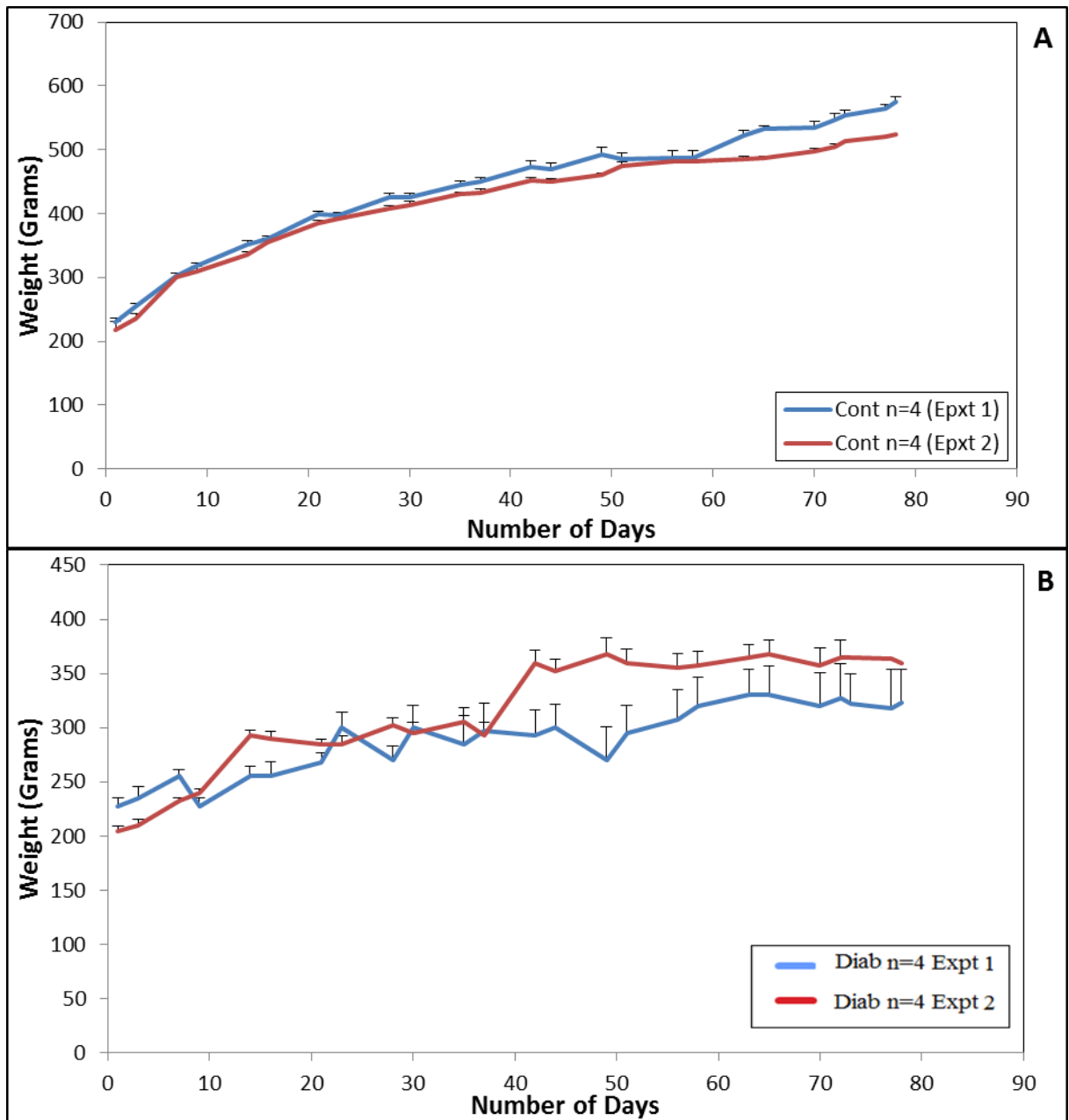


Figure 47: (A) No significant difference in the amount of weight gain observed in CRs from Expt 1 and 2 (B) Significant difference in the amount of weight gained observed in DRs from Expt 2 when compare to DRs from Expt 1 after 40 days post-STZ injection.

III.3.2 Locomotor activity

LMA is defined as the ability of animal to move from one place to another. LABORAS classes walking, running, climbing, jumping in its LMA category. For most of the weeks, DRs were significantly less locomotive than CRs in the 24hrs (Figure 48A), or the dark period (Figure 48B). Please note that it is apparent from the figures that the rats only travelled for about 1 minute in each of the 2.24hrs sections during the whole 24hrs cycle. It should be remembered that, LABORAS measured several activities and so although the rats appear not to be expressing LMA they are carrying out many other activities. Further, it is clear that rats in cages (whether control or diabetic) are quite sedentary compared to when they are free in the wild. Clearly, this does suggest that this LMA may be measured in a slightly artificial situation but it can still show whether CRs and DRs behave different towards this activity. Likewise, the frequency of LMA was reduced in DRs relative to CRs in 24hrs (Figure 49A) or 12hrs dark cycle (Figures 49B and 49C) when the average of the two experiments is determined. However, no difference in LMA behaviour was observed in the 12hrs light cycle for both the duration and the frequency (Figures 48 and 49) indicating that the difference seen between the CRs and DRs occurs during the dark cycle.

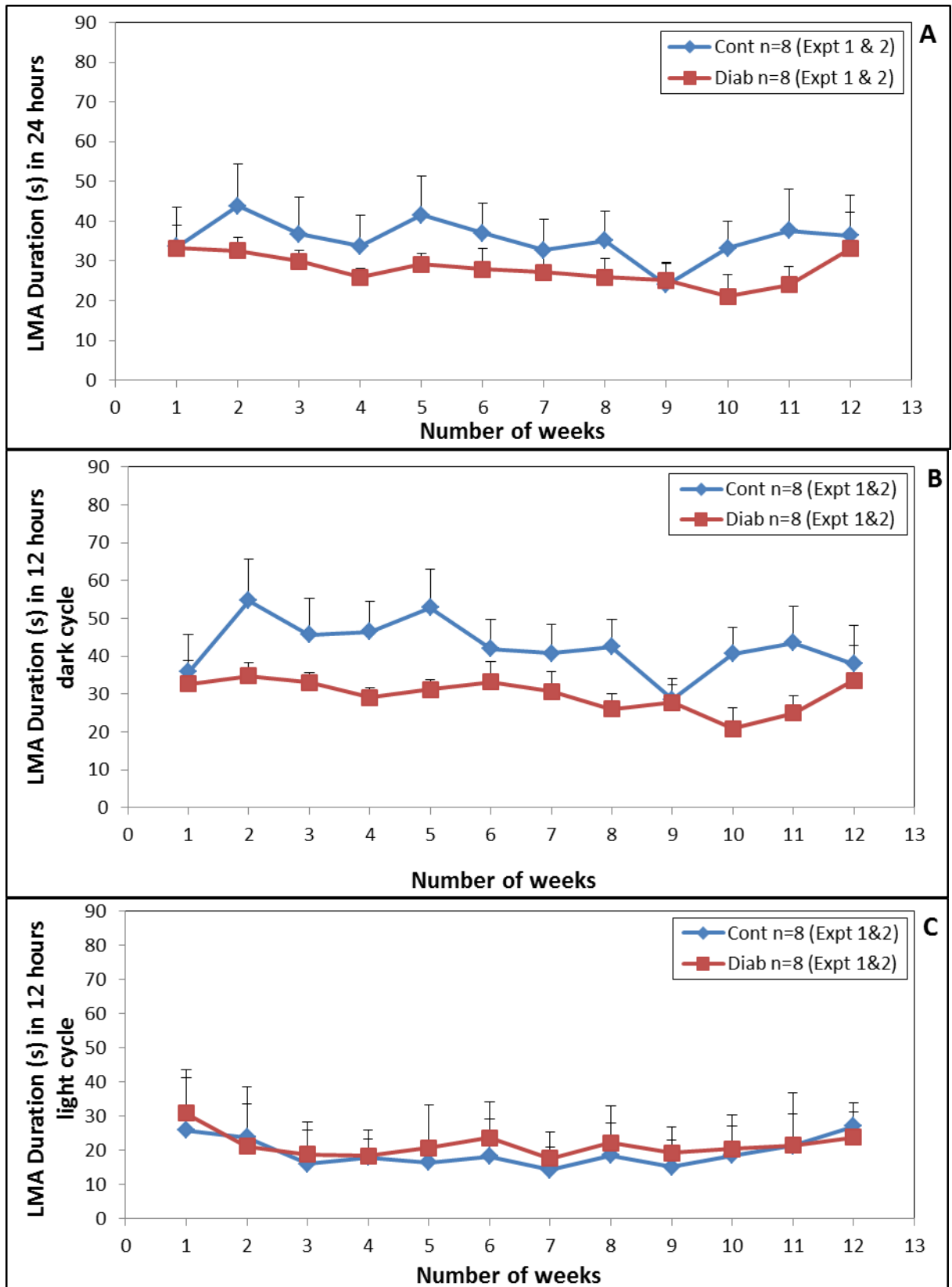


Figure 48: DRs displaced significantly less duration of LMA than CRs for (A) 12hrs dark cycle (B) 24hrs and (C) No significant difference observed in 12hrs light cycle for the Average of Expts 1 and 2

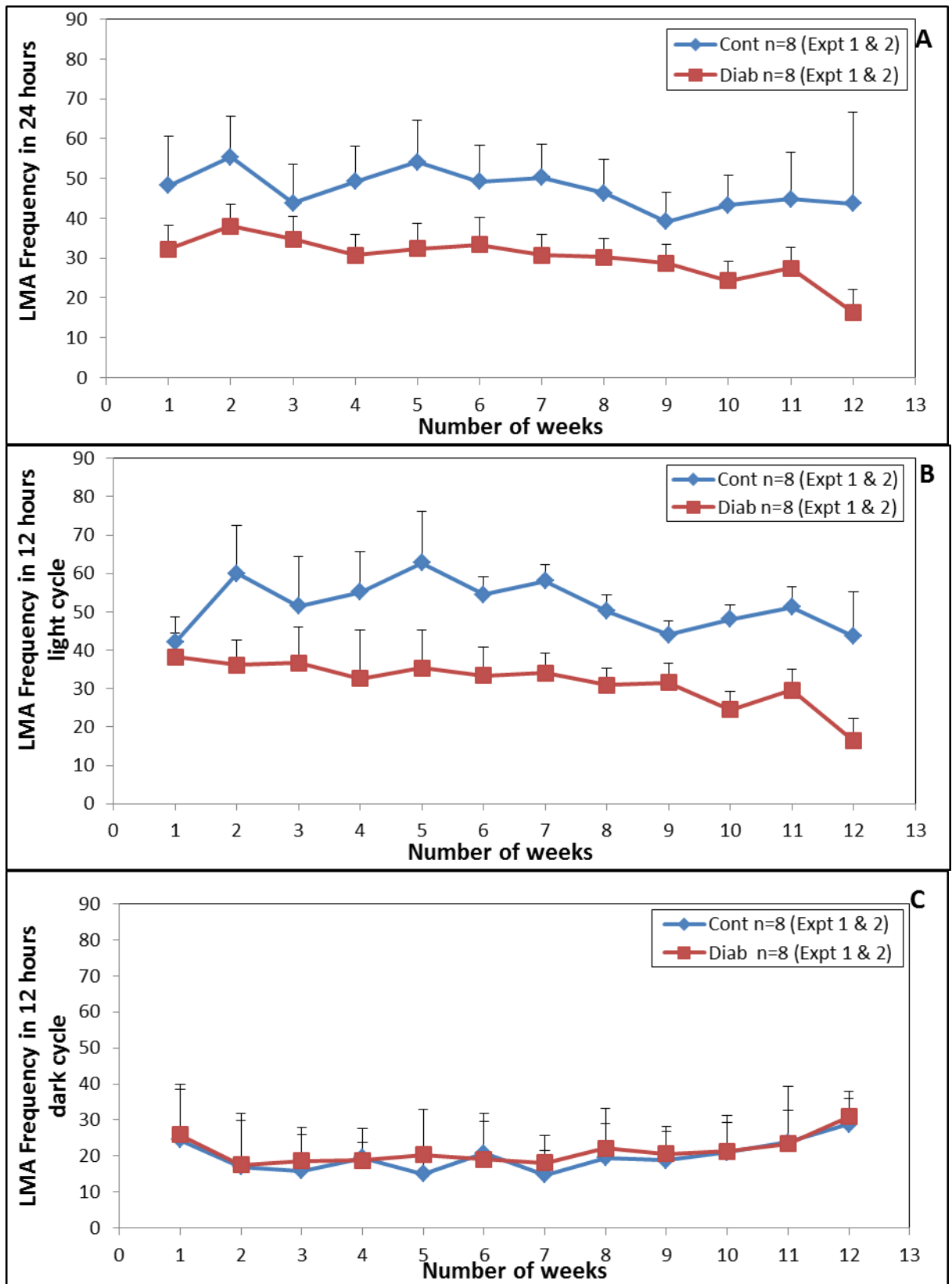


Figure 49: DRs frequency of LMA was significantly less than CRs for (A) 12hrs dark cycle (B) 24hrs and (C) No significant difference observed in 12hrs light cycle for the Average of Expts 1 and 2

In the average speed and distance (Figures 50) covered for expt 1, (Figures 50A) it was observed that the DRs covered a larger average distance with a greater average speed. This can explain why the DRs appear to be less locomotive, but actually cover more distance because they move quicker. However, expt 2 and the average of the two experiments displayed no difference for the 24hrs period (Figures 50B), 12hrs light (Figures 51A) and 12hrs dark period (Figures 51B). This could be because, as previously mentioned, the diabetes induced in the DRs was not similar in both the cases, or the CRs would be less active in one experiment and more in the other. Thus, this experiment needs to be repeated a few more times in order to eliminate and average the discrepancies observed in the two experiments.

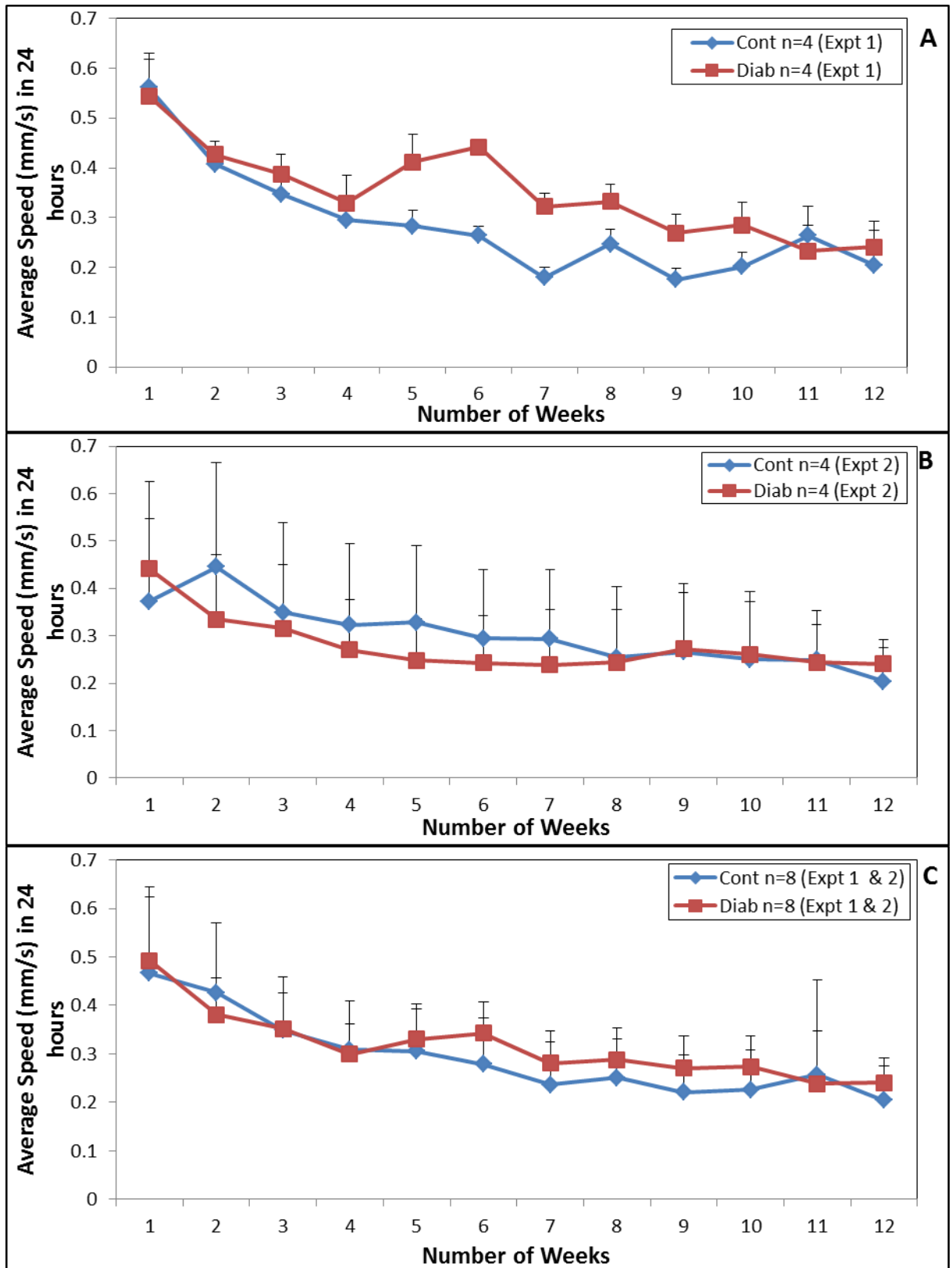


Figure 50: When the average speed of DRs and CRs was compared for 24hrs it was found that in (A) Expt 1 DRs travelled with significantly more speed than CRs from Week 5-10, however for (B) Expt 2 and (C) Average of Expts 1 and Expt 2 no significant difference observed between DRs and CRs.

Similar difference was observed in the 12hrs dark cycle and 12hrs light cycle for both speed and distance covered by the DRs and CRs. However, only the average of the two experiments is presented for these time periods.

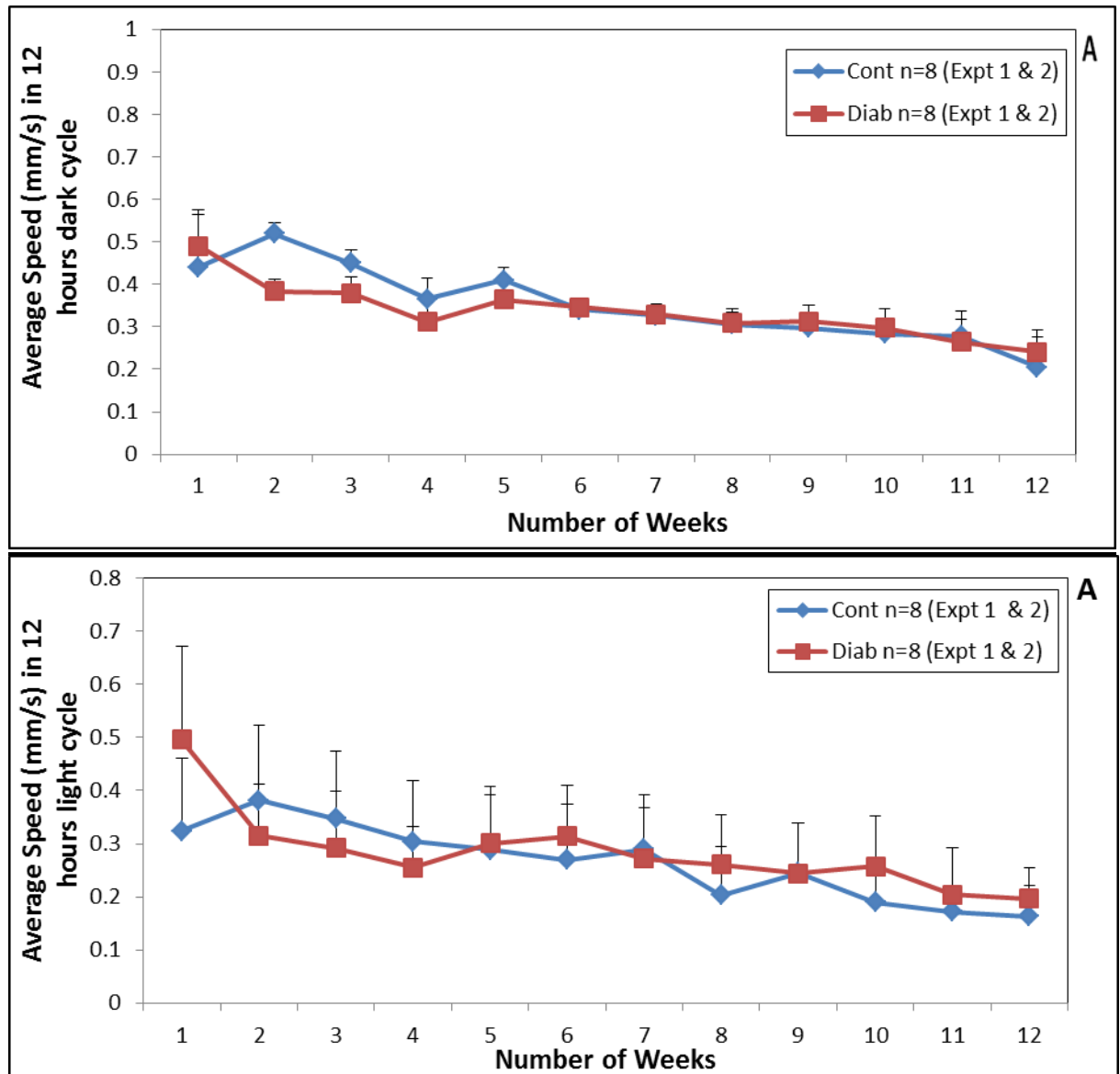


Figure 51: No significant difference in the average speed of DRs and CRs was observed in the average of Expts 1 and Expt 2 in (A) 12hrs dark cycle and (B) 12hrs light cycle.

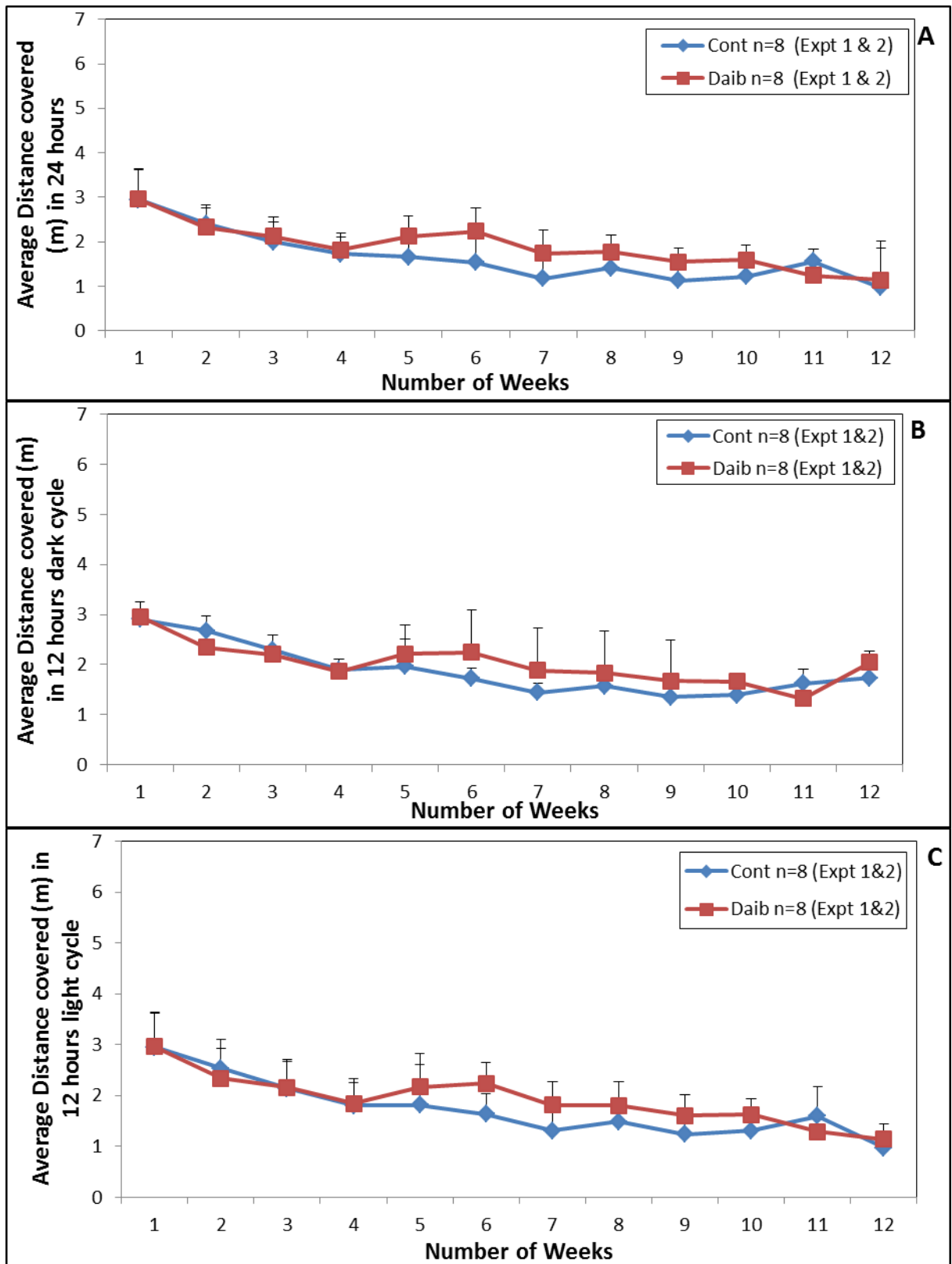


Figure 52: No significant difference in the distance covered by DRs and CRs was observed in the average of Expts 1 and Expt 2 for (A) whole 24hrs (B) 12hrs dark cycle and (C) 12hrs light cycle.

III.3.3: Immobility:

LABORAS describes immobility/resting behaviour as movements that are absent while the animal is in a sitting or lying position. In addition, short movements (e.g. turning over while sleeping) were also classed under immobility. Despite that for most of the weeks as stated in section III.3.2 DRs were less locomotive than the CRs, the duration of time DRs being immobile was significantly less than that for CRs for all the time periods for the average of the two expts (Figures 53A, B and C). However, in expt 2 no difference was observed between the two sets of rats (not shown). Additionally, the frequency of immobility was similar for both the animals for all the time periods (Figures 54A, B and C). It should be noted that, the rats were immobile for most of the time during the study; therefore, not much of difference in the time spent in this behaviour is observed for the entire 24hrs or the dark or light cycle. One result which seems to be consistent between the 2 expts is that the DRs are less immobile (i.e. they are doing some measurable activity) during the light 12hrs period. This suggests that the DRs might respond differently to the light dark cycle. It should also be pointed out there is not a problem between the DRs showing less LMA but also less immobility as this simply means that the DRs must be doing more of some other measurable behaviour.

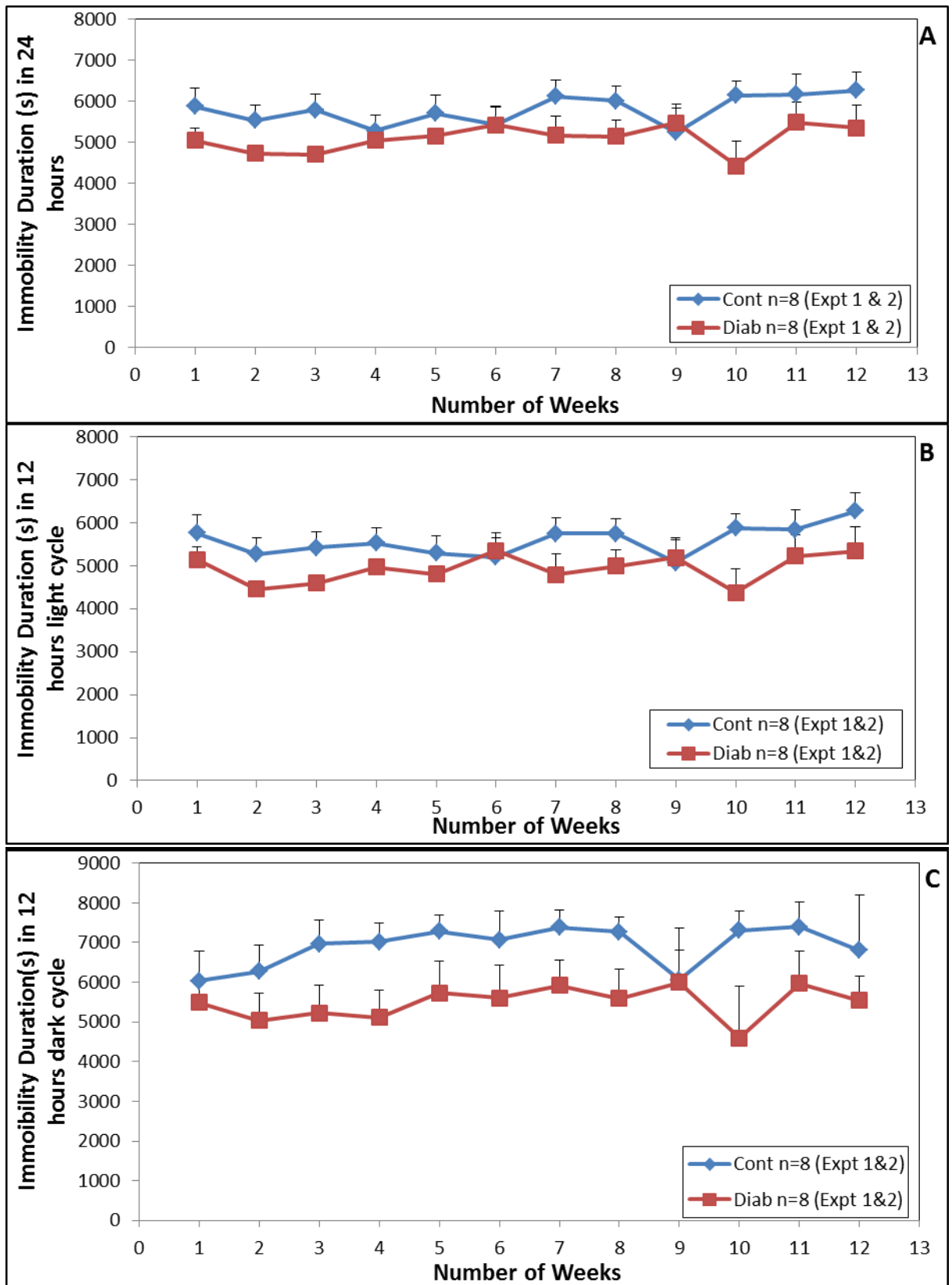


Figure 53: DRs display significantly less duration of immobility than CRs in Average of Expts 1 and 2 for (A) 24hrs, (B) 12hrs dark cycle and (C) 12hrs light cycle.

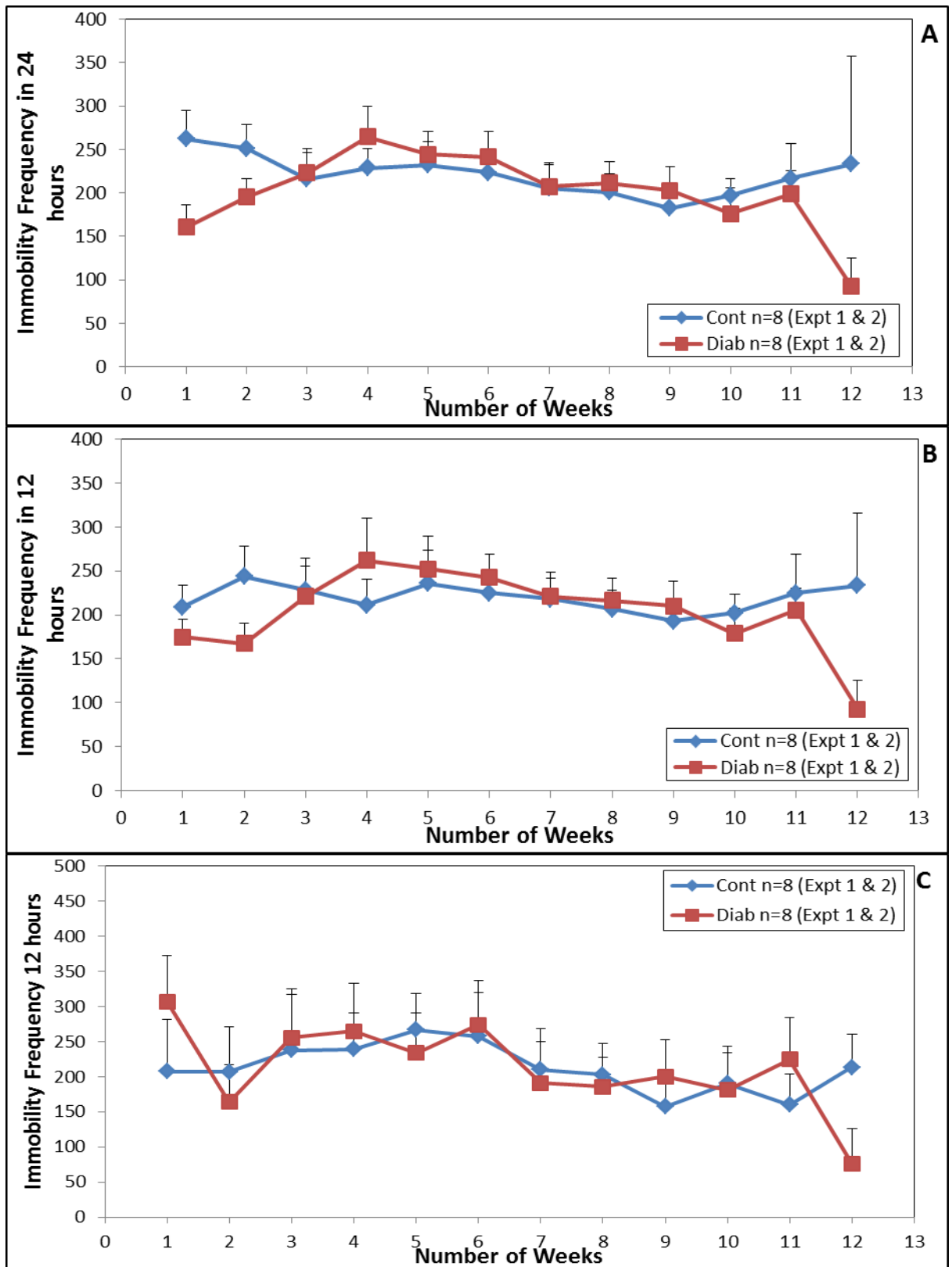


Figure 54: No significant difference in the frequency of immobility observed in CRs and DRs for the average of Expts 1 and 2 in (A) 24hrs, (B) 12hrs dark cycle and (C) 12hrs light cycle.

III.3.4 Rearing

Rearing is defined as the rats standing upright on their hind legs (mostly against the wall of the cage). From the Figures 55A, 55B, 56A and 56B it can be inferred that, the DRs reared significantly less than the CRs, for both duration of monitoring and frequency (from week 3-8 in most of the cases) for the 24hrs and the 12hrs dark cycle. This suggests that the DRs were less keen to explore the surrounding environment. However, individual experiment carried out do not show a significant difference (not shown), but the average does support the conclusion that indeed DRs rear less when compared to CRs. Additionally, no significant difference was observed in rearing during the light cycle (figures 55C and 56C), suggesting that there was a change in nocturnal pattern of the diabetic rats.

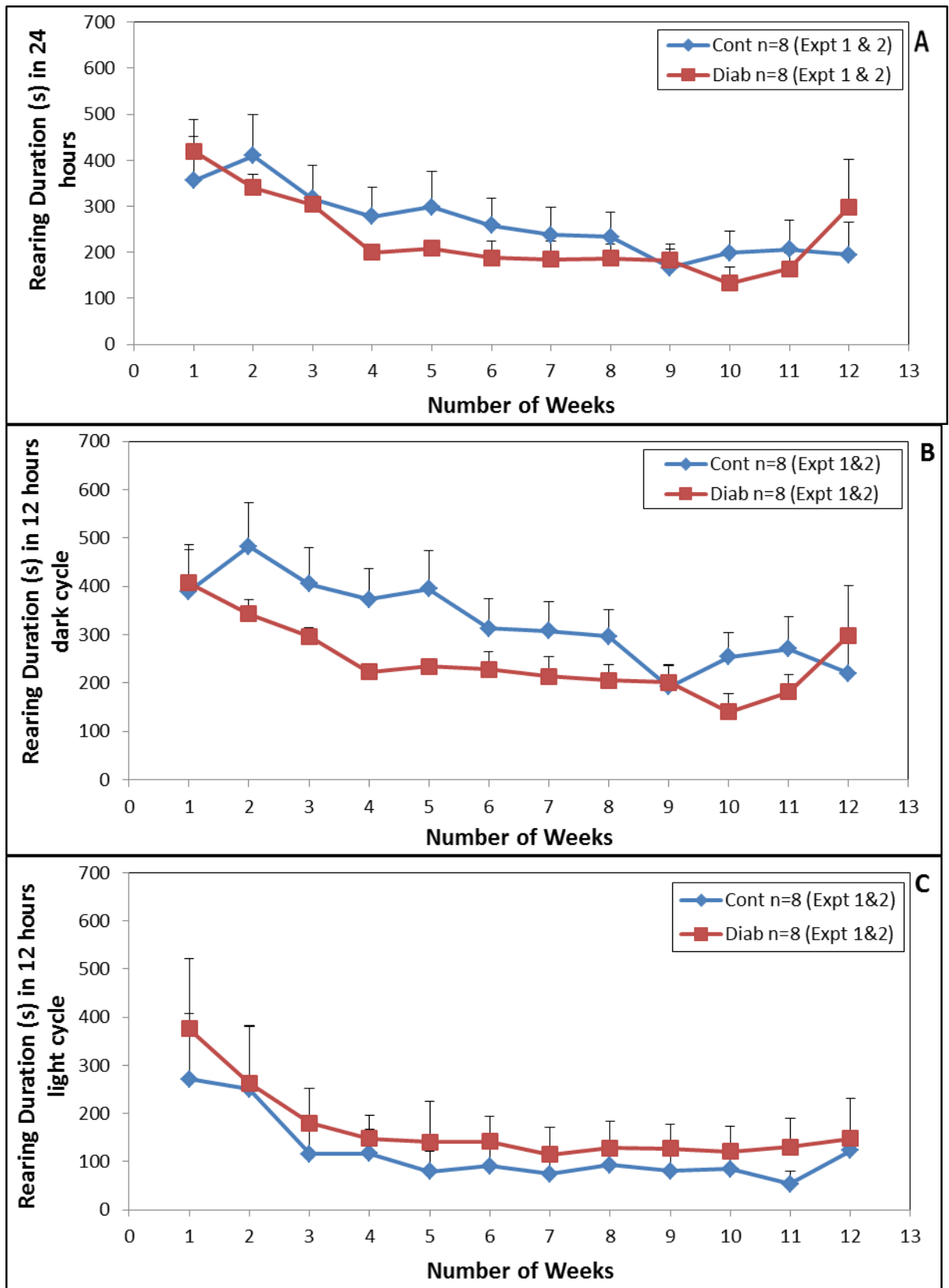


Figure 55: DRs display significantly less duration of rearing in comparison to than CRs in Average of Expts 1 and 2 for (A) 24hrs, (B) 12hrs dark cycle and (C) No Significant difference observed between DRs and CRs for 12hrs light cycle.

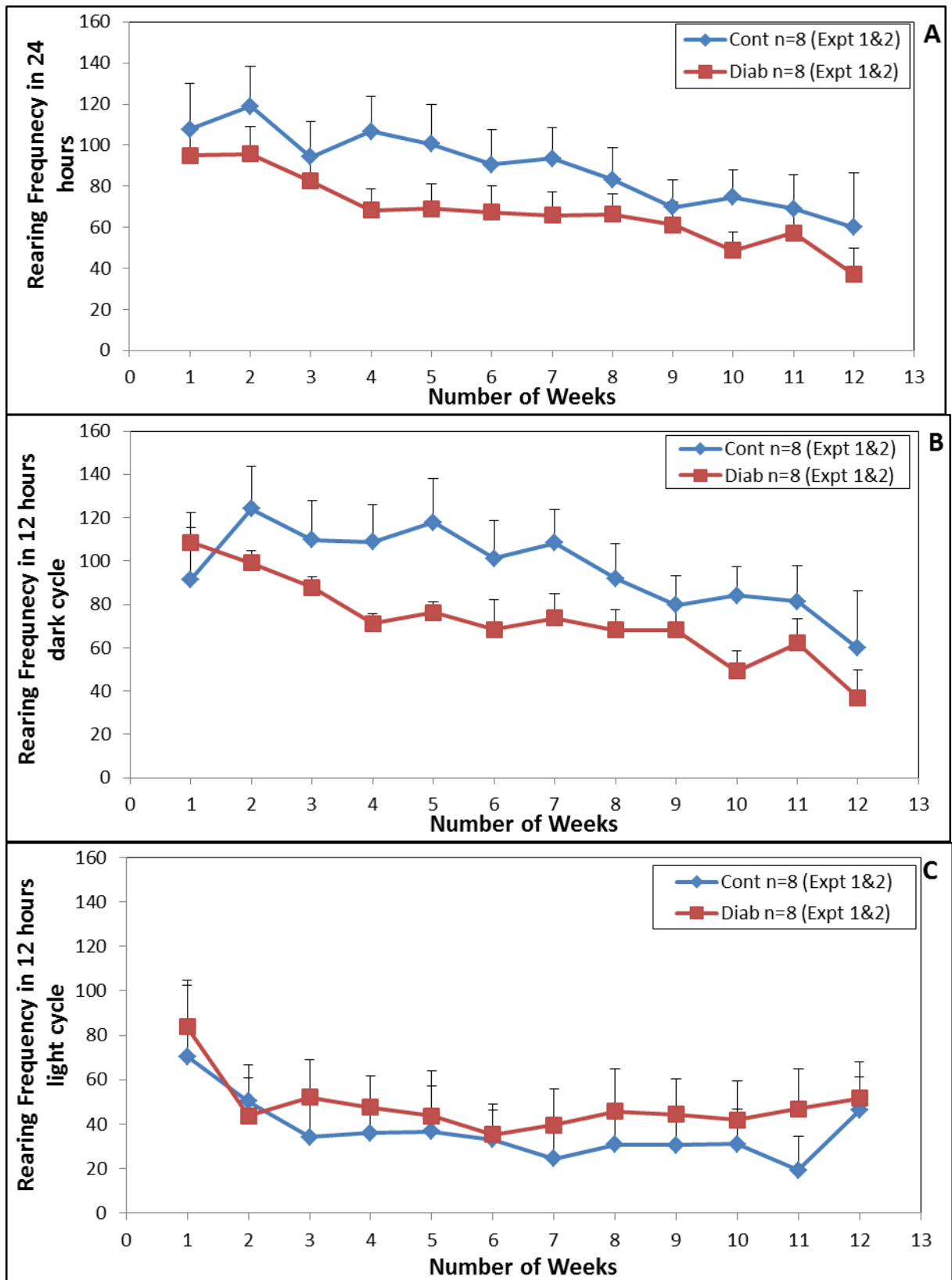


Figure 56: The frequency of rearing in DRs was significantly less than CRs in Average of Expts 1 and 2 for (A) 24hrs, (B) 12hrs dark cycle and (C) No Significant difference observed between DRs and CRs for 12hrs light cycle.

III.3.5 Grooming

The animal shaking, scratching, wiping or licking its fur, snout, ears, tail or genitals is classified as grooming. Results obtained confirm that, no significant difference in the duration of grooming in the DRs and CRs for both 24hrs period (Figures 57A) and 12hrs dark cycle period (Figures 57B). However, the duration of grooming for DRs was significantly more during the light cycle (Figure 57C). This data is very important, as this strongly suggests that, the pattern of activity in the diabetic animals is changed such that, it is more active during the day and considerably less in the night. When the frequency of grooming was monitored in the two groups, it was concluded that DRs groomed more than CRs for all periods (Figures 58).

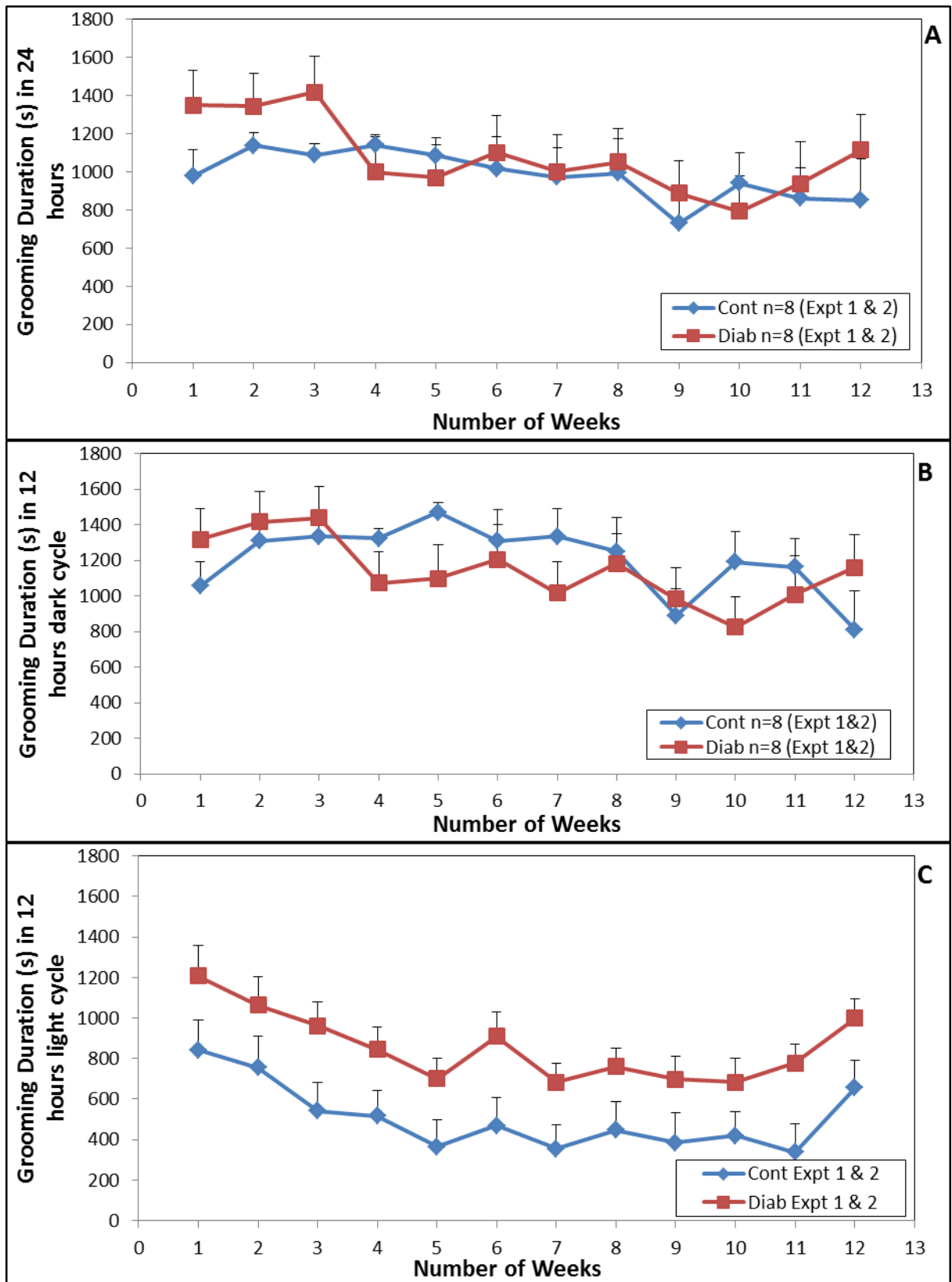


Figure 57: No significant difference in the duration of grooming observed in DRs and CRs in Average of Expts 1 and 2 for (A) 24hrs, (B) 12hrs dark cycle and (C) DRs groomed significantly more than CRs for 12hrs light cycle.

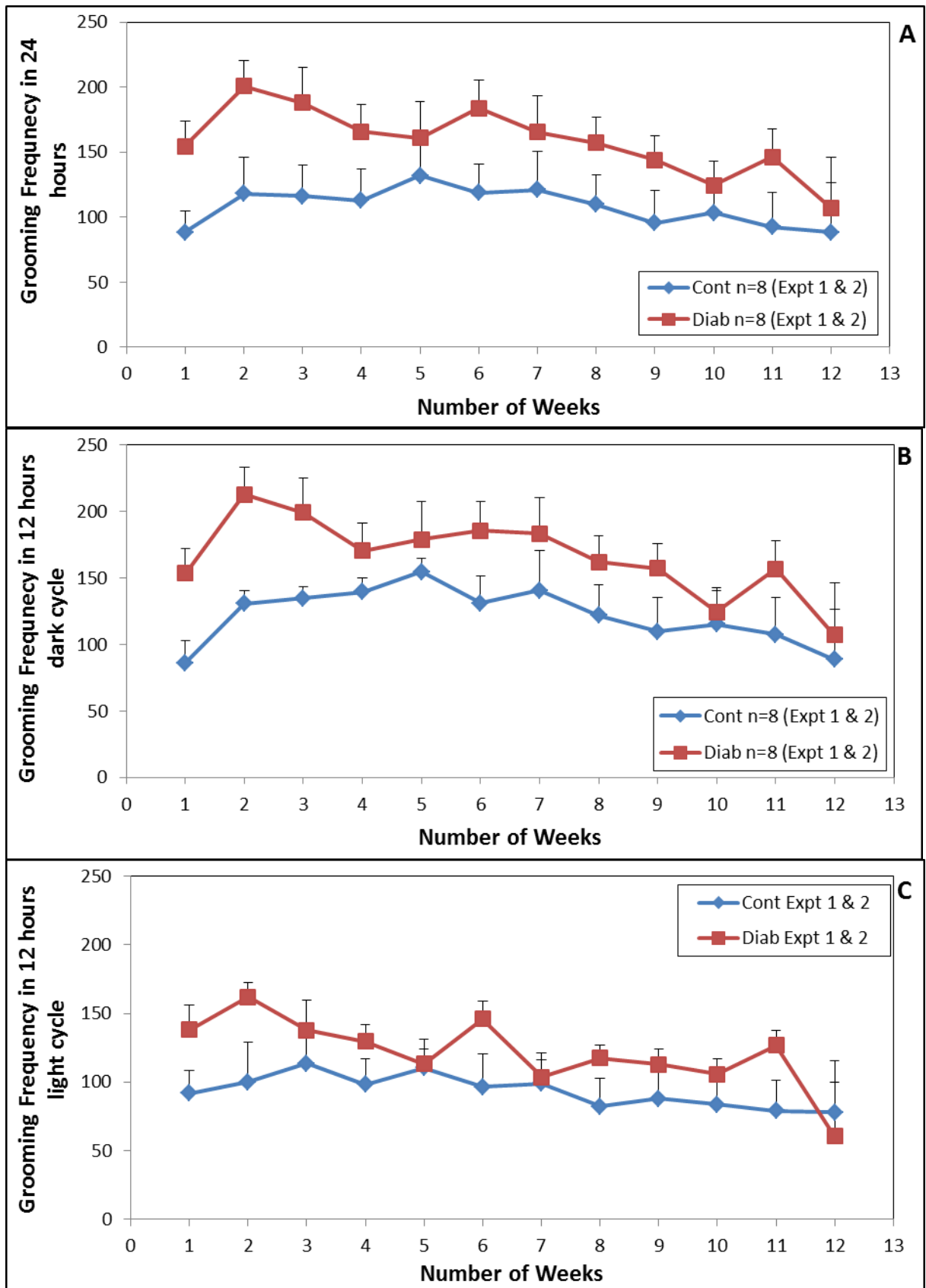


Figure 58: DRs groom significantly more than CRs in Average of Expts 1 and 2 for (A) 24hrs, (B) 12hrs dark cycle and (C) 12hrs light cycle.

III.3.6 Drinking

LABORAS defines drinking behaviour when the rat stands upright gripping the water bottle and licking water. Not surprisingly, we discovered that the DRs drank copious amount of water more frequently as compared to the CRs (Figures 59 and 60). However, it was observed that the difference in duration of time DRs drank more water than CRs was not that great (Figures 59), in contrast to the frequency of times (Figures 60). This data suggests that, the DRs spend less time drinking water, but have it more frequently as compared to the CRs. Additionally, in certain experiments, even though the physical measurements (weighing the water bottle before and after the 24hrs when rat was in cage) indicated that the DRs drank more than CRs (Figure 61), LABORAS did not record significant difference. This suggests either that LABORAS is not accurate in measuring drinking behaviour or just support the fact that the DRs drink more water in less duration of time. This is not surprising for diabetic animals, as it is already known that excess blood sugar, or glucose, in the body draws water from the tissues resulting in feeling dehydrated. This leads the animal to drink more water and thereby causing frequent urination.

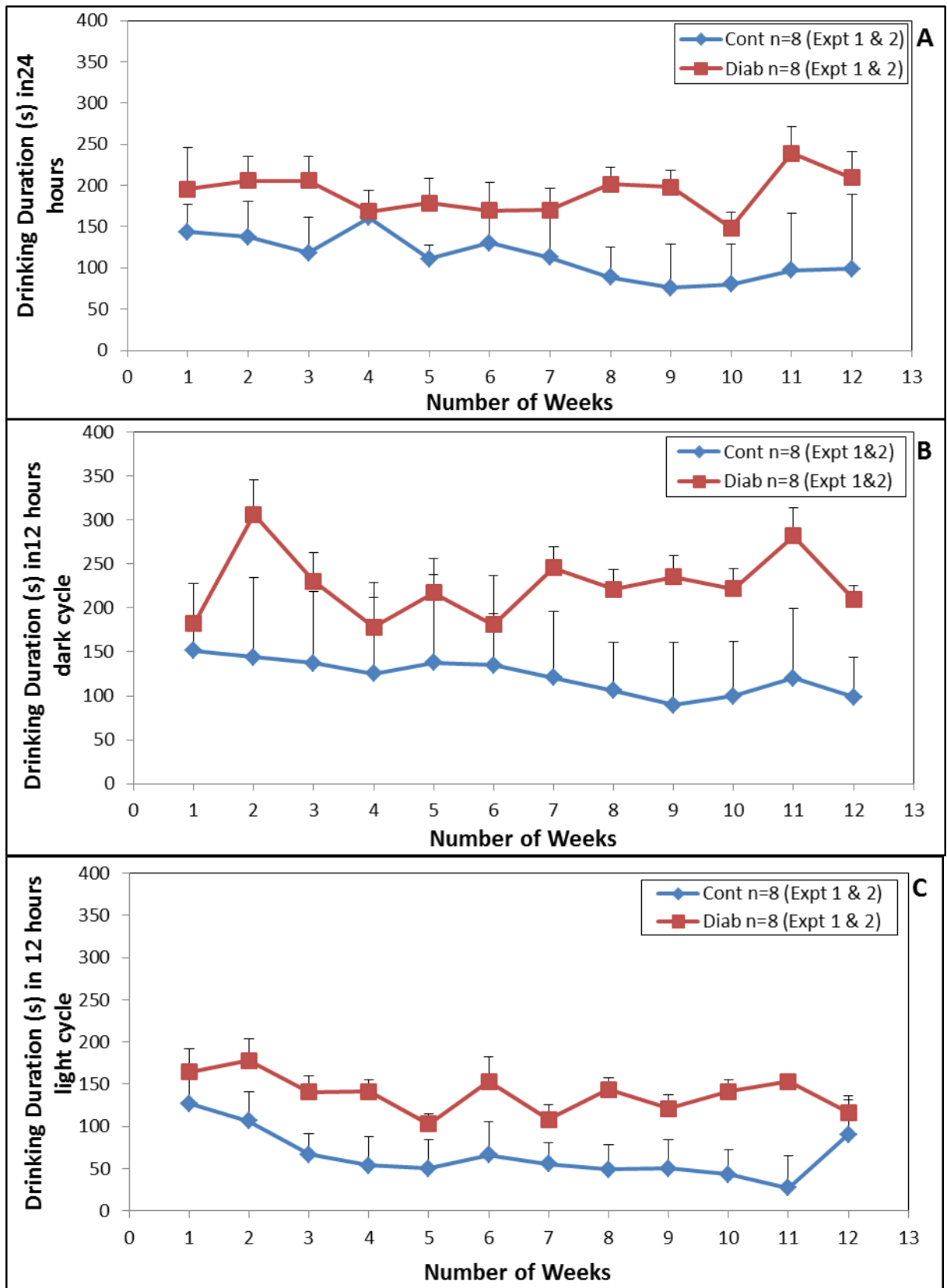


Figure 59: DRs display significantly more duration of drinking in comparison to than CRs in Average of Expts 1 and 2 for (A) 24hrs, (B) 12hrs dark cycle and (C) 12hrs light cycle.

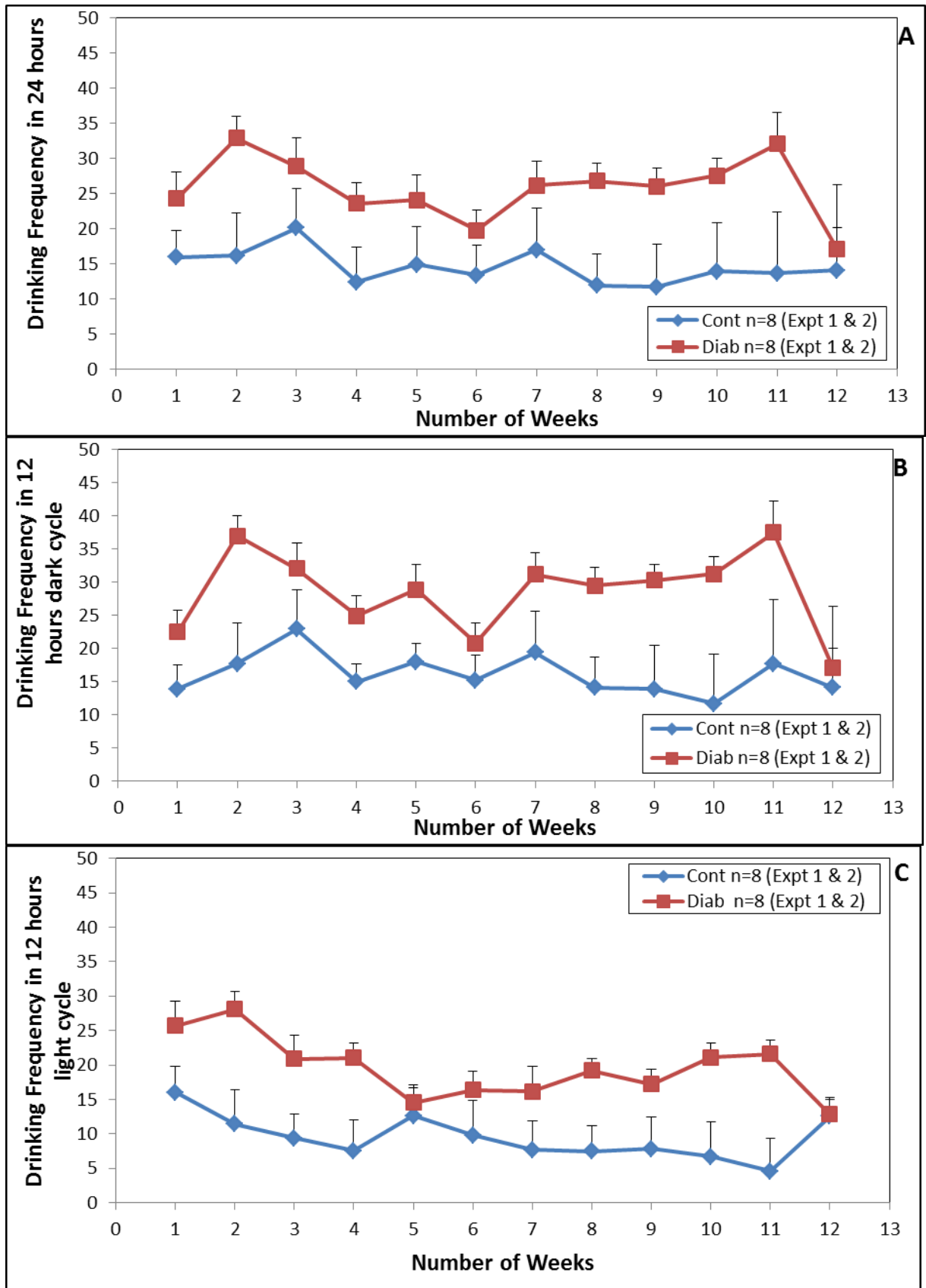


Figure 60: DRs drink more frequently than CRs in Average of Expts 1 and 2 for (A) 24hrs, (B) 12hrs dark cycle and (C) 12hrs light cycle.

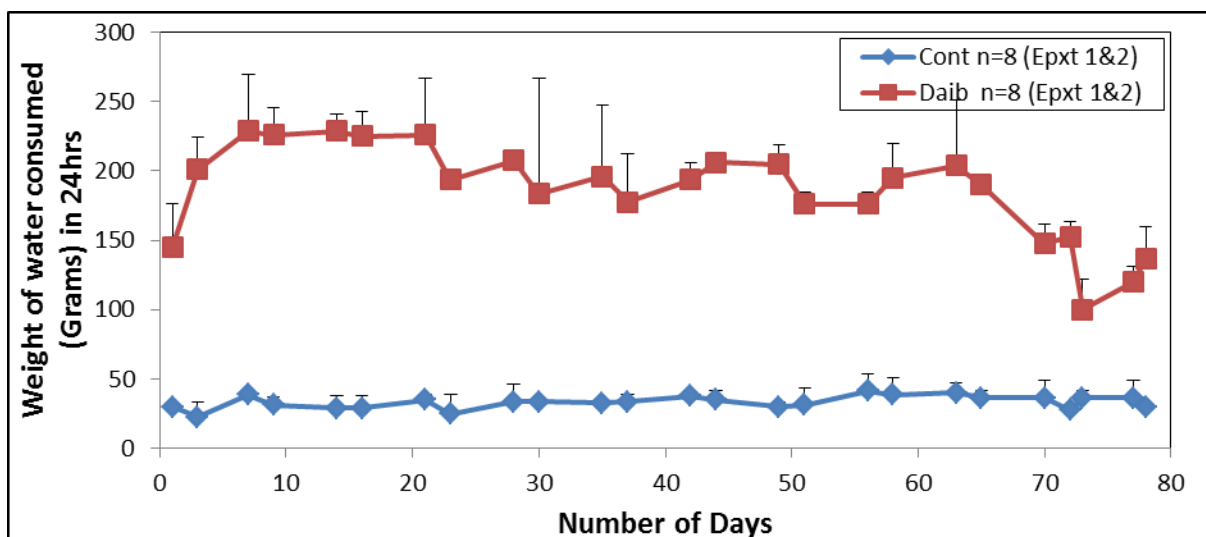


Figure 61: DRs consume significantly more amount of water than CRs in 24hrs for Average of Expts 1 and 2

III.3.7 Eating:

LABORAS classes eating behaviour as the period when rat eats food pellets while standing upright, gripping the bars of the food hopper. It is apparent in all diabetic cases that as the glucose does not get utilized properly by the brain and other parts of the body; the body craves continuously for glucose. This in turn leads to excessive hunger. The DRs thus consumed considerably more food as compared to the CR. In support of this theory, the duration (Figure 62) and frequency (Figure 63) of the eating behaviour for all the experiments and time periods recorded; show that DRs consumed significantly more food than CRs for longer period of time and more frequently. This was confirmed by simply weighing the amount of food added to the cage at time zero and weighing this again after 24hrs, where it was found that there was a significant difference in the amount of food consumed over a 24hrs period (Figure 64). This latter reflects the total consumption over the whole 24hrs period whilst our LABORAS data shows the consumption over an average 2.24hrs period in 24hrs or over an average 2.24hrs period in the 12hrs dark or 12hrs light period.

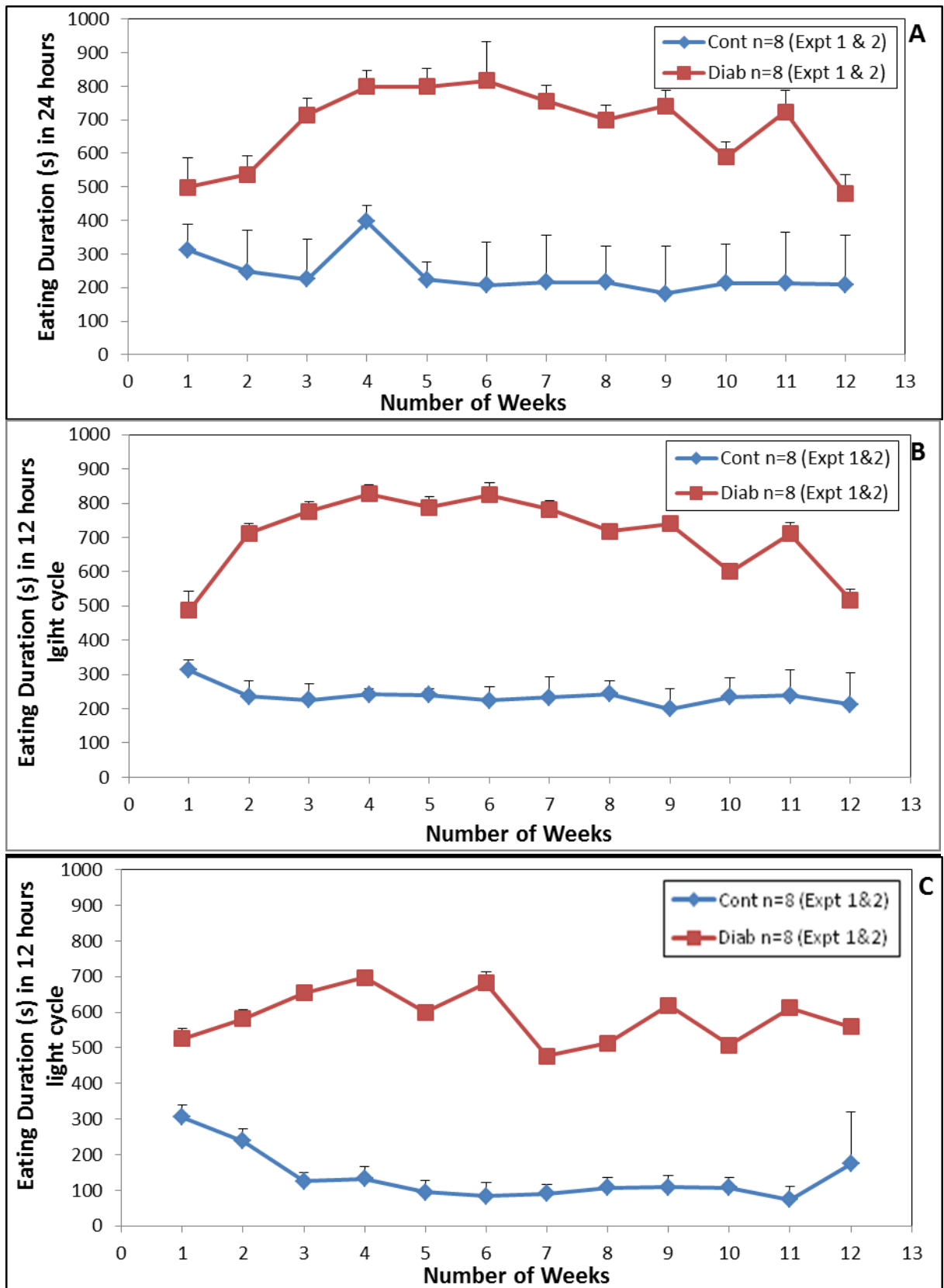


Figure 62: DRs display significantly more duration of eating in comparison to than CRs in Average of Expts 1 and 2 for (A) 24hrs, (B) 12hrs dark cycle and (C) 12hrs light cycle.

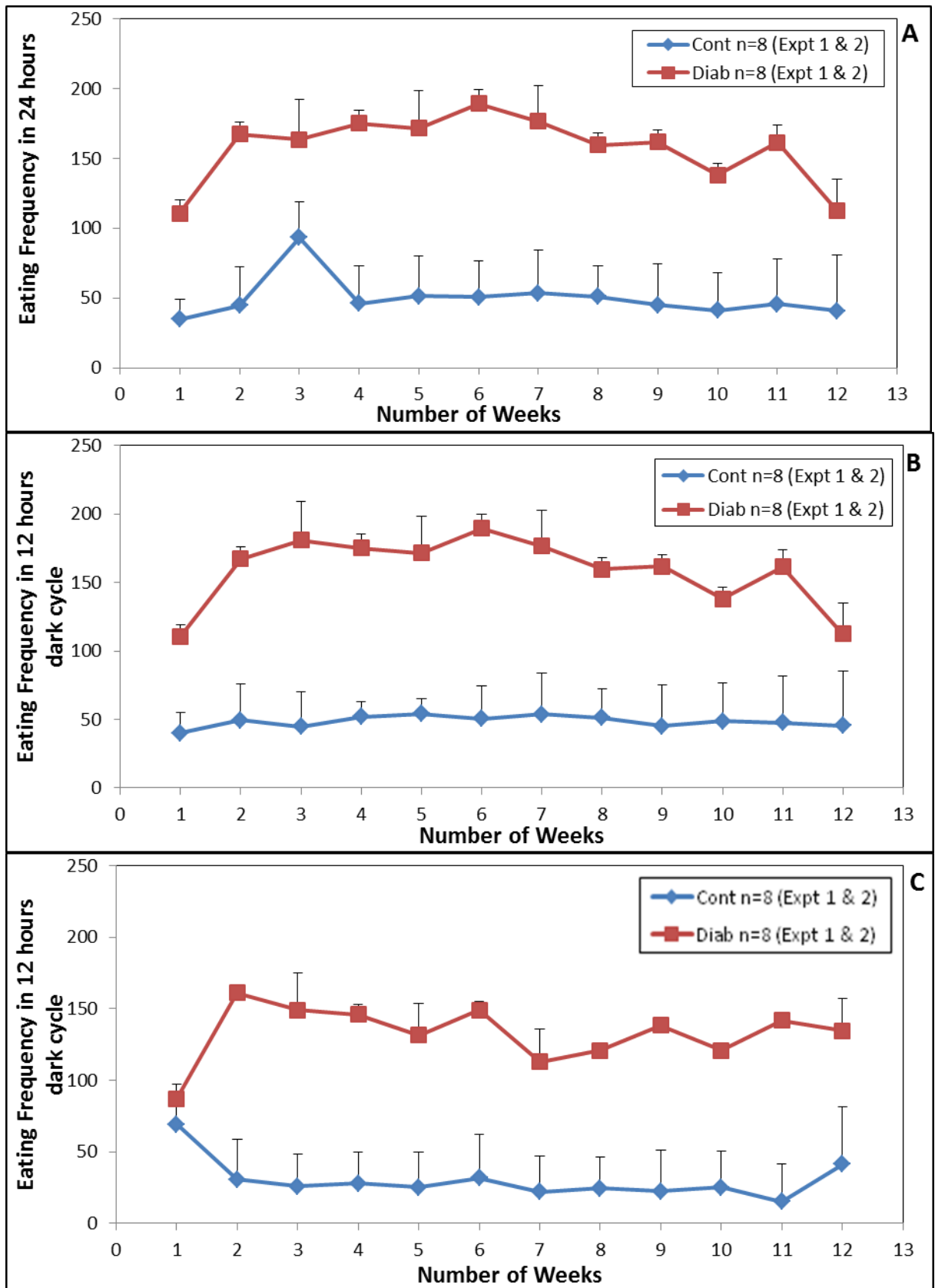


Figure 63: DRs eat frequently than CRs in Average of Expts 1 and 2 for (A) 24hrs, (B) 12hrs dark cycle and (C) 12hrs light cycle.

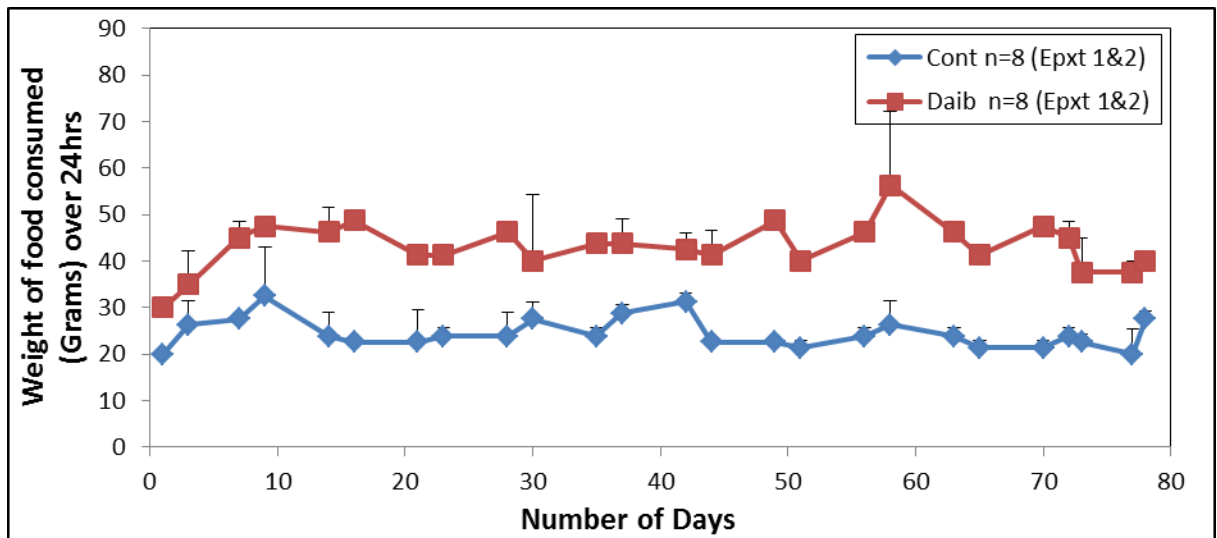


Figure 64: Increase amount of food consumed in DR than CR for 24hrs the Average of Expts 1 and 2.

III.3.8 Undefined:

All behaviours not classified in one of the previous categories are classed as undefined behaviour. From the results obtained, it can be inferred that, DRs displayed significantly larger duration of undefined behaviour in comparison to the CRs when both the experiments were averaged (Figures 65). However, the frequency of undefined behaviour was similar in both sets of rats (Figures 66). It is difficult to interpret these results as we do not know what behaviours are occurring that LABORAS categories as undefined behaviour (i.e. not one of the behaviours that it can distinguish). However, if the relevant software is purchased other behaviours of rats can be analyzed by LABORAS and such software could be used in future experiments to try to determine what some of these undefined behaviours may actually represent.

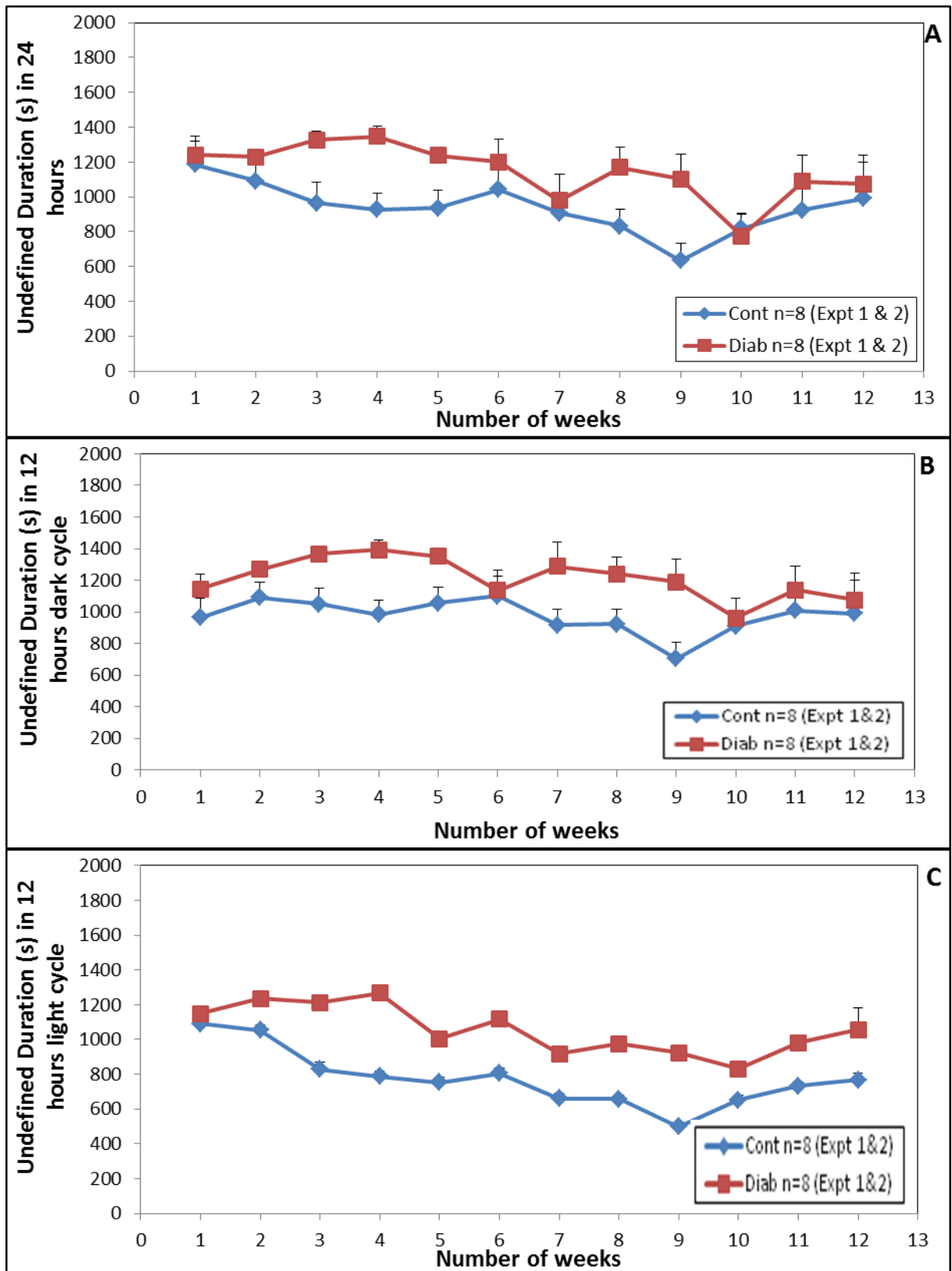


Figure 65: DRs display significantly more duration of undefined behaviour in comparison to than CRs in Average of Expts 1 and 2 for (A) 24hrs, (B) 12hrs dark cycle and (C) 12hrs light cycle.

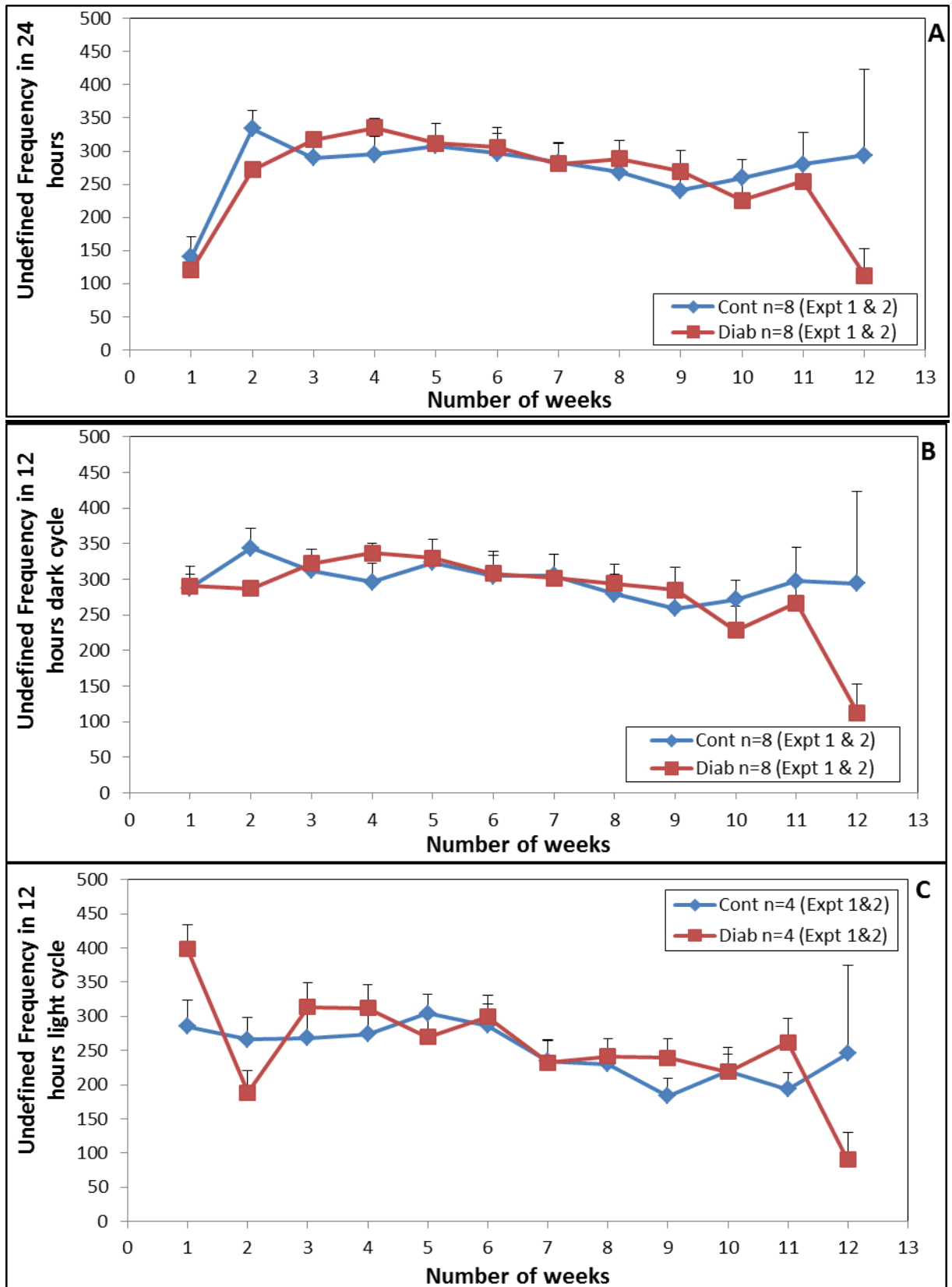


Figure 66: Similar frequency of undefined behaviour observed in DRs and CRs for Average of Expts 1 and 2 for (A) 24hrs, (B) 12hrs dark cycle and (C) 12hrs light cycle.

III.4 Discussion

As characteristic biochemical changes were observed in the diabetic terminals, which may affect synaptic plasticity, the main aim of this study was to observe the behavioural changes that may occur due to the diabetic state. Standard LABORAS software was utilized in these experiments to assess the modification in the LMA, speed, distance, immobility, rearing, grooming, eating, drinking and undefined behaviours. LABORAS has been already a validated system that can perform behavioural recordings and classification in a standardized and non-invasive way, with reduced experimental time required when prolonged periods of examination can be made (Van de Weerd et al., 2001; Quinn et al., 2003).

The weight of the animal, and the amount of food and water consumed were constantly measured throughout the experiment. The results obtained from figures 46, 59-61 and 62-64 illustrate the reduction in the weight gain of the DRs relative to the CRs, despite the higher consumption of water and food by the STZ-treated animals. These measurements confirm the diabetic condition. Weight loss, polyphagia, polydipsia and frequent urination (Kirpichnikov and Sowers, 2001; Latham et al., 2009) are very common symptoms observed in the diabetic state for any animal (including humans). It is well known that, symptoms of diabetes include elevated level of glucose in blood. This leads to the loss of glucose in the urine, thereby causing large urine output leading to dehydration, which consequently causes increased thirst and water consumption (Latham et al., 2009). The lack of insulin in the diabetic animals (and humans) also affects the fat, protein and carbohydrate metabolism, leading to weight loss despite an increase in appetite (Kirpichnikov and Sowers, 2001). It is believed that, the increase in the hunger is because glucose cannot enter into various cells (despite the level of glucose being higher in the blood) due to the lack of insulin. This leads to the body continuously craving glucose and leading to increased hunger.

The results obtained from figure 48A, 48B, 49A and 49B suggest that DRs are less locomotive compared to the CRs. This supports the initial hypothesis as it is well known that when the physical well-being of an individual decreases, it becomes less active. However, the average distance and speed for DRs are

significantly more than CRs (Figures 50, 51 and 52). Additionally no change in the LMA was observed during the light cycle.

The data obtained suggests that DRs are less immobile than CRs (Figures 53 and 54). As discussed already, one might believe that this contradicts with the LMA data obtained but as explained, this is not necessarily the case. Another possible explanation is that because LABORAS measures changes in gravity that exceed 1.45cm/0.25s as LMA (Augustsson et al., 2003), it could be plausible that DRs travel with more speed and cover more distance in shorter periods of time (<1.45 cm/0.25s), thereby not allowing LABORAS to classify this behaviour as LMA. Therefore, the LMA behaviour for DRs appears less than the CRs. However, the average distance and speed is recorded significantly more than the CRs (only in expt 1). This data indicates that, the DRs move more quickly than the CRs. This argument is confirmed by the result obtained by the immobility behaviour. Immobility is registered when the animal moved less than 0.75mm/0.25s (Augustsson et al., 2003).

Thus, it can be concluded that the DRs are more active than CRs, and this may be just due to increase in the anxiety-like behaviour (Casarrubea et al., 2011). Additionally, it should be noted that differences in the two independent experiments (no significant difference in the average speed and distance in Expt 2) is detected. Therefore, these experiments need to be repeated to obtain consistent results.

Additionally, in this initial analysis of the data, all 4 rats were included for both experiments. Therefore, future research could involve going back and examining each of the individual rats for all these behaviours. It may be that in each experimental set there is one rat that is behaving oddly, and it thereby disturbing some of the results e.g. if one rat doesn't move at all or moves too much then this would have a large effect on the average for movement or immobility.

Rearing is a vertical locomotion activity when the animal stands on its hind leg while raising up its forearm in the air or placed on the wall of the cage and this is seen as a survival strategy in assessing the environment for modification. Stimulating CNS increases rearing and inhibiting CNS causes decrease in rearing

behaviour (Aderibigbe et al., 2010). The results obtained from Figures 55A, 55B, 56A and 56B reveals decrease in the rearing behaviour in DRs from an early stage after the induction of diabetes. It can thus be interpreted that, diabetes inhibits the CNS activity (Aderibigbe et al., 2010). Conversely, no difference in rearing is observed in light cycle (Figures 55C and 56C), suggesting that the day rearing activity of the diabetic animals is unchanged as compared to the dark cycle.

A similar decrease in the rearing behaviour was observed by the study conducted by Shoji and Mizoguchi, (2011) in older rats. The present study may suggest that, the diabetic state leads to early ageing in the rodents (as discussed in the Introduction), displaying peculiar characteristics similar to the observed in older rats (Shoji and Mizoguchi, 2011). The decrease in rearing may be due to the decrease in the exploratory activity (Lumley et al., 2001). The rearing behaviour response is regulated by multiple NT systems; including GABA, cholinergic, adrenergic, opioid, serotonin, glutamate and dopamine and their receptors. A decrease in rearing behaviour may be due to potentiation of GABA or inhibition of serotonin, cholinergic and dopamine neurotransmission (Aderibigbe et al., 2010).

Grooming in mammals is a self-directed (Wright et al., 2011), natural, stereotypic behaviour. Grooming is an important behavioural component in animals and is associated with de-arousal (absence of stimulation) in the CNS (Aderibigbe et al., 2010; Casarrubea et al., 2011). First the head is groomed, then body regions, the genital regions and the tail. This cephalocaudal progression of grooming is defined as the “syntactic groom chain.” Previous studies have demonstrated that multiple regions of the rodent brain, mainly brainstem, striatum, and cortex are used to implement the syntactic groom chain (Chen et al., 2010). Grooming stimulates the release of beta-endorphins. This is one physiological reason for why grooming appears to be relaxing (Keverne et al., 1989).

The duration of grooming in DRs seems similar to that of CRs for 24hrs and dark cycle (Figures 57A and 57B). Intriguingly, the light cycle data indicate that DRs groom more than CR (Figure 57C). This further emphasizes that, the DRs display more activity during the day rather than night. In addition, the frequency of

grooming bouts is augmented (Figure 58). This behaviour is pathological and may lead to hair removal (this was not analyzed in this research although it was obvious that there was hair loss).

There are several postulated roles of grooming, which may differ depending on environmental conditions. In addition to its hygiene function, grooming has been assumed to be involved in stress adaptation (Lumley et al., 2001). The stress response may be mediated via corticotropin-releasing hormone or neuropeptides such as neuromedin S, which can act on the amygdala to induce grooming by increasing mesolimbic dopamine secretion (McGowan et al., 2010). Additionally, novelty-induced grooming has been considered to be a displacement behaviour that may decrease stress-induced provocation. Stress hormones, such as glucocorticoids, increase hypothalamic arginine vasopressin and oxytocin in rats.

It is thought that anxious rats groom more often (Casarrubea et al., 2011; Wright et al., 2011). Researchers have shown that activating the anxiogenic effect of various drugs, increases grooming behaviour, and is linked with the activation of serotonergic transmission. Grooming behaviour is due to the involvement of multiple neuromediators and brain regions (Howard et al., 2008). Electrical stimulation of the hypothalamus especially preoptic area also induces grooming in rodents (Lumley et al., 2001).

Excessive grooming in rodents behaviour is very similar to that described for humans with the obsessive-compulsive disorder (OCD) spectrum disorder trichotillomania, where compulsive removal of hair is also a hallmark (Chen et al., 2010).

In an experiment carried out on the *Hoxb8* mutant mice, excessive pathological grooming behaviour was associated with a defect in microglia. Microglia are found in abundance in cortex, including the frontal orbital regions and basal ganglia. Microglia could affect neuronal activity and behaviour by a number of mechanisms. These include the secretion of cytokines that stimulate or inhibit neuronal activity. Such cytokines can work in parallel with NTs. The duration of contact at synapses is dependent on neuronal activity. From the above, it can be concluded that, due to their mobility and dynamic contacts with synapses,

microglia could represent an additional system for stabilizing and managing neural networks (Chen et al., 2010).

The results obtained from the current experiments suggest that, there is an increase in the anxiety in STZ-induced diabetic rats and this is in agreement with earlier experiments carried out by Ramanathan et al., (1998). This study also demonstrated that the augmented anxiety on various experimental paradigms including the social interaction test and the anxiolytic effect of diazepam in DRs (Ramanathan et al., 1998). It is believed that the augmented anxiety-related behaviour may be due to damaged corticosterone and hippocampal serotonergic systems (File and Seth, 2003). In addition, it is assumed that the hippocampus controls anxiety responses, especially the dorsal raphe nucleus. Previous reports suggest that the GABA neurons in the dorsomedial hypothalamus regulate a variety of physiologic and behavioural responses associated with anxiety and stress. It has also been proposed that, the reciprocal neural circuits linking the medial prefrontal cortex, the extended amygdala and the hypothalamus play a crucial role in mediating fear and responses to stress (File and Seth, 2003).

As there are some discrepancies in the results observed in the two independent experiments, it is clear that further LABORAS monitoring needs to be performed.

The data obtained demonstrates a marked increase in undefined behaviour in DRs compared to CRs (Figures 65 and 66). As no specific behaviours are classed under this category, it is difficult to interpret this result. Different software available for LABORAS to measure behaviours such as hind limb licking, scratching, wet dog shakes, head shakes, head twitches and purposeless chewing could be used in the future to define what behaviours may be included in the general umbrella of undefined.

III.5 Conclusions and Future Studies

The results obtained from the current experiments clearly demonstrate that, LABORAS is capable of detecting various behaviours over a long period of time in rats and this can detect differences between rats that have been treated with various pharmacological reagents e.g. STZ. These behavioural deficits can be seen in LABORAS under home cage conditions in the absence of lengthy behavioural pre-training and pharmacological intervention. LABORAS and the social interaction test therefore provide novel, highly sensitive, quantitative methods for establishing differences between CRs and DRs. The DRs were only measured up to 12 weeks following STZ injection. This is because the animal licence being operated under stipulates that the rats only up to 12 weeks following the induction of diabetes can be used. Currently, a new licence is being applied for in which one will be allowed to use rats up to 6-9 months following induction of diabetes. Such rats might show even more obvious behavioural differences compared to the control.

It should be highlighted that LABORAS can only recognise behaviours that have established algorithms. Moreover, the LABORAS system can only be programmed to identify behaviours that produce vibrational signals of significant amplitude and consistency. More complex or refined behaviours such as yawning or disturbances of gait would therefore not be recognised (Quinn et al., 2005). It should be emphasized that, LABORAS continuously records data in real time and that one could chose to analyze what differences are occurring for every 60mins period of the day (or even shorter). Such analysis would enable us to see whether there are differences apparent between the CRs and DRs at particular times during the day and not just in the nocturnal 12hrs period. The current analysis has divided the day into ten 2.24hrs sections and the data presented actually represents the average of these 2.24hrs sections, for either the full 24hrs or 12hrs dark or 12hrs light cycle. Clearly, one could look at longer segments of time including summing all the activities over 24 or 12hrs. However, as this was the first use of LABORAS in this laboratory, it was choosen the times that we have shown. Further analysis may yield further interesting results. It was hoped that if 2.24hrs sections gave a reliable measurement of differences in behaviour then perhaps rat behaviours could be measured just for this short period.

IV. General Conclusions

From the results obtained in chapters II and III it can be concluded that diabetic rats display difference in both biochemical and behaviour when compared to the non-diseased rats.

The biochemical changes suggest that, the L-type VGCCs play a crucial role in regulating the mode of exocytosis evoked by HK5C in control terminals, whilst in the diabetic terminals N-type VGCCs seem to be involved. For the same stimulus, dynamins did not play a role in switching of the modes of exocytosis in control terminals but did in the diabetic terminals. This can be reconciled by stating that only SVs, which are dependent on dynamins, are the RP. The inhibition of PP2A or the activation of PKC switched all SVs to a FF mode in control terminals whereas, in diabetic terminals not all SVs that were undergoing K&R fusion were switched to FF, although, the dual treatment with these drugs did switch all the vesicles to a FF mode by an unknown mechanism. More research needs to be preformed utilizing this dual treatment in order to understand the underlying mechanism for the changes observed.

Monitoring the eating and drinking habits and the weight of rats confirmed that STZ administration induces some classical symptoms of diabetes in such animals. The increase in average speed and distance, decrease in immobility, reduced rearing and increased frequency of grooming signify anxiety and stress induced behaviour in the diabetic rats that can be explained by various neuromediators acting in various brain regions. These initial studies (done over a 6 months period) need to be repeated a few more times to establish some consistent and repeatable behavioural patterns. The two sets of 4 animals (expts 1 and expt 2) varied in some cases and further analysis in the future will indicate whether these differences could be assigned to a rogue (in the sense that not behaving as they should) rat in each of the cohorts. Additionally, various other LABORAS softwares could be helpful to determine the undefined behavioural changes observed in the diabetic rats. Further, some behaviour indicated difference in the activity of DRs during day and the night monitoring. These data signify that DRs perhaps have altered active period in comparison to non-diseased rats. Again, one

could re-analyze the data in the future to choose to look at different periods of time within the 24 hours of data collection.

The results obtained do support the hypothesis that distinct behavioural changes would be apparent in the diabetic rats. This hypothesis was based on the biochemical changes that were observed. The alteration in the behaviour may correlate with the biochemical changes observed and future work will need to be performed to prove this idea. Future experiments need to be performed to determine the effects of the *in vitro* application of either insulin or high glucose levels on control and diabetic terminals, to observe if such conditions could make diabetic terminals behave like controls, or make control terminals behave like diabetic terminals (this would include the measurement of the amount of K&R and the level of $[Ca^{2+}]_i$ induced by a stimulus). Additionally, *in vivo* administration of insulin injections (or slow insulin release with implanted peristaltic pumps) to rats that are made diabetic by STZ can be studied to ascertain whether such treatments now make terminals prepared from these animals identical to control terminals and whether behavioural differences are now corrected. A time course for reversal of diabetic induced effects could be performed in this type of experiment. Again, this could involve both behavioural and biochemical measurements.

Long-term there remains the possibility of testing whether the regulation of neuronal N-type channels in the diabetic rat could reverse the changes seen in the rat. Such a proof of principle experiment could lead to the possibility that these treatments in humans could prevent any long-term synaptic plasticity changes seen in long-term diabetic patients. However, before this can ever be mooted a lot more research has to be carried out with this model of type 1 diabetes. Further, other models of type 1 diabetes and even models of type 2 diabetes could be studied to see whether similar biochemical differences are apparent between these diseased rats and control healthy rats. This would establish the generality and commonality of the changes that have been described in the biochemistry and behaviour of the STZ-type 1 diabetic rats.

V. References

ABIRIA, S. A. & COLBRAN, R. J. 2010. CaMKII associates with Cav1.2 L-type calcium channels via selected β subunits to enhance regulatory phosphorylation. *Journal of Neurochemistry*, **112**, 150-161.

ADAMS, M. M., SHI, L. & LINVILLE, M. C. 2008. Caloric restriction and age affect synaptic proteins in hippocampal CA3 and spatial learning ability. *Experimental Neurology*, **211**, 141-149.

ADERIBIGBE, A. O., ADEYEMI, I. O. & AGBOOLA, O. I. 2010. Central Nervous System Depressant Properties of *Treculia africana* Decne. *Ethnobotanical Leaflets*, **14**, 108-117.

AHMED, M. S. & SIEGELBAUM, S. A. 2009. Recruitment of N-Type Ca^{2+} channels during LTP enhances low release efficacy of hippocampal CA1 perforant path synapses. *Neuron*, **63**, 372-385.

ALÉS, E., TABARES, L., POYATO, J. M., VALERO, V., LINDAU, M. & DE TOLEDO, G. A. 1999. High calcium concentrations shift the mode of exocytosis to the kiss-and-run mechanism. *Nature Cell Biology*, **1**, 40-44.

ALLEN, K. V., FRIER, B. M. & STRACHAN, M. W. J. 2004. The relationship between type 2 diabetes and cognitive dysfunction: longitudinal studies and their methodological limitations. *European Journal of Pharmacology*, **490**, 169-175.

ANDERSON, M. S. 2008. Update in endocrine autoimmunity. *Journal of Clinical Endocrinology & Metabolism*, **93**, 3663-3670.

ANDERSON, R. J., FREEDLAND, K. E., CLOUSE, R. E. & LUSTMAN, P. J. 2001. The prevalence of comorbid depression in adults with diabetes: a meta-analysis. *Diabetes Care*, **24**, 1069-1078.

AOKI, R., KITAGUCHI, T., OYA, M., YANAGIHARA, Y., SATO, M., MIYAWAKI, A. & TSUBOI, T. 2010. Duration of fusion pore opening and the amount of hormone released are regulated by myosin II during kiss-and-run exocytosis. *Biochemical Journal*, **429**, 497-504.

ARTALEJO, C. R., ELHAMDANI, A. & PALFREY, H. C. 2002. Sustained stimulation shifts the mechanism of endocytosis from dynamin-1-dependent rapid endocytosis to clathrin- and dynamin-2-mediated slow endocytosis in chromaffin cells. *Proceedings of the National Academy of Sciences of the United States of America*, **99**, 6358-6363.

ATLAS, D. 2010. Signaling role of the voltage-gated calcium channel as the molecular on/off-switch of secretion. *Cell Signal*, **22**, 1597-1603.

AUGUSTSSON, H., VAN DE WEERD, H. A., KRUITWAGEN, C. L. J. J. & BAUMANS, V. 2003. Effect of enrichment on variation and results in the light/dark test. *Laboratory Animals*, **37**, 328-340.

BANKS, W. A., JASPAN, J. B., HUANG, W. & KASTIN, A. J. 1997. Transport of insulin across the blood-brain barrier: saturability at euglycemic doses of insulin. *Peptides*, **18**, 1423-1429.

BASHKIROV, P. V., AKIMOV, S. A., EVSEEV, A. I., SCHMID, S. L., ZIMMERBERG, J. & FROLOV, V. A. 2008. GTPase cycle of dynamin is coupled to membrane squeeze and release, leading to spontaneous fission. *Cell*, **135**, 1276-1286.

BATIUK, T. D., PAZDERKA, F., ENNS, J., DECASTRO, L. & HALLORAN, P. F. 1995. Cyclosporine inhibition of calcineurin activity in human leukocytes *in vivo* is rapidly reversible. *Journal of Clinical Investigation*, **96**, 1254-1260.

BEISWENGER, K. K., CALCUTT, N. A. & MIZISIN, A. P. 2008. Dissociation of thermal hypoalgesia and epidermal denervation in streptozotocin-diabetic mice. *Neuroscience Letters*, **442** (3), 267-272.

BERRIDGE, K. C. 1989. Progressive degradation of serial grooming chains by descending decerebration. *Behavioural Brain Research*, **33**, 241-253.

BERTOLINO, M. & LLINAS, R. R. 1992. The central role of voltage-activated and receptor-operated calcium channels in neuronal cells. *Annual Review of Pharmacology and Toxicology*, **32**, 399-421.

BEZPROZVANNY, I. 2009. Calcium signaling and neurodegenerative diseases. *Trends in Molecular Medicine*, **15**, 89-100.

BHAT, P. & THORN, P. 2009. Myosin 2 maintains an open exocytic fusion pore in secretory epithelial cells. *Molecular Biology of the Cell*, **20**, 1795-1803.

BIESSELS, G. J., DEARY, I. J. & RYAN, C. M. 2008. Cognition and diabetes: a lifespan perspective. *Lancet Neurology*, **7**, 184-190.

BIESSELS, G. J., KAMAL, A., RAMAKERS, G. M., URBAN, I. J., SPRUIJT, B. M., ERKELENS, D. W. & GISPEN, W. H. 1996. Place learning and hippocampal synaptic plasticity in streptozotocin-induced diabetic rats. *Diabetes*, **45**, 1259–1266.

BINGHAM, E. M., HOPKINS, D., SMITH, D. R., PERNET, A., HALLETT, W., REED, L., MARSDEN, P. K. & AMIEL, S. A. 2002. The role of insulin in human brain glucose metabolism: an ¹⁸fluoro-deoxyglucose positron emission tomography study. *Diabetes*, **51**, 3384-3390.

BORLONGAN, C. V., CAHILL, D. W. & SANBERG, P. R. 1995. Locomotor and passive avoidance deficits following occlusion of the middle cerebral artery. *Physiology & Behavior*, **58**, 909-917.

BRANDS, A. M. A., KESSELS, R. P. C., HOOGMA, R. P. L. M., HENSELMANS, J. M. L., VAN DER BEEK BOTER, J. W., KAPPELLE, L. J., DE HAAN, E. H. F. & BIESELS, G. J. 2006. Cognitive performance, psychological well-being, and brain magnetic resonance imaging in older patients with type 1 diabetes. *Diabetes*, **55**, 1800-1806.

BREUKEL, A. I., BESSELS, E. & GHIJSEN, W. E. 1997. Synaptosomes. A model system to study release of multiple classes of neurotransmitter. *Methods in Molecular Biology*, **72**, 33-47.

BROSE, N. & NEHER, E. 2009. Flowers for Synaptic Endocytosis. *Cell*, **138**, 836-837.

BUCURENCIU, I., BISCHOFBERGER, J. & JONAS, P. 2010. A small number of open Ca²⁺ channels trigger transmitter release at a central GABAergic synapse. *Nature Neuroscience*, **13**, 19-21.

CALCUTT, N. A., COOPER, M. E., KERN, T. S. & SCHMIDT, A. M. 2009. Therapies for hyperglycaemia-induced diabetic complications: from animal models to clinical trials. *Nature Reviews Drug Discovery*, **8**, 417-429.

CASARRUBEA, M., SORBERA, F., MAGNUSSON, M. & CRESCIMANNO, G. 2011. T-pattern analysis of diazepam-induced modifications on the temporal organization of rat behavioral response to anxiety in hole board. *Psychopharmacology*, **215**, 177-189.

CATTERALL, W. A. & FEW, A. P. 2008. Calcium channel regulation and presynaptic plasticity. *Neuron*, **59**, 882-901.

CHANG, C. Y. & MENNERICK, S. 2010. Dynamic modulation of phasic and asynchronous glutamate release in hippocampal synapses. *Journal of Neurophysiology*, **103**, 392-401.

CHAO, C. C., HU, S., SHENG, W. S., BU, D., BUKRINSKY, M. I. & PETERSON, P. K. 1996. Cytokine-stimulated astrocytes damage human neurons via a nitric oxide mechanism. *Glia*, **16**, 276-284.

CHEN, S., TVRDIK, P., PEDEN, E., CHO, S., WU, S., SPANGRUDE, G. & CAPECCHI, M. R. 2010. Hematopoietic Origin of Pathological Grooming in *Hoxb8* Mutant Mice. *Cell*, **141**, 775-785.

CHEUNG, G., JUPP, O. J. & COUSIN, M. A. 2010. Activity-dependent bulk endocytosis and clathrin-dependent endocytosis replenish specific synaptic vesicle pools in central nerve terminals. *Journal of Neuroscience*, **30**, 8151-8161.

CHOWDHURY, S. K. R., ZHEREBITSKAYA, E., SMITH, D. R., AKUDE, E., CHATTOPADHYAY, S., JOLIVALT, C. G., CALCUTT, N. A. & FERNYHOUGH, P. 2010. Mitochondrial respiratory chain dysfunction in dorsal root ganglia of streptozotocin-induced diabetic rats and its correction by insulin treatment. *Diabetes*, **59**, 1082-1091.

CHUNG, C., BARYLKO, B., LEITZ, J., LIU, X. & KAVALALI, E. T. 2010. Acute dynamin inhibition dissects synaptic vesicle recycling pathways that drive spontaneous and evoked neurotransmission. *Journal of Neuroscience*, **30**, 1363-1376.

CINGOLANI, L. A. & GODA, Y. 2008. Actin in action: the interplay between the actin cytoskeleton and synaptic efficacy. *Nature Reviews Neuroscience*, **9**, 344-356.

CLAYTON, E. L., EVANS, G. J. O. & COUSIN, M. A. 2007. Activity-dependent control of bulk endocytosis by protein dephosphorylation in central nerve terminals. *Journal of Physiology*, **585**, 687-691.

COOPER, M. E., BONNET, F., OLDFIELD, M. & JANDELEIT-DAHM, K. 2001. Mechanisms of diabetic vasculopathy: an overview. *American Journal of Hypertension*, **14**, 475-486.

CUKIERMAN, T., GERSTEIN, H. C. & WILLIAMSON, J. D. 2005. Cognitive decline and dementia in diabetes--systematic overview of prospective observational studies. *Diabetologia*, **48**, 2460-2469.

DARIOS, F., WASSER, C., SHAKIRZYANOVA, A., GINIATULLIN, A., GOODMAN, K., MUNOZ-BRAVO, J. L., RAINGO, J., JORGACEVSKI, J., KREFT, M., ZOREC, R., ROSA, J. M., GANDIA, L., GUTIERREZ, L. M., BINZ, T., GINIATULLIN, R., KAVALALI, E. T. & DAVLETOV, B. 2009. Sphingosine facilitates SNARE complex assembly and activates synaptic vesicle exocytosis. *Neuron*, **62**, 683-694.

DAVIDSON, E., COPPEY, L., LU, B., ARBALLO, V., CALCUTT, N. A., GERARD, C. & YOREK, M. 2009. The roles of streptozotocin neurotoxicity and neutral endopeptidase in murine experimental diabetic neuropathy. *Experimental Diabetes Research*, **2009**, 431980-431980.

DESROCHER, M. & ROVET, J. 2004. Neurocognitive correlates of type 1 diabetes mellitus in childhood. *Child Neuropsychology*, **10**, 36-52.

DOLPHIN, A. C. 2006. A short history of voltage-gated calcium channels. *British Journal of Pharmacology*, **147**, S56-S62.

DONATH, M. Y., EHSES, J. A., MAEDLER, K., SCHUMANN, D. M., ELLINGSGAARD, H., EPPLER, E. & REINECKE, M. 2005. Mechanisms of β -cell death in type 2 diabetes. *Diabetes*, **54** (2), 108-113.

DOREIAN, B. W., FULOP, T. G., MEKLEMBURG, R. T. L. & SMITH, C. B. 2009. Cortical F-actin, the exocytic mode, and neuropeptide release in mouse chromaffin cells is regulated by myristoylated alanine-rich C-kinase substrate and myosin II. *Molecular Biology of the Cell*, **20**, 3142-3154.

DU, X. L., EDELSTEIN, D., DIMMELER, S., JU, Q., SUI, C. & BROWNLEE, M. 2001. Hyperglycemia inhibits endothelial nitric oxide synthase activity by posttranslational modification at the Akt site. *Journal of Clinical Investigation*, **108**, 1341-1348.

DUARTE, J. M. N., CARVALHO, R. A., CUNHA, R. A. & GRUETTER, R. 2009. Caffeine consumption attenuates neurochemical modifications in the hippocampus of streptozotocin-induced diabetic rats. *Journal of Neurochemistry*, **111**, 368-379.

DUELLI, R., MAURER, M. H., STAUDT, R., HEILAND, S., DUEMBGEN, L. & KUSCHINSKY, W. 2000. Increased cerebral glucose utilization and decreased glucose transporter Glut1 during chronic hyperglycemia in rat brain. *Brain Research*, **858**, 338-347.

ELHAMDANI, A., AZIZI, F. & ARTALEJO, C. R. 2006. Double patch clamp reveals that transient fusion (kiss-and-run) is a major mechanism of secretion in calf adrenal chromaffin cells: high calcium shifts the mechanism from kiss-and-run to complete fusion. *Journal of Neuroscience*, **26**, 3030-3036.

FARSWAN, M., MAZUMDER, P. M. & PERCHA, V. 2009. Protective effect of *Cassia glauca* Linn. on the serum glucose and hepatic enzymes level in streptozotocin induced NIDDM in rats. *Indian Journal of Pharmacology*, **41**, 19-22.

FDEZ, E. & HILFIKER, S. 2006. Vesicle pools and synapsins: New insights into old enigmas. *Brain Cell Biology*, **35**, 107-115.

FEENER, E. P. & KING, G. L. 1997. Vascular dysfunction in diabetes mellitus. *Lancet*, **350** (1), 9-13.

FERNANDEZ-BUSNADIEGO, R., ZUBER, B., MAURER, U. E., CYRKLAFF, M., BAUMEISTER, W. & LUCIC, V. 2010. Quantitative analysis of the native presynaptic cytomatrix by cryoelectron tomography. *Journal of Cell Biology*, **188**, 145-156.

FERRER, I., BLANCO, R. & CARMONA, M. 2001. Differential expression of active, phosphorylation-dependent MAP kinases, MAPK/ERK, SAPK/JNK and p38, and specific transcription factor substrates following quinolinic acid excitotoxicity in the rat. *Molecular Brain Research*, **94**, 48-58.

FILE, S. E. & SETH, P. 2003. A review of 25 years of the social interaction test. *European Journal of Pharmacology*, **463**, 35-53.

FOURCAUDOT, E., GAMBINO, F., CASASSUS, G., POULAIN, B., HUMEAU, Y. & LUTHI, A. 2009. L-type voltage-dependent Ca²⁺ channels mediate expression of presynaptic LTP in amygdala. *Nature Neuroscience*, **12**, 1093-1095.

FRANCIS, G. J., MARTINEZ, J. A., LIU, W. Q., XU, K., AYER, A., FINE, J., TUOR, U. I., GLAZNER, G., HANSON, L. R., FREY, W. H. & TOTH, C. 2008. Intranasal insulin prevents cognitive decline, cerebral atrophy and white matter changes in murine type I diabetic encephalopathy. *Brain*, **131**, 3311-3334.

FULOP, T. & SMITH, C. 2006. *Physiological stimulation regulates the exocytic mode through calcium activation of protein kinase C in mouse chromaffin cells. Journal of Biochemistry*, **399 (1)**, 111-119.

GIAGTZOGLOU, N., MAHONEY, T., YAO, C. & BELLEN, H. J. 2009. Rab3 GTPase lands Bruchpilot. *Neuron*, **64**, 595-597.

GINIATULLIN, A. R., DARIOS, F., SHAKIRZYANOVA, A., DAVLETOV, B. & GINIATULLIN, R. 2006. SNAP25 is a pre-synaptic target for the depressant action of reactive oxygen species on transmitter release. *Journal of Neurochemistry*, **98**, 1789-1797.

GOLD, S. M., DZIOBEK, I., SWEAT, V., TIRSI, A., ROGERS, K., BRUEHL, H., TSUI, W., RICHARDSON, S., JAVIER, E. & CONVIT, A. 2007. Hippocampal damage and memory impairments as possible early brain complications of type 2 diabetes. *Diabetologia*, **50**, 711-719.

GRAF, E. R., DANIELS, R. W., BURGESS, R. W., SCHWARZ, T. L. & DIANTONIO, A. 2009. Rab3 dynamically controls protein composition at active zones. *Neuron*, **64**, 663-677.

GRAHAM, M. E., O'CALLAGHAN, D. W., MCMAHON, H. T. & BURGOYNE, R. D. 2002. Dynamin-dependent and dynamin-independent processes contribute to the regulation of single vesicle release kinetics and quantal size. *Proceedings of the National Academy of Sciences of the United States of America*, **99**, 7124-7129.

GREENWOOD, C. E. & WINOCUR, G. 2005. High-fat diets, insulin resistance and declining cognitive function. *Neurobiology of Aging*, **26** (1), 42-45.

HAN, B., BALIGA, R., HUANG, H., GIANNONE, P.J. & BAUER, J.A. 2009. Decreased cardiac expression of vascular endothelial growth factor and redox imbalance in murine diabetic cardiomyopathy. *American Journal of Physiology*, **297**(2), H829-35.

HASSELBALCH, S. G., KNUDSEN, G. M., VIDEBAEK, C., PINBORG, L. H., SCHMIDT, J. F., HOLM, S. & PAULSON, O. B. 1999. No effect of insulin on glucose blood-brain barrier transport and cerebral metabolism in humans. *Diabetes*, **48**, 1915-1921.

HENKEL, A. W., KANG, G. & KORNHUBER, J. 2001. A common molecular machinery for exocytosis and the 'kiss-and-run' mechanism in chromaffin cells is controlled by phosphorylation. *Journal of Cell Science*, **114**, 4613-4620.

HILL, J. J., CALLAGHAN, D. A., DING, W., KELLY, J. F. & CHAKRAVARTHY, B. R. 2006. Identification of okadaic acid-induced phosphorylation events by a mass spectrometry approach. *Biochemical and Biophysical Research Communications*, **342**, 791-799.

HOFFMAN, W. H., ANDJELKOVIC, A. V., ZHANG, W., PASSMORE, G. G. & SIMA, A. A. F. 2010. Insulin and IGF-1 receptors, nitrotyrosin and cerebral neuronal deficits in two young patients with diabetic ketoacidosis and fatal brain edema. *Brain Research*, **1343**, 168-177.

HOPKINS, D. F. & WILLIAMS, G. 1997. Insulin receptors are widely distributed in human brain and bind human and porcine insulin with equal affinity. *Diabetic Medicine*, **14**, 1044-1050.

HORIE, K., MIYATA, T., MAEDA, K., MIYATA, S., SUGIYAMA, S., SAKAI, H., VAN YPERSOLE DE STRIHOU, C., MONNIER, V. M., WITZTUM, J. L. & KUROKAWA, K. 1997. Immunohistochemical colocalization of glycoxidation products and lipid peroxidation products in diabetic renal glomerular lesions. Implication for glycoxidative stress in the pathogenesis of diabetic nephropathy. *Journal of Clinical Investigation*, **100**, 2995-3004.

HOSOI, N., HOLT, M. & SAKABA, T. 2009. Calcium dependence of exo- and endocytotic coupling at a glutamatergic synapse. *Neuron*, **63**, 216-229.

HOWARD, O., CARR, G., HILL, T., VALENTINO, R. & LUCKI, I. 2008. Differential blockade of CRF-evoked behaviors by depletion of norepinephrine and serotonin in rats. *Psychopharmacology*, **199**, 569-582.

HUANG, T. J., SAYERS, N. M., FERNYHOUGH, P. & VERKHRATSKY, A. 2002. Diabetes-induced alterations in calcium homeostasis in sensory neurones of streptozotocin-diabetic rats are restricted to lumbar ganglia and are prevented by neurotrophin-3. *Diabetologia*, **45**, 560-570.

HYND, M. R., SCOTT, H. L., DODD, P. R. 2004. Glutamate-mediated excitotoxicity and neurodegeneration in Alzheimer's disease. *Neurochemical International*, **45**, 583–595.

IGARASHI, M. & WATANABE, M. 2007. Roles of calmodulin and calmodulin-binding proteins in synaptic vesicle recycling during regulated exocytosis at submicromolar Ca^{2+} concentrations. *Neuroscience Research*, **58**, 226-233.

JACKSON, M. B. 2007. In search of the fusion pore of exocytosis. *Biophysical Chemistry*, **126**, 201-208.

JACKSON, M. B. & CHAPMAN, E. R. 2006. Fusion pores and fusion machines in Ca^{2+} -triggered exocytosis. *Annual Review of Biophysics and Biomolecular Structure*, **35**, 135-160.

JOHNSON, S. L., FRANZ, C., KUHN, S., FURNESS, D. N., RUTTIGER, L., MUNKNER, S., RIVOLTA, M. N., SEWARD, E. P., HERSCHMAN, H. R., ENGEL, J., KNIPPER, M. & MARCOTTI, W. 2010. Synaptotagmin IV determines the linear Ca^{2+} dependence of vesicle fusion at auditory ribbon synapses. *Nature Neuroscience*, **13**, 45-52.

KAASINEN, V., VILKMAN, H., HIETALA, J., NAGREN, K., HELENIUS, H., OLSSON, H., FARDE, L. & RINNE, J. 2000. Age-related dopamine D2/D3 receptor loss in extrastriatal regions of the human brain *Neurobiology of Aging*, **21**, 683–688.

KAMAL, A., BIESELS, G., GISPEN, W. H. & RAMAKERS, G. M. J. 2006. Synaptic transmission changes in the pyramidal cells of the hippocampus in streptozotocin-induced diabetes mellitus in rats. *Brain Research*, **1073-1074**, 276-280.

KEATING, D. J. 2008. Mitochondrial dysfunction, oxidative stress, regulation of exocytosis and their relevance to neurodegenerative diseases. *Journal of Neurochemistry*, **104**, 298-305.

KESAVAN, J., BORISOVSKA, M. & BRUNS, D. 2007. v-SNARE Actions during Ca^{2+} -Triggered Exocytosis. *Cell*, **131**, 351-363.

KEVERNE, E. B., MARTENSZ, N. D. & TUIITE, B. 1989. Beta-endorphin concentrations in cerebrospinal fluid of monkeys are influenced by grooming relationships. *Psychoneuroendocrinology*, **14**, 155-161.

KIM, J. H. & VON GERSDORFF, H. 2009. Traffic Jams during Vesicle Cycling Lead to Synaptic Depression. *Neuron*, **63**, 143-145.

KIRPICHNIKOV, D. & SOWERS, J. R. 2001. Diabetes mellitus and diabetes-associated vascular disease. *Trends in Endocrinology and Metabolism*, **12**, 225-230.

KLOPPENBORG, R. P., VAN DEN BERG, E., KAPPELLE, L. J. & BIESELS, G. J. 2008. Diabetes and other vascular risk factors for dementia: which factor matters most? A systematic review. *European Journal of Pharmacology*, **585**, 97-108.

KOROGOD, N., LOU, X. & SCHNEGGENBURGER, R. 2007. Posttetanic potentiation critically depends on an enhanced Ca^{2+} sensitivity of vesicle fusion mediated by presynaptic PKC. *Proceedings of the National Academy of Sciences of the United States of America*, **104**, 15923-15928.

KOVACS, M., TOTH, J., HETENYI, C., MALNASI-CSIZMADIA, A. & SELLERS, J. R. 2004. Mechanism of blebbistatin inhibition of myosin II. *Journal of Biological Chemistry*, **279**, 35557-35563.

KRAMER, H. & KAVALALI, E. T. 2008. Dynamin-independent synaptic vesicle retrieval? *Nature Neuroscience*, **11**, 6-8.

KRUPA, B. & LIU, G. 2004. Does the fusion pore contribute to synaptic plasticity? *Trends in Neurosciences*, **27**, 62-66.

KUMASHIRO, S., LU, Y., TOMIZAWA, K., MATSUSHITA, M., WEI, F. & MATSUI, H. 2005. Regulation of synaptic vesicle recycling by calcineurin in different vesicle pools. *Neuroscience Research*, **51**, 435-443.

LADERA, C., MARTÍN, R., BARTOLOMÉ-MARTÍN, D., TORRES, M. & SÁNCHEZ-PRIETO, J. 2009. Partial compensation for N-type Ca²⁺ channel loss by P/Q-type Ca²⁺ channels underlines the differential release properties supported by these channels at cerebrocortical nerve terminals. *European Journal of Neuroscience*, **29**, 1131-1140.

LATHAM, J. R., PATHIRATHNA, S., JAGODIC, M. M., CHOE, W. J., LEVIN, M. E., NELSON, M. T., LEE, W. Y., KRISHNAN, K., COVEY, D. F., TODOROVIC, S. M. & JEVTOVIC-TODOROVIC, V. 2009. Selective T-type calcium channel blockade alleviates hyperalgesia in *ob/ob* mice. *Diabetes*, **58**, 2656-2665.

LAUDERBACK, C. M., HACKETT, J. M., HUANG, F. F., KELLER, J. N., SZWEDA, L. I., MARKESBERY, W. R. & BUTTERFIELD, D. A. 2001. The glial glutamate transporter, GLT-1, is oxidatively modified by 4-hydroxy-2-nonenal in the Alzheimer's disease brain: the role of A β 1-42. *Journal of Neurochemistry*, **78**, 413-416.

LEE, H., YANG, Y., SU, Z., HYEON, C., LEE, T., LEE, H., KWEON, D., SHIN, Y. & YOON, T. 2010. Dynamic Ca²⁺-dependent stimulation of vesicle fusion by membrane-anchored synaptotagmin 1. *Science*, **328**, 760-763.

LEENDERS, A. G. M. & SHENG, Z. H. 2005. Modulation of neurotransmitter release by the second messenger-activated protein kinases: implications for presynaptic plasticity. *Pharmacology & Therapeutics*, **105**, 69-84.

LENZEN, S. 2008. The mechanisms of alloxan- and streptozotocin-induced diabetes. *Diabetologia*, **51**, 216-226.

LEUNER, B., GOULD, E. & SHORS, T. J. 2006. Is there a link between adult neurogenesis and learning? *Hippocampus*, **16**, 216-224.

LLOBET, A., WU, M. & LAGNADO, L. 2008. The mouth of a dense-core vesicle opens and closes in a concerted action regulated by calcium and amphiphysin. *Journal of Cell Biology*, **132**, 1017-1028.

LODISH, H., BERK, A., ZIPURSKY, S. L., MATSUDAIRA, P., BALTIMORE, D. & DARNELL, J. 2008. *Molecular Cell Biology*, New York: W.H. Freeman.

LOU, X., KOROGOD, N., BROSE, N. & SCHNEGGENBURGER, R. 2008a. Phorbol esters modulate spontaneous and Ca²⁺-evoked transmitter release via acting on both Munc13 and protein kinase C. *Journal of Neuroscience*, **28**, 8257-8267.

LOU, X., PARADISE, S., FERGUSON, S. M. & DE CAMILLI, P. 2008b. Selective saturation of slow endocytosis at a giant glutamatergic central synapse lacking dynamin 1. *Proceedings of the National Academy of Sciences of the United States of America*, **105**, 17555-17560.

LU, W., MA, H., SHENG, Z. H. & MOCHIDA, S. 2009. Dynamin and activity regulate synaptic vesicle recycling in sympathetic neurons. *Journal of Biological Chemistry*, **284**, 1930-1937.

LUMLEY, L. A., ROBISON, C. L., CHEN, W. K., MARK, B. & MEYERHOFF, J. L. 2001. Vasopressin into the preoptic area increases grooming behavior in mice. *Physiology & Behavior*, **73**, 451-455.

LUNDMARK, R. & CARLSSON, S. R. 2009. SNX9 - a prelude to vesicle release. *Journal of Cell Science*, **122**, 5-11.

LYNCH, K. L., GERONA, R. R. L., KIELAR, D. M., MARTENS, S., MCMAHON, H. T. & MARTIN, T. F. J. 2008. Synaptotagmin-1 utilizes membrane bending and SNARE binding to drive fusion pore expansion. *Molecular Biology of the Cell*, **19**, 5093-5103.

MCDONOUGH, S. I., SWARTZ, K. J., MINTZ, I. M., BOLAND, L. M. & BEAN, B. P. 1996. Inhibition of calcium channels in rat central and peripheral neurons by ω -conotoxin MVIIC. *Journal of Neuroscience*, **16**, 2612-2623.

MCEWEN, J. M. & KAPLAN, J. M. 2008. UNC-18 promotes both the anterograde trafficking and synaptic function of syntaxin. *Molecular Biology of the Cell*, **19**, 3836-3846

MCGOWAN, B. M. C., MINNION, J. S., MURPHY, K. G., WHITE, N. E., ROY, D., STANLEY, S. A., DHILLO, W. S., GARDINER, J. V., GHATEI, M. A. & BLOOM, S. R. 2010. Central and peripheral administration of human relaxin-2 to adult male rats inhibits food intake. *Diabetes, Obesity and Metabolism*, **12**, 1090-1096.

MCMAHON, H. T., KOZLOV, M. M. & MARTENS, S. 2010. Membrane curvature in synaptic vesicle fusion and beyond. *Cell*, **140**, 601-605.

MELDRUM, B. S. 2000. Glutamate as a neurotransmitter in the brain: review of physiology and pathology. *Journal of Nutrition*, **130**, 15.

MENG, S. Z., OZAWA, Y., ITOH, M. & TAKASHIMA, S. 1999. Developmental and age-related changes of dopamine transporter, and dopamine D1 and D2 receptors in human basal ganglia. *Brain Research*, **843**, 136-144.

MESSIER, C. 2004. Glucose improvement of memory: a review. *European Journal of Pharmacology*, **490**, 33-57.

MIN, L., LEUNG, Y. M., TOMAS, A., WATSON, R. T., GAISANO, H. Y., HALBAN, P. A., PESSIN, J. E. & HOU, J. C. 2007. Dynamin Is Functionally

Coupled to Insulin Granule Exocytosis. *Journal of Biological Chemistry*, **282**, 3530–33536.

MOLLER, D. E. 2001. New drug targets for type 2 diabetes and the metabolic syndrome. *Nature*, **414**, 821-827.

MORIMOTO, C., KIYAMA, A., KAMEDA, K., NINOMIYA, H., TSUJITA, T. & OKUDA, H. 2000. Mechanism of the stimulatory action of okadaic acid on lipolysis in rat fat cells. *Journal of Lipid Research*, **41**, 199-204.

MORTON, A. J., FAULL, R. L. & EDWARDSON, J. M. 2001. Abnormalities in the synaptic vesicle fusion machinery in Huntington's disease. *Brain Research Bulletin*, **56**, 111–117.

MUNTON, R. P., TWEEDIE-CULLEN, R., LIVINGSTONE-ZATCHEJ, M., WEINANDY, F., WAIDELICH, M., LONGO, D., GEHRIG, P., POTTHAST, F., RUTISHAUSER, D., GERRITS, B., PANSE, C., SCHLAPBACH, R. & MANSUY, I. M. 2007. Qualitative and quantitative analyses of protein phosphorylation in naive and stimulated mouse synaptosomal preparations. *Molecular & Cell Proteomics*, **6**, 283-293.

NACHMAN-CLEWNER, M., ST JULES, R. & TOWNES-ANDERSON, E. 1999. L-type calcium channels in the photoreceptor ribbon synapse: localization and role in plasticity. *Journal of Comparative Neurology*, **415**, 1-16.

NEHER, E. & SAKABA, T. 2008. Multiple roles of calcium ions in the regulation of neurotransmitter release. *Neuron*, **59**, 861-872.

NEWTON, A. J., KIRCHHAUSEN, T. & MURTHY, V. N. 2006. Inhibition of dynamin completely blocks compensatory synaptic vesicle endocytosis. *Proceedings of the National Academy of Sciences of the United States of America*, **103**, 17955-17960.

NEWTON, I. G., FORBES, M. E., LINVILLE, M. C., PANG, H., TUCKER, E. W., RIDDLE, D. R. & BRUNSO-BECHTOLD, J. K. 2008. Effects of aging and caloric restriction on dentate gyrus synapses and glutamate receptor subunits. *Neurobiology of Aging*, **29**, 1308–1318.

NGARMUKOS, C., BAUR, E. L. & KUMAGAI, A. K. 2001. Co-localization of GLUT1 and GLUT4 in the blood-brain barrier of the rat ventromedial hypothalamus. *Brain Research*, **900**, 1-8.

NICHOLLS, D. G., SIHRA, T. S. & SANCHEZ-PRIETO, J. 1987. Calcium-dependent and independent release of glutamate from synaptosomes monitored by continuous fluorometry. *Journal of Neurochemistry*, **49**, 50-57.

OBROSOVA, I. G. 2005. Increased sorbitol pathway activity generates oxidative stress in tissue sites for diabetic complications. *Antioxidants and Redox Signaling*, **7**, 1543-1552.

OHYAMA, A., HOSAKA, K., KOMIYA, Y., AKAGAWA, K., YAMAUCHI, E., TANIGUCHI, H., SASAGAWA, N., KUMAKURA, K., MOCHIDA, S., YAMAUCHI, T. & IGARASHI, M. 2002. Regulation of exocytosis through Ca^{2+} /ATP-dependent binding of autophosphorylated Ca^{2+} /calmodulin-activated protein kinase II to syntaxin 1A. *Journal of Neuroscience*, **22**, 3342-3351.

OMIATEK, D. M., CANS, A. S., HEIEN, M. L. & EWING, A. G. 2010. Analytical approaches to investigate transmitter content and release from single secretory vesicles. *Analytical and Bioanalytical Chemistry*, **397**, 3269-3279.

OPAZO, F., PUNGE, A., BUCKERS, J., HOOPMANN, P., KASTRUP, L., HELL, S. W. & RIZZOLI, S. O. 2010. Limited intermixing of synaptic vesicle components upon vesicle recycling. *Traffic*, **11**, 800-812.

PANG, Z. P., CAO, P., XU, W. & SUDHOF, T. C. 2010. Calmodulin controls synaptic strength via presynaptic activation of calmodulin kinase II. *Journal of Neuroscience*, **30**, 4132-4142.

PARK, Y. & KIM, K. T. 2009. Short-term plasticity of small synaptic vesicle (SSV) and large dense-core vesicle (LDCV) exocytosis. *Cell Signal*, **21**, 1465-1470.

PERETZ, A., ABITBOL, I., SOBKO, A., WU, C. F. & ATTALI, B. 1998. A Ca^{2+} /calmodulin-dependent protein kinase modulates *Drosophila* photoreceptor K^+ currents: a role in shaping the photoreceptor potential. *Journal of Neuroscience*, **18**, 9153-9162.

PERSON, A. L. & RAMAN, I. M. 2010. Deactivation of L-type Ca current by inhibition controls LTP at excitatory synapses in the cerebellar nuclei. *Neuron*, **66**, 550-559.

PETERS, A., PALAY, S. L., & WEBSTER, H. D. F. 1991. *The Fine Structure of the Nervous System*, Oxford, Oxford University Press.

PUCADYIL, T. J. & SCHMID, S. L. 2008. Real-time visualization of dynamin-catalyzed membrane fission and vesicle release. *Cell*, **135**, 1263-1275.

PUENTE, E. C., SILVERSTEIN, J., BREE, A. J., MUSIKANTOW, D. R., WOZNIAK, D. F., MALONEY, S., DAPHNA-IKEN, D. & FISHER, S. J. 2010. Recurrent moderate hypoglycemia ameliorates brain damage and cognitive dysfunction induced by severe hypoglycemia. *Diabetes*, **59**, 1055-1062.

QUINN, L. P., GRUNDY, R. I., CAMPBELL, C. A., COLLIER, S., LAWMAN, A., STEAN, T. O., BILLINTON, A., PARSONS, A. A., UPTON, N., DUXON, M. S. & IRVING, E. A. 2005. A novel behavioural registration system LABORAS and the social interaction paradigm detect long-term functional deficits following middle cerebral artery occlusion in the rat. *Brain Research*, **1031**, 118-124.

QUINN, L. P., STEAN, T. O., TRAIL, B., DUXON, M. S., STRATTON, S. C., BILLINTON, A. & UPTON, N. 2003. LABORAS: Initial pharmacological

validation of a system allowing continuous monitoring of laboratory rodent behaviour. *Journal of Neuroscience Methods*, **130**, 83-92.

RAMAKRISHNAN, R., PRABHAKARAN, K., JAYAKUMAR, A. R., GUNASEKARAN, P., SHEELADEVI, R. & SUTHANTHIRARAJAN, N. 2005. Involvement of Ca²⁺/calmodulin-dependent protein kinase II in the modulation of indolamines in diabetic and hyperglycemic rats. *Journal of Neuroscience Research*, **80**, 518-528.

RAMANATHAN, M., JAISWAL, A. K. & BHATTACHARYA, S. K. 1998. Differential effects of diazepam on anxiety in streptozotocin induced diabetic and non-diabetic rats. *Psychopharmacology*, **135**, 361-367.

RANDALL, A. & TSIEN, R. W. 1995. Pharmacological dissection of multiple types of Ca²⁺ channel currents in rat cerebellar granule neurons. *Journal of Neuroscience*, **15**, 2995-3012.

REICHARD, P. & PIHL, M. 1994. Mortality and treatment side-effects during long-term intensified conventional insulin treatment in the Stockholm Diabetes Intervention Study. *Diabetes*, **43**, 313-317.

REZAZADEH, S., CLAYDON, T. W. & FEDIDA, D. 2006. KN-93 (2-[N-(2-hydroxyethyl)]-N-(4-methoxybenzenesulfonyl)]amino-N-(4-chlorocinnamyl)-N-methylbenzylamine), a calcium/calmodulin-dependent protein kinase II inhibitor, is a direct extracellular blocker of voltage-gated potassium channels. *Journal of Pharmacology & Experimental Therapeutics*, **317**, 292-299.

RICHARDS, D. A. 2009. Vesicular release mode shapes the postsynaptic response at hippocampal synapses. *Journal of Physiology*, **587**, 5073-5080.

RIZO, J. 2010. Synaptotagmin-SNARE coupling enlightened. *Nature Structural & Molecular Biology*, **17**, 260-262.

RIZO, J. & ROSENMUND, C. 2008. Synaptic vesicle fusion. *Nature Structural & Molecular Biology*, **15**, 665-674.

RIZZOLI, S. O. & BETZ, W. J. 2005. Synaptic vesicle pools. *Nature Structural & Molecular Biology*, **6**, 57-69.

RIZZOLI, S. O. & JAHN, R. 2007. Kiss-and-run, collapse and 'readily retrievable' vesicles. *Traffic*, **8**, 1137-1144.

ROBINSON, P. J. 2007. Neuroscience. How to fill a synapse. *Science*, **316**, 551-553.

ROHRBOUGH, J. & BROADIE, K. 2005. Lipid regulation of the synaptic vesicle cycle. *Nature Reviews Neuroscience*, **6**, 139-150.

ROMERO-AROCA, P., MENDEZ-MARIN, I., BAGET-BERNALDIZ, M., FERNENDEZ-BALLART, J. & SANTOS-BLANCO, E. 2010. Review of the relationship between renal and retinal microangiopathy in diabetes mellitus patients. *Current Diabetes Reviews*, **6**, 88-8101.

ROY, S., TRUDEAU, K., BEHL, Y., DHAR, S. & CHRONOPOULOS, A. 2010. New insights into hyperglycemia-induced molecular changes in microvascular cells. *Journal of Dental Research*, **89**, 116-127.

RUSNAK, F. & MERTZ, P. 2000. Calcineurin: form and function. *Physiological Reviews*, **80**, 1483-1521.

SANTOS, M. S., LI, H. & VOGLMAIER, S. M. 2009. Synaptic vesicle protein trafficking at the glutamate synapse. *Neuroscience*, **158**, 189-203.

SATOH, E. & TAKAHASHI, A. 2008. Experimental diabetes enhances Ca²⁺ mobilization and glutamate exocytosis in cerebral synaptosomes from mice. *Diabetes Research and Clinical Practice*, **81**, 14-17.

SERRA, S. A., CUENCA-LEON, E., LLOBET, A., RUBIO-MOSCARDO, F., PLATA, C., CARRENO, O., FERNÁNDEZ-CASTILLO, N., COROMINAS, R., VALVERDE, M. L. A., MACAYA, A., CORMAND, B. & FERNANDEZ, J. M. 2010. A mutation in the first intracellular loop of CACNA1A prevents P/Q channel modulation by SNARE proteins and lowers exocytosis. *Proceedings of the National Academy of Sciences of the United States of America*, **107**, 1672-1677.

SERULLE, Y., SUGIMORI, M. & LLINAS, R. R. 2007. Imaging synaptosomal calcium concentration microdomains and vesicle fusion by using total internal reflection fluorescent microscopy. *Proceedings of the National Academy of Sciences of the United States of America*, **104**, 1697-1702.

SHIN, O. H., LU, J., RHEE, J. S., TOMCHICK, D. R., PANG, Z. P., WOJCIK, S. M., CAMACHO-PEREZ, M., BROSE, N., MACHIUS, M., RIZO, J., ROSENMUND, C. & SUDHOF, T. C. 2010. Munc13 C₂B domain is an activity-dependent Ca²⁺ regulator of synaptic exocytosis. *Nature Structural & Molecular Biology* **17**, 280-288.

SHOJI, H. & MIZOGUCHI, K. 2011. Aging-related changes in the effects of social isolation on social behavior in rats. *Physiology & Behavior*, **102**, 58-62.

SHU, S., LIU, X. & KORN, E. D. 2005. Blebbistatin and blebbistatin-inactivated myosin II inhibit myosin II-independent processes in Dictyostelium. *Proceedings of the National Academy of Sciences of the United States of America*, **102**, 1472-1477.

SHUPLIAKOV, O. 2009. The synaptic vesicle cluster: A source of endocytic proteins during neurotransmitter release. *Neuroscience*, **158**, 204-210.

SIEGEL, G. J., AGRANOFF, B. W., ALBERS, W., FISHER, S. K. & UHLER, M. D. 1999. *Basic Neurochemistry: Molecular, Cellular and Medical Aspects*, Philadelphia: Lippincott-Raven, American Society for Neurochemistry.

SIMPSON, I. A., APPEL, N. M., HOKARI, M., OKI, J., HOLMAN, G. D., MAHER, F., KOEHLER-STECH, E. M., VANNUCCI, S. J. & SMITH, Q. R. 1999. Blood-brain barrier glucose transporter: effects of hypo- and hyperglycemia revisited. *Journal of Neurochemistry*, **72**, 238-247.

STRANAHAN, A. M., ARUMUGAM, T. V., CUTLER, R. G., LEE, K., EGAN, J. M. & MATTSON, M. P. 2008. Diabetes impairs hippocampal function through glucocorticoid-mediated effects on new and mature neurons. *Nature Neuroscience*, **11**, 309-317.

SUDHOF, T. C. 1995. The synaptic vesicle cycle: a cascade of protein-protein interactions. *Nature*, **375**, 645-653.

SUDHOF, T. C. & MALENKA, R. C. 2008. Understanding synapses: past, present, and future. *Neuron*, **60**, 469-476.

SUH, S. W., AOYAMA, K., MATSUMORI, Y., LIU, J. & SWANSON, R. A. 2005. Pyruvate administered after severe hypoglycemia reduces neuronal death and cognitive impairment. *Diabetes*, **54**, 1452-1458.

SUNYER, B., DIAO, W. & LUBEC, G. 2008. The role of post-translational modifications for learning and memory formation. *Electrophoresis*, **29**, 2593-2602.

SWAINSON, R., HODGES, J. R., GALTON, C. J., SEMPLE, J., MICHAEL, A., DUNN, B. D., IDDON, J. L., ROBBINS, T. W. & SAHAKIAN, B. J. 2001. Early detection and differential diagnosis of Alzheimer's disease and depression with neuropsychological tasks. *Dementia and Geriatric Cognitive Disorders*, **12**, 265-280.

SZE, C. I., BI, H., KLEINSCHMIDT-DEMASTERS, B. K., FILLEY, C. M. & MARTIN, L. J. 2000. Selective regional loss of exocytotic presynaptic vesicle

proteins in Alzheimer's disease brains. *Journal of Neurological Sciences*, **175**, 81–90.

TERRY, A. V. & BUCCAFUSCO, J. J. 2003. The cholinergic hypothesis of age and Alzheimer's disease-related cognitive deficits: recent challenges and their implications for novel drug development. *Journal of Pharmacological and Experimental Therapeutics*, **306**, 821-827.

TFAYLI, H. & ARSLANIAN, S. 2009. Pathophysiology of type 2 diabetes mellitus in youth: the evolving chameleon. *Arquivos Brasileiros de Endocrinologia & Metabologia*, **53**, 165-174.

THOMAS, V. S., DARVESH, S., MACKNIGHT, C. & ROCKWOOD, K. 2001. Estimating the prevalence of dementia in elderly people: a comparison of the Canadian Study of Health and Aging and National Population Health Survey approaches. *International Psychogeriatrics*, **13** (1), 169-175.

THOMPSON, H. M. & MCNIVEN, M. A. 2006. Discovery of a new 'dynasore'. *Nature Chemical Biology*, **2**, 355-356.

THORNALLEY, P. J. 2002. Glycation in diabetic neuropathy: characteristics, consequences, causes, and therapeutic options. *International Review of Neurobiology*, **50**, 37-57.

TOKUOKA, H. & GODA, Y. 2006. Myosin light chain kinase is not a regulator of synaptic vesicle trafficking during repetitive exocytosis in cultured hippocampal neurons. *Journal of Neuroscience*, **26**, 11606-11614.

TOMLINSON, D. R. & GARDINER, N. J. 2008. Glucose neurotoxicity. *Nature Reviews Neuroscience*, **9**, 36-45.

UNGER, J. W., LIVINGSTON, J. N. & MOSS, A. M. 1991. Insulin receptors in the central nervous system: localization, signalling mechanisms and functional aspects. *Progress in Neurobiology*, **36**, 343-362.

URANGA, R. M., BRUCE-KELLER, A. J., MORRISON, C. D., FERNANDEZ-KIM, S. O., EBENEZER, P. J., ZHANG, L., DASURI, K. & KELLER, J. N. 2010. Intersection between metabolic dysfunction, high fat diet consumption, and brain aging. *Journal of Neurochemistry*, **114**, 344-361.

VAN DE WEERD, H. A., BULTHUIS, R. J. A., BERGMAN, A. F., SCHLINGMANN, F., TOLBOOM, J., VAN LOO, P. L. P., REMIE, R., BAUMANS, V. & VAN ZUTPHEN, L. F. M. 2001. Validation of a new system for the automatic registration of behaviour in mice and rats. *Behavioural Processes*, **53**, 11-20.

VAN DUINKERKEN, E., KLEIN, M., SCHOONENBOOM, N. S. M., HOOGMA, R. P. L. M., MOLL, A. C., SNOEK, F. J., STAM, C. J. & DIAMANT, M. 2009. Functional brain connectivity and neurocognitive functioning in patients with long-standing type 1 diabetes with and without microvascular complications: a magnetoencephalography study. *Diabetes*, **58**, 2335-2343.

VANGUILDER, H. D., BRUCKLACHER, R. M., PATEL, K., ELLIS, R. W., FREEMAN, W. M. & BARBER, A. J. 2008. Diabetes downregulates presynaptic proteins and reduces basal synapsin I phosphorylation in rat retina. *European Journal of Neuroscience*, **28**, 1-11.

VERMA, D., GUPTA, Y. K., PARASHAR, A. & RAY, S. B. 2009. Differential expression of L- and N-type voltage-sensitive calcium channels in the spinal cord of morphine+nimodipine treated rats. *Brain Research*, **1249**, 128-134.

VERONA, M., ZANOTTI, S., SCHAFFER, T., RACAGNI, G. & POPOLI, M. 2000. Changes of synaptotagmin interaction with t-SNARE proteins *in vitro* after calcium/calmodulin-dependent phosphorylation. *Journal of Neurochemistry*, **74**, 209-221.

VRLJIC, M., STROP, P., ERNST, J. A., SUTTON, R. B., CHU, S. & BRUNGER, A. T. 2010. Molecular mechanism of the synaptotagmin-SNARE interaction in Ca²⁺-triggered vesicle fusion. *Nature Structural & Molecular Biology*, **17**, 325-331.

WASSER, C. R. & KAVALALI, E. T. 2009. Leaky synapses: Regulation of spontaneous neurotransmission in central synapses. *Neuroscience*, **158**, 177-188.

WESSELS, A. M., ROMBOUTS, S. A. R. B., REMIJNSE, P. L., BOOM, Y., SCHELTENS, P., BARKHOF, F., HEINE, R. J. & SNOEK, F. J. 2007. Cognitive performance in type 1 diabetes patients is associated with cerebral white matter volume. *Diabetologia*, **50**, 1763-1769.

WHEELER, D. G., BARRETT, C. F., GROTH, R. D., SAFA, P. & TSIEN, R. W. 2008. CaMKII locally encodes L-type channel activity to signal to nuclear CREB in excitation-transcription coupling. *Journal of Cell Biology*, **183**, 849-863.

WIDMAIER, E. P., RAFF, H. & STRANG, K. T. 2006. *Vander's Human Physiology- The mechanism of body function*. 10. Europe: McGraw-Hill Education.

WIERDA, K. D. B., TOONEN, R. F. G., DE WIT, H., BRUSSAARD, A. B. & VERHAGE, M. 2007. Interdependence of PKC-dependent and PKC-independent pathways for presynaptic plasticity. *Neuron*, **54**, 275-290.

WOOLLEY, M. L., PEMBERTON, D. J., BATE, S., CORTI, C. & JONES, D. N. C. 2008. The mGlu2 but not the mGlu3 receptor mediates the actions of the mGluR2/3 agonist, LY379268, in mouse models predictive of antipsychotic activity. *Psychopharmacology (Berlin)*, **196**, 431-440.

WRIGHT, C. E. & ANGUS, J. A. 1996. Effects of N-, P- and Q-type neuronal calcium channel antagonists on mammalian peripheral neurotransmission. *British Journal of Pharmacology*, **119**, 49-56.

WRIGHT, T., LANGLEY-EVANS, S. C. & VOIGT, J. P. 2011. The impact of maternal cafeteria diet on anxiety-related behaviour and exploration in the offspring. *Physiology & Behavior*, **103**, 164-172.

WU, X. S., MCNEIL, B. D., XU, J., FAN, J., XUE, L., MELICOFF, E., ADACHI, R., BAI, L. & WU, L. G. 2009. Ca²⁺ and calmodulin initiate all forms of endocytosis during depolarization at a nerve terminal. *Nature Neuroscience*, **12**, 1003-1010.

WYKES, R. C. E., BAUER, C. S., KHAN, S. U., WEISS, J. L. & SEWARD, E. P. 2007. Differential regulation of endogenous N- and P/Q-type Ca²⁺ channel inactivation by Ca²⁺/calmodulin impacts on their ability to support exocytosis in chromaffin cells. *Journal of Neuroscience*, **27**, 5236-5248.

XIA, X., LESSMANN, V. & MARTIN, T. F. J. 2009. Imaging of evoked dense-core-vesicle exocytosis in hippocampal neurons reveals long latencies and kiss-and-run fusion events. *Journal of Cell Science*, **122**, 75-82.

XU, J., MCNEIL, B. D., WU, W., NEES, D., BAI, L. & WU, L.G. 2008. GTP-independent rapid and slow endocytosis at a central synapse. *Nature Neuroscience*, **11**, 45-53.

XUE, M., CRAIG, T. K., XU, J., CHAO, H. T., RIZO, J. & ROSENMUND, C. 2010. Binding of the complexin N terminus to the SNARE complex potentiates synaptic-vesicle fusogenicity. *Nature Structural & Molecular Biology*, **17**, 568-575.

XUE, M., LIN, Y. Q., PAN, H., REIM, K., DENG, H., BELLEN, H. J. & ROSENMUND, C. 2009. Tilting the balance between facilitatory and inhibitory

functions of mammalian and *Drosophila* Complexins orchestrates synaptic vesicle exocytosis. *Neuron*, **64**, 367-380.

YAMASHITA, T., EGUCHI, K., SAITOH, N., VON GERSDORFF, H. & TAKAHASHI, T. 2010. Developmental shift to a mechanism of synaptic vesicle endocytosis requiring nanodomain Ca^{2+} . *Nature Neuroscience*, **13**, 838-844.

YAMAUCHI, T. 2005. Neuronal Ca^{2+} /calmodulin-dependent protein kinase II-discovery, progress in a quarter of a century, and perspective: implication for learning and memory. *Biological and Pharmaceutical Bulletin*, **28**, 1342-1354.

YANG, L., WANG, Z., WANG, B., JUSTICE, N. J. & ZHENG, H. 2009. Amyloid precursor protein regulates $\text{Ca}_v1.2$ L-type calcium channel levels and function to influence GABAergic short-term plasticity. *Journal of Neuroscience*, **29**, 15660-15668.

YOON, E. J., HAMM, H. E. & CURRIE, K. P. M. 2008. G protein $\beta\gamma$ subunits modulate the number and nature of exocytotic fusion events in adrenal chromaffin cells independent of calcium entry. *Journal of Neurophysiology*, **100**, 2929-2939.

ZHANG, Q., CAO, Y. Q. & TSIEN, R. W. 2007. Quantum dots provide an optical signal specific to full collapse fusion of synaptic vesicles. *Proceedings of the National Academy of Sciences of the United States of America*, **104**, 17843-17848.

ZHANG, Q., LI, Y. & TSIEN, R. W. 2009. The dynamic control of kiss-and-run and vesicular reuse probed with single nanoparticles. *Science*, **323**, 1448-1453.

ZHANG, Z. & JACKSON, M. B. 2010. Membrane bending energy and fusion pore kinetics in Ca^{2+} -triggered exocytosis. *Biophysical Journal*, **98**, 2524-2534.

ZHAO, W. Q., CHEN, H., QUON, M. J. & ALKON, D. L. 2004. Insulin and the insulin receptor in experimental models of learning and memory. *European Journal of Pharmacology*, **490**, 71-81.

ZHU, L. Q., LIU, D., HU, J., CHENG, J., WANG, S. H., WANG, Q., WANG, F., CHEN, J. G. & WANG, J. Z. 2010. GSK-3 β inhibits presynaptic vesicle exocytosis by phosphorylating P/Q-type calcium channel and interrupting SNARE complex formation. *Journal of Neuroscience*, **30**, 3624-3633.

ZHU, Y., XU, J. & HEINEMANN, S. F. 2009. Synaptic vesicle exocytosis-endocytosis at central synapses: Fine-tuning at differential patterns of neuronal activity. *Communicative & Integrative Biology*, **2**, 418-419.

Website References

<http://www.labx.com/v2/adsearch/detail3.cfm?adnumb=367614>

http://www.metris.nl/en/products/laboras/laboras_information/

VI. Appendices

IV.1 Settings for plate reader

Table VI.1.1: Tecan GENios Pro™ microtitre plate reader's settings for the measurement of glutamate release:

Greiner 96 well, flat transparent bottom microtitre plate
Fluorescence, Kinetics
Part of the plate: 1-9/7-12
Excitation wavelength: 340 nm
Emission wavelength: 465 nm
Gain: 70
Measurement mode: Bottom of the plate
No. of cycles: 21/14
Shake duration: 3s before the measurement and 1s in between the cycle

Table VI.1.2: Tecan GENios Pro™ microtitre plate reader's settings for the measurement of FM2-10 dye release:

Greiner 96 well, flat bottom black microtitre plate
Fluorescence, Well Kinetics
Part of the plate: 1-4/ 5-8
Excitation wavelength: 485 nm
Emission wavelength: 555 nm
Gain: 40
Measurement mode: Top of the plate
No. of cycles: 461
No. of flashes: 10: lag time 0 μ s
Mirror type: Dichroic 3
Integration time: 40 μ s
Injector volume and speed: 40 μ L
Injection mode: Every injection refill.
Shake duration: 1s

Table VI.1.3: Tecan GENios Pro™ microtitre plate reader's settings for the measurement of the changes in intracellular $[Ca^{2+}]_i$:

Greiner 96 well, flat bottom black microtitre plate
Fluorescence, Well Kinetics
Part of the plate: 1/2/3/4/5/6/7/8/9/10/11/12
Excitation wavelength: 340 nm/ 390 nm
Emission wavelength: 535 nm
Gain: 30
Measurement mode: Top of the plate
No. of cycles: 40/160
No. of flashes: 10: lag time 0 μ s
Mirror type: Dichroic 3
Integration time: 40 μ s
Injector volume and speed: None/ 40 μ L
Injection mode: Every injection refill.
Shake duration: 1s

Buffers used in the experiments

Table VI.1.4: Homogenization Buffer (pH 7.4)

Components	Concentration	Amount in 1 litre
Sucrose	0.32M	109.54g
Hepes	10mM	2.383g

Table VI.1.5: L0 Buffer (pH 7.4)

Components	Concentration	Amount in 1 litre
NaCl	125mM	7.305g
KCl	5mM	0.373g
MgCl ₂	1mM	0.203g
Hepes	20mM	4.766g
Glucose	10mM	10mL*

*** Solution of 1.8 g glucose made in 10mL water before adding it to the buffer as glucose alone will not dissolve in the buffer**

IV.2 Calculations

All the data produced in the glutamate release, FM2-10 dye release and Fura-2 assay were analyzed by methods outlined in appendix 6C (p121), appendix 6D (p129) and appendix 6E (p155) in the thesis of Pooja Mohanrao Barbar (Barbar, 2010). As this information represents 46 pages of text, it was deemed reasonable just to cite these methods of analysis rather than repeating this text.

LABORAS Calculation:

After 24 hours of monitoring, LABORAS provides data as shown below:

Raw Data

A	B	C	D	E	F	G	H	I	J	K	L	M	N	O
WI ND O W	T-BEGIN	T-END	S E S I O N		A N I C E		U N D E F _ D	L O C O M _ D	I M M O B _ D	R E A R _ D	G R O O M _ D	D R I N _ K _ D	E A T _ D	T O T A L _ D
							[s]	[s]	[s]	[s]	[s]	[s]	[s]	[s]
1	000:00:00	002:24:00	2	1	0	0	900.24	20.3	6384.99	80.47	1018.12	86.76	149.15	8640
2	002:24:00	004:48:00	2	1	0	0	1233.3	38.1	4324.49	517.25	2077.23	189.44	260.18	8640
3	004:48:00	007:12:00	2	1	0	0	611.84	7.35	6832.52	193.79	774.94	20.79	198.77	8640
4	007:12:00	009:36:00	2	1	0	0	423.95	0.51	7868.18	25.42	199.26	92.94	29.74	8640
5	009:36:00	012:00:00	2	1	0	0	950.53	74.4	4086.04	741.8	1831.41	130.41	825.43	8640
6	012:00:00	014:24:00	2	1	0	0	820.87	61.2	4742.44	498.73	1811.47	245.33	459.96	8640
7	014:24:00	016:48:00	2	1	0	0	447.64	11.7	7669.21	36.93	458.47	0	16.06	8640
8	016:48:00	019:12:00	2	1	0	0	743.57	63.7	4539.82	460.56	1812.83	106.34	913.17	8640
9	019:12:00	021:36:00	2	1	0	0	733.53	63.8	4706.8	803.22	1553.05	86.47	693.12	8640
10	021:36:00	024:00:00	2	1	0	0	1880.9	50.1	3390.33	694.29	1862.88	402.38	359.16	8640
1	000:00:00	002:24:00	2	2	0	0	1746.6	104	3064.11	1087.48	1706.95	168.85	762.3	8640
2	002:24:00	004:48:00	2	2	0	0	1168.4	10.1	5825.69	207.34	906.88	91.96	429.66	8640
3	004:48:00	007:12:00	2	2	0	0	1211.8	21.6	5162.28	539.57	922.23	173.73	608.8	8640
4	007:12:00	009:36:00	2	2	0	0	1378.1	23.7	5797.7	328.87	785.37	92.04	234.27	8640
5	009:36:00	012:00:00	2	2	0	0	1213.5	79.1	4897.13	826.51	1080.35	83.18	460.24	8640

6	012:00:00	014:24:00	2	2	0	0	854.91	19.3	6906.26	194.48	558.24	53	53.77	8640
7	014:24:00	016:48:00	2	2	0	0	1023.7	46.7	5596.29	568.65	854.75	112.57	437.37	8640
8	016:48:00	019:12:00	2	2	0	0	919.46	32.6	5519.39	568.91	1101.37	27.38	470.88	8640
9	019:12:00	021:36:00	2	2	0	0	1273.4	65.2	4214.23	814.27	1554.15	115.21	603.58	8640
10	021:36:00	024:00:00	2	2	0	0	1724.4	67.5	4376.24	830.45	1055.67	119.04	466.72	8640
1	000:00:00	002:24:00	2	3	0	0	1345.6	32.7	5470.09	351.83	1439.77	0	0	8640
2	002:24:00	004:48:00	2	3	0	0	2024.5	28.6	4541.97	599.63	1439.2	0	6.12	8640
3	004:48:00	007:12:00	2	3	0	0	2117.3	9.45	4734.75	590.71	1182.01	0	5.82	8640
4	007:12:00	009:36:00	2	3	0	0	1143	5.92	6392.43	251.83	846.8	0	0	8640
5	009:36:00	012:00:00	2	3	0	0	1459.5	105	3884.57	1211.63	1662.41	19.94	296.83	8640
6	012:00:00	014:24:00	2	3	0	0	1118.2	24.2	5817.9	209.35	1194.63	71.32	204.4	8640
7	014:24:00	016:48:00	2	3	0	0	1188.4	33.6	5215.64	570.7	1575.68	0	56	8640
8	016:48:00	019:12:00	2	3	0	0	1383.9	32.5	5105.27	550.89	1546.18	0	21.29	8640
9	019:12:00	021:36:00	2	3	0	0	1731	26	5595.42	368.57	834.36	0	84.66	8640
10	021:36:00	024:00:00	2	3	0	0	1951.9	55.5	3265.38	1013.06	2224.41	0	129.76	8640
1	000:00:00	002:24:00	2	4	0	0	1619.9	95.3	3594.84	892.97	1512.67	382.56	541.76	8640
2	002:24:00	004:48:00	2	4	0	0	1419.2	73	3034.63	684.17	2441.07	445.6	542.38	8640
3	004:48:00	007:12:00	2	4	0	0	1068	0	7391.89	53.9	45.63	27.94	52.64	8640
4	007:12:00	009:36:00	2	4	0	0	936.15	21.2	5582.92	382.16	1164.94	182.12	370.55	8640
5	009:36:00	012:00:00	2	4	0	0	1091.3	118	4234.73	997.63	1647.62	267.37	283.58	8640
6	012:00:00	014:24:00	2	4	0	0	1071.7	43.3	6845.4	113.15	504.4	43.64	18.37	8640
7	014:24:00	016:48:00	2	4	0	0	993.79	13.7	5893.27	296.51	1097.33	182.4	163.03	8640
8	016:48:00	019:12:00	2	4	0	0	874.57	43.2	5026.94	638.5	1231.72	295.25	529.83	8640
9	019:12:00	021:36:00	2	4	0	0	756.64	19.6	6384.5	289.03	874.04	204.5	111.69	8640
10	021:36:00	024:00:00	2	4	0	0	1152.3	99.5	3953.41	1065.1	1655.56	180.76	533.31	8640

P	Q	R	S	T	U	V	W	X	Y	Z	AA	AB
UNDEF _F	LOC OM_ F	IMMO B_F	REAR _F	GRO OM_ F	DR IN K_ F	EAT_ F	TOTAL _F	SPD_M AX	T_SP D_M X	SPD_ LAV G	SPD_AVG	DISTAN CE
[count s]	[cou nts]	[counts]	[cou nts]	[cou nts]	[cou nts]	[cou nts]	[counts]	[mm/s]	[s]	[mm /s]	[mm/s]	[m]
376	22	357	24	80	14	50	923	111	4723	64	0.129284	1.117
284	48	167	128	183	25	59	894	235	1099	74	0.495	4.277
186	5	166	35	47	3	22	464	168	6256	73	0.279418	2.414
153	1	150	8	19	8	6	345	59	1452	51	0.013429	0.116
244	78	105	174	157	13	59	830	234	5845	75	1.217602	10.52
247	65	137	133	135	28	40	785	236	142	77	0.866094	7.483
161	14	145	18	13	0	4	355	118	6179	65	0.05268	0.455
238	76	135	149	143	18	82	841	275	4451	76	1.071967	9.262
213	71	110	152	108	11	71	736	249	1768	73	0.973893	8.414
466	67	290	137	209	43	50	1262	245	2974	78	0.759057	6.558
547	101	351	253	192	29	102	1575	245	7722	74	1.3908	12.017
477	10	418	54	87	15	44	1105	213	6469	67	0.254578	2.2
528	30	431	126	111	31	95	1352	169	6799	69	0.551471	4.765

553	17	467	71	66	10	32	1216	209	4140	69	0.354261	3.061
417	82	320	183	112	14	58	1186	282	5948	77	1.047931	9.054
319	24	268	54	54	5	11	735	192	350	72	0.171335	1.48
408	52	305	130	78	17	40	1030	208	8500	68	0.5769	4.984
338	41	248	160	86	4	40	917	244	4156	71	0.62219	5.376
384	79	236	209	162	17	70	1157	234	1228	72	0.761447	6.579
531	68	439	166	129	17	91	1441	247	3426	76	0.930666	8.041
414	27	357	66	108	0	0	972	234	1	81	0.401227	3.467
454	29	277	131	140	0	1	1032	213	1398	71	0.574992	4.968
657	10	522	107	101	0	1	1398	270	4682	67	0.470104	4.062
311	7	257	51	67	0	0	693	169	5608	68	0.168353	1.455
381	116	192	249	154	6	23	1121	243	7176	81	1.121285	9.688
415	23	363	70	111	4	32	1018	312	65	98	0.195884	1.692
384	36	278	114	109	0	11	932	320	3315	81	0.442153	3.82
349	42	243	102	99	0	2	837	265	8202	76	0.337594	2.917
510	25	425	92	105	0	10	1167	253	1420	76	0.276601	2.39
598	47	420	201	210	0	9	1485	261	2866	75	0.739725	6.391
480	96	301	195	197	53	85	1407	271	6134	76	1.197135	10.343
377	85	212	168	254	50	130	1276	260	5577	71	0.974442	8.419
389	0	385	13	9	4	21	821	53	5109	49	0.005656	0.049
331	26	245	98	110	20	61	891	181	2700	75	0.512255	4.426

354	124	234	231	163	32	57	1195	302	7148	82	1.267996	10.955
402	40	365	40	30	7	5	889	202	1918	78	0.298889	2.582
354	17	306	66	82	20	27	872	179	5424	71	0.280503	2.424
272	44	170	134	108	28	57	813	241	6401	77	0.823831	7.118
299	25	253	75	76	19	26	773	242	5508	76	0.299285	2.586
301	113	142	258	167	18	90	1089	304	3984	87	1.484556	12.827

After obtaining the raw data, behaviours from the four cages are grouped together into two sections for each behaviour; one for duration of behaviour and other for frequency as shown in the next section.

Grouping the data for undefined behaviour:

	Cage 1	Cage 2	Cage 3	Cage 4
002:24:00	900.24	1746.55	1345.59	1619.89
004:48:00	1233.28	1168.42	2024.49	1419.15
007:12:00	611.84	1211.79	2117.26	1068
009:36:00	423.95	1378.08	1143.02	936.15
012:00:00	950.53	1213.52	1459.46	1091.33
014:24:00	820.87	854.91	1118.17	1071.74
016:48:00	447.64	1023.65	1188.42	993.79
019:12:00	743.57	919.46	1383.85	874.57
021:36:00	733.53	1273.37	1731.04	756.64
024:00:00	1880.89	1724.4	1951.92	1152.33
002:24:00	900.24	1746.55	1345.59	1619.89

As the first experiment for the week was started by 8.30-8.45 AM the 24 hour monitoring was divided accordingly as shown below and thereafter every consequent experiment was rounded to its nearest time point. 8.6 and 32.6 signified same time point.

8.6	900.24	1746.55	1345.59	1619.89
11	1233.28	1168.42	2024.49	1419.15
13.4	611.84	1211.79	2117.26	1068
15.6	423.95	1378.08	1143.02	936.15
18.2	950.53	1213.52	1459.46	1091.33
20.6	820.87	854.91	1118.17	1071.74
23	447.64	1023.65	1188.42	993.79
25.4	743.57	919.46	1383.85	874.57
27.8	733.53	1273.37	1731.04	756.64
30.2	1880.89	1724.4	1951.92	1152.33
32.6	900.24	1746.55	1345.59	1619.89

Such adjusted time points from the other set of data obtained were averaged such that three points were obtained. The average for all the time points for week 1 was classed under 24hrs period, data from 11-18.2 and 32.6 were classed under 12hrs light cycle and data from 18.2-30.2 was classed under 12hrs dark cycle. The reason for the overlap in the time point 18.6 was due to the fact that as this software could only divide the measurement duration into 10 time points (2.24hrs each) the measurement for 7PM was included between the 18.2 and 20.6.

Average for duration of undefined behaviour for day 1 and 3 control rats undefined behaviour.

	A	B	C	D	E	F	G	H	I
1	8.6								
2	11	900.24	1746.55	1345.59	1619.89	1317.08	566.05	2409.52	677.82
3	13.4	1233.28	1168.42	2024.49	1419.15	1261.39	1301.99	1796.33	740.35
4	15.6	611.84	1211.79	2117.26	1068	1265.72	1164.11	2482.96	1934.47
5	18.2	423.95	1378.08	1143.02	936.15	816.77	900.38	2038.85	1075.52
6	20.6	950.53	1213.52	1459.46	1091.33	1208.23	1234.49	2457.63	1523.28
7	23	820.87	854.91	1118.17	1071.74	1346.82	1817.92	1261.89	978.12
8	25.4	447.64	1023.65	1188.42	993.79	1039.28	1063.48	1851.33	1129.19
9	27.8	743.57	919.46	1383.85	874.57	687.18	607.41	1008.99	566.94
10	30.2	733.53	1273.37	1731.04	756.64	977.1	640.83	1118.42	641.2
11	32.6	1880.89	1724.4	1951.92	1152.33	1022.39	1413.27	1746.31	788.41

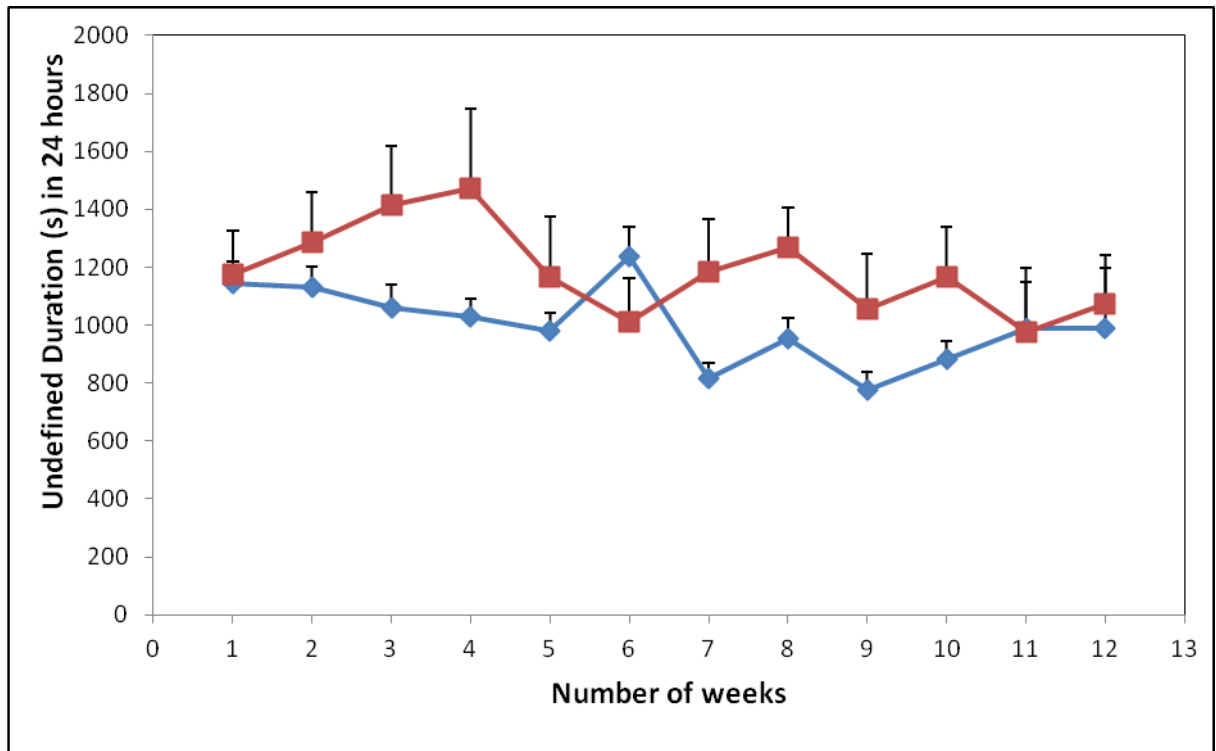
Average:

	Average	STD	SEM=STD/SQT (N)
24hrs: 11-32.6	1219.834	470.2855	166.271
12hrs light 11- 18.2 and 32.6	1344.423	509.49	180.1319
12hrs dark 18.2- 30.2	1094.219	404.0054	142.8375

Such average were obtained for duration and counts for diabetic and control rats and for individual and the average of the two independent experiment (N=16) for all the behaviours and such data obtained were plotted on the graph.

UNDEF_D	Average		SEM	
No. of weeks	Cont	Diab	Cont	Diab
1	1219.834	1174.333	166.271	152.3483
2	1131.413	1285.041	70.2782	173.5174
3	1061.835	1415.279	77.66578	204.774
4	1028.014	1473.159	61.98718	274.1098
5	980.5696	1166.966	62.89767	205.9138
6	1239.763	1011.173	97.86969	149.5993
7	814.5125	1186.246	53.17262	179.7136
8	952.2577	1269.343	70.79017	136.2126
9	777.9513	1057.475	59.85152	190.2915
10	885.0213	1165.721	58.8881	175.0355
11	989.7521	973.9916	208.5064	176.248
12	989.7521	1074.571	208.5064	167.3297

A typical graph obtained



Please note for presentational purposes it was not possible to plot for the whole time period. As the data obtained was enormous, this data can be represented in various different ways. The current analysis has divided the day into ten 2.24hrs sections and the data presented actually represents the average of these 2.24hrs sections either for the full 24hrs or the 12hrs dark and 12hrs light cycle. Clearly, we could look at longer segments of time including summing all the activities over 24 or 12 hours. However, as this was the first use of LABORAS in this laboratory, the times that have shown were chosen to be presented. Further future analysis by members of the laboratory may yield further interesting results. It was hoped that if 2.24hrs sections gave a reliable measurement of differences in behaviour then perhaps rat behaviours could be measured just for this short period.